

**Design, Synthesis and SAR Evaluation of Novel
Antituberculosis Agents.**



Fatimah Mohammed Alsalem

Submitted in the requirements for the degree of Doctor of
Philosophy

Biosciences Institute

Newcastle University

June 2024

Abstract

Abstract

There is an urgent need to discover and develop novel therapeutic alternatives for treatment of *Mycobacterium tuberculosis* (*Mtb*) infection, especially for infections caused by drug-resistant strains, to mitigate the global burden of tuberculosis disease. Initially within our group, a benzoxa-[2,1,3]-diazole moiety was employed in these investigations; however, the group has recently adopted a scaffold hopping strategy to generate several structurally diverse examples while maintaining antitubercular efficacy, often enhancing antitubercular activity. The pharmacophores imidazo[1,2-a]pyridine and 3,5-dinitrobenzene *N*-amino acid substituted hydrazides are of particular interest. The results for imidazo[1,2-a]pyridine substituted amino acid hydrazide compounds demonstrated increased activity with unsubstituted side chains on the amino acid and variable activity depending on the position of the halogen in the aromatic hydrazine. Furthermore, compared to the prior series, the results showed a higher level of action against bacteria with the 3,5-dinitrobenzene moiety substituted amino acid hydrazide, indicating the potential utility of these compounds as future antitubercular medications. Furthermore, this research was conducted to explore the coupling of the *N*-amino acid hydrazide structure with a scaffold comprising a one nitrogenous group in Pretomanid and 7-chloro-4-nitrobenzo-2-oxa-1,3-diazole (NBD-Cl). Unfortunately, these attempts were not successful, but it is worthwhile considering modifications for future endeavours.

Acknowledgments

ACKNOWLEDGEMENT

First and foremost, praises and thanks to Allah (God), for his never-ending grace, mercy and provision, for his showers of blessings throughout my research work to complete the research successfully. I am very grateful for offering me the opportunity and will to follow through my plan to obtain my PhD so far.

Then, i would like to express my deep and sincere gratitude to my research supervisor, Dr. Jon D Sellars, for the invaluable guidance and unwavering support you have provided me throughout my research work. I am truly grateful for the opportunity you have given me to pursue my PhD. Also, thanks is extend to Dr. Alistair Brown for his assistance and advice with the biology aspect of my thesis.

Furthermore, I would like to thank Dr C. Wills and Dr C. Dixon for NMR spectroscopy assistance, also Dr P. Waddell for his assistance with X-ray crystallography, and Dr. Alex Charlton for his assistance with the Mass spectroscopy.

Moreover, thanks is extend to the examiners of my thesis Dr. Judith Hall and Dr. Christopher Coxon for their valuable comments on the thesis.

In addition, i would like to express sincere thanks to the Saudi Ministry of Education and King Khalid University for the financial sponsorship of my PhD study. I would also like to express my sincere thanks to Newcastle University for their accessibility to all the needs.

I would also like to express my deepest appreciation to my family for their unwavering love, support, and sacrifices throughout my academic journey. I am extremely grateful to my loving Mam and Dad (who is sadly is no more) for their love, prayers, caring and sacrifices for educating and preparing me for my future.

To my dear husband, Ibrahim, thank you for your unwavering support, kindness, and patience. Your love and encouragement have been a source of strength for me, and I am truly blessed to have you by my side. Also, thanks to my sons, Khalid and Tariq, your presence and encouragement have been a constant source of motivation for me, and I am grateful for the love and joy you bring into my life.

Acknowledgments

Lastly, i would like to extend my heartfelt thanks to my friends Haya, Noor and Aminah, who offered both distractions when need and encouragement when it seems difficult to continue. My research experience has been improved by the discussions and solid support of them, making this trip not only possible but also pleasant, your encouragement and friendship have made this journey truly special, also thanks extend to Dr. Ahmed Aljohani, for his help at beginning of my PhD journey. Also, thanks extend for collogues in the crystallography site, Lina, Max, Tom and Jake for help during my laboratory time, I am grateful to work with you all.

Publication

- 1) Brown, A. K.; Aljohani, A. K. B.; Alsalem, F. M. A.; Broadhead, J. L.; Gill, J. H.; Lu, Y.; Sellars, J. D. Identification of Substituted Amino Acid Hydrazides as Novel Anti-Tubercular Agents, Using a Scaffold Hopping Approach. *Molecules* **2020**, 25 (10), 2387.

Poster Participation

1. Royal Society of Chemistry Chemical Biology Community Meeting 11-12th September 2023 School of Chemistry, University of Leeds, “*Design, Synthesis and SAR Evaluation of Novel Antituberculosis Agents*”
2. Chemical Biology Workshop, Newcastle University, 1st July 2022, “*Design, Synthesis and SAR Evaluation of Novel Antituberculosis Agents*”

Table of Abbreviations

Abbreviations

ACP	Acyl carrier protein
AG	Arabinogalactan
AMK	Amikacin
AMS	Alveolar macrophages
ATP	Adenosine triphosphate synthase
BCG	Bacille Calmette-Guerin
BDQ	Bedaquiline
CAP	Capreomycin
CI	Chemical ionisation
CNS	Central nervous system
DAT	Diacyltrehalose
DCS	D-cycloserine
Dd	Doublet doublet
Ddn	Dependent nitroreductase
DIPEA	<i>N,N</i> -diisopropylethylamine
DLM	Delamanid
DMF	Dimethyl formamide
DMSO	Dimethyl sulfoxide
DMSO-d ₆	Deuterated dimethyl sulfoxide
DMTMM	4-(4,6-Dimethoxy-1,3,5-triazin-2-yl)-4-methyl-morpholinium
DNA	Deoxyribonucleic acid
DOTS	Directly Observed Standard Therapy
EI	Electron Ionisation
EMB	Ethambutol
ESAT6	Early secreted antigenic target 6
ESI	Electroscopy
EPTB	Extrapulmonary TB
ETH	Ethionamide
FDA	Food and Drug Administration
FQ	Fluroquionolone
HBTU	2-(1 <i>H</i> -benzotriazol-1-yl)-1,1,3,3-tetramethyluronium hexafluorophosphate
HOBt	1-hydroxybenzotriazole
HNP-1	Human neutrophil tetradecapeptide
KAN	Kanamycin
KatG	Catalase-peroxidase
LAM	Lipoarabinomannan
LM	Lipomannan

Table of Abbreviations

LP	Lipopolysaccharide
LTBI	Latent TB infection
LZD	Linezolid
mAGP	Mycolyl arabinogalactan-peptidoglycan
ManLAM	Mannosylated lipoarabinomannan
MDMs	Monocyte-produced macrophages
MDR	Multidrug-resistant TB
MIC	Minimum inhibitory concentration
m.p.	Melting Point
<i>Mtb</i>	<i>Mycobacterium tuberculosis</i>
MurNAc	N-acetylmuramic acid
NAD	Nicotinamide Adenine Dinucleotide
NBD-Cl	7-chloro-4-nitrobenzo-2-oxa-1,3-diazole
NF- κ B	Nuclear factor kappa-light-chain-enhancer of activated B cells
NLRs	Nucleotide-binding oligomerization domain-like receptors
NO	Nitric oxide
PA	Pyrazinoic acid
PAMP	Pathogen-associated molecular patterns
PAS	<i>Para</i> - amino salicylic acid
PAT	Polyacetyltrehalose
PA-824	Pretomanid
PDF	Formylmethionine deformylase
PDIM	Phthiocedimycocerosate
Ph	Phenyl
PIMs	Phosphatidyl-myo-inositol mannosides
PIP ₃	Phosphatidylinositol 3-phosphate
PknG	Protein kinase G
PTH	Prothionamide
5-OH-PA	5-hydroxy-pyrazinoic acid
5-OH-PZA	Hydroxy-pyrazinamide
Ppm	Parts per million
PZA	Pyrazinamide
Q	Quartet
QcrB	Cytochrome bcc complex
RD	Regions of differences
REMA	Resazurin Microtiter Assay
Rf	Retention Factor
RIF	Rifampin
RNA	Ribonucleic acid
Rt	Room Temperature

Table of Abbreviations

S	Singlet
SAR	Structure-activity relationship
SGL	Sulfoglycolipid
SPPS	Solid phase peptide synthesis
SZD	Sutezolid
T	Triplet
TB	Tuberculosis
TBM	Tuberculous meningitis
TBAI	Tetra butyl ammonium iodide
TDM	Trehalose dimycolate;
TDR-TB	total drug-resistant strains
THF	Tetrahydrofuran
TLC	Thin Layer Chromatography
TLRs	Toll-like receptors
TMM	Trehalose monomycolate
UDP	Uridine diphosphate
WHO	World health organization
XDR	Extensively drug-resistant TB
Δ	Chemical shift
°	Degrees

Originality Statement.

Originality Statement

I hereby declare that this submission is my own work and to the best of my knowledge it contains no materials previously published or written by another person, or substantial proportions of material which have been accepted for the award of any other degree or diploma at University of Newcastle or any other educational institution, except where due acknowledgment is made in the thesis. Any contribution made to the research by others, with whom I have worked at University of Newcastle or elsewhere, is explicitly acknowledged in the thesis. I also declare that the intellectual content of this thesis is the product of my own work, except to the extent that assistance from others in the project's design and conception or in style, presentation and linguistic expression is acknowledged.'

Fatimah Mohammed Alsalem.

Date:10/06/2024

Table of Contents.

Table of Contents

1. Introduction.....	1
1.1 Tuberculosis Epidimology.	1
1.2 Tuberculosis Pathology.	3
1.2.1 Mycobacterium tuberculosis cell wall structure.	4
1.2.2 Expression of <i>Mtb</i> into phagocytes.	7
1.3 Tuberculosis Immunology.....	9
1.3.1 Defensive mechanism of macrophages and granuloma development.	9
1.3.2 Latent Tuberculosis Infection.....	12
1.4 Control and treatment.	13
1.4.1 Vaccination.....	13
1.4.2 First-line anti-tuberculosis drugs.....	14
1.4.2.1 Isoniazid	15
1.4.2.2 Rifampicin.	16
1.4.2.3 Pyrazinamide.	17
1.4.2.4 Ethambutol.	18
1.4.3 Second-line anti-tuberculosis drugs.	19
1.4.3.1 <i>Para</i> - Amino Salicylic acid.	19
1.4.3.2 Aminoglycosides	20
1.4.3.3 Fluoroquinolones.	21
1.4.3.4 Ethionamide and Prothionamide.....	22
1.4.3.5 Cycloserine.....	22
1.4.4 New candidate anti-tuberculosis drugs.	23
1.4.4.1 Bedaquiline.	23
1.4.4.2 Delamanid and Pretomanid.....	25
1.4.4.3 Linezolid and Sutizolid.....	27
1.4.4.4 Q203.	28
1.4.4.5 Antimycobacterial activity of peptides.	29
1.4.4.6 Antimycobacterial activity of hydrazides.	31
1.5 Drug Resistant Tuberculosis.....	33
1.5.1 Overview of drug-resistant tuberculosis	33

Table of Contents.

1.5.2 Resistance mechanism to anti-tuberculosis drugs.	35
1.5.2.1 Resistance to the first line anti-tuberculosis.....	35
1.5.2.2 Resistant of the second line drugs anti-tuberculosis.	37
1.6. Previous work with in the group.....	41
1.6.1 Enantiomeric purity determination.....	43
1.7 Scaffold hopping approach.	45
1.8 Aim and objectives.....	48
2. Chapter 2: Synthesis and SAR evaluation of imidazo[1, 2<i>a</i>] pyridine substituted aminoacid hydrazide compounds.	50
2.1 Introduction.....	50
2.2 Synthesis of the imidazo[1,2 <i>a</i>] pyridine amino acid hydrazides	52
2.3 Synthesis of the imidazo[1,2 <i>a</i>]pyridine-3-carboxylic acid precursor	53
2.4 Synthesis of amino acids hydrazides intermediates.	54
2.4.2 Enantiomeric purity determination.....	59
2.5 Synthesis of imidazo[1,2 <i>a</i>]pyridine substituted amino acid hydrazide compounds.	60
2.6 Structure activity relationship evaluation of imidazo[1,2 <i>a</i>]pyridine substituted amino acids hydrazide compounds.....	63
2.6.1 Antimycobacterial susceptibility test.	63
2.6.2 Structure activity relationship exploration of imidazo[1,2 <i>a</i>]pyridine substituted amino acid hydrazide compounds.	64
3. Chapter 3: Synthesis and structural activity relationship evaluation of 3,5-dinitrobenzene substituted amino acid hydrazide compounds.	76
3.1 Introduction.....	76
3.2 Synthesis of 3,5-dinitrobenzene substituted amino acid hydrazide compounds. .	79
3.3 Synthesis of amino acid hydrazide intermediates.	81

Table of Contents.

3.4 Synthesis of the 3,5-dinitrobenzene substituted amino acid hydrazide compounds.....	81
3.5 Structural activity relationship evaluation of the 3,5-dinitrobenzene substituted amino acid hydrazide compounds.	84
4. Chapter4: Attempts to synthesise of 4-nitroimidazole and NBD scaffolds substituted amino acid hydrazide compounds.	94
4.1 Introduction.....	94
4.2 Synthesis of the 4-nitroimidazole precursor.	95
4.3 Attempts to synthesise the 4-nitroimidazole amino acid hydrazide compounds..	96
4.3.1 Introduction.....	96
4.3.2 Mitsunobu reaction.....	97
4.3.2 Tosylation reaction.....	99
4.4 Reaction of the NBD-Cl with amino acid hydrazide compound	100
4.5 Conclusion and Future work	102
4.5.1 Thesis Conclusion.....	102
4.5.2 Future work and additional studies	103
4.5.2.1 Synthesis of NBD-substituted amino acid hydrazide compound using alkyl ester amino acid.	103
4.5.2.2 Synthesis of adamantyl substituted amino acid hydrazide compounds.	105
4.5.2.3 <i>In vivo</i> phenotypic screening.	106
4.5.2.4 Evaluation of the Q203 analogues for anti-cancer and anti-proliferation activity.	107
5. General Experimental information.	108
5.1 Analysis	108
5.1.1 Synthesis of N-protected Hydrazides – General Procedure.....	109
5.1.2 General procedure for synthesis of imidazo[1,2 α] pyridine substituted amino acid hydrazide compounds.....	133
5.1.3 General procedure for synthesis of 3,5-dinitrobenzene substituted amino acid hydrazide compounds.....	169

Table of Contents.

5.1.4 General procedure for synthesis of 1-admantyl substituted amino acid hydrazide compounds.....	206
5.2 General Experimental Information of Biological Assessment	213
5.2.1 Cell Lines.....	213
5.2.2 Bacterial Growth Conditions	214
5.2.3 <i>In vitro</i> bacterial inhibitory assay.....	214
5.2.4 Cytotoxicity assay method.....	215
5.2.5 Calculation of the percentage yield of the compound.....	215
6. References	217
7. Appendix	214
7.1 The biological data for <i>in vitro</i> evaluating antitubercular activity	214
7.1.1 Q203 analogues MIC values.....	214
7.1.2 3,5-dinitrobenzene amino acid hydrazide compounds MIC values.....	222
7.2 Crystal structure determination of: jds220006 (C₁₄H₂₀ClN₃O₃).....	232

Chapter 1: Introduction

1. Introduction.

Tuberculosis (TB) disease continues to be the leading cause of mortality worldwide among infectious diseases¹. Drug-resistant *Mycobacterium tuberculosis* (*Mtb*) infections are becoming more common, which constitutes a worldwide health threat². The significance of the problem has so far been estimated globally through surveillance and survey. In each year, new hotspots emerge and more instances of drug-resistant tuberculosis are reported³. Despite the availability of effective short-course therapy, tuberculosis remains the primary factor in mortality of an infectious disease.

This thesis provides research on three main areas: 1) the design of new chemical compounds that show potential antitubercular agents and selectivity for *Mycobacterium tuberculosis* based on a scaffold hopping approach, 2) the synthesis of novel *N*-amino acid hydrazides substituted with imidazo[1, 2*a*] pyridine and 3,5-dinitrobenzene moieties, 3) the investigation of the structure-activity relationship of novel *N*-substituted amino acid hydrazide imidazo[1,2 *a*] pyridine and 3,5-dinitrobenzene compounds utilising a resazurin microtiter assay (REMA) assay.

This chapter will specifically address the recent tuberculosis epidemiology, with a particular focus on *Mycobacterium tuberculosis* background and its pathology, also treatment and resistance mechanisms of antituberculosis agents. Then, chapter 2 and chapter 3 will describe the successful synthesis and structure-activity relationship (SAR) analysis of new antitubercular compounds utilising amino acid hydrazides substituted with imidazo[1,2 *a*] pyridine and 3,5-dinitrobenzene scaffolds, respectively. Lastly, chapter 4 will describe the unsuccessful attempts to synthesise a *N*-substituted amino acid hydrazides with 4-nitroimidazole and 7-chloro-4-nitrobenzo-2-oxa-1,3-diazole (NBD-Cl) scaffolds as well as potential future work, followed by the detail of the experimental procedures used in this project.

1.1 Tuberculosis Epidemiology.

There had been progress in reducing the TB obligation up until 2019, but this was interrupted by the COVID 19 pandemic, which reversed the previous

Chapter 1: Introduction

achievements. In 2020, the significant decline in individuals seeking treatment for the disease, coupled with insufficient recovery in 2021, led to an increase in tuberculosis-related mortality and incidence. In 2022, World Health Organisation report indicated that tuberculosis remained the second largest cause of death globally from a single infectious agent, following COVID-19. The recorded deaths from tuberculosis in 2022 reached to 1.13 million, more than double that of HIV/AIDS, which reported 0.63 million deaths. In 2014 and 2015, all World Health Organisation (WHO) and United Nations Member States (UN) pledged to eradicate the global tuberculosis epidemic by endorsing the WHO End TB Strategy and United Nations Sustainable Development Goal. The goal is to lower the incidence rate of tuberculosis by 50% between 2015 and 2025. These agreements were reaffirmed at two high-level United Nations sessions on tuberculosis, in 2018 and most recently in September 2023, further objectives concerning funding, treatment provision for individuals with TB sickness or infection, and the accessibility of novel TB vaccines were established. Nevertheless, the global community, along with many sectors and nations, remains significantly far from achieving the milestones and targets set by the End TB Strategy (Figure 1)⁴.

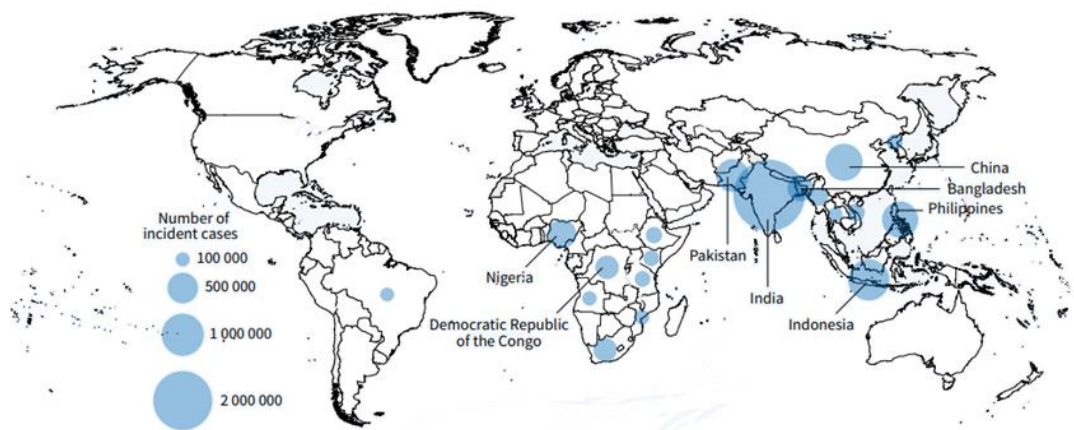


Figure 1: Estimated TB incidence in 2022, for countries with at least 100 000 incident cases⁴.

Tuberculosis is a contagious illness resulting from infection with the pathogenic bacteria *Mycobacterium tuberculosis*. Mainly it infects the lungs, but it can also infect other organs such as the kidney, brain, and spinal cord. Spreading of the

Chapter 1: Introduction

infection from one person to another occurs when sneezing, coughing, spitting or direct contact and breathing air contaminated with bacteria. Tuberculosis follows two known patterns of infection, one of which is the infected person does not develop symptoms as the bacteria is inactive inside the body, so the disease is not contagious in this case⁵.

After the initial infection with *Mtb*, certain individuals quickly developed active disease, typically referred to as primary or primary-progressive TB, which is more common in children but often affects adults⁶. Active disease may occur after several years after exposure to others who carry the initial infection and are subsequently assumed to be latently infected. With latent infection, people having a 5 - 10 % lifetime risk of developing active TB, called reactivation or post-primary TB⁷. The complexity of this disease is often underestimated and oversimplified because of the significant variations observed among individuals with active tuberculosis. The entire manifestation of symptoms and diagnostic tests can involve systemic symptoms, such as fever, weight loss, and night sweats, as well as localised effects of infection, such as cough and haemoptysis, particularly in respiratory illnesses. Approximately 500,000 children develop TB annually, with 20-30% of them suffering extrapulmonary TB (EPTB)⁸. Therefore, infants, young children, and children infected with HIV are frequently afflicted with serious symptoms of TB, such as disseminated TB or tuberculous meningitis (TBM). Meningitis is the most typical sign of an *Mtb* infection in the central nervous system (CNS). Furthermore, tuberculous meningitis is the most prevalent and severe form of central nervous system tuberculosis in children, particularly in underdeveloped nations⁹. It leads to significant consequences and continues to be a socioeconomic concern. If left untreated, it can lead to severe cognitive, intellectual, and endocrine consequences, perhaps resulting in disability, particularly in nations with limited resources¹⁰.

1.2 Tuberculosis Pathology.

Tuberculosis predominantly impacts the respiratory system, with around 75% of reported cases being pulmonary. Approximately 15 to 20 % of current cases of tuberculosis result in extrapulmonary manifestations, where the infection extends

Chapter 1: Introduction

beyond the respiratory organs and affects other parts of the body. The occurrence of this phenomenon is commonly noted in individuals with compromised immune systems and the paediatric population. The observed occurrences of this condition are most frequently found in the lymphatic system, pleura, bones and joints (particularly the spine). In exceptional cases, TB may disseminate extensively throughout the body, resulting in a condition known as "Miliary TB"⁷. The manifestation of tuberculosis symptoms is not evident until the infection has progressed to the pulmonary region. In contrast to other bacterial species, *Mycobacterium tuberculosis* exhibits a comparatively prolonged replication cycle, resulting in a delayed onset of symptoms that may manifest several years following initial infection. The symptoms associated with active TB are generally nonspecific and vary depending on the precise site of infection¹¹.

Individuals who have been diagnosed with active pulmonary tuberculosis can release infected aerosol particles into the surrounding environment by actions such as coughing, spitting, or sneezing. Each instance of sneezing or coughing results in the discharge of approximately 40,000 droplets of water, which have the potential to linger in the air for several hours¹². Consequently, this prolonged presence of droplets in the air elevates the risk of infection. Due to the low infectious dose of tuberculosis, inhaling a single droplet can lead to infection, as the inhalation of only 10 bacteria is sufficient to cause an illness¹³.

Among the most distinctive features of mycobacteria is their intricate cell wall. As a result, a complete understanding of cell wall biosynthesis has been a major research objective over the last decade¹⁴.

1.2.1 *Mycobacterium tuberculosis* cell wall structure.

Mycobacteria are a wide group of unicellular species, known as prokaryotic cells since there is no true nucleus. These microscopic organisms, having cell walls, capsules, DNA, pili, flagellum, cytoplasm, and ribosomes, comprise a basic physical structure. Typically, bacteria are divided into two main types of bacteria, Gram-positive and Gram-negative. The cell wall structure of the Gram-positive bacteria consists of a single-layer thick peptidoglycan that forms a rigid and dense structure. It also has phosphate and teichoic acid in its cell wall. In addition, Gram-positive bacteria are bacteria that are classified based on their reaction to the

Chapter 1: Introduction

staining procedure. The staining technique employs crystal violet dye, which is retained by the dense peptidoglycan cell wall found in Gram-positive organisms and cannot be removed by acetone or alcohol. When observed under a microscope, this process imparts a blue hue to Gram-positive organisms. On the other hand, the Gram-negative bacteria have an outer membrane as well as a thin peptidoglycan layer. The Gram-stained results in pink cell colour staining, which can be removed by alcohol, also, it is more resistant to antibiotics as a consequence (Figure 2)¹⁵.

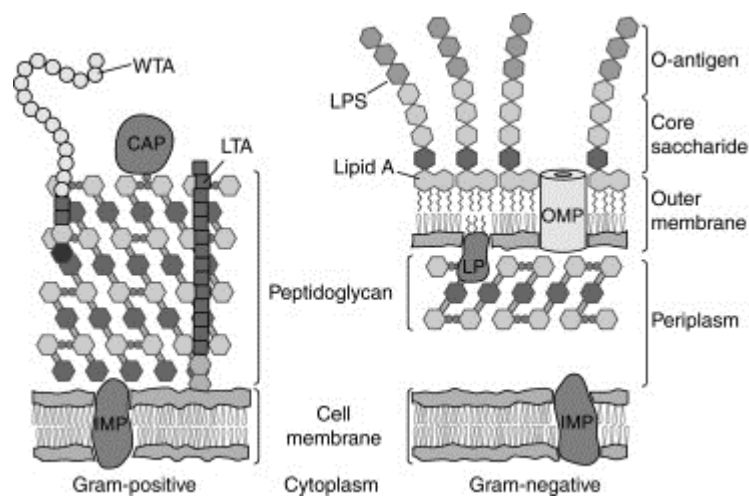


Figure 2. Illustration of Gram-positive and Gram-negative cellular membranes, CAP $\frac{1}{4}$ covalently attached protein; IMP, integral membrane protein; LP, lipoprotein; LPS, lipopolysaccharide; LTA, lipoteichoic acid; OMP, outer membrane protein; WTA, wall teichoic acid¹⁶.

Mycobacterium tuberculosis (*Mtb*) is classified as an obligate aerobe, characterised by its nonmotile rod-shaped morphology, its inability to produce spores and its possession of a distinct cell wall. *Mycobacterium tuberculosis*, which primarily infects the lungs¹⁷, has a unique cell wall structure which is characterised via the cell wall envelope that consists of three main structural components: (a) the characteristic long-chain mycolic acids, (b) a highly branched arabinogalactan (AG) polysaccharide, and (c) a cross-linked network of peptidoglycan.

Mtb is part of the genus of mycobacterium, but its cell wall is not graded as either Gram-positive or Gram-negative as the structure of its cell wall is unusual and unique. Firstly, the peptidoglycan layer contains *N*-glycolyl muramic acid rather than *N*-acetyl muramic acid. Furthermore, the *Mtb* cell wall has more distinctive characteristics, which include lipids up to 60% of its cell wall, which are mostly

Chapter 1: Introduction

specific long-chain fatty acids (60-90 carbon), defined as mycolic acid. The mycolic acid replaces 10 % of the residue of arabinose. Moreover, the cell wall also includes a lipid which cannot be separated from the main skeleton. Peptidoglycan is located outside to the mycobacterial inner membrane, providing rigidity, integrity, and shape to the cell¹⁸. It is a polysaccharide consisting of alternating *N*-acetylglucosamine and muramic acid (either *N*-acetylated or *N*-glycolylated) residues connected by β (1→4) linkages¹⁹. Arabinogalactan is a branching polysaccharide consisting of arabinose (Araf) and galactose (Galf) residues in the furanose form. Mycolic acids are associated with the arabinose component of the arabinogalactan complex. The ultimate product, arabinogalactan, consists of a linear galactan with highly branching arabinans attached to it. The arabinan binds the mycolic acids, constituting the mycolyl-arabinogalactan-peptidoglycan (mAGP) complex. In addition to the mAGP complex, the mycobacterial cell wall contain lipomannan (LM), lipoarabinomannan (LAM), and phosphatidyl-myo-inositol mannosides (PIMs). These lipids are bound to the inner membrane and are crucial for the proliferation, survival, and virulence of *Mtb*. Trehalose-containing glycolipids and phthiocerol dimycoserates alternate with mycolic acids in the outer membrane. These lipids are essential for their interactions with the host and its immunological response (Figure 3)¹⁹.

Chapter 1: Introduction

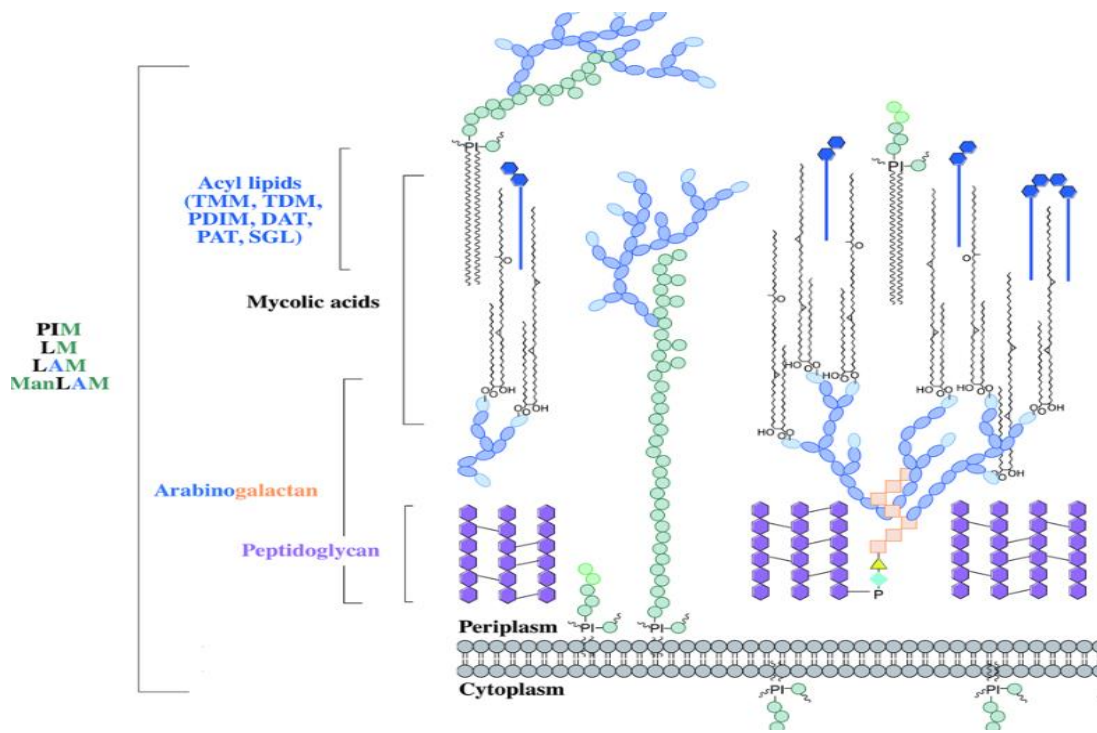


Figure 3: Schematic illustration of the mycobacterial cell wall, highlighting key characteristics such as glycolipids. (PIMs, phosphatidyl-myo-inositol mannosides; LM, lipomannan; LAM, lipoarabinomannan; ManLAM, mannosylated lipoarabinomannan), peptidoglycan, arabinogalactan and mycolic acids. The acyl lipids are inserted into the mycolate layer. (including TMM, trehalose monomycolate; TDM, trehalose dimycolate; DAT, diacyltrehalose; PAT, polyacyltrehalose; PDIM, phthiocedimycocerosate; SGL, sulfolipid)²⁰.

This cell wall structural components function as an insoluble residue that retains the whole cell's viability. Overall, the special structure and waxy cell wall contribute to low drug permeability and consequently, low drug concentration which makes effective therapy a challenge²¹. This is due to presence lipid-rich cell wall which creates a low-permeability barrier that protects *Mtb* from most drugs. This represents one of the numerous obstacles confronting tuberculosis drug development and the primary reason for the ineffectiveness of medication target-based screening¹⁹.

1.2.2 Expression of *Mtb* into phagocytes.

The initial stage of the infection involves the identification of Mycobacteria as a foreign pathogen by the innate immune system. Therefore, macrophages and dendritic cells are capable of recognising *Mtb* through various receptors, including Toll-like receptors (TLRs), nucleotide-binding oligomerization domain-like receptors (NLRs), and C-type lectins²². Accordingly, the alveolar macrophage engulfs the Mycobacteria, enclosing it within a phagosome²³.

Chapter 1: Introduction

Phagosomes represent a specific type of endosome that serves as tiny vesicles employed by cells to internalise extracellular substances from the surrounding environment²⁴. The typical pathway for a phagosome involves fusion with the lysosome, where the contents of the bacteria are ultimately broken down and digested. Upon entering the phagosome, *Mycobacterium tuberculosis* (*Mtb*) initiates a cascade of defensive mechanisms to ensure its survival such as secretion of protein kinase G (PknG), a virulence component essential for lysosomal escape, aids in metabolic adaptability, enhancing mycobacterium survival. PknG, blocks phagosome-lysosome fusion by increasing signal transduction in host cells. Another significant way for *Mtb* to suppress phagosome-lysosome fusion by inhibition of releasing the pro-inflammatory transcription factor NF- κ B, Studies have indicated that the NF- κ B controls the release of lysosomal enzymes into phagosomes, therefore regulating pathogen death. Furthermore, NF- κ B increases the production of membrane transport molecules, which regulates phagolysosome fusion during an infection. Moreover, Phosphatidylinositol 3-phosphate (PI3P) is a key component of the macrophage cell membrane found on the initial endosome and phagosome surface. After *Mtb* infection, decreased produce and trafficking of the toxin lipoarabinomannan (LAM), as well as calmodulin-dependent PI3P production, impede the process of phagosome-lysosome fusion process (Figure 4)^{25, 26}.

Chapter 1: Introduction

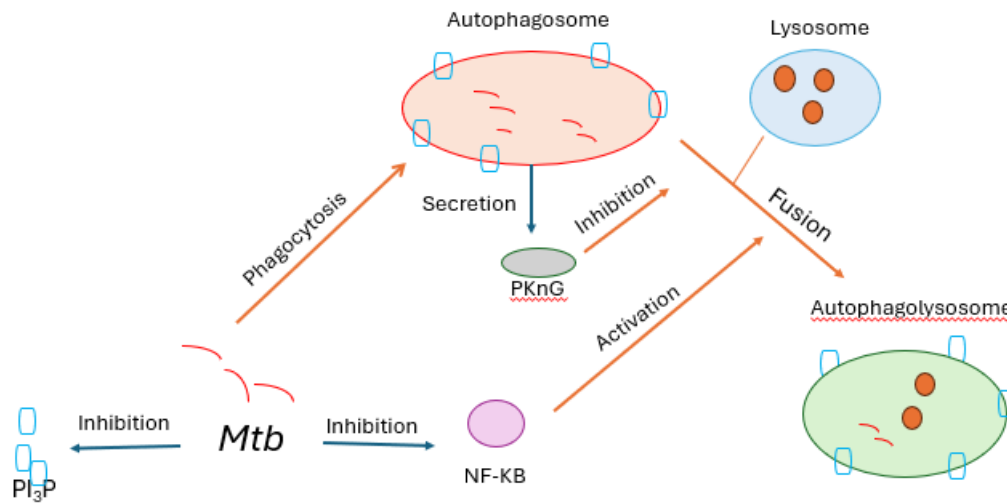


Figure 4: *Mycobacterium tuberculosis* evades the immune system by preventing the fusion of lysosomes with phagosomes. PknG (Protein kinase G) secreted by phagocytic *Mtb* limits the fusion of phagosomes with lysosomes, while the inhibition of NF-κB also reduces this fusion. Lower production and increased hydrolysis of PIP3 (Phosphatidylinositol 3-phosphate) on the phagosome surface inhibit fusion, allowing *Mtb* to escape²⁷.

1.3 Tuberculosis Immunology

1.3.1 Defensive mechanism of macrophages and granuloma development.

Macrophages serve as the main barrier of defence in the immune system's efforts to thwart infection. The extensive mycobacterial lipoarabinomannan provides resistance against macrophages. The consequent phase of phagocytosis by macrophages triggers a series of events that leads to either effective containment of the infection, resulting in latent tuberculosis, or advancement towards active disease, known as primary progressive tuberculosis. Moreover, macrophages are the initial cells that encounter *Mtb* in the lungs, however, it is worth noting that neutrophils and monocytes can also identify and become infected by *Mtb*. Various components of the microbe, such as cell wall constituents, DNA, cytosolic proteins, superoxide dismutase A, and heat shock proteins, can function as pathogen-associated molecular patterns (PAMP). TLRs, Nod-like receptors, C-type lectin receptors, complement receptors, Fc receptors, GPI-anchored membrane receptors, and scavenger receptors all recognise these antigenic components. Detection of these pathogen-associated molecular patterns (PAMPs) initiates a series of reactions in macrophages, such as the internalisation of *Mtb* by lysosomes, the maturation and acidification of phagosomes, the release of cytokines, the inhibition of vacuole maturation, and

Chapter 1: Introduction

the increased production of intracellular nitric oxide. All these processes collectively contribute to the elimination of *Mtb*. The occurrence of these events alone does not trigger the formation of granuloma. However, the inability to eradicate *Mtb* and terminate the defensive mechanisms launched by *Mtb* as a response to these events leads to the initiation of granuloma²⁸. The granuloma is composed of a heterogeneous collection of immune cells, mostly consisting of resident alveolar macrophages (AMs) and monocyte-produced macrophages (MDMs) (Figure 5)²⁹.

Chapter 1: Introduction

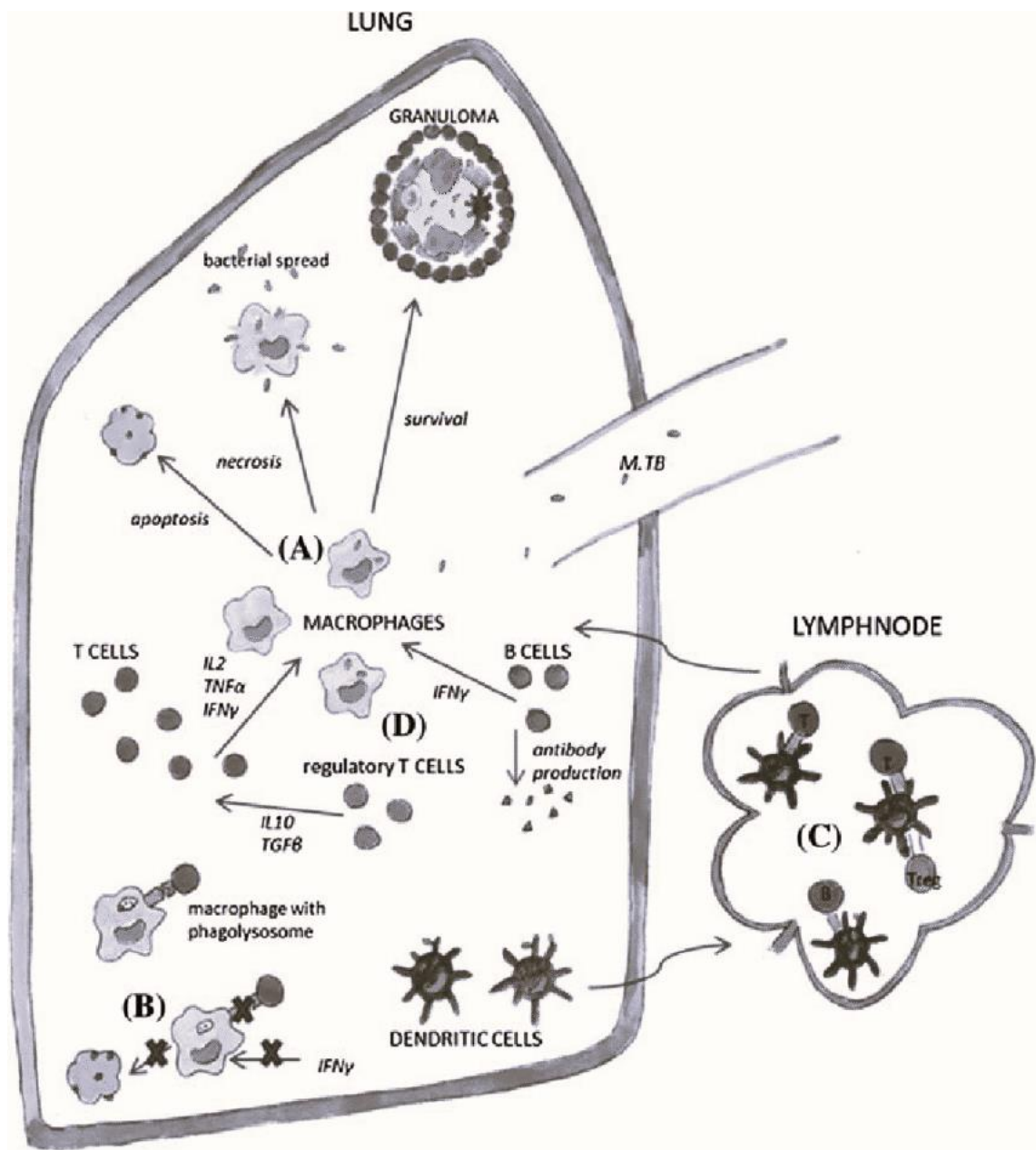


Figure 5: Diagram illustrating primary immune responses to mycobacterial infections in the lung and lymph nodes. Macrophages and dendritic cells first encounter *Mtb* in the lungs. A Following intake, macrophages have the potential to undergo apoptosis or necrosis. Bacterial dispersion may occur following necrosis. Macrophages that survive contribute to the first creation of granulomas, which can either result in the elimination of the infection or the establishment of clinical latency. B Mycobacteria can avoid the immune response by preventing the development of phagolysosomes and apoptosis, and by limiting the response of macrophages to IFN γ . C Lung resident dendritic cells can migrate to nearby lymph nodes, where they offer live mycobacteria and mycobacterial antigen to activate naive T-cells, B-cells, and regulatory T-cells. D Activated T-cells and B-cells recruited to the lung by chemokines regulate bacterial growth through the generation of cytokines and antibodies. Regulatory T-cells manage inflammation by producing IL-10 and TGF- β ³⁰.

The formation of the granuloma is commonly referred to as caseous necrosis, which is characterised by reduced oxygen levels, acidic pH and a restricted supply of essential nutrients. This situation imposes limitations on subsequent

Chapter 1: Introduction

growth and generates a state of latency. In individuals possessing an adequate immune system, lesions typically acquire fibrosis and calcification, effectively managing the infection. The patient may have no signs of symptoms after bacteria invasion, however, during periods of dormancy, it is possible for the host's immune system to become compromised at certain stages of their life and consequently development of active TB will occur. This condition is commonly referred to as latent tuberculosis. It is possible that during the advanced phase of the disease, the proliferation of bacteria inside the lung region leads to consequential damage to the lung tissue and as a result, the untreated tissues can lead to death.

1.3.2 Latent Tuberculosis Infection.

Approximately 2 billion individuals have latent TB infection (LTBI) today. Humans are the primary reservoir of *Mtb*, and human-to-human transmission occurs predominantly through inhalation of *Mtb*-containing respiratory aerosols and secretions exhaled by a patient with active pulmonary TB³¹. The main complex, also known as the early inflammatory process, produced by *Mtb* is localised to a small area in immunocompetent individuals and may involve local lymph nodes. However, the immune response may not always totally eradicate the main complex, which can result in a persistent infection that can arise due to the survival of infections³². Various factors can exert an influence on the progression of a disease, and these factors are interconnected with the immune response of the afflicted individual and the virulence of the specific strain involved. One of the primary factors contributing to the pathogenicity of mycobacteria is their capacity to persist within macrophages. Furthermore, *Mtb* exhibits the ability to halt its metabolic processes and inhibit replication, thereby entering a dormant state characterised by increased resistance to both host defence mechanisms and pharmaceutical interventions³³. This emphasises the significance of addressing the molecular biology of *Mtb* to enhance comprehension of its pathogenic mechanisms and virulence factors, as well as to make valuable contributions to the advancement of novel vaccines and medicines. Undoubtedly, the research conducted in this sector has produced extremely beneficial outcomes, resulting in the identification and characterization of several pathogenic mechanisms.

Chapter 1: Introduction

However, it is important to note that despite these advancements, a significant number of pathogenic mechanisms remain unidentified and drug resistance continues to emerge³⁴.

1.4 Control and treatment.

1.4.1 Vaccination.

The only known preventive measure for TB is the administration of the Bacille Calmette-Guerin (BCG) vaccine, which is generated from a weakened strain of *Mycobacterium bovis*. The BCG vaccination is well recognised as a cost-effective and reliable immunisation method, making it the most administered vaccine among the global population. However, it is important to note that its protective effects are limited to the prevention of tuberculosis meningitis in babies, infants and young children³⁵. Despite being administered worldwide for over a century, the mechanism behind the protective immunity conferred by the BCG vaccine remains unknown. The efficacy of this vaccination in adults exhibits significant variability, nevertheless, it does not confer protection against tuberculosis infection in adult individuals^{36, 37}. The lack of efficacy of BCG can be attributed to its incomplete appearance of *Mtb* within the host. Accordingly, it was observed that 23% of the T cell epitopes that are known to be physiologically retained in the *Mtb* complex were not detected in BCG³⁸. Therefore, it may be concluded that BCG lacks some *Mtb* virulence characteristics, despite the significant genetic similarities observed between *Mycobacterium bovis* and *Mtb*, which are believed to have originated from a common genetic origin. The attenuation process of *Mycobacterium bovis* led to the additional removal of many genes linked to virulence, which were in regions known as regions of differences (RD). One of the deleted areas, RD1, contained the genetic information for a protein secretion system called Esx1. This system is responsible for the secretion of ESAT6, a virulence factor that plays a role in modulating the host's innate and adaptive immune responses. The lack of capacity of Bacillus Calmette-Guérin (BCG) to stimulate an immunological response comparable to *Mtb* infection results in its inability to effectively deliver protection against *Mtb*³⁹. Therefore, there is a need for new vaccines for tuberculosis that protect against adult pulmonary disease in geographical regions where BCG is not effective. However, BCG could remain

Chapter 1: Introduction

integral to TB control programmes because neonatal BCG protects against disseminated forms of childhood TB⁴⁰.

1.4.2 First-line anti-tuberculosis drugs.

Where effective preventative measures are not available, medication therapy continues to be the primary method for managing tuberculosis disease. The management of tuberculosis poses significant challenges due to the necessity of timely diagnosis, screening for medication susceptibility, and the implementation of efficacious combination treatment protocols.

The first antituberculosis agent, streptomycin, was developed as an antibiotic in 1943 in the laboratory of Selman Waksman at Rutgers University.⁴¹ The initial comprehensive clinical trial of streptomycin in tuberculosis patients was performed by the British Medical Research Council in 1948⁴²⁻⁴⁴.

Following the introduction of streptomycin, two other antimycobacterial drugs, namely thioacetazone **1** and para-aminosalicylic acid, were subsequently introduced into clinical practice (Figure 6).

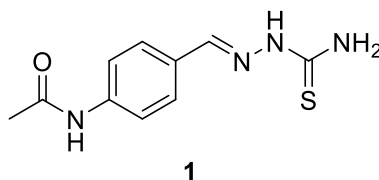


Figure 6: Chemical structure of thioacetazone 1.

The clinical results in streptomycin-resistant cases were enhanced with combination therapy involving either of these medicines in conjunction with streptomycin. Later, the introduction of isoniazid in the 1950s brought about a significant enhancement in the treatment of tuberculosis. Isoniazid rapidly emerged as the preferred pharmaceutical agent. Following the introduction of isoniazid, subsequent medicines were also developed.

Several drugs were introduced during this period, including pyrazinamide in 1952, cycloserine in 1952, ethionamide in 1956 and rifampin. The drugs isoniazid and ethambutol were developed in 1957 and 1962, respectively⁴⁵. The primary

Chapter 1: Introduction

medicines applied in the initial treatment protocols for tuberculosis (TB) consist of isoniazid **2**, rifampicin **3**, pyrazinamide **4**, and ethambutol **5** (Figure 7)⁴⁶.

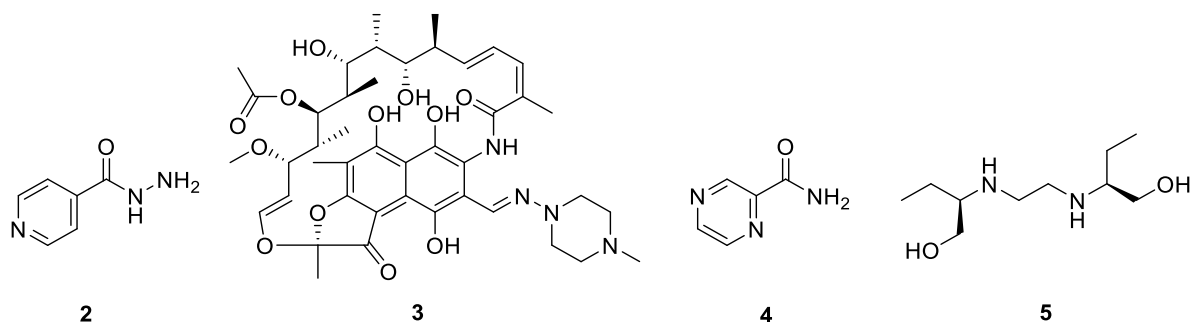


Figure 7: First-line anti TB drugs.

Due to its slow growth rate and high resistance, treatment of TB requires a minimum duration of six months under the Directly Observed Standard Therapy (DOTS) programme. This treatment approach consists of two different stages. The initial phase occupies two months and involves the administration of four first-line drugs, which are isoniazid **2**, rifampicin **3**, pyrazinamide **4**, and ethambutol **5**. Afterwards, the treatment continues for an additional four months with a combination of isoniazid and rifampicin.

1.4.2.1 Isoniazid

Isoniazid **2** is an analogue of the antitubercular drug thioacetazone **1** which was used successfully in TB patients in the 1940s but unfortunately, has toxic side-effects. Therefore, in an effort to modified thioacetazone compound, the phenyl ring was substituted with a pyridine ring due to the fact that nicotinamide hindered the growth of *Mtb*⁴⁷. When treating drug-susceptible TB, isoniazid (INH, commonly referred as isonicotinic acid hydrazide) is typically used. In addition, INH **2** is a prodrug that is transformed to isonicotonic acyl radical **6** by Mycobacterial catalase-peroxidase (KatG), which generates a nicotinoyl-NAD adduct **7**. Consequently, the strong binding of the active metabolite **7** to the enzyme enoyl acyl carrier protein reductase (InhA), a precursor in mycolic acid biosynthesis, impairs fatty acid chain elongation, therefore inhibit *Mtb* cell wall synthesis (Figure 8).

Chapter 1: Introduction

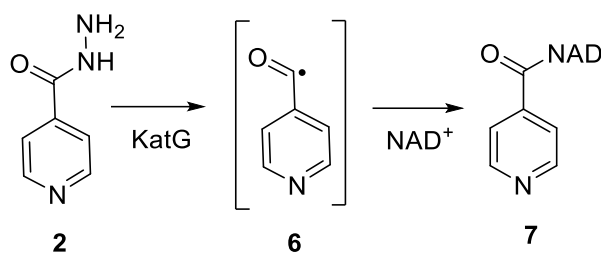


Figure 8: Schematic representation of (INH) **2** activation.

The metabolism of the INH **2** occurs in the liver by acetylation and converted to acetylisoniazide and isonicotinic acid. Nausea, vomiting, and stomach pain are frequently observed as minor adverse effects in association with isoniazid INH administration. However, it is important to note that the significant side effects of INH have the potential to manifest as psychosis, convulsive seizures, mental confusion, and coma. Peripheral neuritis is an additional potential manifestation, although the occurrence of this condition can be readily controlled with the use of pyridoxine⁴⁸.

1.4.2.2 Rifampicin.

Rifampin **3** plays an essential role in the treatment of tuberculosis. This medication has been employed since 1966, with a minimum inhibitory concentration (MIC) ranging from 0.05 to 0.50 μM ⁴⁹. Rifampin **3** is a semi-synthetic antibiotic produced from the Gram-positive bacteria *Amycolatopsis rifamycinica* and has been considered a bactericidal drug that effectively eliminates both active and non-active bacilli. The duration of tuberculosis treatment can be reduced to a period of six months by combining the administration of rifampin **3** with pyrazinamide **4**. The mechanism of action involves the inhibition of DNA-dependent RNA polymerase, hence inhibiting the synthesis of messenger RNA and protein in the bacillus. Consequently, this blockage hinders the gene transcription process in mycobacteria, ultimately leading to cellular death⁵⁰. One frequently encountered minor adverse effect involves the colouring of bodily fluids such as sweat, tears, and urine. Therefore, it is significant to alert patients about the possibility of this side effect. Additionally, it is important to note that exanthema, a serious adverse reaction occurs as a skin rash accompanying a disease, requiring the urgent discontinuation of the medication^{51, 52}.

Chapter 1: Introduction

1.4.2.3 Pyrazinamide.

The discovery of pyrazinamide occurred in 1952 as a bacteriostatic, although it may have bactericidal properties against replication *Mtb*⁴⁹. Pyrazinamide (PZA) exhibits minimum inhibitory concentrations (MIC) ranging from 20 to 100 µg/mL against *Mtb*. While most medicines function by inhibiting protein function when bonded to their targets, recent findings indicate that pyrazinoic acid functions as a mild enzyme inhibitor. Consequently, the traditional tuberculosis medication pyrazinamide demonstrates antibacterial efficacy by acting as a target degrader. This mechanism of action has recently surfaced as an efficacious strategy in pharmacological development across several illness indications⁵³.

Pyrazinamide **4** is a prodrug that undergoes conversion into the active drug pyrazinoic acid by *Mtb* under acidic conditions⁵⁴. PZA undergoes hepatic metabolism mainly via amidase, which transforms PZA into pyrazinoic acid (PA) **8**. PA can undergo further oxidation through the action of xanthine oxidase, resulting in the formation of 5-hydroxy-pyrazinoic acid **10** (5-OH-PA). Alternatively, PZA can undergo oxidation by xanthine oxidase to produce 5-hydroxy-pyrazinamide **9** (5-OH-PZA), which is then hydrolysed by amidase to make 5-hydroxy-pyrazinoic acid (5-OH-PA) that was suggested to be more hepatotoxic than PA (Figure 9)^{55, 56}.

Chapter 1: Introduction

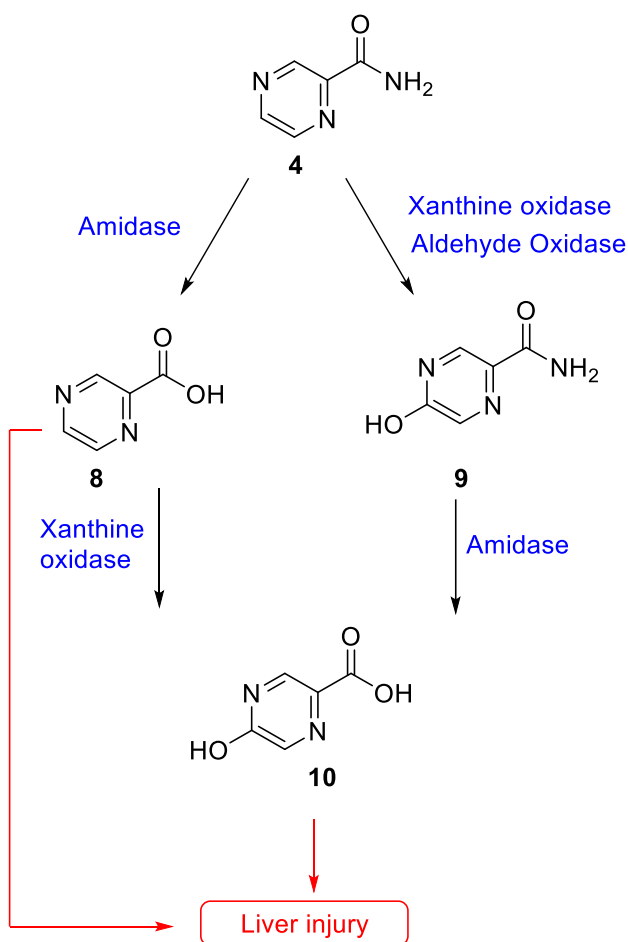


Figure 9: Pyrazinamide **4** and proposed hepatotoxicity produced in the metabolic process. (Adapted from ⁵⁵)

1.4.2.4 Ethambutol.

Since 1961, ethambutol **5** has been used for the treatment of tuberculosis. Ethambutol is a compound derived from *N,N'*-diisopropylethylenediamine **11**, which was initially discovered by random screening⁵⁷. The compound exhibits its effects on both intracellular and extracellular environments, with a primary focus on quickly proliferating bacilli and its minimum inhibitory concentration 1-5 µg / mL. Ethambutol inhibits the formation of the primary polysaccharides on mycobacterial cells. Therefore, the inhibition of the arabinosyltransferase enzyme, which is responsible for the polymerization of arabinose to arabinogalactan, results in the suppression of arabinogalactan synthesis leading to cell death⁵⁴. Through combinatorial synthesis, additional optimisation of ethambutol led to the development of a novel chemical termed SQ-109 **12** which is a highly lipophilic drug that exhibits a distinct mechanism of action compared to ethambutol (Figure 10).

Chapter 1: Introduction

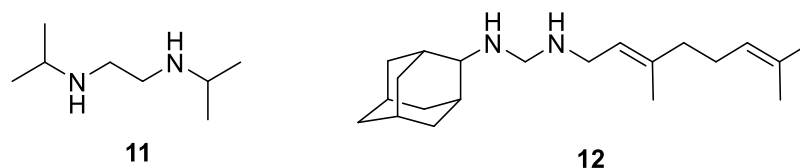


Figure 10: chemical Structures of *N,N*-diisopropylethylenediamine **11** and SQ109 drug **12**.

1.4.3 Second-line anti-tuberculosis drugs.

The second and third-line medications were not originally developed to be antitubercular treatments, however, they have been discovered to be effective in the treatment of tuberculosis due to their ability to target and combat *Mtb* and its drug-resistant forms. In comparison to first-line medications, it is commonly seen that they exhibit reduced activity, increased toxicity, and higher costs. Generally, the scope of their application is restricted to the treatment of instances involving multidrug-resistant (MDR) or extensively drug-resistant (XDR) tuberculosis. More details on drug treatment for resistant TB will be given below.

1.4.3.1 *Para*- Amino Salicylic acid.

In 1946 Lehmann discovered that salicyclates and benzoate increase the respiratory capacity of tuberculosis bacilli and it was therefore proposed that these compounds are important for the normal metabolism of the organism and therefore can be used as anti-tuberculosis targets. One of these compounds that interfere with *Mtb* metabolism is *para*- amino salicylic acid (PAS) **13**. PAS is recognised as a structural analogue of *p*-aminobenzoic acid **14** and hinders the production of folic acid by targeting dihydrofolate reductase and/or iron reduction in *Mtb* (Figure 11).

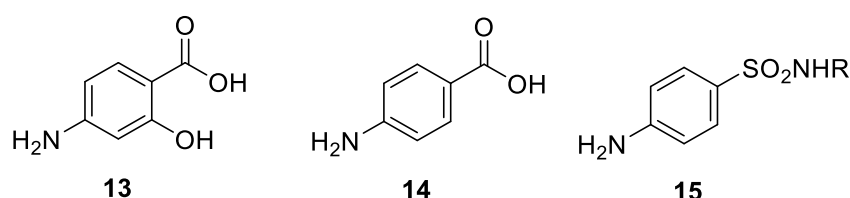


Figure 11: Chemical structure of PAS **13** and its analogues *p*-amino benzoic acid **14** and sulfonamides **15**.

Moreover, PAS exhibits a distinct range of activity compared to sulfonamides **15**, as it is specifically effective against *Mtb*⁵⁷. PAS is specifically targeting tuberculosis, therefore its selectivity may be due to differences in the affinity for

Chapter 1: Introduction

folate synthetase of TB rather than other bacteria^{58, 59}. Although PAS is considered one among the earliest compounds used as an antitubercular drug, its precise mechanism of action remains unclear. Moreover, the use of PAS is restricted only to the management of extensively drug-resistant tuberculosis (XDR-TB) instances due to its severe gastrointestinal toxicity⁶⁰.

1.4.3.2 Aminoglycosides

Kanamycin (KAN) **16**, Amikacin (AMK) **17**, and capreomycin **18** (CAP) are injectable medications utilised in the treatment of multidrug-resistant tuberculosis (MDR-TB) (Figure 12).

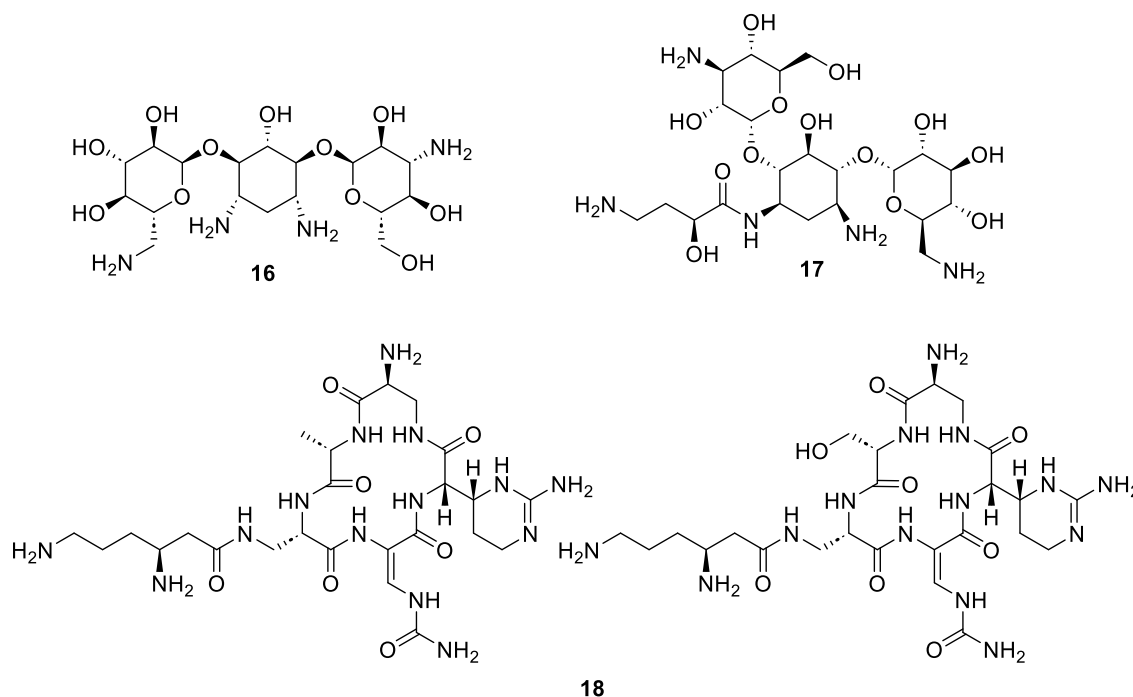


Figure 12: Chemical structures of the injectable aminoglycosides (KAN)**16**, (AMK) **17** and (CAP) **18**.

Each of these substances disrupts the process of protein synthesis by targeting protein translation⁶¹. The use of AMK/KAN and CAP-based therapies are associated with the development of nephrotoxicity, which limits their effectiveness due to the high rate of cross-resistance in *Mtb* strains^{62, 63}. Nevertheless, Kanamycin (KAN) is widely utilised as the primary injectable agent for the treatment of multidrug-resistant tuberculosis (MDR-TB)⁶⁴.

Chapter 1: Introduction

1.4.3.3 Fluoroquinolones.

The Fluoroquinolones (ciprofloxacin **19**, ofloxacin **20**, levofloxacin **21**, gatifloxacin **22** and moxifloxacin **23**) are broad-spectrum antibiotics which are widely used for the treatment of gastrointestinal, respiratory, and urinary tract bacterial infections as well as sexually transmitted diseases (Figure 13)⁶⁵.

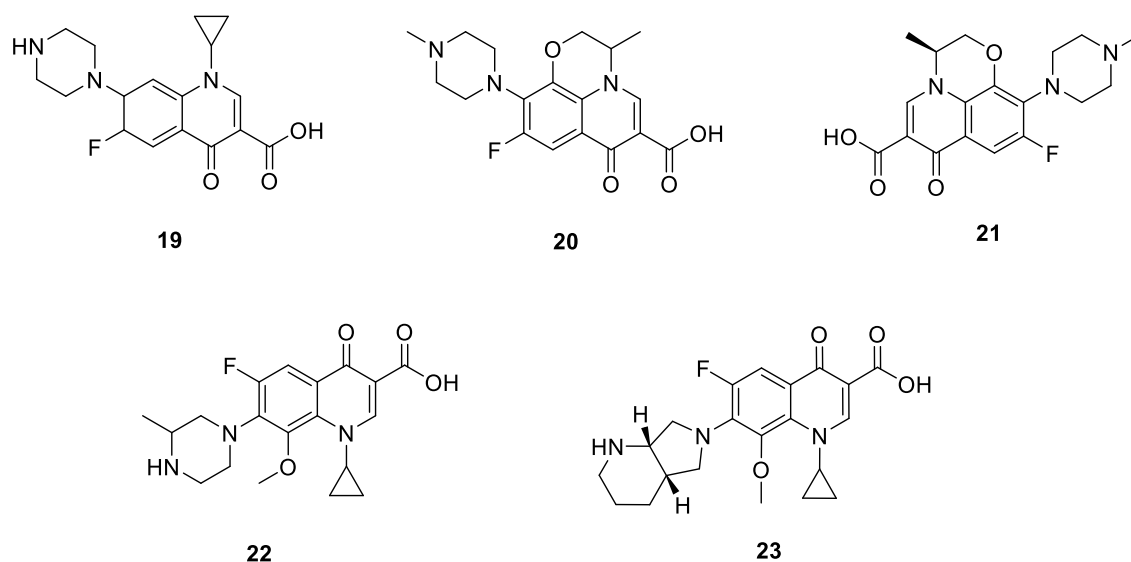


Figure 13: Chemical structures of ciprofloxacin **19**, ofloxacin **20** levofloxacin **21**, gatifloxacin **22** and moxifloxacin **23**.

Fluoroquinolones (FQs) exhibit significant efficacy against *Mtb* with their primary cellular targets being the bacterial DNA gyrase and topoisomerase IV⁶⁶. The above-mentioned treatments are regarded as the most safe and efficient antitubercular medications following INH and RIF, however, with increased exposure to fluoroquinolones and the introduction of newer agents, more significant adverse effects have become evident. In particular, tendon rupture, photosensitivity, and QT prolongation in cardiac signalling are now significant adverse effects that cannot be ignored⁶⁷.

Chapter 1: Introduction

1.4.3.4 Ethionamide and Prothionamide.

Ethionamide (ETH) **24** and prothionamide (PTH) **25** are isonicotinic acid derivatives that have been used as anti-tubercular medicines since 1956 (Figure 14).

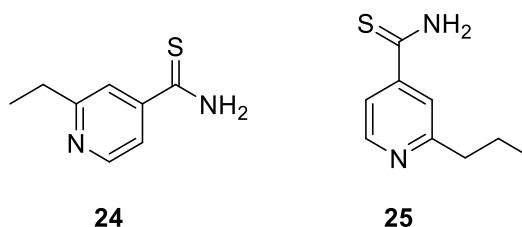


Figure 14: Chemical structures of ethionamide **24** and prothionamide **25**.

Both substances act as prodrugs and have an identical mode of action, wherein isoniazid (INH) interferes with the mycolic acid synthesis⁶⁸. Nevertheless, the identification of active metabolite forms of ETH and PTH have not yet been achieved⁶⁹. Multiple studies have shown evidence that *Mtb* strains that are resistant to ethionamide (ETH) also exhibit cross-resistance to prothionamide (PTH) and isoniazid (INH)⁶⁹. The usage of these drugs is restricted to the treatment of MDR-TB due to their propensity to induce significant gastrointestinal adverse reactions. The co-administration of *p*-amino salicylic acid with these medications is not recommended due to its association with hypothyroidism, which ultimately reduces their therapeutic efficacy as a second-line treatment^{70, 71}.

1.4.3.5 Cycloserine.

D-cycloserine (DCS) **26** is a natural antibiotic produced by *Streptomyces* with excellent bioavailability and a wide range of activity (Figure 15)⁷².

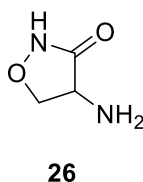


Figure 15: Structure of D-cycloserine **26**.

DCS mode of action involves targeting enzymes which are necessary in the D-alanyl-D-alanine dipeptide unit synthesis, a key feature of the peptidoglycan

Chapter 1: Introduction

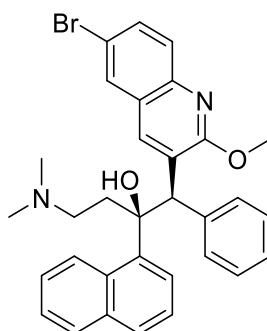
structure. DCS functions as a competitive inhibitor of D-alanyl-D-alanine ligase, which forms the D-alanyl-D-alanine dipeptide from two D-alanine amino acids⁷³. As a result, the integrity of the bacterial cell wall is compromised, and cell death occurs. D-Cycloserine does not exhibit cross-resistance to other compounds. However, it is associated with the occurrence of severe adverse psychological effects. Consequently, DCS is considered a secondary option in drug treatment⁷⁴.

1.4.4 New candidate anti-tuberculosis drugs.

The development of extensively drug-resistant tuberculosis (XDR-TB) has further complicated the management of this disease. XDR-TB is tuberculosis that is caused by mycobacteria that have developed resistance to the primary medications used for treatment, mainly isoniazid and rifampicin alongside resistance to secondary drugs, such as fluoroquinolones and either injectable aminoglycoside⁷⁵. The growth of multidrug-resistant (MDR) and extensively drug-resistant (XDR) tuberculosis underscores the pressing requirement for novel anti-TB medications that can reduce the treatment period while maintaining high effectiveness and safety standards. Medications being developed for the treatment of XDR-TB are described below.

1.4.4.1 Bedaquiline.

Bedaquiline (BDQ) **27** is classified as a diarylquinoline pharmaceutical agent. Bedaquiline possesses a core heterocyclic nucleus that consists of a quinoline ring, alongside an alcohol and amine side chains. These side chains are responsible for the compound's anti-tuberculosis activity (Figure 16)⁷⁶.



27

Figure 16: Chemical structure of bedaquiline **27**.

Chapter 1: Introduction

Investigating the derivatisation of BDQ has shown that the quinoline structure is essential for activity against *Mtb*, with enhanced activity observed through modifications of the amine and alcohol sites (Figure 17)⁷⁷.

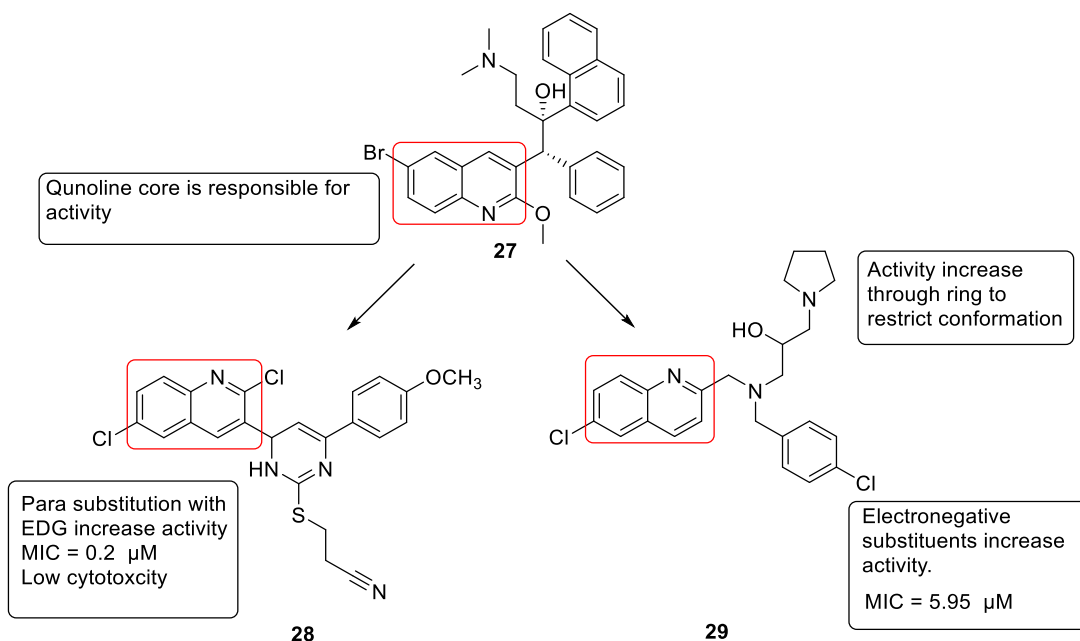


Figure 17: Structure-activity relationship of Bedaquiline derivatives **28** and **29** as antitubercular agents (Adapted from ⁷⁷)

During a high throughput phenotypic screening aimed at identifying compounds with action against saprophytic mycobacteria, specifically *Mycobacteria smegmatis*, a compound was discovered. Additional research found that this drug also exhibited activity against *M. bovis BCG* and *Mtb*. By blocking mycobacterial adenosine triphosphate synthase (ATP), a key membrane-bound enzyme, bedaquiline kills both dormant and actively replicating mycobacteria, interfering with energy production, and altering intracellular metabolism via blocking ATP synthase which is a key enzyme in *Mtb* ATP production. Binding of ATP synthase results in the suppression of ATP synthesis, which results in bacterial death⁷⁸. A phase III clinical trial of BDQ is currently being conducted to confirm its efficacy from earlier phase II clinical trials and to collect further safety data since BDQ has a black box warning for patients and healthcare professionals, as it may prolong the QT interval and cause an irregular cardiac rhythm⁷⁹. Consequently, BDQ is considered part of a combination therapy for individuals with MDR pulmonary TB when other treatment options are unavailable. In consideration of the use of BDQ

Chapter 1: Introduction

in TB treatment, 50 nations reported receiving BDQ for the treatment of over 2,500 patients by the end of 2015. According to WHO reports, as of the end of 2017, 68 countries had introduced or initiated the use of BDQ for the treatment of MDR/XDR TB. Although BDQ is a recommended drug for increasing the efficacy of MDR-TB treatment, improper or insufficient use of BDQ may hasten the emergence of resistant strains⁷⁶. The resistance mechanism suggested results from mutations in the *atpE* gene, which codes for a transmembrane protein of the F1/F0-ATP synthase enzyme⁸⁰.

1.4.4.2 Delamanid and Pretomanid.

Many antibiotics of the nitroimidazole class such as metronidazole, have been developed to treat anaerobic bacterial and protozoan infections, however, they are ineffective against *Mtb*⁸¹. Delamanid (DLM) **30** is a newly developed pharmacological drug that recently obtained approval from both the European Union and Japan for their utilisation in combination with other treatments for the control of multidrug-resistant tuberculosis (MDR-TB). Pretomanid **31**, referred to as PA-824, is classified as a nitroimidazole medication, similar to delamanid **30** (Figure 18).

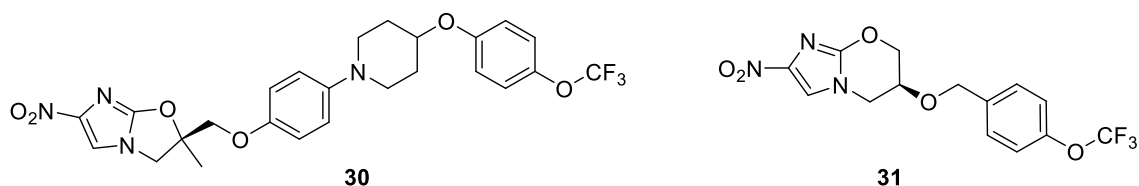


Figure 18: Structure of delamanid **30** and pretomanid **31**.

In addition, pretomanid demonstrates efficacy against both replicating and hypoxic nonreplicating strains of *Mtb*. Delamanid and pretomanid are prodrugs that require activation by the enzymatic action of deazaflavin (F420)-dependent nitroreductase (Ddn). The process of redox cycling involving the deazaflavin cofactor 420, also known as F420, plays a critical role in this process, which is facilitated by glucose-6-phosphate dehydrogenase (Figure 19)

Chapter 1: Introduction

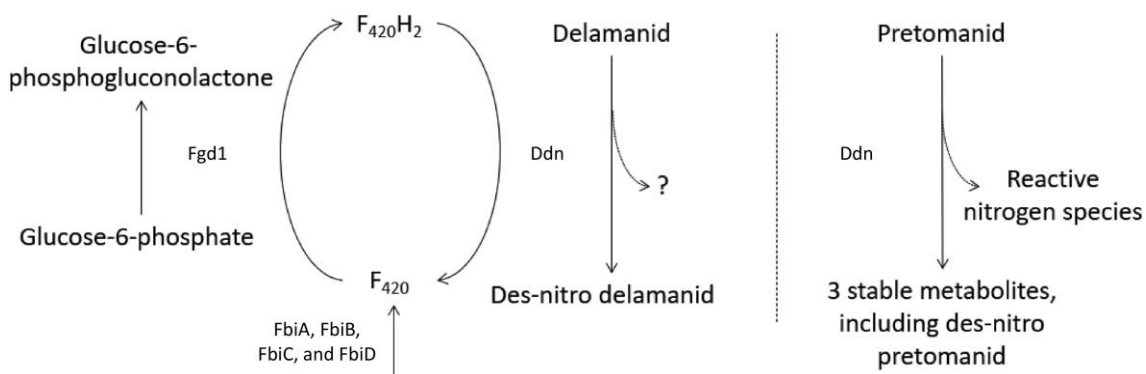


Figure 19: Schematic overview of the metabolic activation of delamanid and pretomanid by mycobacteria, adapted with permission from Liu et al. and Rifat et al. Delamanid and pretomanid are prodrugs that require activation by deazaflavin (F420)-dependent nitroreductase (Ddn). Redox cycling of deazaflavin cofactor 420, or F420, is crucial in this process, which is mediated by glucose-6-phosphate dehydrogenase (Fgd1) and Ddn.10, Synthesis of F420 depends on FbiA, FbiB, FbiC and FbiD. Bio-activation of delamanid by Ddn results in the formation of inactive des-nitro-imidazooxazole. The active intermediate for delamanid has not yet been identified. Activation of pretomanid, on the other hand, generates three stable, inactive metabolites, as well as reactive nitrogen species which are responsible for respiratory poisoning by pretomanid⁸².

The inhibitory mechanism of delamanid involves its release of reactive radicals, such as nitric oxide (NO), which play a vital role in the mammalian defence against mycobacterial infections. In consideration of the SAR studies of the delamanide and pretomanid, it is evident that the stereochemistry and presence of nitro group is essential for the activity (Figure 20)⁸³.

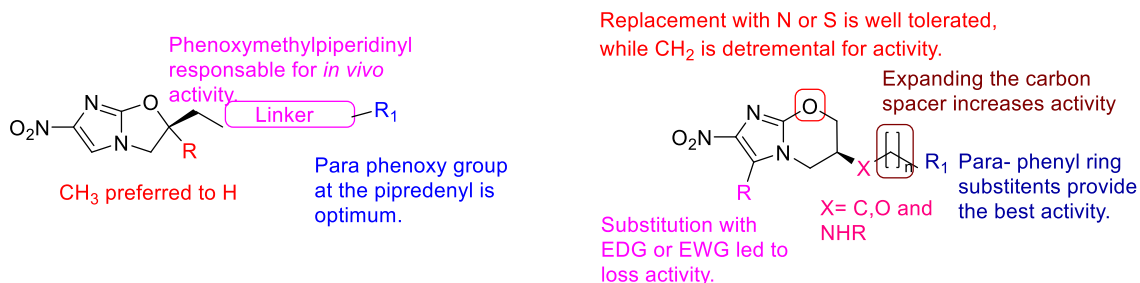


Figure 20: Structural activity relationship of Delamanid **30** and Pretomanid **31** derivatives. (Adapted from⁸³)

The compound TBA-354 exhibits promising characteristics as a new generation nitroimidazole molecule as it has superior efficacy compared to pretomanid.⁸⁴ The structure of this compound closely resembles that of Pretomanid, and it is now undergoing preclinical research (Figure 21)⁸³.

Chapter 1: Introduction

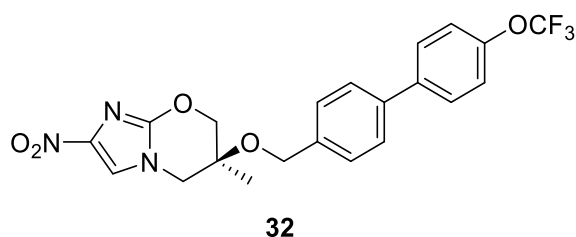
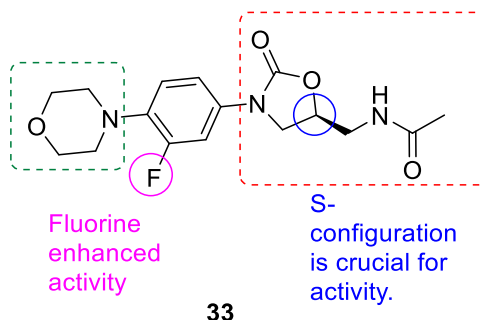


Figure 21: Chemical structure of TBA-354 **32**.

1.4.4.3 Linezolid and Sutizolid.

Oxazolidinones have exhibited favourable efficacies against *Mtb* both *in vitro* and *in vivo*. The unique mode of action exhibited by these compounds involves binding to the 23S ribosome, hence inhibiting microbial protein synthesis. Oxazolidinones have been suggested as a potential therapeutic option for addressing the challenge of multiple drug resistance tuberculosis (MDR-TB). The US Food and Drug Administration (FDA) granted approval to linezolid (LZD) **33** in 2000 for the purpose of treating infections caused by drug resistant Gram-positive bacteria (Figure 22)⁸⁵.

Morpholine group improve pharmacokinetic properties, replaced with thiomorpholine led to improved safety profile.



33

Figure 22: Structure activity relationship of linezolid **33**⁵.

It demonstrated remarkable efficacy in combating drug-resistant tuberculosis and non-tuberculous mycobacterial infections. However, the extended use of LZD can result in severe hematologic and neurologic adverse effects. As a result, dose reduction or withdrawal of LZD is typically necessary to mitigate these adverse effects⁸⁶. Sutezolid (SZD) **34** is a thiomorpholinyl analogue of linezolid (LZD) that has shown preliminary evidence of having greater efficacy against *Mtb* (Figure 23)⁸⁷.

Chapter 1: Introduction

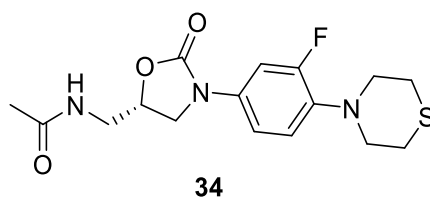


Figure 23: Chemical structure of sutezolid **34**.

The safety profile of SZD was determined to be generally advantageous, since it was well tolerated by individuals with tuberculosis. Additionally, SZD exhibited significant bactericidal action in both sputum and blood samples. In contrast, SZD exhibits a superior safety profile and demonstrates antimycobacterial activity greater than that of linezolid⁵. SDZ exhibits synergistic effects when used with SQ109 and has demonstrated efficacy when used in conjunction with other novel tuberculosis medications⁸⁸.

1.4.4.4 Q203.

The latent form of *Mtb* exhibits reduced energy consumption for its survival by suppressing several biosynthetic processes. Consequently, medications that specifically target these biochemical pathways demonstrate diminished efficacy. As a result, there is a growing interest in investigating the energy metabolism of *Mtb* as a potential target for therapeutic interventions. One of those compounds that exert their action through targeting the energy metabolism pathway is Q203 **35** (Figure 24)⁸⁹.

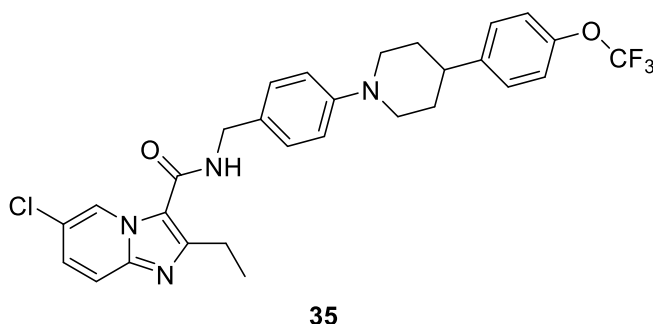


Figure 24: Chemical structure of the Q203 **35** compound.

It is an imidazopyridine amide compound that was discovered via phenotypic high-throughput screening and is now undergoing phase II clinical trials. The compound exhibits activity against (MDR) and (XDR) strains of *Mtb*. It interrupts

Chapter 1: Introduction

the energy metabolism of *Mtb* by specifically binding to the b subunit of the respiratory cytochrome bcc complex, commonly known as QcrB, which is encoded by the qcrB gene⁹⁰. The results of structure-activity relationship investigations indicate that the presence of a carboxamide linker with N-benzyl functionality is essential for antimycobacterial activity (Figure 25).

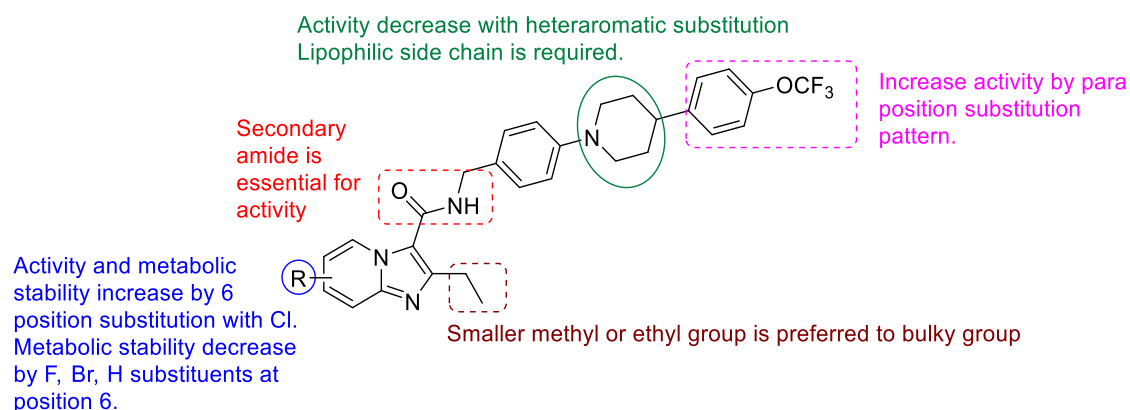


Figure 25: Structure activity relationship of Q203 35 (adapted from ⁵ and ⁸⁹)

The lipophilicity of the linker that connects the benzyl group and the para-substituted phenyl group exhibits a beneficial influence on the antimycobacterial activity.

New classes of antibiotics with different biological targets are needed to provide a broader spectrum of antimicrobial action as drug-resistant infections are becoming increasingly prevalent and can make existing antibiotic treatments ineffective. In this context, the following subsections cover some new antimicrobial drugs and their mechanisms of action.

1.4.4.5 Antimycobacterial activity of peptides.

Naturally occurring peptides and their derivatives such as antimicrobial peptides (AMPs) are currently undergoing clinical trials for the treatment of various diseases, including cancer, inflammation, and bacterial and viral infections. For example, the synthetic membrane-lytic peptide LTX-109 is currently undergoing phase II clinical trials for the treatment of Methicillin-resistant *Staphylococcus aureus* (MRSA) nasal infections, while NZ2114, a plectasin derivative, is in preclinical development targeting systemic drug-resistant infections, including MRSA⁹¹. The advantages of peptides can be related to enhanced target affinity,

Chapter 1: Introduction

fewer off-target side reactions, and consequently, a lower incidence of side effects⁹². Research on the antimicrobial properties of these peptides present in human and rabbit neutrophils has demonstrated their effectiveness against *Mycobacterium* species, with (MIC) values ranging from 2.5 to 50 µg/mL⁹¹. Human neutrophil tetradecapeptide (HNP-1) is one of six human α-defensins that are part of the innate immunity arsenal to combat infectious microorganisms (Figure 26).

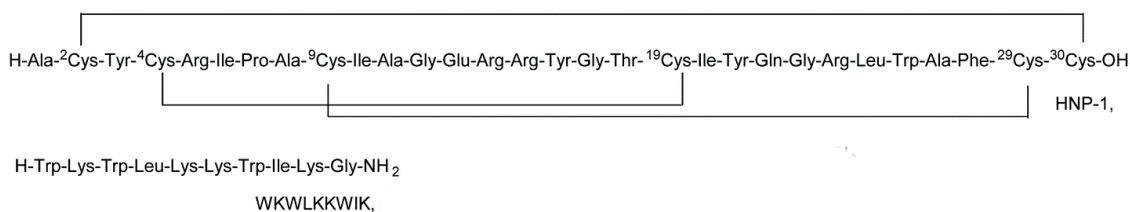


Figure 26 : Peptide sequence of HNP-1 and its analogue⁹³.

A three-stranded β-sheet core stabilized by three intramolecular disulfides is the main structural feature of α-defensins. It has been thought that the bactericidal activity involves microbial membrane disruption. According to one study, HNP-1 exhibits potent bactericidal activity against *Mtb* via increasing the permeability of the mycobacterial cell envelope. Therefore, HNP-1 is considered to be a potential solution to the increasing issue of antibiotic resistance in mycobacteria, mainly by facilitating the penetration of medications into the mycobacterial cell⁹⁴. The synthesis of HNP-1 and analogues can be achieved using conventional solid phase peptide synthesis protocols, however there are some limitations associated with HNP-1 as it has limited stability in plasma and is expensive to produce. In contrast to HNP-1, a short synthetic nonapeptide, H-WKWLKKWIK-NH₂ (Figure 26) has recently been discovered to display antibacterial activity as well as enhanced anti-TB activity. Additionally, nonapeptide synthesis was carried out utilising standard Fmoc-SPPS, and because of its short peptide sequence, nonapeptide processing on a large scale is thought to be viable and achievable in a cost-effective manner⁹³.

BB-3497 **36** is a peptidomimetic that inhibits the basic bacterial metalloenzyme *N*-formylmethionine deformylase (PDF) which is essential enzyme for bacterial

Chapter 1: Introduction

of these hydrazides and their derivatives as synthons for various heterocyclic compounds, which incorporate one or more heteroatoms, has been demonstrated. These compounds have demonstrated significant pharmacological and biological applications. The heating of appropriate hydrazides of carboxylic or heterocarboxylic acids with different aldehydes or ketones in various organic solvents like ethanol, methanol or butanol is the main synthesis route of hydrazide, hydrazones compounds. The anti-TB activity of the 2-hydroxy-1-naphthaldehyde isonicotinoyl hydrazone **38** can serve as a novel inhibitor of *Mtb* methionine aminopeptidases (Figure 29).

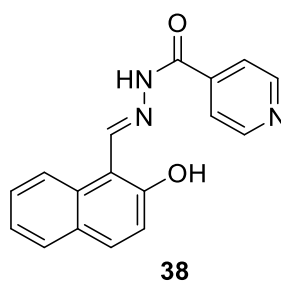


Figure 29: Chemical structure of 2-hydroxy-1-naphthaldehyde isonicotinoyl hydrazone **38**.

A series of hydrazide-hydrazones produced from indole-pyridine has been synthesised and compounds evaluated against susceptible strains of *Mtb*. Based on the information gathered, it was observed that the hydrazide-hydrazone derivative exhibited the highest potency among the investigated compound **39** against the H37Rv strain of *Mtb* with (MIC) of 0.05 µg/mL (Figure 30).

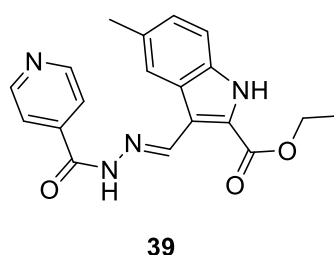


Figure 30: The indole pyridine hydrazide compound **39** with MIC=1.43 µM

A recent investigation has shown a novel examination of the synthesis of 2H-chromene or coumarin compounds, whereby several substituted hydrazide-hydrazone pharmacophores are linked to the chromene ring at the 3-position. The synthesised compounds were assessed for their antimycobacterial activity

Chapter 1: Introduction

against the *Mtb* H37Rv strain. The findings from the SAR analysis indicate that the antimycobacterial action of the synthesised compounds cannot be solely attributed to their lipophilic characteristics. These derivatives exhibiting strong charge donation (electron-donating groups) and delocalisation within the hydrazone moiety exhibited highest antimycobacterial activity. For example, 4-methoxyphenyl chromene hydrazone containing compound **40** showed the highest antimycobacterial effect and exhibited low cytotoxicity (Figure 31)⁹⁷.

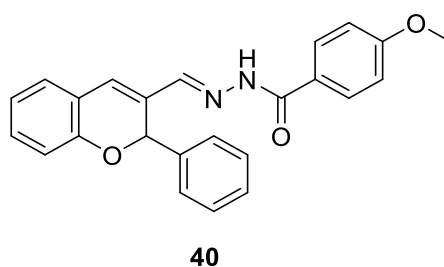


Figure 31: The most effective compound of chromene substituted hydrazone series with MIC 0.13 μ M.

Whereas isoniazid **2**, the common anti-TB hydrazone, has a significant antimycobacterial action, the development of resistance to isoniazid **2** can be considered as a hallmark of MDR-TB. Given the significant personal and societal implications of the epidemic of tuberculosis, particularly the drug-resistant TB in both forms (MDR-TB and XDR-TB), it is crucial to comprehend their mechanisms to be able to establish effective preventive therapies against TB infection⁹⁸.

1.5 Drug Resistant Tuberculosis.

1.5.1 Overview of drug-resistant tuberculosis

The control strategies for TB involve two key elements: prompt identification of new cases and immediate implementation of treatment protocols to enable efficient cessation of transmission. The disruption of these factors can lead to the emergence of drug resistance in TB, resulting in the rapid development of multidrug-resistant (MDR-TB), extensive drug-resistant (XDR-TB) and in the worst-case scenario total drug-resistant strains (TDR-TB). Multidrug-resistant tuberculosis (MDR-TB) is characterised by the resistance of tuberculosis strains to a minimum of two medications, mainly isoniazid and rifampin. The diminished effectiveness of first-line medications requires the substitution of second-line drugs to tackle the issues caused by (MDR TB). The second-line drugs are

Chapter 1: Introduction

typically more costly and associated with a higher incidence of adverse effects⁹⁹. The incidence of drug-resistant tuberculosis has increased because of insufficient care, predominantly attributed to improper therapeutic approaches. There are additional factors that have been associated with the development of drug-resistant tuberculosis, particularly misuse and inadequate quality of second-line drugs. Furthermore, the implementation of insufficient supervision strategies, such as a patient management system, promotes patient adherence to the prescribed treatment regimen. In addition, there is a shortage of private-sector healthcare facilities to address tuberculosis cases in both developed and low-resource nations. Furthermore, the poor quality of TB services in the private sector includes the healthcare professionals responsible for TB care. For example, if they are aware of the potential of drug resistance, they should have access to laboratories that can provide early and accurate diagnostic testing, so that appropriate care can be given as quickly as possible¹⁰⁰. Another significant issue related to resistant strain tuberculosis is XDR-TB which is characterised by the patient's resistance to both rifampicin and isoniazid as well as resistance to fluoroquinolones and at least one of the three injectable second-line drugs, namely kanamycin, amikacin, and/or capreomycin¹⁰¹. The incidence of XDR-TB creates serious challenges for healthcare practitioners and HIV researchers¹⁰². For instance, the prevalence of tuberculosis in South Africa is increasing, particularly due to the co-occurrence of HIV infection because people with HIV are at high risk of acquiring active tuberculosis in comparison to individuals without HIV. HIV weakens the immune system, hindering the body's ability to combat illnesses such as tuberculosis¹⁰³. Accordingly, the rapid transmission of infection among individuals with impaired immune systems accelerates the development of tuberculosis medication resistance, hence, monitoring drug-resistant tuberculosis globally poses significant challenges, demanding substantial time and resources as it is complex, very expensive and requires experienced clinics, in addition to high levels of resources and good quality second-line drugs¹⁰⁴. Moreover, the molecular approaches provide more accurate and rapid results in comparison to susceptible test methods to detect

Chapter 1: Introduction

resistance, particularly in the context of identifying resistance by DNA sequencing^{105, 106}.

1.5.2 Resistance mechanism to anti-tuberculosis drugs.

1.5.2.1 Resistance to the first line anti-tuberculosis

The first resistance that was identified was for isoniazid **2**. As stated before, INH **2** is a prodrug that is activated by an enzyme called catalase-peroxidase KatG. This produces an active species that reacted with NAD to form an INH-NAD adduct, that ultimately inhibits enoyl CAP reductase InhA, then suppresses mycolic acid biosynthesis leading to cell death. The major resistance mechanism of INH is a mutation in the KatG, therefore changing the activator of the INH (Figure 32).

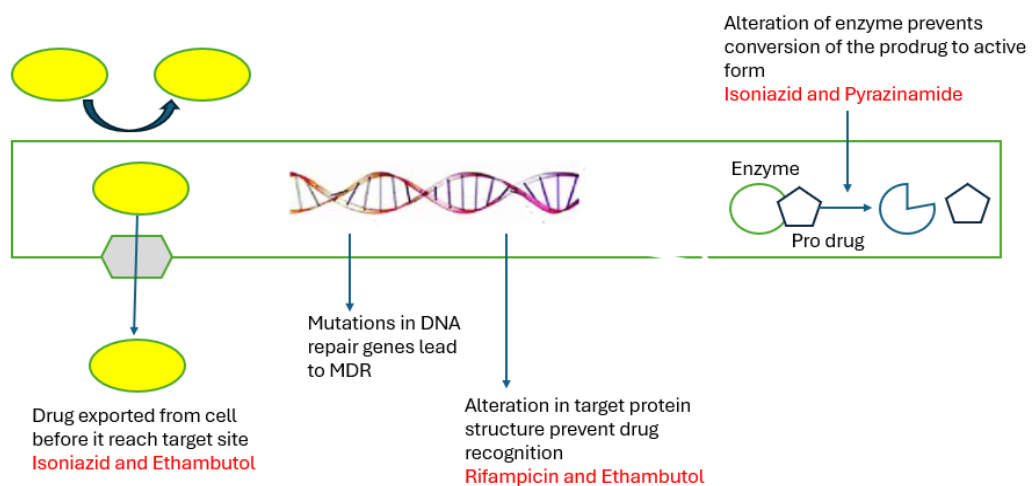


Figure 32: Resistance mechanism of the first line anti TB drugs¹⁰⁷, mutation of the target protein leads to resistance such as in rifampicin and ethambutol, also mutation in the enzyme responsible to activate the drugs such as isoniazid and pyrazinamide lead to resistance.

Furthermore, it has been found in 94% of the resistant clinical isolates that the specific variant in KatG is S315T. In addition, the proposed second resistant mechanism is a mutation at InhA (C-15t) which is a promoter region that results in overexpression and leads to decreased drug concentration. Also, the defect in the NADH dehydrogenase (Ndh), results in lowering the rate of NADH/NAD ratio.

Chapter 1: Introduction

When the amount of NADH increases, the formation of the isonicotinic acyl NADH or may be displacement of the isonicotinic acyl NADH from InhA.

With regards rifampicin **3** resistance, it has been proposed that one-step mutation in the bacterial DNA dependant polymerase (RNAP) results in a high level of resistance. This can be defect in the *rop* β gene that encodes the B subunit of RNAP leads to a change in the polymerase properties such as transcription process¹⁰⁸. Also, the single mutation, Ser531Leu in B subunit protein has been found as predominant in different studies. Another resistance mechanism was found that the multiple amino acids change in 516, 526 and 531 residues¹⁰⁸.

Like INH **2**, pyrazinamide **3** is a prodrug that needs activation to the active form pyrazinoic acid (POA) by the enzyme pyrazinamidase (PZase) encoded by *pncA* gene. Alterations in this gene significantly influence the development of resistance to pyrazinamide (PZA) in *Mtb*. The presence of these mutations significantly reduces the enzymatic activity of pyrazinamidase, which is crucial for the transformation of PZA into its active form, pyrazinoic acid. Mutations often occur in particular areas of the *pncA* gene, encompassing the 561bp (base pairs) and 82bp regions, the open reading frame (ORF), and flanking regions. These modifications impair the enzyme's normal action, resulting in resistance. Another way for PZA **3** resistance is the mutation in the ribosomal protein S1(RpsA), which is the protein essential in protein synthesis, transcription, and ribosomal-sparing process. As mentioned, S1 inhibits the trans-translation activity required for protein synthesis efficiently, therefore, the mutation in *rpsA* (RV 1630,1446 nucleotides) that encodes the S1 protein leads to alteration in binding of the POZ, thus could be mediated for PZA **3** resistance in *Mtb* strain. Furthermore, mutation of the gene called PanD which encodes aspartate alpha decarboxylase enzyme which is involved in the β -alanine synthesis that is a precursor of the coenzyme A and pantothenate biosynthesis which analysis was revealed via whole genome sequencing (Figure 33)^{109, 110}.

Chapter 1: Introduction

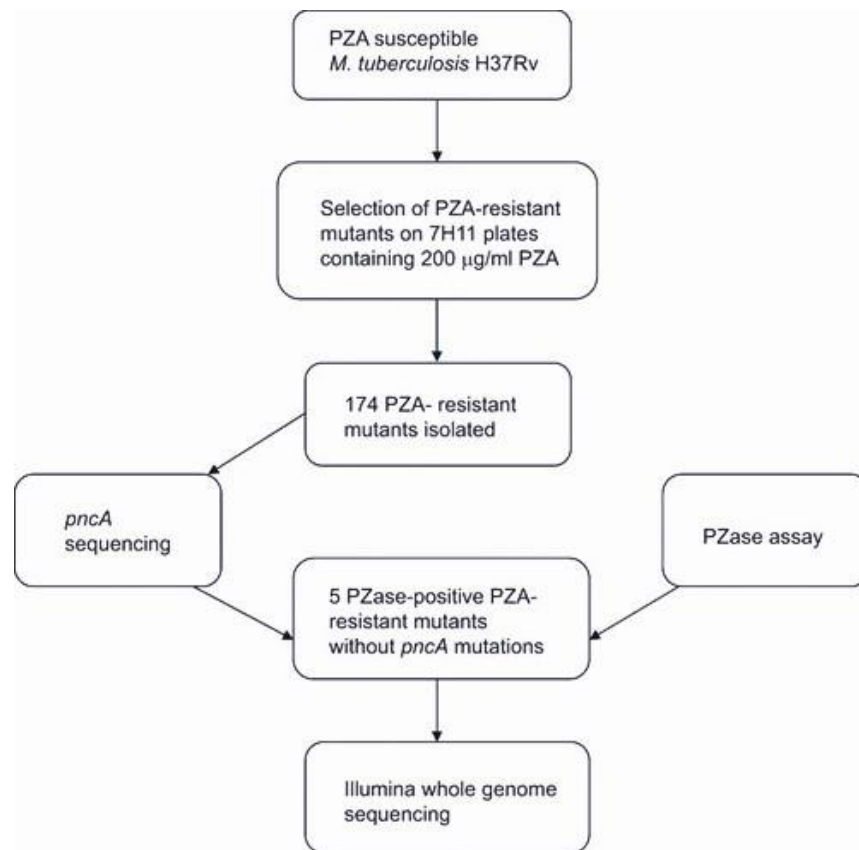


Figure 33: The figure illustrates a flowchart describing the isolation and characterisation of in vitro mutants exhibiting resistance to PZA. The wild type *Mtb* strain H37Rv showed susceptibility to 100 µg/mL PZA. Early stationary phase cultures were inoculated onto 7H11 agar plates, producing 300 mutants. Following thorough testing, 174 samples exhibited persistent resistance to PZA¹¹⁰.

Turning now to ethambutol **4** which inhibits the arabinosyl transferases enzyme, encoded by the *embCAB* operon gene that cause inhibition of the cell wall biosynthesis via arabinogalactan and lipoarabinomannan. At the bacterial genetics, the mutation of *embB*, particularly the mutations of the *embB306* are believed to be a major cause of EMB resistance in *Mtb* though some studies have shown that both EMB-resistant and EMB-susceptible mycobacteria mutations have been reported regarding tuberculosis strain¹¹¹.

1.5.2.2 Resistant of the second line drugs anti-tuberculosis.

The fluoroquinolone cellular target in *Mtb* is DNA gyrase, a type II topoisomerase enzyme consisting of two subunits A and B encoded by the genes *gyrA* and *gyrB* respectively (Figure 34).

Chapter 1: Introduction

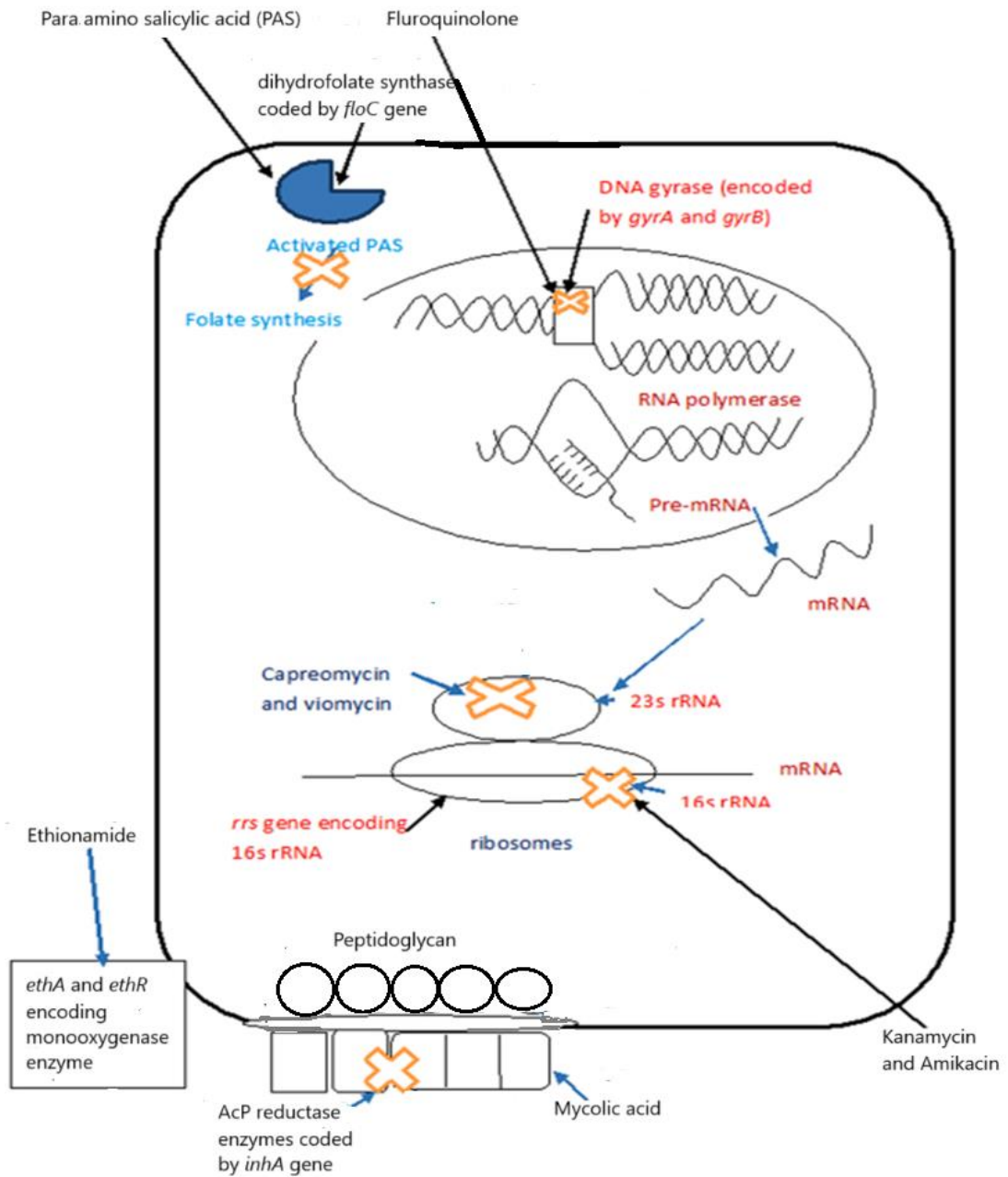


Figure 34: Resistant mechanism for the second line drugs. Mutation in each of the enzymes causes resistance to each of the drugs¹¹². For example, mutation in monooxygenase enzyme responsible for oxidation of ethionamide leads to resistance. Moreover, mutation in the DHFS enzyme is the main mechanism for para-aminosalicylic acid resistant. For the fluoroquinolone drugs, mutation in DNA gyrase enzyme is responsible for resistance. Aminoglycoside drugs (Kanamycin, Amikacin) developed resistant by mutation in RNA.

The principal mechanism of fluoroquinolone (FQ) resistance in *Mycobacterium tuberculosis* (Mtb) is mutations in the quinolone resistance-determining region (QRDR) of the *gyrA* gene. These mutations are predominantly located in codons 90, 91, and 94, with the Asp94 mutation being particularly prevalent¹¹³. The Ser95Thr codon 95 mutation is a naturally occurring polymorphism that is

Chapter 1: Introduction

unrelated to fluoroquinolone resistance. This mutation can be found in both fluoroquinolone-resistant and fluoroquinolone-sensitive strains. However, Codon 88 is a less common involvement. The clinical isolates typically have a significantly lower frequency of *GyrB* mutations. To achieve higher resistance levels, it is necessary to have two mutations in the *gyrA* gene or mutations in both the *gyrA* and *gyrB* genes simultaneously¹¹⁴.

Regarding aminoglycosides such as AMK, KAN, and CAP, they primarily affect protein synthesis in *Mtb*, consequently alterations in 16S rRNA are linked to tuberculosis and treatment resistance. This mutation in 16S rRNA gene results in a significant increase in resistance to AMK and KAN, while simultaneously decreasing resistance to CAP. The C1402T mutation is linked to resistance against CAP and low-level KAN, but the G1484T mutation is related with significant resistance to AMK, KAN, and CAP. Furthermore, the occurrence of low-level resistance to KAN can be linked to mutations in the promoter region of the gene that encodes the acetyltransferase aminoglycoside, a protein known as enhanced intracellular survival protein in *Mtb* (Eis)¹¹⁴. Additionally, the *tlyA* gene encodes a putative 2'-O-methyltransferase responsible for methylating nucleotide C1402 in helix 44 of 16S rRNA and nucleotide C2158 in helix 69 of 23S rRNA. These alterations are essential for the effective binding of CAP to the ribosome, and mutations in *tlyA* may hinder this process, causing resistance.

Capreomycin binds to the ribosome of 70S and prevents translocation of mRNA-tRNA. Furthermore, *tlyA* methylation is assumed to improve capreomycin's antimicrobial activity, therefore disruption of *tlyA* contributes to capreomycin resistance because the nonmethylated ribosome is insensitive to the drugs.

With regards to ethionamide resistance, the *InhA* (NADH-dependent enoyl-ACP reductase) of the mycolic acid synthesis pathway is activated by *EthA* (NADPH-specific flavin adenine dinucleotide-containing monooxygenase). Then, ETH, in its active form, undergoes a reaction with NAD⁺ to produce an ETH-NAD adduct. This adduct works as an inhibitor of *InhA*, resulting in the suppression of mycolic acid production. ETH undergoes activation via two oxidative steps until delivered into the bacterial cell (Figure 35)¹¹⁵.

Chapter 1: Introduction

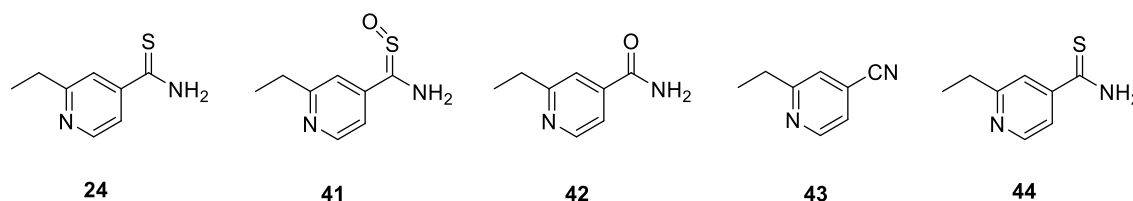


Figure 35: Structures of ETH **24** and its reported oxidation metabolites: active ETH-SO **41** and inactive metabolites **42–44**¹¹⁵.

The initial oxidation produces the ethionamide S-oxide derivative (ETH-SO) **41**. Subsequent oxidation of ETH-SO **41**, by means of an undiscovered process, leads to the formation of stable and non-reactive final products. The compounds referred to as 2-ethylpyridine-4-carboxamide **42** and 2-ethylpyridine-4-carbonitrile **43**, lastly, the intracellular metabolite 2-ethylpyridine-4-carboxylic acid **44**¹¹⁵. Ethionamide resistant resistance can be achieved through two mechanisms, either inhibiting the activation of ETH by modifying its activators, such as ethA, or the suppression of InhA by the ETH-NAD adduct that can be blocked by alterations in inhA or its promoter region¹¹⁶.

As mentioned before (*cf* section 1.4.3.1), one of the first antibiotics which demonstrated anti-TB activity, p-amino salicylic acid (PAS) **13** was used in combination with isoniazid **2** and streptomycin¹¹⁷. PAS incorporated into the folate structure through the actions of dihydropteroate synthase (DHPS) and dihydrofolate synthase (DHFS). This integration results in the production of a hydroxyl dihydrofolate antimetabolite, which subsequently hinders the enzymatic activity of dihydrofolate reductase (DHFR) within *Mtb*. Therefore, the PAS resistance involves blocking of DHPS or mutation in DHFS, which hinders the synthesis of the antimetabolite¹¹⁸.

Following the discussion on tuberculosis (TB) control and treatment, in addition to the aspects of drug resistance TB and the need to tackle TB resistance issue, the subsequent section will describe our group's prior efforts in synthesising novel anti-TB agents featuring benzoxa-[2,1,3]-diazole-substituted amino acid hydrazides, which demonstrate potential as antitubercular drugs.

Chapter 1: Introduction

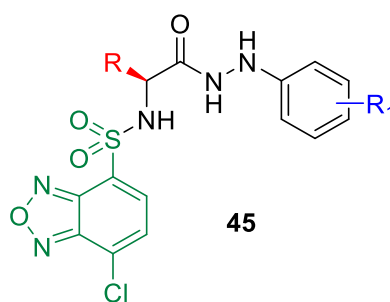
1.6. Previous work with in the group.

In earlier work within the group, led to the development of a small library (≈ 100 molecules) of various bioactive compounds. These compounds include, benzo-[2,1,3]-diazoles flavones, indolin-2-ones, purine, quinolines, thiocumarine. In previous studies by the group, resazurin microtiter assays (REMA) were performed at a constant concentration (128 $\mu\text{g/mL}$) to evaluate the efficacy of putative antibacterial agents against a broad spectrum of drug-sensitive bacteria, including Gram-positive, Gram-negative, and mycotic bacteria. Some classes were effective in inhibiting bacterial growth, while others were not effective even at these extremely high concentrations¹¹⁹. However, the significance of the amino acid and hydrazide moieties in benzoxa-[2,1,3]- diazole-substituted amino acid hydrazides for specific therapeutic efficacy against Mt has been demonstrated previously.

Subsequently, experiments were undertaken to synthesise a range of benzo-[2,1,3]-diazoles to investigate their efficacy against *Mtb*. This investigation was conducted to acquire more understanding of the potential of this molecular architecture in terms of anti-tuberculosis activity. A subsequent SAR study of the library was conducted, resulting in the identification of a category of compounds that demonstrate efficacy against mycolata bacteria.

To establish the MIC of these compounds, REMA experiments were performed on a specific group of compounds containing a benzo-[2,1,3]-diazole scaffold substituted amino acid hydrazides moiety. This allowed both simple and branched amino acids, coupled with different phenyl hydrazine substitution patterns, to be investigated. Results demonstrated specificity and efficacy against *Mtb* bacteria above that of broad-spectrum Gram-positive and Gram-negative bacteria (Table1).

Chapter 1: Introduction



MIC (μM)

R	R ₁	Compound No	<i>M. tuberculosis mc 27000</i> (MIC)	Mammalian Cell Toxicity	<i>S. aureus (MRSA)</i>	<i>M. luteus</i>	<i>B. subtilis</i>	<i>B. cereus</i>	<i>E. faecal</i>	<i>E. faecium</i>	<i>S. agalactiae</i>	<i>S. pyogenes</i>	<i>Y. enterocolitica</i>	<i>S. marcescens</i>	<i>E. coli</i>	<i>M. smegmati</i>
Gly	4-CF ₃	45a	31.1	>90%	-	-	-	-	-	-	-	-	-	-	-	-
Gly	H	45b	36.7	0 %	-	-	-	-	-	-	-	-	-	-	-	-
Gly	4-F	45c	20	60 %	-	-	-	-	-	-	-	-	-	-	-	-
Gly	4-Cl	45d	19.2	80 %	-	-	-	-	-	-	-	-	-	-	-	-
Gly	3-Cl	45e	19.2	45 %	-	-	-	-	-	-	-	-	-	-	-	-
Gly	2-Cl	45f	19.2	70 %	-	-	-	-	-	-	-	-	-	-	-	-
Phg	4-CF ₃	45g	60.7	>90 %	-	-	-	-	-	-	-	-	-	-	-	-
Pro	4-CF ₃	45h	16.3	>90 %	-	-	-	-	-	-	-	-	-	-	-	-
Phe	4-CF ₃	45i	59.3	>90 %	-	-	-	-	-	-	-	-	-	-	-	-
Ala	4-CF ₃	45m	17.3	>90%	-	-	-	-	-	-	-	-	-	-	-	-

Table 1: Antibacterial activity against Gram-positive, -negative and mycolata bacteria. Mammalian cell toxicity assay of benzoxa-[2,1,3]-diazole substituted amino acid hydrazides (cells used Macrophages), percentage of toxicity, (-) = No activity from the REMA assay at the maximum assay concentration 128 $\mu\text{g/ml}$ ¹¹⁹.

Chapter 1: Introduction

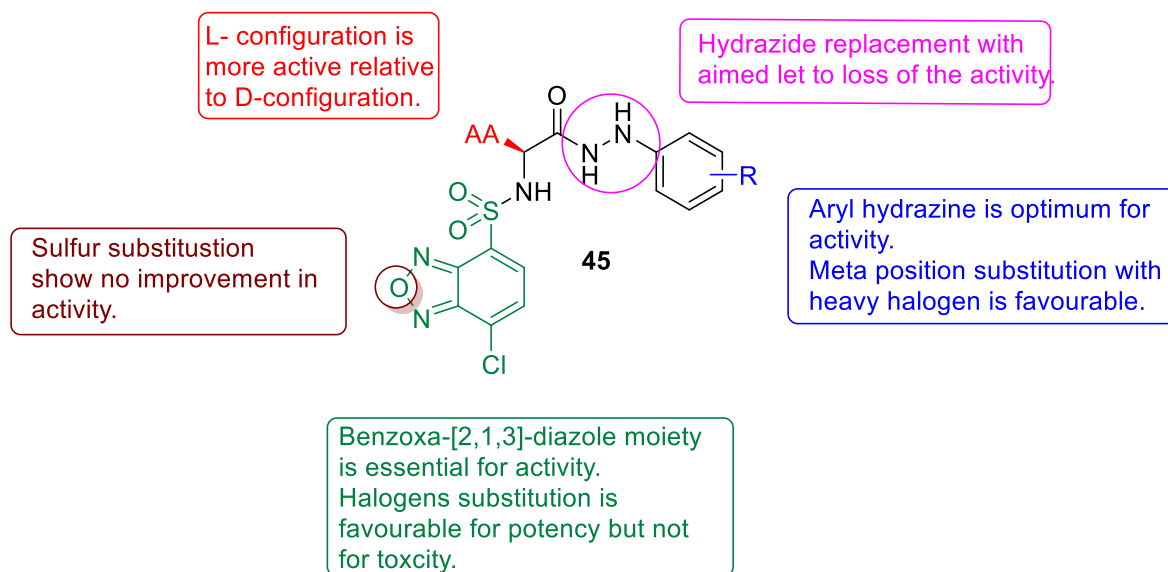


Figure 36: SAR studies of the prior amino acid hydrazide benzoxa-[2,1,3]-diazole architecture investigated within the group.

Following the discussion of previous group work in the synthesis of amino acid hydrazide benzoxa-[2,1,3]-diazole compounds as prospective anti-tuberculosis agents, it is essential to ensure that chirality is preserved throughout the entire process, considering these compounds are chiral molecules.

1.6.1 Enantiomeric purity determination.

The biological effects of chiral compounds are significantly impacted by their stereochemical configurations. Chirality is significant because different enantiomers of pharmacological compounds can show substantial variations in pharmacodynamics and pharmacokinetics¹²⁰. For example, anti-TB drug bedaquiline **27** shows anti-TB activity with (1*R*,2*S*) stereoisomer while reduced activity toward the bacteria observed with (1*R*,2*R*) stereoisomer (Figure 37)¹²¹.

Chapter 1: Introduction

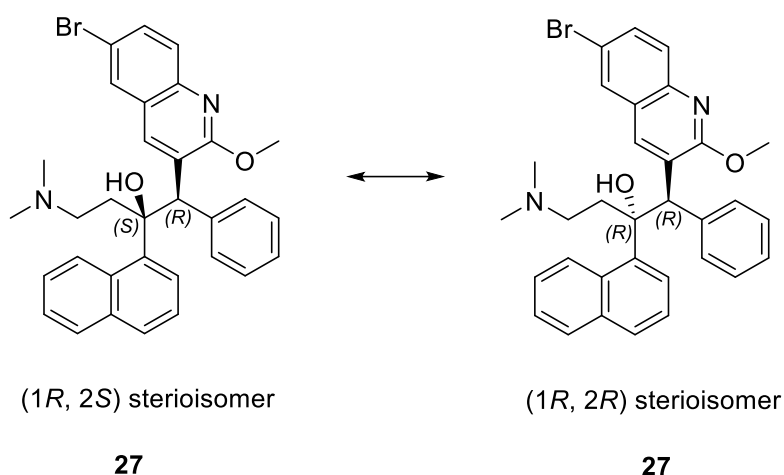


Figure 37: Activity against *Mtb* observed with (1R, 2S) stereoisomer, while reduced activity showed with (1R, 2R) stereoisomer¹²¹.

Enantiomers of chiral substances share identical chemical structures but display distinct optical activity. One enantiomer rotates plane-polarized light anticlockwise and is laevorotatory, denoted by a minus (-) sign. The other enantiomer rotates light clockwise and is dextrorotatory, indicated by a plus (+) sign¹²². Therefore, due to the possibility of anticipated racemization of the chiral carbon in amino acid during the initial synthesis phase while activating the carboxylic acid with HBTU, it was crucial to examine the chiroptical characteristics of the resulting hydrazides.

Therefore, determination was done using polarimeter to define the optical activity for L and D amino acid hydrazide. A polarimeter was utilised to determine the specific optical rotation ($[\alpha]_D$) of hydrazides with the S enantiomer of alanine and with the R enantiomer of alanine¹²². The results consistent with the prediction of a single enantiomer, as the S enantiomer of the amino acid was used in the synthetic process. In addition, HPLC was used to confirm the chiral purity of hydrazides before their biological evaluation. The hydrazides containing the S enantiomer and R enantiomer of alanine were individually analysed using a chiral HPLC system with a Daicel Chiralpak® IB column (flow rate of 1 mL/minute, solvent composition of 94:5:1 acetonitrile:methanol:0.1% formic acid) to verify that the hydrazides were present as a single enantiomer¹²³. Consequently, initial group examinations have established that chirality is conserved by the presence of a single enantiomer S substance.

Chapter 1: Introduction

The prior group work has shown that antibacterial activity may be altered by modifying the hydrazine and amino acid components, while preserving species selectivity. Thus, we broadened our investigation by substituting the benzoxa-[2,1,3]-diazole moiety by scaffold hopping to assess its effectiveness in reducing toxicity. Additional information regarding this method will be presented in the next section.

1.7 Scaffold hopping approach.

As mentioned earlier (*cf* section 1.5), the necessity for lengthy, toxic tuberculosis treatments that are less effective against multidrug-resistant (MDR) and extensively drug-resistant (XDR) tuberculosis significantly contributes to the continuous increase in tuberculosis infections. An effective approach for tackling the challenging development of drug-resistant TB is to identify a novel chemical compound with a unique mode of action, therefore providing a new pathway for TB treatment. Different methods exist to accomplish this, such as scaffold hopping, which is, a strategic approach used by medicinal chemists, involves altering the central core structure of established bioactive compounds to create unique chemotypes with enhanced properties.¹²⁴ This approach is a strategy that is employed not only in the field of drug discovery but also in the subsequent phase of the lead optimisation process. Occasionally, this process involves altering the side chains and central cores of parent scaffolds, wherein side chain modifications are employed to address unfavourable characteristics, while alterations to the central core may be required under specific circumstances.¹²⁵ A significant portion of medications that are currently on the market were previously created by scaffold modification from natural compounds, hormones, and other medications such as morphine and tramadol¹²⁶.

As explained earlier (*cf*. section 1.6), our research group has identified benzoxa-[2,1,3]-diazole substituted amino acid and hydrazides as selective therapeutic agents against *Mtb*, modulating antibacterial activity while maintaining species selectivity, but cytotoxicity remains a concern¹¹⁹. From this perspective, scaffold hopping has been employed to substitute the benzoxa-[2,1,3]-diazole component with known anti-TB pharmacophores (Figure 38).

Chapter 1: Introduction

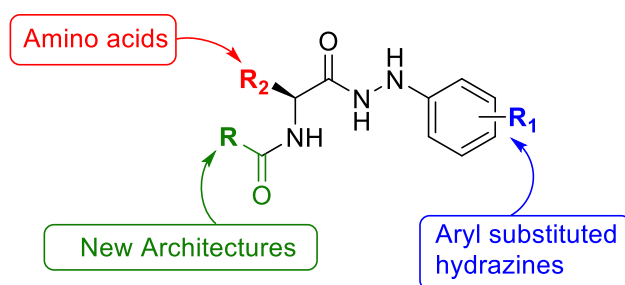


Figure 38: Key modification of the benzoxa-[2,1,3]-diazole moiety to be replaced with known anti-TB pharmacophores¹²⁷.

These pharmacophores include imidazo-[1, 2a] pyridine moiety of the first in class cytochrome *bc1* complex inhibitor Q203 **35** and the dinitrobenzamide (DNB) **46** moiety which has been shown from a HTS to produce excellent antitubercular activity (Figure 39)^{128, 129}.

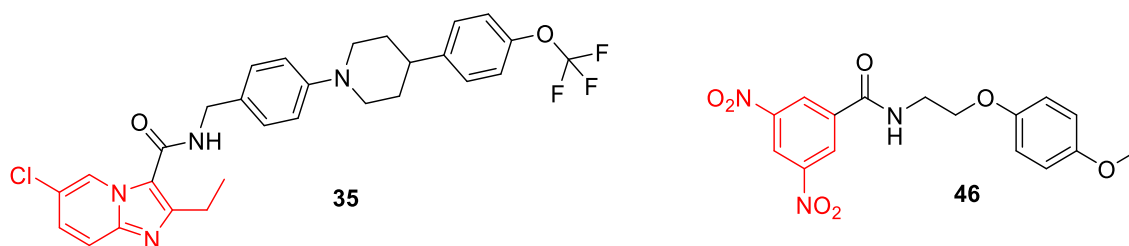
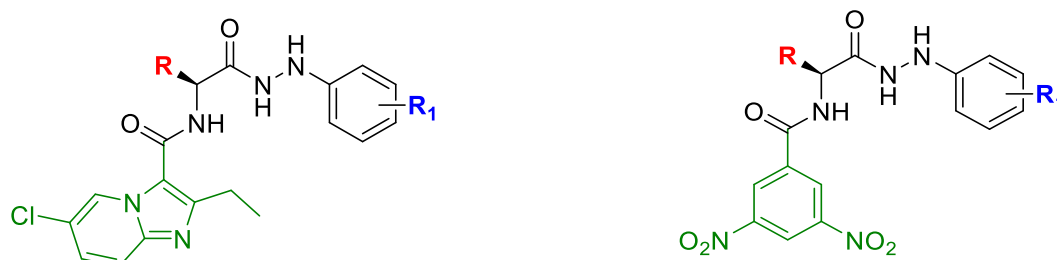


Figure 39: Scaffold hopping architecture (red) within known anti TB active compounds Q203 **35** and DNB **46**.

The main goal of this project was to perform a structure-activity relationship analysis of these substrates to achieve a comprehensive understanding of the specific molecules critical for their efficacy against *Mtb*. The compounds resulting from the modification were screened against both susceptible and resistant strains of *Mtb* using a Resazurin Microtiter Assay (REMA). The imidazo[1,2 a] pyridine amino acid hydrazide compounds exhibited enhanced activity with straightforward sidechains on the amino acid, and their activity varied based on the halogen position of the aromatic hydrazine. The 3,5-dinitrobenzamide component exhibited a higher level of effectiveness against the bacteria in comparison to the previous group. This suggests that these molecules may serve as potential antitubercular agents in the future (Figure 40).

Chapter 1: Introduction



R	R ₁	WT	MIC (μM)		R	R ₁	WT	MIC (μM)	
			INH _R	RIF/INH _R				INH _R	RIF/INH _R
Gly	3-Br	71	71	71	Leu	4-Br	16	8	16
Gly	3-Cl	39	39	39	Leu	3-CF ₃	16	8	16
Ala	3-Cl	34	34	34	Phe	3-Br	16	16	30
Ala	3-Br	69	138	69	Hph	3-Cl	8	8	8

Figure 40: MIC values using REMA assay for imidazo[1,2 a] pyridine amino acid hydrazide compounds and the 3,5-dinitrobenzene substituted amino acid hydrazide compounds against susceptible and resistant *Mtb* strains. The results demonstrated low MIC values with 3,5-dinitrobenzene containing compared to imidazo[1,2 a] pyridine containing compounds. R= various amino acid, R₁= halogen substituted phenyl hydrazine. MIC test was done by Dr.A. Brown.

Alternative scaffolds have been explored as substitutes for benzoxa-[2,1,3]-diazole, including nitrogenous scaffolds such as nitroimidazole found in the pretomanid **31** drug, likewise, 4-chloro-7-nitrobenzofurazan (NBD-Cl) **47** which is a fluorescent fluorophore that is utilised in biology and biomedicine as a fluorescent marker for various biomolecules such as peptides or proteins (Figure 41)¹³⁰.

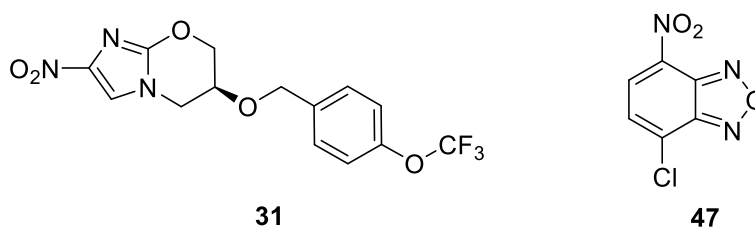


Figure 41: Chemical structure of pretomanid **31** containing nitroimidazole and NBD-Cl structure **47**.

The purpose of this was to observe the impact of the coupling with amino acids hydrazide moiety and generate SAR study by conducting REMA assay, however, this was not accomplished. More details about this will follow in chapter 4. Overall, it has successfully produced a small library of compounds that possess anti-TB activity, and it was able to produce the SAR study with regards to MIC values for sensitive and resistant *Mtb* strains using REMA assay.

Chapter 1: Introduction

In conclusion, this chapter covers knowledge on global tuberculosis epidemiology, *Mtb*-pathology and immunology, TB vaccination and treatments, and the increasing incidence of drug-resistant strains of TB, particularly MDR-TB and XDR-TB. It also discussed previous group efforts in discovering new anti-TB agents that have driven this project to use scaffold hopping approach. Although there has been a rise in the number of research endeavours intended for discovering novel antibiotics, resistant TB infections to antibiotics continues to be a challenging task¹³¹. Furthermore, treatment with conventional antibiotics such as INH **2** and RIF **3** often can be ineffective due to the prolonged duration of therapy and associated side effects. Consequently, the objective of this research was to develop novel antitubercular agents that have anti *Mtb* activity. The purpose is to tackle the continuous and substantial impact of TB disease, as well as the limitations in effectiveness and cost that are associated with current medications. Therefore, in this research, the *N*-amino acid substituted hydrazine framework has coupled with the imidazo[1, 2*a*] pyridine and 3,5-dinitrobenzene moieties to afford potential anti-tubercular agents.

The following chapter will start with the imidazo[1, 2*a*] pyridine substituted amino acid hydrazides compounds detailing their synthesis and SAR analysis.

1.8 Aim and objectives.

As previously highlighted (*cf.* section 1.4.3 and 1.4.4), the demand for highly toxic and less efficacious tuberculosis treatments with prolonged durations for the management of multidrug-resistant tuberculosis (MDR-TB) or extensively drug-resistant tuberculosis (XDR-TB) is the primary factor driving the persistent rise in tuberculosis infections. One strategy to combat the growing threat of drug-resistant tuberculosis involves the discovery of new chemical entities with innovative mechanisms of action, thereby offering other therapeutic alternatives for tuberculosis. Previous investigations within the group have demonstrated that the architecture of benzo-[2,1,3]-diazole peptidomimetics displays significant selectivity and mycobacterial efficacy (*cf.* section 1.7). The primary objective of this thesis is to conduct a structural activity relationship investigation to elucidate

Chapter 1: Introduction

the molecular components critical for activity against *Mtb*, utilising a scaffold hopping approach.

Therefore, this were accomplished through synthesising a diverse library of novel imidazo[1,2 a] pyridine substituted amino acid hydrazides and 3,5 dinitrobenzene substituted amino acid hydrazides. Following this, an exploration was performed to assess how structural modifications might affect the inhibition of mycobacterial growth by screening the produced compounds against both susceptible and resistant *Mtb* strains using a Resazurin Microtiter Assay (REMA).

Conducted a structure-activity relationship (SAR) analysis on imidazo[1,2a] pyridine and 3,5 dinitrobenzene substituted amino acid hydrazides to explore the relationship between chemical structure and biological activity. This investigation aims to enhance comprehension of molecular modifications that may improve antitubercular efficacy and identify potent hits compounds.

The cytotoxicity of novel imidazo[1,2a] pyridine-substituted amino acid hydrazide compounds and 3,5-dinitrobenzene-substituted amino acid hydrazide compounds was assessed on mammalian cell lines.

2. Chapter 2: Synthesis and SAR evaluation of imidazo[1, 2a] pyridine substituted aminoacid hydrazide compounds.

2.1 Introduction

As previously stated in Chapter 1, the TB drug resistance problem remains a major global challenge. Given the prevailing requirement for superior antibiotic medicines capable of eliminating aggressive tuberculosis infectious illnesses, a range of various strategies have been developed to overcome the issue of antibiotic resistance. In this research, we utilised a scaffold hopping strategy to modify the benzoxa-[2,1,3]-diazole compound **45** by including a pharmacophore with proven anti-TB activity. We aimed to enhance the anti-*Mtb* activity, particularly against drug-resistant strains of *Mtb*.

The first scaffold chosen in this research was the imidazo[1,2 a]pyridine (IPs) which is a fused bicyclic heterocycle currently gaining attention as a scaffold due to its extensive uses in the field of medicinal chemistry research. Until recently, it has shown substantial antituberculosis activity in addition to its anticancer, antileishmanial, anticonvulsant, antibacterial, antiviral, antidiabetic, proton pump, and insecticidal modes of action (Figure 42)¹³².

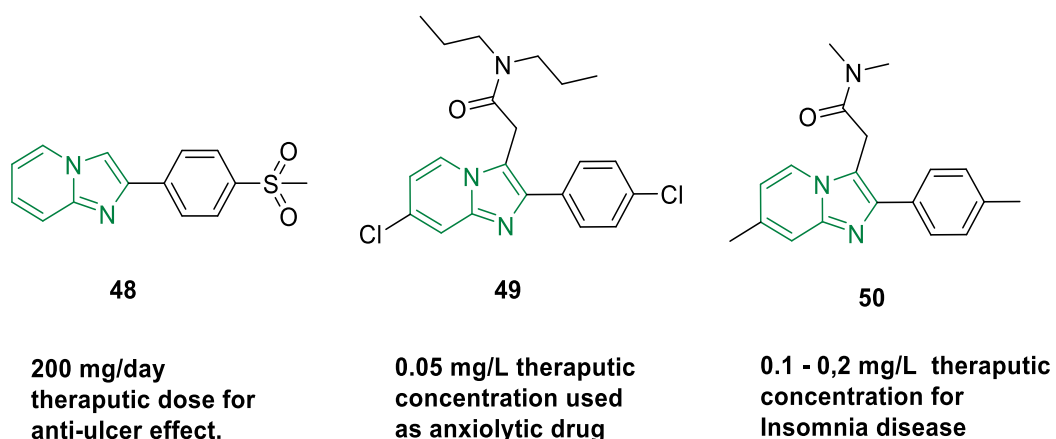


Figure 42: Examples of imidazo[1,2 a] pyridine-containing drugs used currently in the market, Zolimidine (gastroprotective drug) **48**, (anxiolytic drug) **49**, and Zolpidem (insomnia drug) **50** respectively^{133, 134}.

Several studies have begun to examine using imidazo[1,2 a]pyridine as a scaffold in antituberculosis agents. For instance, according to a study reported a set of nine 2,7-dimethylimidazo[1,2 a]pyridine-3-carboxamides compounds **51** have

demonstrated *in vitro* activity against both replicating and non-replicating forms of TB. The minimum inhibitory concentration (MIC_{90}), which refers to the lowest concentration of the compound resulting in a 90% reduction in bacterial growth, ranges from (0.4 to 1.9 μM), MDR (MIC_{90} 0.07–2.2 μM) and XDR (MIC_{90} 0.07–0.14 μM) strains. A subsequent SAR study of **51** led to the development of a bulky, more lipophilic biaryl ether compound **52** with excellent anti-TB activity in addition to its *in vivo* promising pharmacokinetics profile such as ($t_{1/2}$ 13.2 h and bioavailability 31.1%). The pharmacokinetics of the drug involves four main processes, commonly summarised by the abbreviation ADME, absorption, distribution, metabolism and excretion (Figure 43).

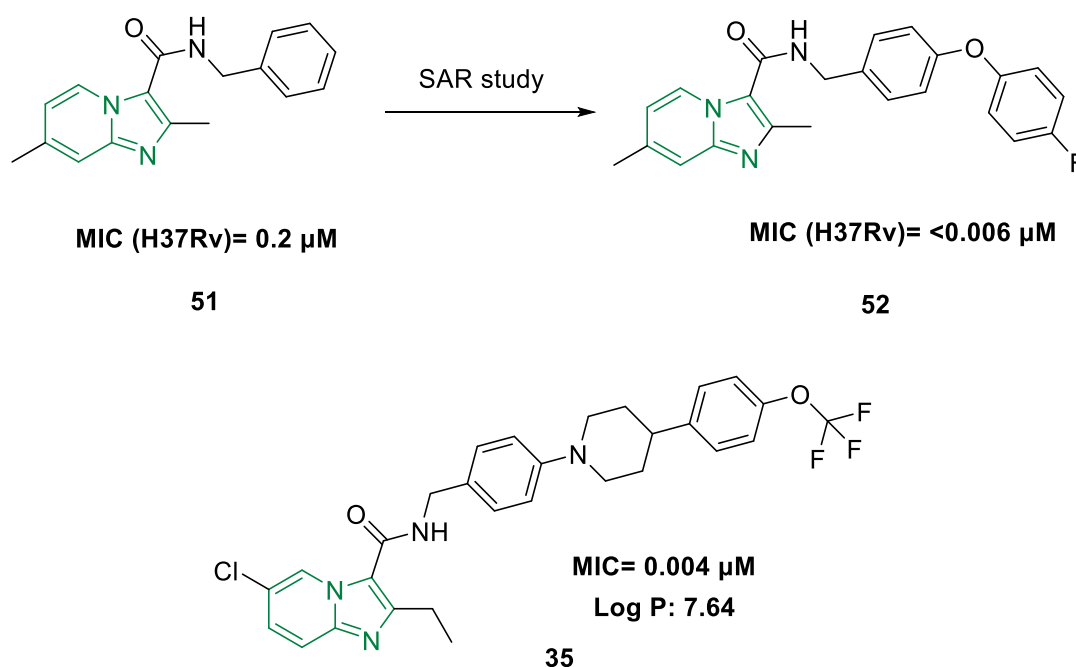


Figure 43: Imidazo[1,2 a]pyridine core-based compounds in research of development of the antituberculosis agents¹³².

Numerous endeavours have been undertaken to explore novel imidazo[1,2 a]pyridine amide (IPAs) compounds. Among these, the compound Q203 **35** has been effectively evaluated as a prospective clinical candidate due to its established antitubercular activity against both MDR and XDR strains and its excellent pharmacokinetic profile¹³². The long hydrophobic side chain produces a log *P* value of 7.64 and helps the selectivity index to be > 3700 with no blockage of hERG channels, suggesting an absence of cardiotoxicity⁹⁰.

2.2 Synthesis of the imidazo[1,2 a] pyridine amino acid hydrazides

Taken together the scaffold hopping strategy and the importance of imidazo[1,2 a]pyridine as a scaffold, we were able to replace the benzoxa [2,1,3] diazole core in the amino acid hydrazide backbone **45** with the imidazo[1,2 a]pyridine core of Q203 **35** synthesising the amino acid hydrazide imidazo[1,2 a]pyridine compound **53** and determine a structural activity relationship study (Figure 44).

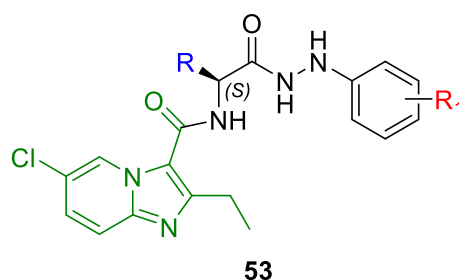


Figure 44: Amino acid hydrazide imidazo[1,2 a]pyridine compound structure **53**. **R**, different amino acids, **R₁** is diverse halogens substituents.

Initially, a retrosynthetic analysis of **53** took place with the first disconnection cleaving the amide link to generate the imidazo[1,2 a]pyridine-3- carboxylic acid **54** and the amino acid hydrazide **55**. Further, cleaving amino acid hydrazide **55** at the hydrazide bond produces the aryl hydrazines **56** and *N*-protected amino acids **57** (Figure 45).

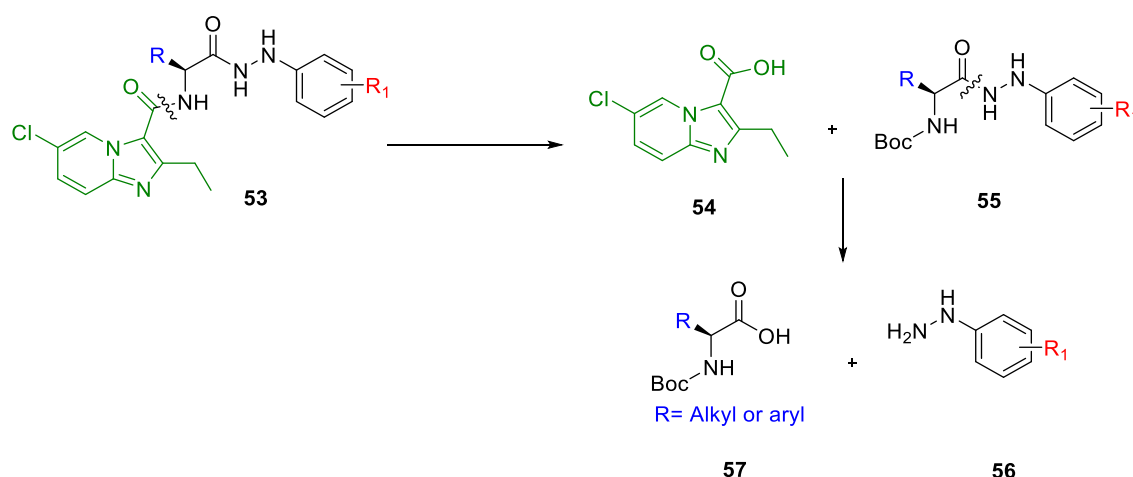


Figure 45: Retrosynthetic analysis of the target compound **53**.

The imidazo[1,2 a]pyridine-3-carboxylic acid **54** is not commercially available and as such had to be synthesised. Consequently, the retrosynthetic analysis of **53** with the hydrolysis to **58** and the subsequent cleavage to produce the 2-amino-

5-chloropyridine **59** and 2-bromopropionylacetate **60A** as an intermediate derived from the commercially available ethyl propionyl acetate **60** (Figure 46).

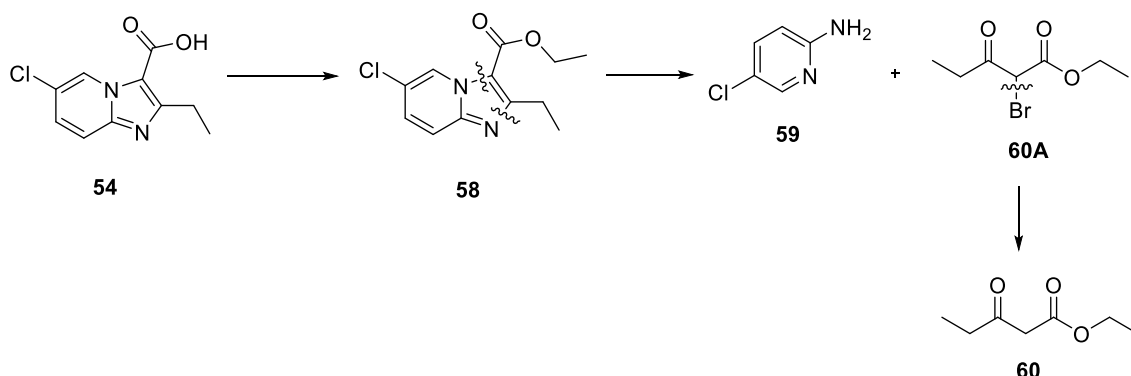
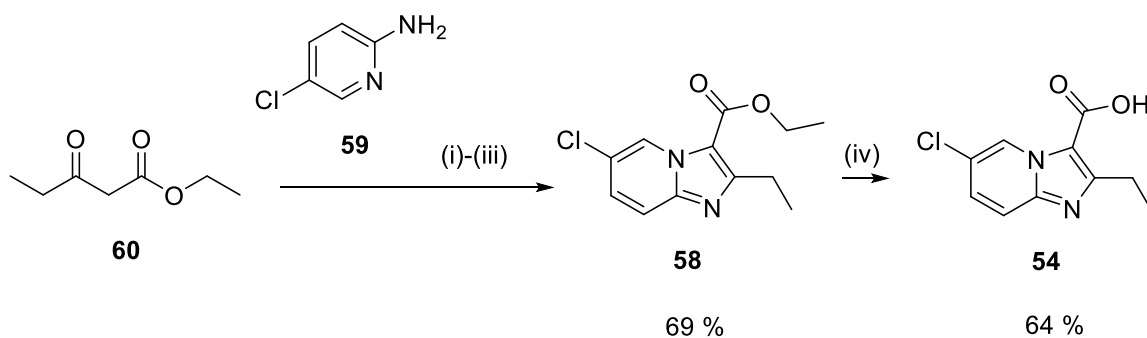


Figure 46: Retrosynthetic scheme for imidazo[1,2 a]pyridine -3-carboxylic acid **54**.

2.3 Synthesis of the imidazo[1,2 a]pyridine-3-carboxylic acid precursor

To begin our study, we were required to synthesise the imidazo[1,2 a] pyridine core to facilitate coupling with the *N*-amino acid hydrazide framework. To achieve this, we followed the literature procedure providing the carboxylic acid product **54** in high yield over 4 steps. The first step was the regioselective bromination of commercially available ethyl propionylacetate **60** with *N*-bromosuccinimide (NBS). Using NBS as a convenient brominating agent. The intermediate 2-bromopropionylacetate was not isolated but condensed with 2-amino-5-chloropyridine **59** in ethanol to afford the corresponding imidazopyridine ester **58** in high yield after purification by column chromatography. Subsequent hydrolysis with an aqueous solution of lithium hydroxide in EtOH gave the corresponding carboxylic acid **54** in quantitative yield with no further chromatography needed (Scheme 1)¹³⁵.



Scheme 1: Reagents and conditions. (i)-(iii), NBS, NH₄OAc, EtOH, 80 °C overnight. (iv) LiOH.H₂O, EtOH, rt 4 hr, (%) percentage yield.

The ^1H NMR spectrum of 6-chloro imidazo[1,2a] pyridine ester **58** displayed seven distinct signals, indicating the presence of the molecule. The ethyl signal observed on the alkyl region of the spectrum as a triplet around 1.5 ppm matches the CH_3 group and the quartet at 3.3 ppm corresponds to CH_2 . Also, similar signal multiplicity was observed for the ethyl ester but deshielded so appeared around 1.5 ppm for the CH_3 and 4.5 ppm for CH_2 . In addition, the protons on the heterocyclic ring appeared in the phenyl ring region of the spectrum. These signals match the literature data (Figure 47)¹³⁵

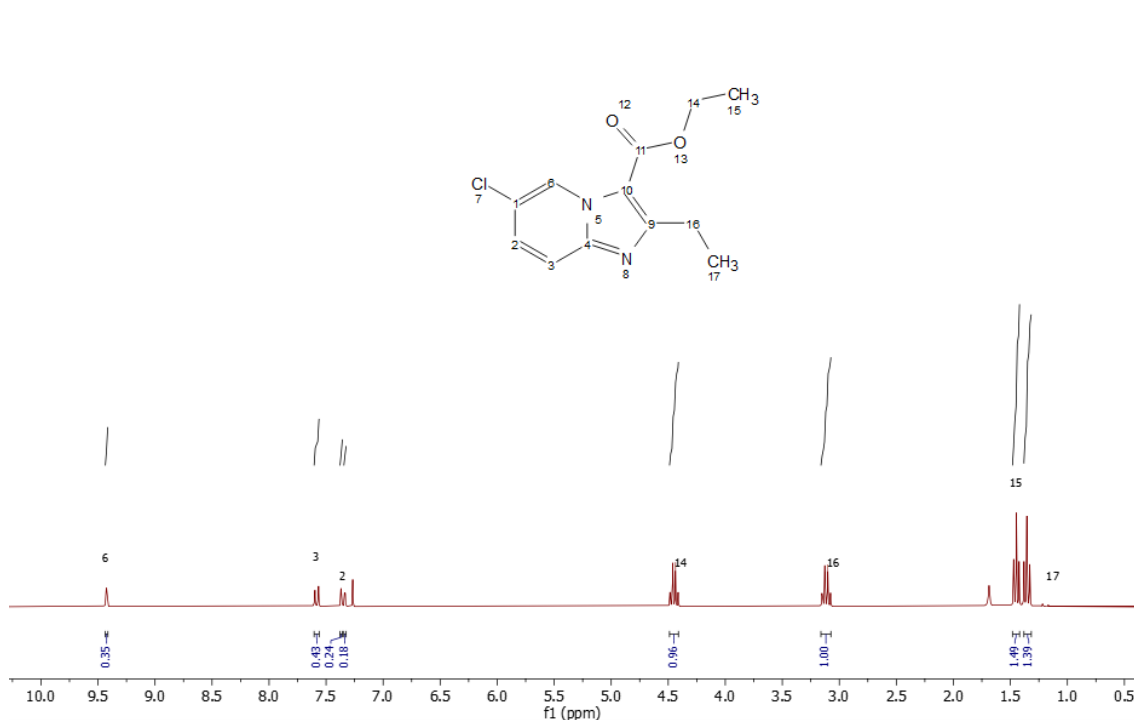


Figure 47: ^1H NMR spectrum of the 6-chloro-imidazo[1,2-a]pyridine ester **58** annotated to the proton signals matching the data source.

With imidazo[1,2-a]pyridine-3-carboxylic acid **54** in place, attention turned to the synthesis of the amino acid hydrazide compounds.

2.4 Synthesis of amino acids hydrazides intermediates.

The L-amino acids utilised in this research extend from unsubstituted amino acid glycine to the large side chain substituted amino acids such as phenylalanine and homophenylalanine. Since halogens are increasingly used in medical chemistry, the aryl hydrazine fragment was substituted with halogen¹³⁶. For instance chloramphenicol **61** a chlorinated drug used as an antimicrobial drug¹³⁷ and evafireniz **62**, a trifluoromethyl group containing compound act as an antiretroviral medication for HIV disease¹³⁸. In addition, previously mentioned bromide

substituted diarylquinoline (*cf.* Section 1.4.4.1), bedaquiline **27** the anti-TB drug (Figure 48).

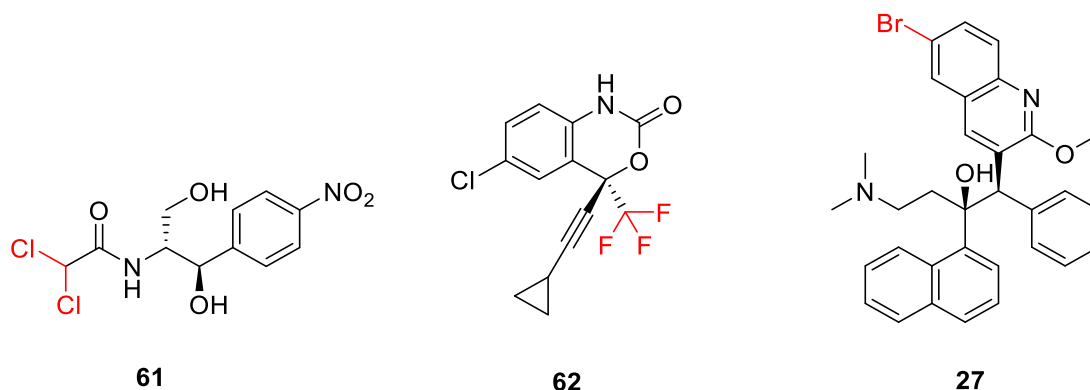
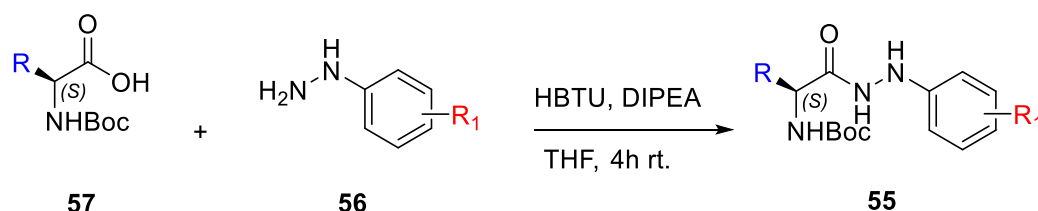


Figure 48: Examples of halogenated medications, chloramphenicol **61**, evafireniz **62** and bedaquiline **27** used as antibacterial, anti-HIV and anti-TB respectively^{137, 138}

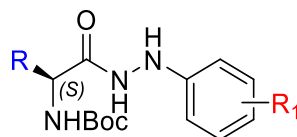
Furthermore, prior work within the group has demonstrated that the inclusion of chlorine in the *meta* position, together with larger side chains of the L-amino acid fragment, exhibits significant potential for antitubercular activity¹¹⁹. Additionally, the mono substitution pattern, *meta* or *para* positions, on the aryl hydrazine component were shown to be the best for antimycobacterial activity¹²⁷. Therefore, coupling of the amino acids with the *meta* and *para*-substituted phenyl hydrazine was made to produce the amino acid hydrazide compounds in fair to good yields (50 % - 70%).

To achieve the synthesis of *N*- amino acid hydrazide backbone **55**, we followed a standard coupling procedure used within the group¹¹⁹. This utilised a conventional peptide coupling reaction in which the *N*-Boc-amino acid **57** was coupled with monosubstituted aryl hydrazine **56** to produce the protected amino acid hydrazide intermediate **55** (Scheme 2).



Scheme 2: Peptide bond formation between amino acid **57** and substituted phenyl hydrazine **56** to form the protected amino hydrazide product **55**.

The reaction was able to provide amino acid hydrazides **55** with high yield (above 80 %) and purity and no need, in most cases, for chromatography to proceed to the next synthetic process (Table 2).



61a - 67f

R	R ₁	Entry	Yield (%)	R	R ₁	Entry	Yield (%)
Gly	3-Cl	61a	59%	Gly	4-Cl	61d	40%
	3-Br	61b	47%		4-Br	61e	88%
	3-CF ₃	61c	70%		4-CF ₃	61f	50%
Ala	3-Cl	62a	64%	Ala	4-Cl	62d	74%
	3-Br	62b	58%		4-Br	62e	78%
	3-CF ₃	62c	68%		4-CF ₃	62f	46%
Met	3-Cl	63a	82%	Met	4-Cl	63d	74%
	3-Br	63b	59%		4-Br	63e	70%
	3-CF ₃	63c	64%		4-CF ₃	63f	55%
Leu	3-Cl	64a	45%	Leu	4-Cl	64d	81%
	3-Br	64b	38%		4-Br	64e	57%
	3-CF ₃	64c	72%		4-CF ₃	64f	82%
Ile	3-Cl	65a	52%	Ile	4-Cl	65d	41%
	3-Br	65b	55%		4-Br	65e	65%
	3-CF ₃	65c	74%		4-CF ₃	65f	55%
Phe	3-Cl	66a	62%	Phe	4-Cl	66d	64%
	3-Br	66b	79%		4-Br	66e	80%
	3-CF ₃	66c	84%		4-CF ₃	66f	51%
Hph	3-Cl	67a	82%	Hph	4-Cl	67d	75%
	3-Br	67b	59%		4-Br	67e	70%
	3-CF ₃	67c	64%		4-CF ₃	67f	55%

Table 2: Amino acids hydrazides intermediates percentage yields. Compound percentage yield with very good yield (above 80%), good yield (above 70%), fair to poor yield (less than 50%).

Synthesis of the amino acid hydrazides was confirmed using ¹H NMR, for example, 4-chloroalanine hydrazide compound **62d** showed the characteristic signal assigned to the chiral proton, present in all amino acid hydrazide intermediates, around 4.4 ppm. Also, the spectrum showed a singlet signal corresponding to the Boc protecting group around 1.3 ppm. In addition, the protons of the aryl hydrazine fragment appear as doublets at 6.5 and 7.2 ppm. Moreover, the alkyl protons for alanine (CH₃) were observed in the alkyl region as a doublet at 1.4 ppm (Figure 49).

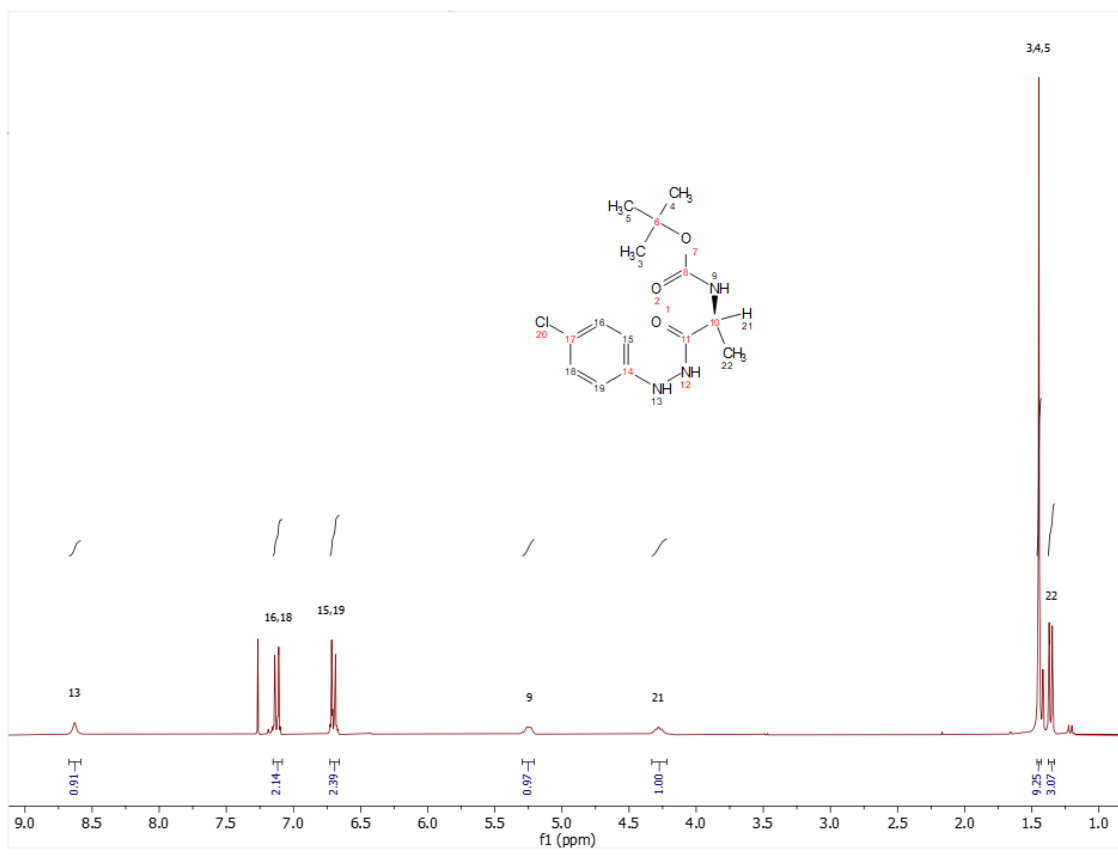


Figure 49: Crude ¹H NMR spectrum of the 4-chlorophenyl alanine hydrazide **62d** showing the characteristics signals indicating the presence of the compound.

Another example is phenylalanine-3-bromophenyl hydrazide compound **66b** which also showed a singlet signal corresponding to the Boc group in the alkyl region at 1.5 ppm, while protons of the benzyl group for the phenylalanine appear as doublets downfield of the alkyl region at 3.3 ppm. Also, the chiral proton signal of the amino acid hydrazide was observed at around 4.4 ppm. In addition, aryl protons were observed as multiplet in the aryl region of the spectrum around 6.5 to 7.0 ppm. As mentioned earlier, both amino acid hydrazide compounds **62d** and **66b** were used as crude before being converted to the desired compound in the following synthetic step (Figure 50).

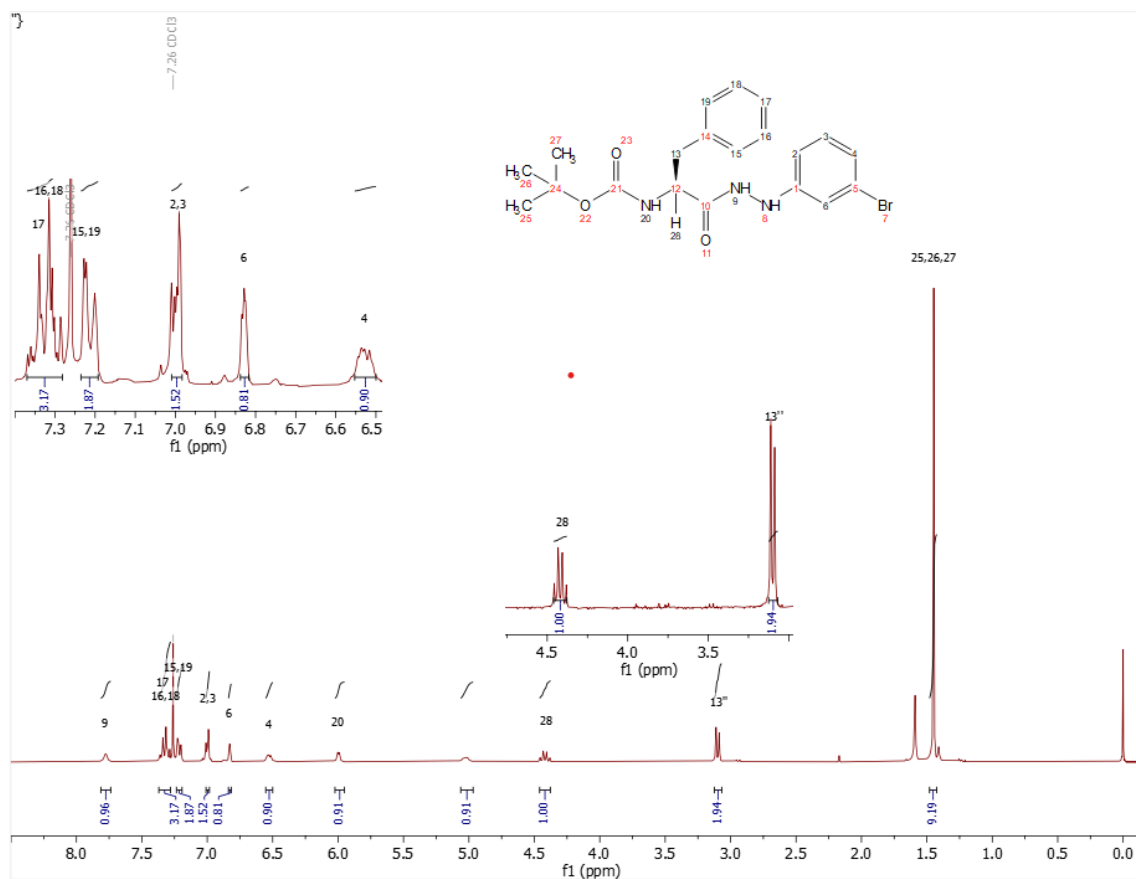
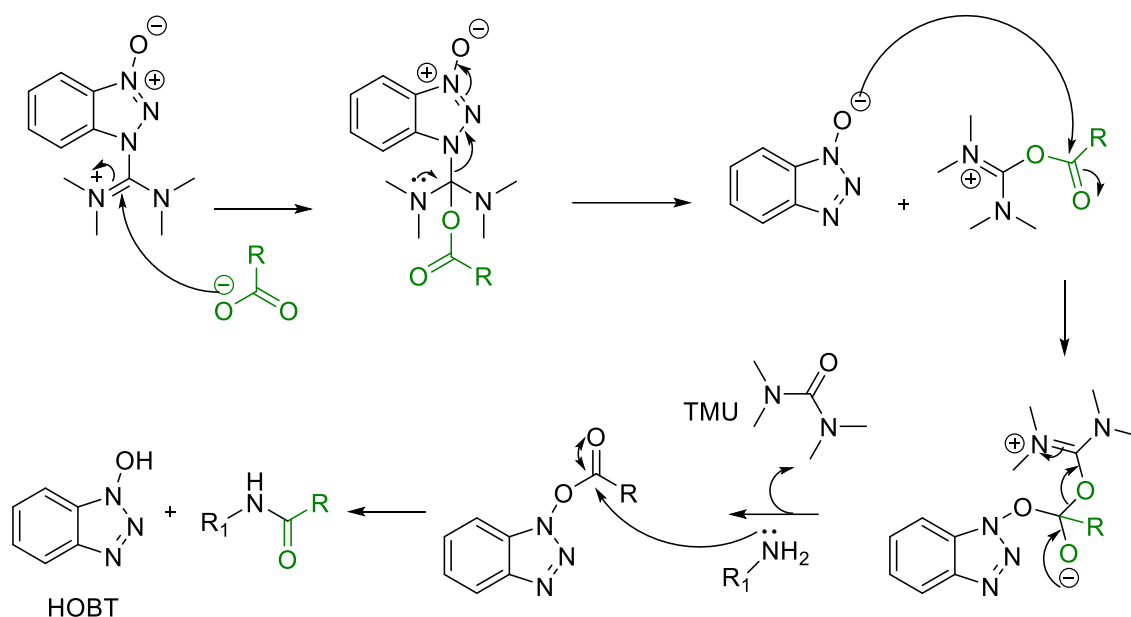


Figure 50: ¹H NMR for 3-bromophenylalanine hydrazide compound **66b** were produced via HBTU coupling reagent without chromatography.

HBTU (Hexafluorophosphate Benzotriazole Tetramethyl Uronium) was the most appropriate coupling reagent used in the coupling reactions as it produces the tetramethyl urea by-product which is readily removed through extraction whilst other reagents had been used, such as dicyclohexylcarbodiimide (DCC) required chromatography for the removal of the byproduct (Scheme 3)¹³⁹.



Scheme 3: Mechanism for the coupling of the activated carboxylic acid with amine using HBTU as coupling reagent in which tetramethyl urea (TMU) by product is produced.

N,N-diisopropylethylamine (DIPEA) was also used to deprotonate the carboxylic acid and to naturalise the phenyl hydrazine hydrochloride salts were present.

2.4.2 Enantiomeric purity determination.

As explained, in previous group work (*cf.* Chapter 1, Section 1.6.1), we examined the chiroptical characteristics of amino acid hydrazides, which may be racemized during the initial synthesis phase. The optical activity of L and D amino acid hydrazides was determined using a polarimeter, revealing a single enantiomer. Moreover, the chiral HPLC system was used to confirm the chiral purity of the hydrazides before their biological evaluation. The hydrazides containing the S and R enantiomers of alanine were individually analysed using a Daicel Chiralpak® IB column to confirm the presence of the hydrazides as a single enantiomer. Consequently, based on prior group work, the absolute configuration integrity of the amino acid hydrazide molecule has been confirmed, showing that the chirality remains unaltered.¹²³ Furthermore, we successfully acquired the crystal structure of compound **62d**, which includes L-alanine, through the slow evaporation of a dichloromethane solution. The findings suggest the coupling process does not cause racemization of the chiral centre.

The crystal structure analysis clearly identifies the structure of hydrazide **62d** and the determination of its absolute stereochemistry to be the correct enantiomer (Figure 51).

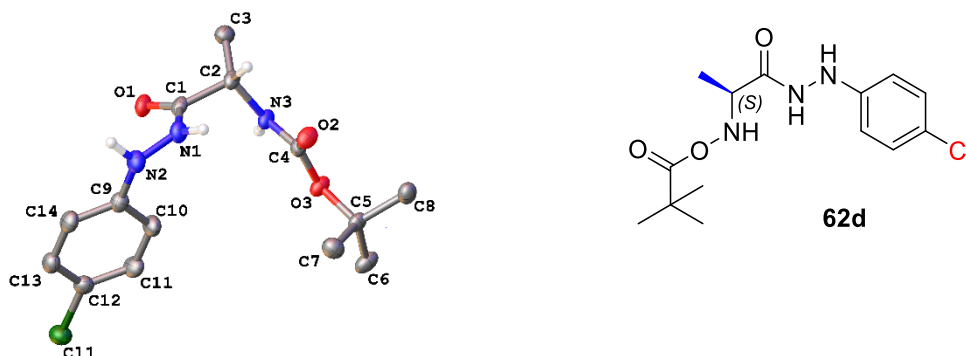
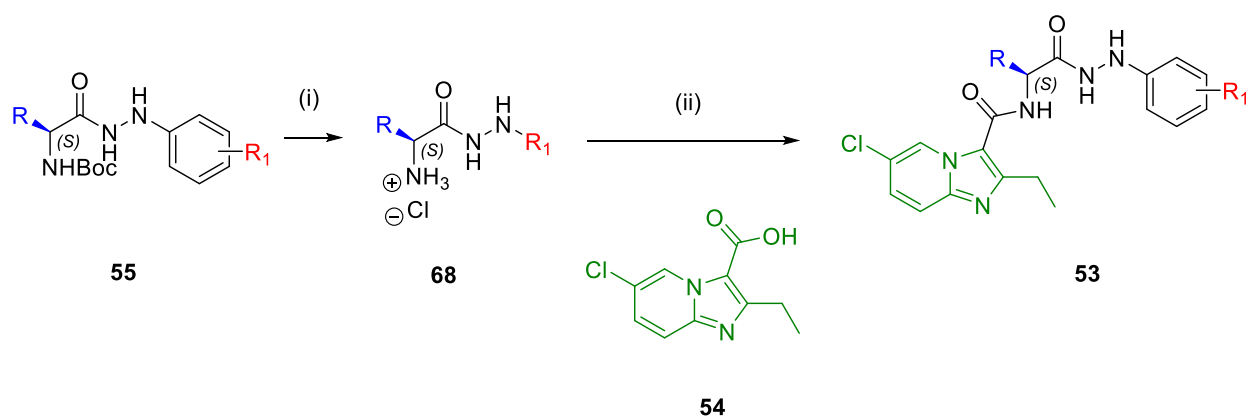


Figure 51: Crystal structure of L- alanine-4- chlorophenyl hydrazide compound **62d**.

2.5 Synthesis of imidazo[1,2 a]pyridine substituted amino acid hydrazide compounds.

Following the successful coupling reaction between the protected amino acid and the substituted aryl hydrazine components, the focus shifted to the deprotection of the Boc (*tert*-butyloxycarbonyl) amino acid hydrazide intermediates using 4M HCl in dioxane. By adhering to our established procedure, we successfully synthesised the amine-HCl salt after precipitating the reaction using a mixture of EtOH and diethyl ether as antisolvent¹⁴⁰.

Next, the required imidazo[1,2 a]pyridine scaffold is installed to generate the target compounds **53** via the previously mentioned deprotection step followed by a final peptide coupling reaction (Scheme 4).

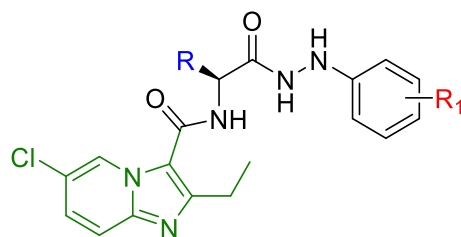


$\text{R} = \text{H}, \text{CH}_3, (\text{CH}_2)_2\text{SCH}_3, \text{CH}_2\text{CH}(\text{CH}_3)_2, \text{CH}(\text{CH}_3)\text{CH}_2\text{CH}_3, \text{CH}_2\text{Ph}, (\text{CH}_2)_2\text{Ph}$

$\text{R}_1 = 3\text{-Cl}, 3\text{-Br}, 3\text{CF}_3, 4\text{-Cl}, 4\text{-Br}, 4\text{CF}_3$

Scheme 4: Synthesis of 6-chloro-imidazo[1,2-a]pyridine amino acid hydrazide compounds. Reagents and conditions (i). 4N HCl in dioxane, 90 min, r t. (ii) **54**, HBTU, DIPEA, THF, 4hr, rt.

In this manner, a library of compounds can be efficiently synthesised using a key set of protection/deprotection and coupling processes, therefore, with the synthesis outlined, we began by deprotecting the protected *N*-hydrazides **61a** - **67f** and reacting these with the imidazo[1,2-a]pyridine-3-carboxylic acid scaffold to yield the desired product **69a** - **75f** in acceptable yields. For instance, compound **69b** yields very good (exceeding 80%), whereas compound **70d** yields poorly (below 40%), however, the yield was entirely sufficient to proceed with the compound investigation for the MIC test (Table 3).



69a - 75f

R	R ₁	Entry	Yield (%)	R	R ₁	Entry	Yield (%)
Gly	3-Cl	69a	36	Gly	4-Cl	69d	34
	3-Br	69b	88		4-Br	69e	51
	3-CF ₃	69c	50		4-CF ₃	69f	53
Ala	3-Br	70b	20	Ala	4-Cl	70d	23
	3-CF ₃	70c	33		4-Br	70e	59
Met	3-Br	71b	49	Met	4-Cl	71d	50
	3-CF ₃	71c	35		4-Br	71e	35
Leu	3-Cl	72a	67	Leu	4-Cl	72d	76
	3-Br	72b	59		4-Br	72e	37
	3-CF ₃	72c	94		4-CF ₃	72f	28
Ile	3-Cl	73a	60	Ile	4-Cl	73d	19
	3-Br	73b	76		4-Br	73e	40
	3-CF ₃	73c	60		4-CF ₃	73f	29
Phe	3-Cl	74a	76	Phe	4-Cl	74d	30
	3-Br	74b	48		4-Br	74e	53
	3-CF ₃	74c	64		4-CF ₃	74f	38
Hph	3-Cl	75a	63	Hph	4-Cl	75d	33
	3-Br	75b	43		4-Br	75e	63
	3-CF ₃	75c	36		4-CF ₃	75f	66

Table 3: Imidazo[1,2 a]pyridine substituted amino acid hydrazide compounds with percentage yields. Compound percentage yield with very good yield (above 80%), good yield (above 70%), fair to poor yield (less than 50%).

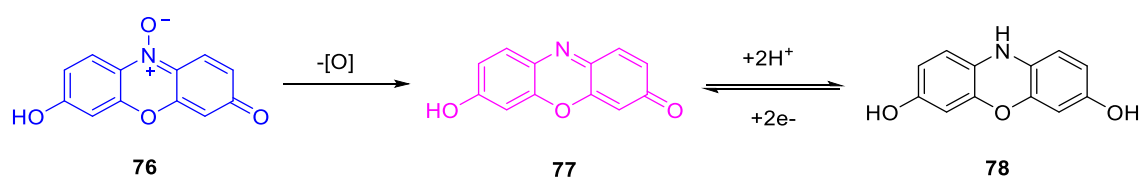
The imidazo[1,2 a]pyridine substituted amino acid hydrazide compounds were confirmed using ¹H NMR, ¹³C NMR, 2D data NMR and MS techniques. Where

MS analysis was undertaken, high-resolution mass spectroscopy was used and confirming that all compounds measured masses correlated with their respective molecular formulas.

2.6 Structure activity relationship evaluation of imidazo[1,2 a]pyridine substituted amino acids hydrazide compounds.

2.6.1 Antimycobacterial susceptibility test.

All compounds were screened against *Mtb* using a Resazurin microtiter assay (REMA). This assay utilises a colorimetric redox indicator method that has been established and approved by the WHO for testing medication susceptibility in non-reference laboratories¹⁴¹. It utilises resazurin (7-hydroxy-3-oxo-3H-phenoxazine 10-oxides) **76** which is a redox indicator that exhibits a colour transition from blue to pink. This colour change reveals the irreversible conversion of resazurin **76** to resorufin **77**, indicating metabolic activity (Scheme 5)¹⁴².



Scheme 5: Irreversible reduction of the resazurin dye **76** to the resorufin **77** with color change from blue purple to pink which can be observed when compound is not active against *Mtb*.

The redox potential of resorufin **77** can be visually inspected for colour changes measured using a spectrophotometer. Experiments were conducted in 96-well plates, with four replicates for each concentration of two compounds per plate. Each compound was dissolved in DMSO to create solutions with a concentration of 10 mg/mL. The solution was further diluted to achieve the desired initial concentration. The highest concentration of 64 $\mu\text{g/mL}$ was added onto the first column and then diluted through the plate using a 2-fold serial dilution. Then a further 2-fold dilution was used by adding *Mtb* bacteria culture to all wells in the growth media, except for the negative control, then the plates were incubated at 37 °C for five days, then resazurin (0.2% w/v in water) was added to each well. The plates were read ~48 hours later for the colour change. The control wells were checked first to verify the plates had not been contaminated. The negative control should not have any bacteria and should maintain the blue-

purple colour of resazurin. Conversely, the positive controls that consist only of *Mtb* without any experimental compounds, are expected to exhibit a pink colour, indicating metabolic activity. The minimum inhibitory concentration (MIC) is defined as the lowest concentration of a drug that causes no colour change for resazurin (purple), whilst the persistence of a dark blue colour indicates that compounds can inhibit mycobacterial growth by 95-100% (Figure 52)¹⁴¹.

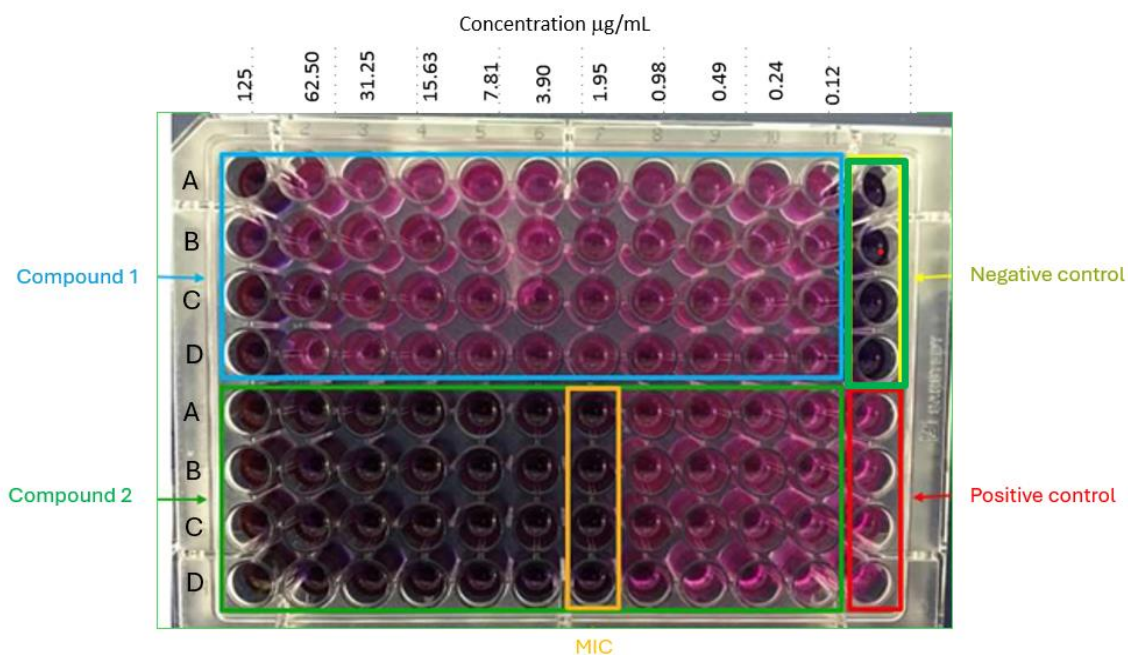


Figure 52: Determination of the MIC using REMA assay method via 96 wall plate.

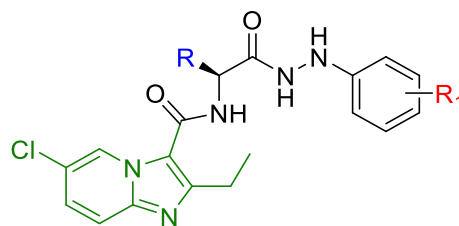
For data validation, MIC measurements of established anti-tubercular medicines such as isoniazid, rifampicin and ethambutol were also evaluated at the same time. The MIC values of these medicines were consistent with values in the literature, proving that the data for the novel compounds is reliable.

2.6.2 Structure activity relationship exploration of imidazo[1,2 a]pyridine substituted amino acid hydrazide compounds.

Following the successful coupling reactions resulting in the generation of the imidazo[1,2 a]pyridine substituted amino acid hydrazide library of compounds. It has been possible to investigate the structure-activity relationship of these compounds against different *Mtb* strains. Therefore, to evaluate their anti-tubercular potency, we measured the antituberculosis activity against wild-type *Mtb*, isoniazid-resistant strain and multi-resistant *Mtb* strains, utilising a REMA

assay. This allowed us to conduct a comparative analysis of the minimum inhibitory concentrations of these compounds.

Known anti-tubercular drugs were tested in addition to the compounds being studied. The minimum inhibitory concentrations (MIC) for rifampicin, isoniazid, ethambutol, and ethionamide were determined as 0.05 μM , 0.15 μM , 2.45 μM , and 6.02 μM against susceptible strain, respectively. In most cases, the imidazo[1,2-*a*]pyridine compounds **69a** – **75f** demonstrated anti-tuberculosis activity against sensitive and resistant *Mtb* strains (Table 4 and 5).



69a - 75f

R	R ₁	Entry	7902 WT (μ M)	8245 INH ^R (μ M)	8250 RIF/INH ^R (μ M)	8258 RIF/INH ^R (μ M)	Mammalian Cell Survivability (%)
Gly	3-Cl	69a	39	39	39	39	29
	3-Br	69b	71	71	71	71	95
	3-CF ₃	69c	-	-	-	-	95
	4-Cl	69d	79	79	79	79	56
	4-Br	69e	71	35	35	35	31
	4-CF ₃	69f	36	36	36	36	18
Ala	3-Br	70b	69	138	-	69	81
	3-CF ₃	70c	-	-	-	-	86
	4-Cl	70d	-	-	-	-	90
	4-Br	70e	152	152	152	152	47
Met	3-Br	71b	-	-	-	-	100
	3-CF ₃	71c	125	125	125	125	-2
	4-Cl	71d	-	-	-	-	82
	4-Br	71e	-	-	-	-	93
Leu	3-Cl	72a	-	-	-	-	1
	3-Br	72b	126	126	126	126	-2
	3-CF ₃	72c	-	-	-	-	95
	4-Br	72e	-	-	-	-	85
Ile	3-Br	73b	-	-	-	-	100
	3-CF ₃	73c	-	-	-	-	18
	4-Cl	73d	-	-	-	-	97
	4-Br	73e	-	-	-	-	91
Phe	3-Cl	74a	-	-	-	-	58
	3-Br	74b	-	-	-	-	95
	3-CF ₃	74c	-	-	-	-	102
	4-Cl	74d	-	-	-	-	84
	4-Br	74e	-	-	-	-	12
	4-CF ₃	74f	60	60	60	60	3
Hph	3-Cl	75a	-	-	-	-	2
	3-Br	75b	-	-	-	-	86
	3-CF ₃	75c	-	59	-	-	5
	4-Cl	75d	-	-	-	-	87
	4-Br	75e	-	-	-	-	64
	4-CF ₃	75f	118	118	118	118	0.03

Table 4: MIC values of the imidazo[1,2-a]pyridine compounds using REMA assay against susceptible and resistant *Mtb* strains. (-) = Not active at the maximum assay concentration (64 μ g/mL). Mammalian survivability test at (50 μ M), cell type= Human NCI-H460 lung carcinoma cells to the agents were determined using MTT assay, cell numbers= 2000, MIC and MTT assays were done by Dr A. Brown.

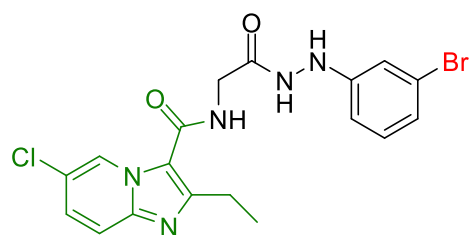
R	R ₁	Entry	7000 WT (μ M)	7002 RIF ^R (μ M)	7021 INH ^R (μ M)	Mammalian Cell Survivability (%)
Leu	4-Cl	72d	-	-	-	87
	4-CF ₃	72f	-	-	-	2
Ile	3-Cl	73a	65	-	65	101
	4-CF ₃	73f	-	-	-	102

Table 5: MIC values of the imidazo[1,2 a]pyridine compounds using REMA assay against susceptible and resistant *Mtb* strains. (-) = Not active at the maximum assay concentration (64 μ g/mL). Mammalian survivability test at (50 μ M), cell type= Human NCI-H460 lung carcinoma cells to the agents were determined using MTT assay, cell numbers= 2000, MIC and toxicity assays were done by Dr A. Brown.

The observed difference in minimum inhibitory concentration (MIC) values between imidazo[1,2 a]pyridine compounds substituting glycine hydrazide in compounds **69a - 69f** and imidazo[1,2 a]pyridine compounds substituting lengthy side chain amino acid hydrazides, such as in imidazopyridine containing homophenylalanine hydrazide in compound **75a - 75f**, is a notable result. This observation suggests that the anti-tubercular activity has been influenced by the side chain size of the amino acid hydrazide component.

Furthermore, it was shown that the halogen substituents in the aryl hydrazine component failed to provide a significant decrease in the minimum inhibitory concentration (MIC). Likewise, the substitution pattern did not lead to any enhancement in the MIC outcomes. (*cf.* **69a** vs **75a**), (*cf.* **69b** vs **75b**), (*cf.* **70b** vs **74b**), (*cf.* **70d** vs **74e**), (*cf.* **69a** vs **74a**), (*cf.* **69b** vs **70a**).

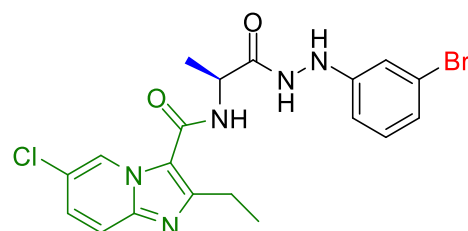
In light of the results, the modification of the amino acid typically led to a rise in the MIC due to the lengthening of the side chain. Consequently, the compounds exhibited less favourable MIC results against both susceptible and resistant *Mtb* strains. Moreover, the increasing in the lipophilicity characteristic of the compounds represented by the Log P value seems to not have a significant effect on the inhibitory activity in this instance (Figure 53).



69b

71 μM wt. *Mtb*
 71 μM INH^R *Mtb*
 71 μM INH/Rif^R *Mtb*

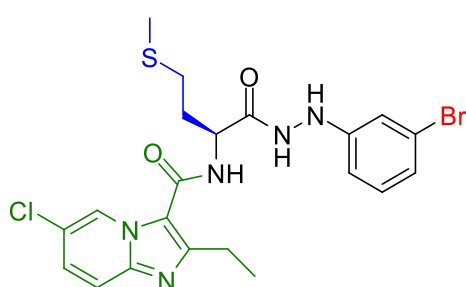
Log P: 2.7



70b

69 μM wt. *Mtb*
 138 μM INH^R *Mtb*
 69 μM INH/Rif^R *Mtb*

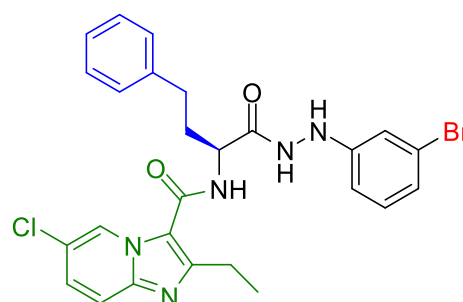
Log P: 3.19



71b

- μM wt. *Mtb*
 - μM INH^R *Mtb*
 - μM INH/Rif^R *Mtb*

Log P: 3.53



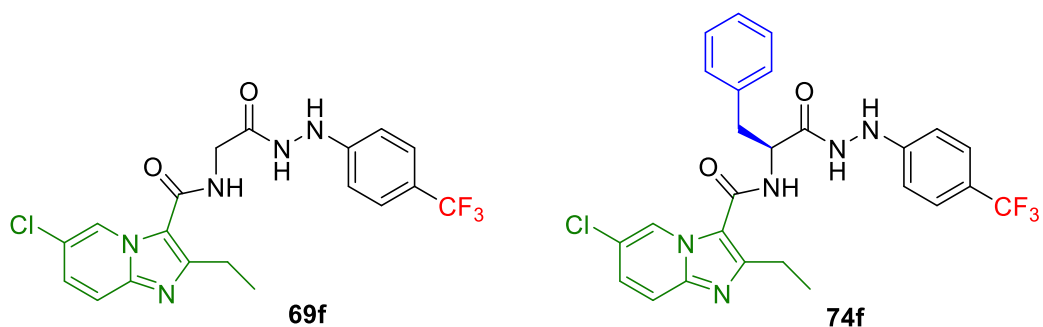
75b

- μM wt. *Mtb*
 - μM INH^R *Mtb*
 - μM INH/Rif^R *Mtb*

Log P: 5.28

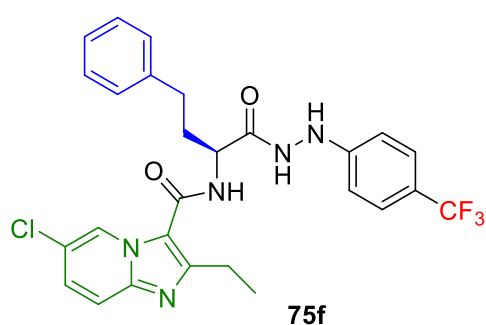
Figure 53: Significant loss of activity against susceptible and resistance *Mtb* strains observed when increasing the amino acid side chain from compound **69b** to **75b** regardless of the *meta*-bromo substitution on the phenyl hydrazide part and Log P values observed.

Following the preliminary study conducted by the group, it was found that the substitution of the aryl hydrazine fragment with a *para*-trifluoromethyl group resulted in potent anti-TB activity¹²⁷. Furthermore, upon assessing compound **69a**, **74f** and **75f**, which also contain the *para*-trifluoromethyl group, it appears that these compounds exhibit activity against both sensitive and resistant strains of *Mtb*. This effect may be attributed to the hydrophobicity of the trifluoromethyl group, leading to increased lipophilicity, therefore compounds expected to gain more penetration through the *Mtb* membrane. In addition, the anti-TB activity decreases upon adaption of the amino acid side chain in these compounds, emphasising the impact of the side chain amino acid substituent regarding the anti-tuberculosis activity (Figure 54).



36 μM wt. *Mtb*
 36 μM INH_R *Mtb*
 36 μM INH_R/Rif_R *Mtb*

60 μM wt. *Mtb*
 60 μM INH_R *Mtb*
 60 μM INH_R/Rif_R *Mtb*



118 μM wt. *Mtb*
 118 μM INH_R *Mtb*
 118 μM INH_R/Rif_R *Mtb*

Figure 54: Anti-tuberculosis activity observed with para-CF₃ substituent on the phenyl hydrazide component in compound **69f**, **74f** and **75f**.

When examining compounds **69b**, **70b**, and **72b**, which have the *meta* position substituted with a bromo phenyl hydrazide, it was revealed that these compounds have modest action (36 μM , 60 μM and 118 μM) respectively, against both susceptible and resistant strains of *Mtb* suggested that this favourable to produce activity. Additionally, it was noted that the MIC value significantly increases with the amplification of the *N*-side chain in these compounds against both sensitive and resistant *Mtb* strains (Figure 55).

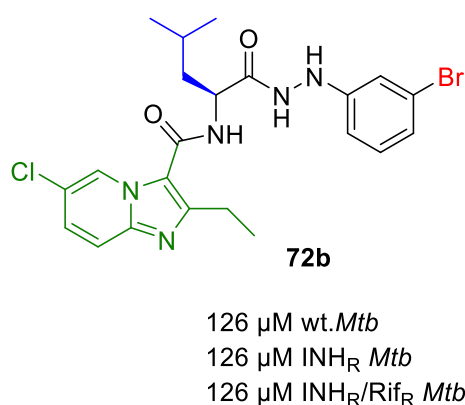
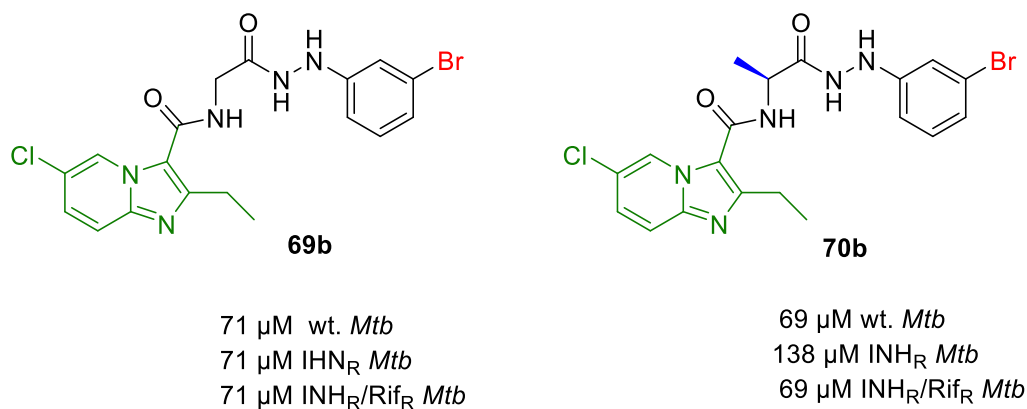


Figure 55: Observed anti-tuberculosis activity within **69b**, **70b**, and **72b** with notice of increasing in the MIC values against sensitive and resistant strains.

Looking specifically at compounds **69b**, **69e**, **70b**, and **70e** with bromide in *meta* and *para* positions in the glycine and alanine phenyl hydrazide, respectively. A MIC value of 71 μM was observed with compound **69b** against susceptible and resistant *Mtb* strains while compound **69e** showed a 2-fold decrease in MIC toward resistant *Mtb* strain. In contrast, compound **70b** showed comparable to low inhibitory activity (69 μM) compared to compound **69e** with MIC of (71 μM), while compound **70d** showed a significant increase in the MIC values (152 μM) for both susceptible and resistant strains of *Mtb* (Figure 56).

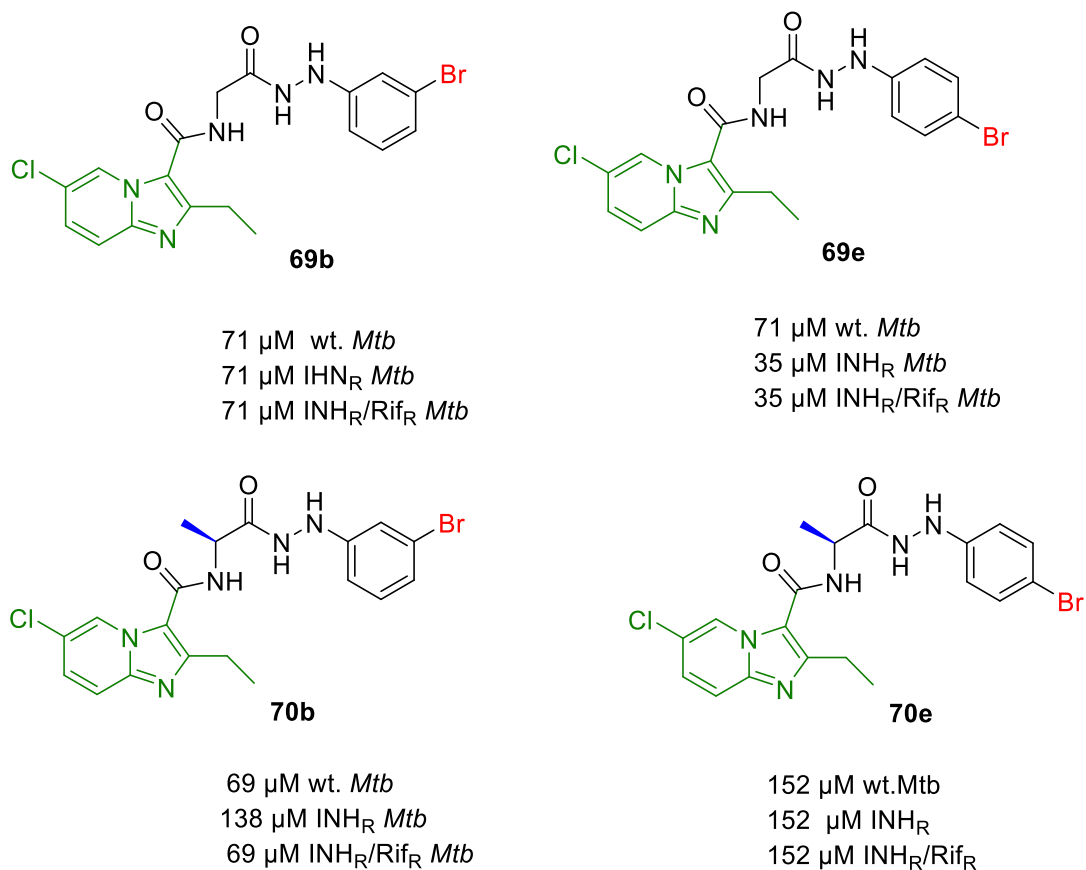
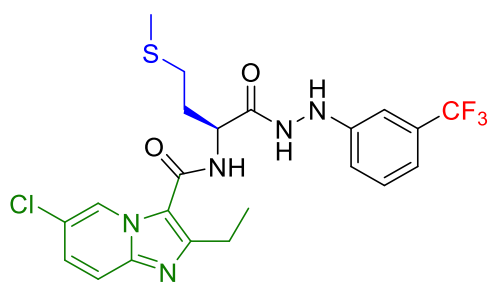


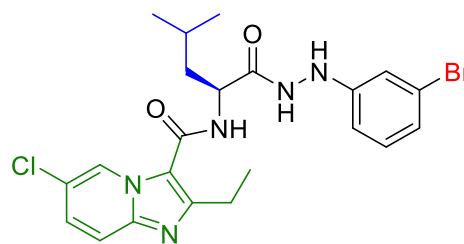
Figure 56 : Comparison between MIC values of glycine and alanine substituted bromo phenyl hydrazide in meta and para positions in compounds **69b**, **69e**, **70b** and **70e**.

Further investigation into the impact of elongating the side chain of the amino acid component on the molecules' inhibitory activity demonstrated minimal enhancement in the MIC results. For example, leucine, isoleucine, and methionine containing compounds such as **71a** and **72b** shows no to minimal antituberculosis activity (125 μM) against sensitive and resistant strains (Figure 57).



71a

125 μ M Wt *Mtb*
 125 μ M INH^R *Mtb*
 125 μ M INH/Rif^R *Mtb*

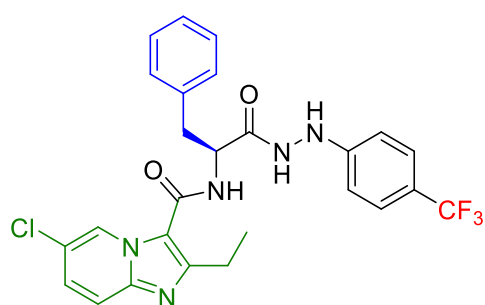


72b

125 μ M Wt *Mtb*
 125 μ M INH^R *Mtb*
 125 μ M INH/Rif^R *Mtb*

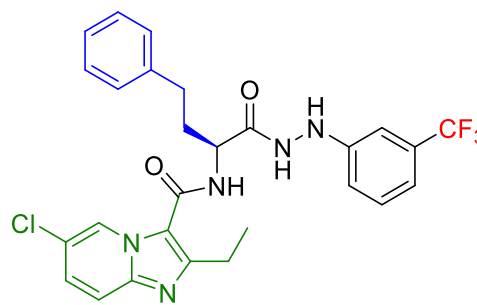
Figure 57: High MIC values observed with the increased size of side chain in imidazo[1,2-a]pyridine substituted amino acid hydrazide compounds seen in methionine and leucine-containing compounds **71a** and **72b**.

Furthermore, examining the impact of incorporating a hydrophobic side chain amino acid on the anti-*Mtb* activity was conducted. To achieve this, we specifically examined the inclusion of phenylalanine and the unnatural amino acid homophenylalanine in the amino acid fragment. This modification was chosen because it would increase the log P value, indicating a higher lipophilicity characteristic for the compounds would promote enhanced passing of the molecules across the *Mtb* lipid cell membrane. However, the compounds **74f** and **75c** exhibited a lack of significant if any, anti-tuberculosis activity by a MIC of 60 μ M against both susceptible and resistant strains (Figure 58).



74f

60 μ M Wt *Mtb*
 60 μ M INH^R *Mtb*
 60 μ M INH/Rif^R *Mtb*
 Log P: 4.96



75c

- μ M Wt *Mtb*
 59 μ M INH^R *Mtb*
 - μ M INH/Rif^R *Mtb*
 Log P: 5.38

Figure 58: Negative impact on antituberculosis activity upon incorporation of the bulky hydrophobic amino acid side chain as seen in compounds **74f** and **75c**.

Despite the importance of lipophilicity and log P value in drug incorporation through the dense lipid membrane of *Mtb*, there are exceptions, where compounds that have low log P values and afford low MIC values, can still be effective as potent anti-*Mtb* drugs such as zolpidem **50** which is an imidazo[1,2 a]pyridine containing compound used for treatment of insomnia but was repurposed for TB disease with MIC activity of 10 μ M (Figure 59)¹⁴³.

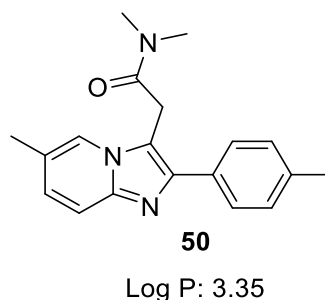


Figure 59: Structure of the zolpidem drug with low Log P value¹⁴³.

As a general trend, imidazo[1,2 a]pyridines coupled with unsubstituted amino acid side chains showed higher activity than the large hydrophobic side chain amino acid hydrazide backbone. In particular, imidazo[1,2 a]pyridine substituted glycine hydrazides were shown to be the most active than overall the imidazo[1,2 a]pyridine substituted side chain amino acid hydrazide compound regardless of the position or the type of substituents present in the hydrazine fragment such as compound **69f** which was the highest active compound by a MIC of 36 μ M against both sensitive and resistant *Mtb* strains .

Moreover, examining the structure of the imidazo[1,2 a]pyridine substituted amino acid hydrazides compounds and with connection to the SAR study of Q203 structure, it has been shown that altering the carboxamide linker with tertiary carboxamide, reversed amide, inserting a methylene group between the IP ring, and adding amide functionality resulted in an impairment of activity¹³². Therefore, by comparing with the side chain in the amino acid part in imidazo[1,2 a]pyridine core, it is emphasised that the unsubstituted amino acid side chain is crucial to producing anti-tuberculosis activity (Figure 60).

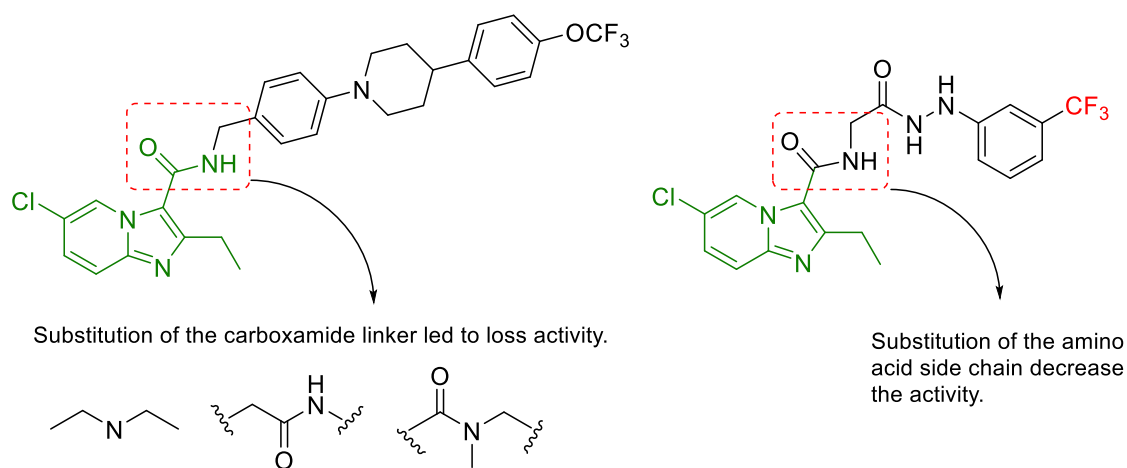


Figure 60: SAR of the Q203 showing that the modification of the carboxamide linker produces a total loss of activity and compared with the structure of most active imidazo[1,2 a]pyridine substituted glycine hydrazide compound **69f**¹³².

Concerning the cytotoxicity of the imidazo[1,2 a]pyridine substituted amino acid hydrazides compounds **69a** – **75f**, the majority of the compound shows no significant toxicity against macrophages, indicating their potential utility as drug molecules. For instance, compounds **69b**, **70b** and **73a** show a high percentage of the viable cells being tested under 50 μM of the compound (95 %, 81 % and 100%) respectively. On the other hand, compounds **72b**, **75f** and **74f** show significant mammalian cell toxicity (-2 %, 0.03 % and 3 %) respectively, indicating their limited use as therapeutic agents.

To conclude, as mentioned earlier (*cf.* Chapter 1, Section 1.5), there is an increasing demand for new medications with unique mechanisms of action to treat both drug-sensitive and drug-resistant tuberculosis. Owing to this, the scaffold hopping approach was used to design these molecules, this method aims to synthesise and evaluate new chemical compounds to identify the most potent and selective inhibitor of *Mtb* growth. The exploration of the IPs scaffold upon coupling with the amino acid hydrazide farmwork and producing their SAR analysis study was conducted. Furthermore, the amino acid hydrazide backbone was successfully synthesised and coupled with the imidazo[1,2 a]pyridine scaffold to produce a series of imidiaz[1,2 a]pyridine substituted amino acid hydrazide compounds capable of determining the *in vitro* antitubercular potency via screening against sensitive and resistant *Mtb* strain utilising Resazurin Microtiter Assay (REMA). The compounds were confirmed their chemical structures using ^1H NMR ^{13}C NMR, 2D data NMR and MS analysis. The SAR

finding of the imidazo[1,2 *a*]pyridine substituted amino acid hydrazide compounds reveal that unsubstituted side chain amino acid hydrazide is more favourable than substituted side chain amino acid hydrazide components and the lipophilicity of these compounds seemingly has no impact on the anti-*Mtb* activity. Hence, to achieve the research objective, it is necessary to synthesise superior compounds to combat TB. The upcoming chapter will discuss the synthesis and SAR of 3,5-dinitrobenzene substituted amino acid hydrazide compounds as potential anti-TB agents

3. Chapter 3: Synthesis and structural activity relationship evaluation of 3,5-dinitrobenzene substituted amino acid hydrazide compounds.

3.1 Introduction

In the previous chapter, novel imidazo[1,2 a]pyridine substituted amino acid hydrazide compounds as potential anti-*Mtb* agents was evaluated using a scaffold hopping method. However, it did not demonstrate sufficient effectiveness against *Mtb* strains being examined. Therefore, we decided to investigate another scaffold which is the 3,5-dinitrobenzene core, to study its impact on enhancing the anti-tubercular activity. The 3,5-dinitrobenzene moiety has been recently utilised in many research and development endeavours focused on antituberculosis activities¹⁴⁴.

Generally, nitro-based compounds have been recognised for their elevated toxicity, which encompasses hepatotoxicity, genotoxicity, mutagenicity, and carcinogenic effects attributed to the production of superoxide anions.¹⁴⁵ However, there are numerous examples of medicinal applications that involve nitro-based derivatives, for instance utilising as antiparasitic antineoplastic, antibiotic, antihypertensive and antiparasitic agents¹⁴⁶. Furthermore, compounds containing nitro groups are considered to be excellent as they demonstrate a wide range of biological activities such as anti-*Mtb* activity¹⁴⁷. Recently, researchers have identified electron-deficient nitroaromatic compounds as a novel and highly efficient group of anti-TB agents¹⁴⁸. These compounds have been recognised as inhibitors of the enzyme DprE1 (Decaprenylphosphoryl- β -D-ribose oxidase). This enzyme plays a vital role in the synthesis of decaprenylphosphoryl arabinose, which is the basic donor of arabinosyl residues for the synthesis of arabinose polymers in the mycobacterial cell wall biosynthesis process¹⁴⁹. Moreover, these putative DprE1 inhibitors were active against both *Mtb* and *Mycobacterium smegmatis* (*Msm*) (Figure 61)^{150, 151}.

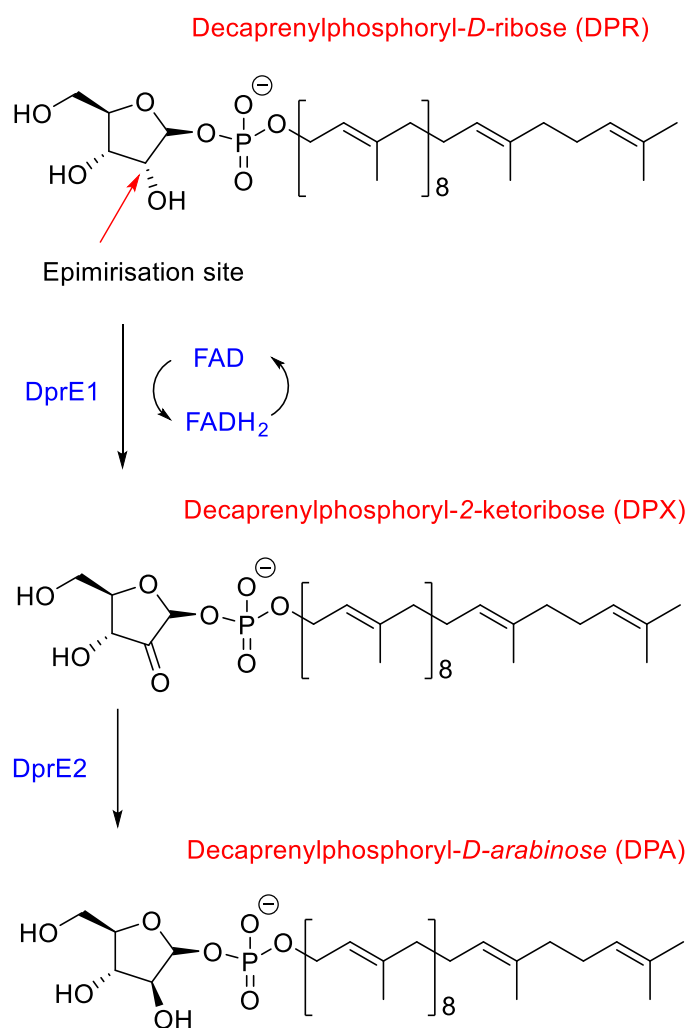


Figure 61: Epimerization of 2-OH group by DprE1 and DprE2 into arabinose in the presence of the cofactor flavine adenine dinucleotide (FAD) in an oxygen-free environment. The Decaprenylphosphoryl-*D*-arabinose (DPA) is a substrate for arabinosyltransferase and plays an important role in the synthesis of the *Mtb* cell wall polysaccharides¹⁴⁹.

Particularly, dinitrobenzamide (DNB1) **76** and benzothiazinones (BTZs) analogue **77** were identified using the high throughput screening (HTS) technique. They exhibited considerable activity against MDR-TB and XDR-TB in clinical isolates, in addition to the activity against intracellular *Mtb* bacilli. Furthermore, the compounds demonstrated no cellular toxicity when applied to traditional cytotoxicity assays on uninfected cells, indicating their toxicity is low (Figure 62)^{144, 150}.

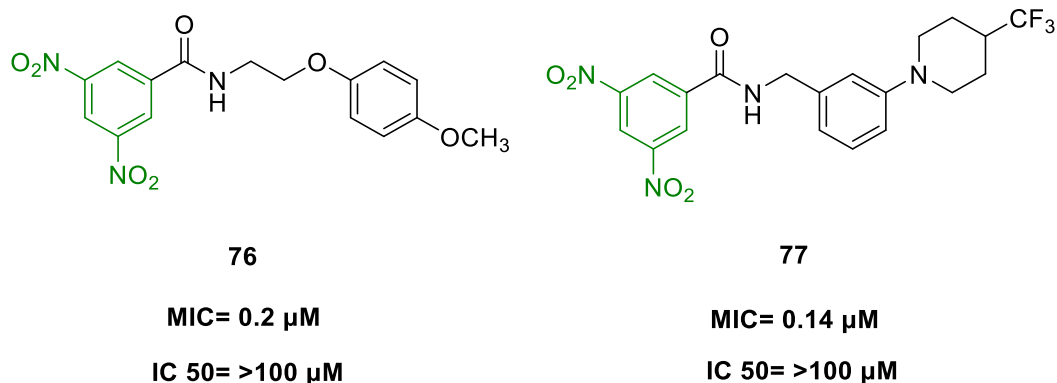


Figure 62: Dinitrobenzamide (DNB1) **76** and (BTZs) **77** bearing 3,5 dinitrobenzene pharmacophore, were identified for their high anti-tuberculosis activity^{144, 150}.

Furthermore, a novel series of 1,3,4-oxadiazole-2-thiols and tetrazole-5-thiol-based compounds which contain a 3,5-dinitrobenzene moiety have been recognised with substantial anti-*Mtb* activity. All compounds possessing the 3,5-dinitrobenzylsulfanyl group showed outstanding effectiveness against drug-sensitive *Mtb* and also exhibited significant activity against resistant *Mtb* both MDR and XDR (MIC value < 0.5 μ M). Interestingly, the antimycobacterial activity was significantly influenced by the locations of the two nitro groups. For instance, the antimycobacterial potency of the 3,5-dinitro-substituted derivatives was much greater than the 2,4-dinitro-substituted derivatives in this series of compounds. In addition, no cytotoxicity to primary human hepatocytes and low mutagenicity were obtained when examined in the viability cell assay (MTS Assay) and *in vitro* mutagenicity assay, respectively (Figure 63)^{152, 153}.

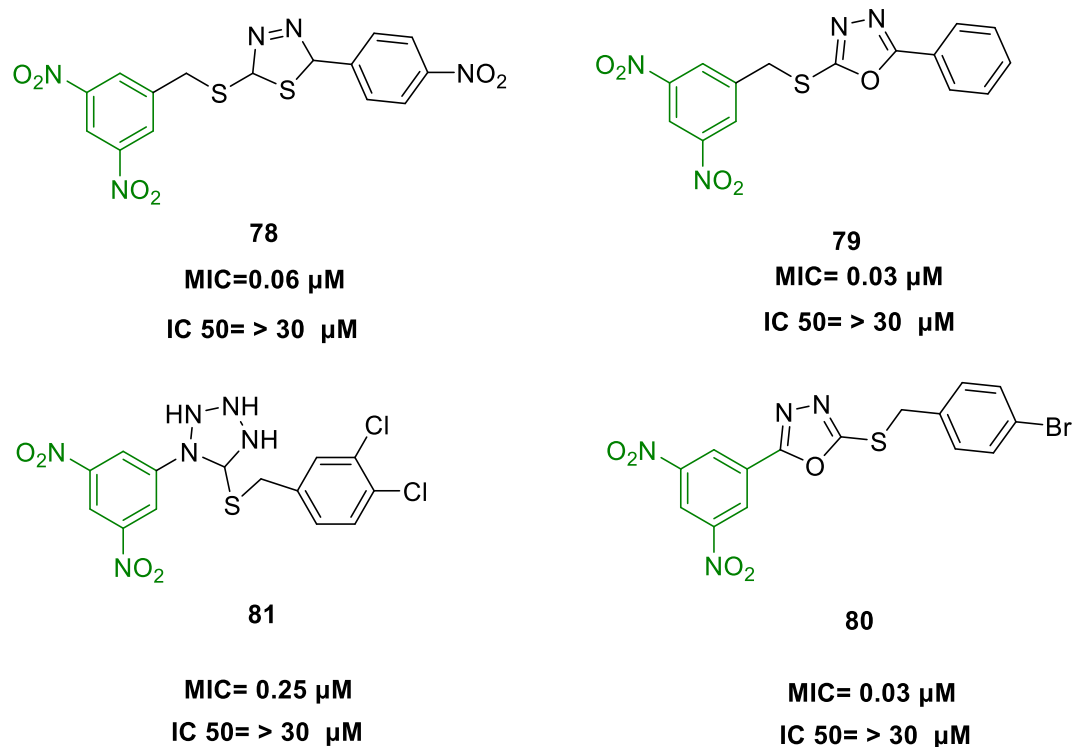
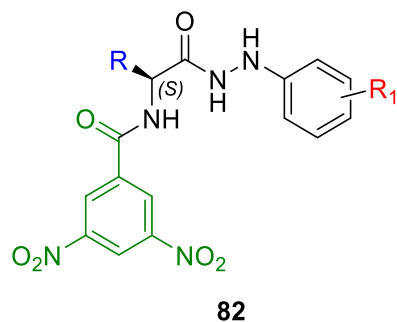


Figure 63: Novel 3,5-dinitrobenzylsulfanyl-1,3,4-oxadiazole and thiadiazole-based analogues **78**, **79**, **80** and tetrazole-5-thiol-based derivatives **81** exhibited high inhibitory activity against *Mtb* and this mainly attributed to presence of the 3,5 dinitrobenzene pharmacophore^{152, 153}.

3.2 Synthesis of 3,5-dinitrobenzene substituted amino acid hydrazide compounds.

The significance of the 3,5-dinitrophenyl group in medicinal chemistry, especially in the discovery of anti-mycobacterial drugs, prompted us to employ the scaffold hopping method. Consequently, we have used 3,5-dinitrobenzoic acid as a scaffold and successfully achieved coupling with the amino acid hydrazide framework to give rise to the 3,5-dinitrobenzene substituted amino acid hydrazide compounds **82** and screened them against sensitive and resistant *Mtb* strains, where this enables us to evaluate their SAR, in addition to examine the cytotoxicity assay against mammalian cell lines (Figure 64).



MIC Wt= 2 - 129 μ M

MIC INH^R/Rif^R= 2- 124 μ M

MTS (50 μ M) %= 9 -109 %

Figure 64: General structure of the 3,5-dinitrobenzene substituted amino acid hydrazide compounds **82** with range of the MIC values in μ M for the 3,5-dinitrobenzene substituted amino acid hydrazide compounds against sensitive and resistant *Mtb* strains. Mammalian cell cytotoxicity assay, survivability % range (9 – 109 %)

Firstly, a retrosynthetic analysis of molecule **82** was undertaken. The initial disconnection breaks the amide bond in compound **82**, resulting in the formation of 3,5-dinitrobenzoic acid **83** and amino acid hydrazide **55**. In addition, when amino acid hydrazide **55** is split at the hydrazide bond, it generates aryl hydrazine **56** and *N*-protected amino acids **57** (Figure 65).

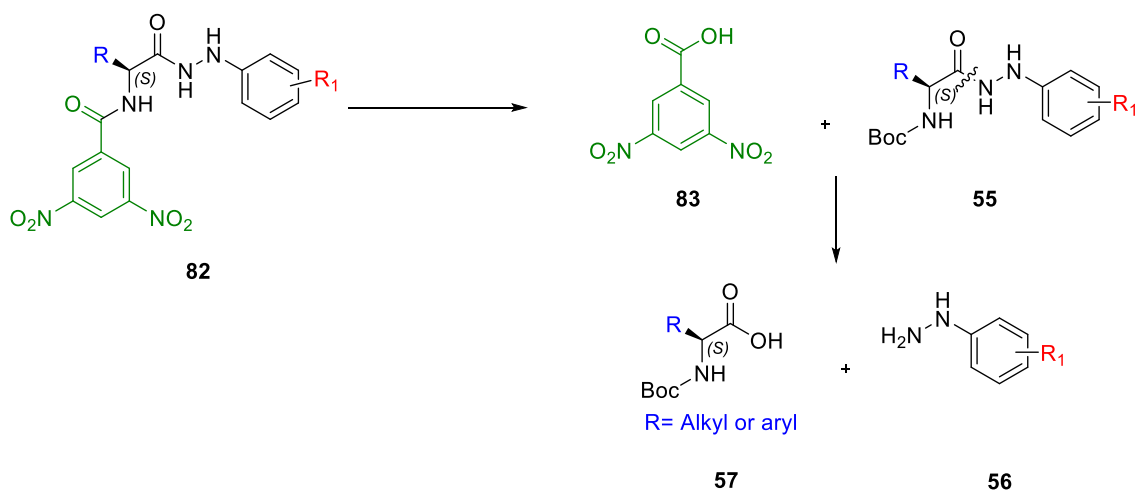


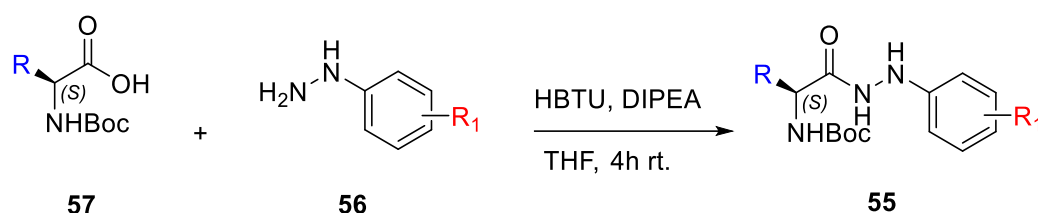
Figure 65: Retrosynthetic analysis of the target molecule **82**.

The desired compounds can be generated by initiating a peptide coupling reaction between different *N*-protected amino acids **57** and diverse aryl hydrazine **56**, which results in the synthesis of hydrazides **55**. After a successful coupling, the Boc protecting group will be removed from intermediates **55**. This will release the free amine, allowing it to react with the free carboxylic acid **83** of the commercially available 3,5-dinitrobenzoic acid. The outcome of the reaction will

be the formation of the target compound **82**, which is a 3,5-dinitrobenzene substituted amino acid hydrazide.

3.3 Synthesis of amino acid hydrazide intermediates.

As explained in Chapter 2 (*cf.* Section 2.4), synthesis of *N*-amino acid hydrazide backbone **55**, was achieved using a standard coupling procedure used within the group.¹¹⁹ This reaction utilised conventional peptide coupling reagents in which the *N*-Boc-amino acid **57** coupled with monosubstituted aryl hydrazine **56** produces the protected amino acid hydrazide intermediate **55** (Scheme 6).



Scheme 6: Peptide bond formation between amino acid **57** and substituted phenyl hydrazine **56** to form the protected amino hydrazide product **55**.

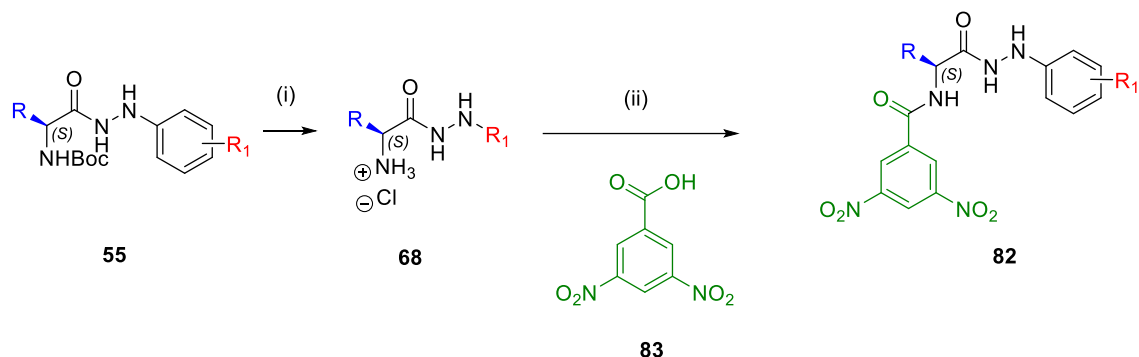
The peptide coupling provides amino acid hydrazides **55** with high yield and purity and there is no need, in most cases, for chromatography to carry the hydrazides to the next synthetic process. Additionally, *N,N*-diisopropylethylamine (DIPEA) was used to protonate the carboxylic acid and to naturalise the phenyl hydrazine hydrochloride where salts were present.

Moreover, L-amino acids with variations of the *para*, *meta* and *ortho*-substituted phenyl hydrazine molecules were used to evaluate the impact of the substitution pattern on the antituberculosis activity.

3.4 Synthesis of the 3,5-dinitrobenzene substituted amino acid hydrazide compounds.

With a successful reaction between the protected amino acid and the substituted aryl hydrazine components, attention turned to removing the Boc (*tert*-butyloxycarbonyl) group from the intermediates using 4M HCl in dioxane. By following our established procedure, we effectively produced the amine-HCl salt with a high conversion rate, precipitating the salt using a combination of EtOH and diethyl ether as an antisolvent.

Following this, the 3,5-dinitrobenzoic acid **83** was coupled with the deprotected amino acid mono substituted hydrazide compound **68** to produce the desired molecules **82** through the final peptide coupling reaction (Scheme 7).

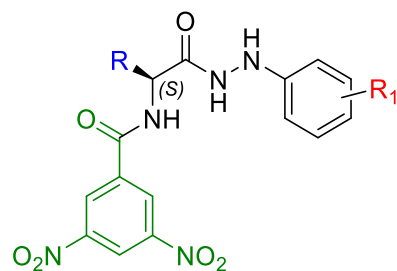


R= H, CH₃, (CH₂)₂SCH₃, CH₂CH(CH₃)₂, CH₂Ph, (CH₂)₂Ph

R₁= 3-Cl, 4-Cl, 2-Br, 3-Br, 4-Br, 2-CF₃, 3-CF₃, 4-CF₃

Scheme 7: Synthesis of 3,5-dinitrobenzen amino acid hydrazide compounds **82**. Reagents and conditions (i).4N HCl in dioxane, 90 min, r t.(ii) **83**, HBTU, DIPEA, THF, 4hr, rt.

As a result of the coupling, deprotection and final coupling set of reactions, this allowed us to produce the required 3,5-dinitrobenzene substituted amino acid hydrazide compounds **84a** – **89h** with very good yields (above 80%), good yield (70% - 50%) and fair to poor yield (less than 50%) (Table 6).



84a - 89h

R	R ₁	Entry	Yield (%)	R	R ₁	Entry	Yield (%)
Gly	3-Cl	84a	46	Leu	3-Cl	87a	46
	4-Cl	84b	26		4-Cl	87b	62
	2-Br	84c	58		2-Br	87c	63
	3-Br	84d	59		3-Br	87d	52
	4-Br	84e	37		4-Br	87e	62
	2-CF ₃	84f	29		2-CF ₃	87f	70
	3-CF ₃	84g	43		3-CF ₃	87g	46
	4-CF ₃	84h	65		4-CF ₃	87h	47
Ala	4-Cl	85a	56	Met	4-Cl	88a	68
	2-Br	85b	68		2-Br	88b	49
	3-Br	85c	37		3-Br	88c	69
	4-Br	85d	36		4-Br	88d	69
	2-CF ₃	85e	21		2-CF ₃	88e	35
	3-CF ₃	85f	43		3-CF ₃	88f	62
Phe	3-Cl	86a	54	Hph	3-Cl	89a	83
	4-Cl	86b	60		4-Cl	89b	54
	2-Br	86c	44		2-Br	89c	63
	3-Br	86d	31		3-Br	89d	69
	4-Br	86e	54		4-Br	89e	63
	2-CF ₃	86f	70		2-CF ₃	89f	62
	3-CF ₃	86g	72		3-CF ₃	89g	44
	4-CF ₃	86h	43		4-CF ₃	89h	26

Table 6: Synthesis of the 3,5-dinitrobenzene substituted amino acid hydrazide compounds with percentage yield.

Moreover, the 3,5- dinitrobenzene substituted amino acid hydrazide compounds **84a – 89h** were confirmed by their structures using ^1H NMR, ^{13}C NMR, 2D data NMR and high-resolution mass spectroscopy (HR-MS). This enables us to confirm the structures and purity of the resulting compounds.

3.5 Structural activity relationship evaluation of the 3,5-dinitrobenzene substituted amino acid hydrazide compounds.

As mentioned earlier (*cf.* Chapter 2, Section 2.6) the compounds used in this thesis were tested for inhibitory activity against strains of *Mtb* using a REMA assay. Therefore, the 3,5-dinitrobenzene substituted amino acid hydrazide compounds were examined against three strains of *Mtb*: wild type (WT), isoniazid-resistant (INH_R) or rifampicin-resistant (Rif_R) and doubly resistant strains (INH_R/Rif_R) (Tables 7).

R	R ₁	Entry	7902 WT (μ M)	8245 INH ^R (μ M)	8250 RIF/INH ^R (μ M)
Gly	3-Cl	84a	41	20	41
	4-Cl	84b	41	10	20
	2-Br	84c	18	18	18
	3-Br	84d	-	-	-
	4-Br	84e	9	9	9
	2-CF ₃	84f	37	37	37
	3-CF ₃	84g	19	9	9
	4-CF ₃	84h	19	9	9
Ala	4-Cl	85a	20	10	20
	2-Br	85b	35	35	35
	3-Br	85c	18	18	18
	4-Br	85d	35	35	35
	2-CF ₃	85e	18	18	18
	3-CF ₃	85f	36	36	36
Phe	3-Cl	86a	8	4	4
	4-Cl	86b	17	17	8
	3-Br	86c	15	15	30
	4-Br	86d	-	-	-
	2-CF ₃	86e	4	4	4
	3-CF ₃	86f	124	124	124
	4-CF ₃	86g	16	16	16
Leu	3-Cl	87a	18	9	9
	4-Cl	87b	18	9	18
	2-Br	87c	16	16	8
	3-Br	87d	129	64	129
	4-Br	87e	16	8	16
	2-CF ₃	87f	8	8	8
	3-CF ₃	87g	17	8	17
	4-CF ₃	87h	8	4	8
Met	4-Cl	88a	34	16	34
	2-Br	88b	16	16	16
	3-Br	88c	63	63	31
	4-Br	88d	125	63	125
	2-CF ₃	88e	16	16	16
	3-CF ₃	88f	32	16	32
Hph	3-Cl	89a	8	8	8
	4-Cl	89b	16	16	16
	2-Br	89c	2	2	2
	3-Br	89d	7	4	7
	4-Br	89e	15	7	30
	2-CF ₃	89f	30	15	30
	3-CF ₃	89g	60	30	60
	4-CF ₃	89h	15	8	8

Table 7: MIC results of the 3,5-dinitrobenzene substituted amino acid hydrazide compounds against *Mtb* strains using REMA assay. (-) = Not active at the assay maximum concentration of 64 μ g/mL. MIC assay was done by Dr. A. Brown.

Following the synthetic approach discussed earlier (*cf.* Section 3.3), The 3,5-dinitrobenzene-substituted amino acid hydrazides were assessed, providing their MIC values using the REMA assay, enabling a SAR analysis. Consequently, depending on the MIC results, most of the compounds have a low minimum inhibitory concentration with MIC range (2 μ M - 18 μ M), which indicates their ability to block the growth of *Mtb* strains, both sensitive and resistant strains.

This demonstrated that the inclusion of the 3,5-dinitrobenzene scaffold has a positive impact on the antituberculosis potency. Moreover, this series of compounds has provided insights into the impact of the amino acid side chain in addition to the effect of the different halogen substituents and their substitution pattern in the aryl hydrazine fragment, for example (**84a** vs **86a**), (**84c** vs **89c**), (**87d** vs **87e**), (**87e** vs **87f**), (**86a** vs **68b**), (**89e** vs **89d**) and (Tables 7).

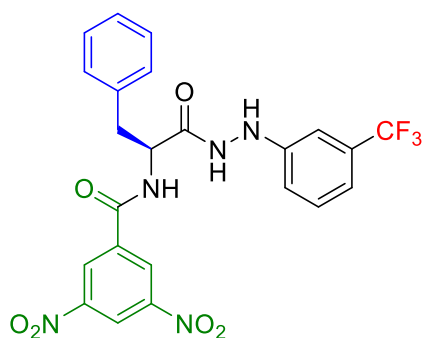
The objective of the SAR analysis being conducted is to evaluate the importance of the 3,5-dinitrobenzene scaffold in the context of the antituberculosis potency toward the development of compounds with improved anti-*Mtb* activity, specifically, against drug-resistant *Mtb*.

The biological data agreed with the idea that modifying the side chain of the amino acid component in the compounds leads to changes in the lipophilicity parameter, which in turn can decrease the inhibitory concentration value. For instance, the most active compound obtained **89c** which is 3,5-dinitrobenzene substituted homophenylalanine-2-bromohydrazide by an MIC value of (2 μ M) against susceptible, mono resistant and doubly resistant strains, suggested that the optimum lipophilicity (log P value = 4.15) of the amino acid side chain has an additional effect to the presence of 3,5-dinitrobenzene moiety within the compound. This is also realised in compound **86f**, which is 3,5-dinitrobenzene substituted phenylalanine-2-trifluoromethyl hydrazide (Log P value = 3.79), that exhibits low MIC value (4 μ M) for both sensitive and resistance *Mtb* strains.

Whereas compound **84f** which is a glycine-2-trifluoromethyl hydrazide-containing compound (Log P value = 1.99) produced a rise in the MIC value (37 μ M), this increase in the MIC was also observed with alanine-2-trifluoromethyl hydrazide containing compound **85e** (Log P value = 2.31) with a MIC (18 μ M) against susceptible and resistance strains, suggesting that the hydrophobic amino acid

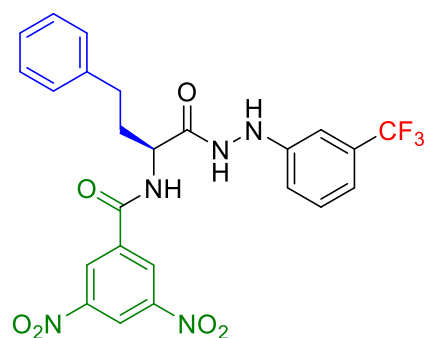
side chain might influence the lipophilicity characteristic of the compounds leads to promising anti-tuberculosis activity.

On the other hand, the compounds 3,5-dinitrobenzene substituted phenylalanine and homophenylalanine *meta*-substituted trifluoromethyl hydrazides **86g** and **89g**, respectively, led to a significant loss of activity against both susceptible and resistant *Mtb* strains. This could be attributed to the strong electron-withdrawing effect of the (CF₃) may influence interactions within the binding site. This can be emphasised when comparing with the 3,5-dinitrobenzene substituted phenylalanine and homophenylalanine *meta*-substituted chloro hydrazides **86a** and **89a**, respectively, which exhibit a noticeable rise in antituberculosis activity for both susceptible and resistant strains suggesting that chloride in *meta* position is more favourable than trifluoromethyl groups when inhibiting the growth of *Mtb* (Figure 66).



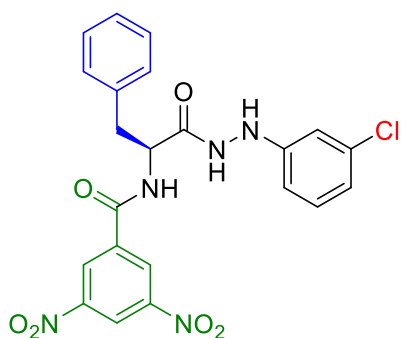
86g

124 μM wt.*Mtb*
 124 μM INH_R
 124 μM INH_R/Rif_R



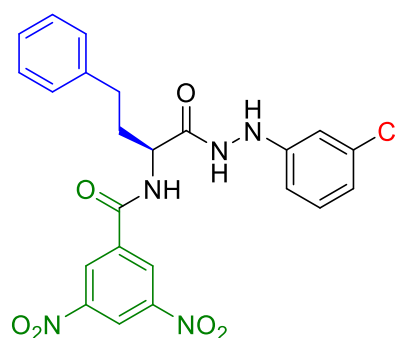
89g

60 μM wt.*Mtb*
 30 μM INH_R
 60 μM INH_R/Rif_R



86a

8 μM wt.*Mtb*
 4 μM INH_R
 4 μM INH_R/Rif_R

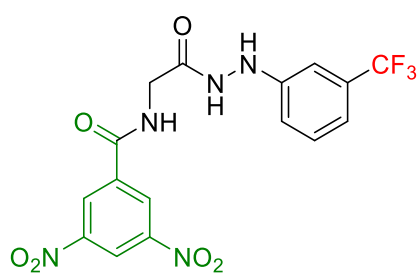


89a

8 μM wt.*Mtb*
 8 μM INH_R
 8 μM INH_R/Rif_R

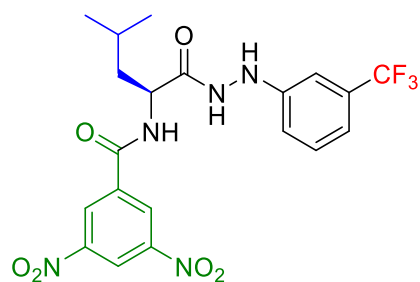
Figure 66: High MIC values observed with meta-(CF₃) substituent in compounds **86g** and **89g**, while low MIC values obtained with meta-(Cl) substituent in compounds **86a** and **89a**.

Notably, several 3,5-dinitro compounds have shown selectivity against the isoniazid-resistant strain containing *meta* trifluoromethyl amino acid hydrazide, as it has a lower MIC value compared with the wild-type *Mtb* strain, suggesting the scaffold hopping approach has potential for developing medicines that may effectively target drug-resistant *Mtb* (Figure 67).



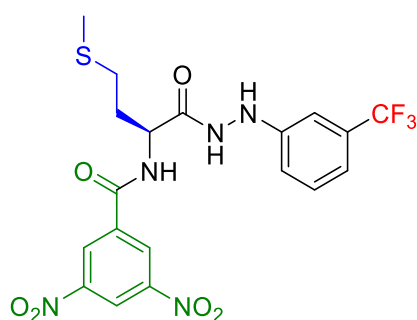
84g

19 μM wt.Mtb
9 μM INH_R



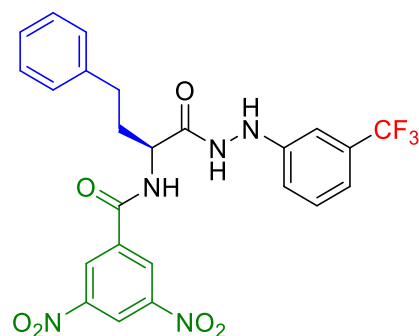
87g

17 μM wt.Mtb
8 μM INH_R



88f

32 μM wt.Mtb
16 μM INH_R



89g

60 μM wt.Mtb
30 μM INH_R

Figure 67: Low MIC value toward the INH resistant strains perceived with *meta*-(CF₃) substituent compounds **84g**, **87g**, **88f** and **89g**.

Moreover, the 3,5-dinitrobenzene glycine containing hydrazides **84a**, **84b**, **84g**, and **84h** have moderate to low MIC values ranging from 37 μM to 9 μM . These compounds also show selectivity towards the INH-resistant strain, implying the possibility of manipulation towards the development of the molecules with demonstrated activity against MDR-TB. However, these compounds have a high minimum inhibitory concentration against the Rif_R strain, indicating potential gene mutation might occurred within this strain leading to an increase MIC value in this instance. This can be related to specific mutations in the *rpoB* gene, which encodes the β -subunit of RNA polymerase. These mutations modify the rifampin target site, diminishing the drug's effectiveness and resulting in elevated MIC values¹⁵⁴ (Figure 68).

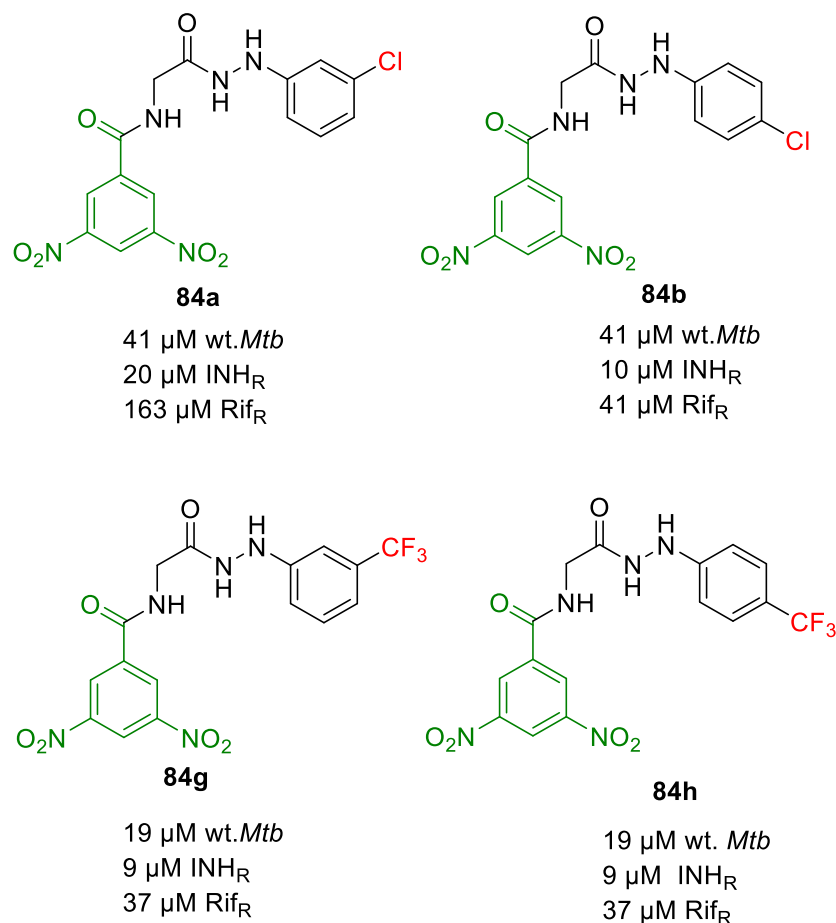


Figure 68: High MIC values obtained against Rif_R strain while lowering concentration observed against INH_R with compounds **84a**, **84b**, **84g**, and **84h**.

Likewise, the 3,5-dinitrobenzene substituted alanine hydrazides (**85a - e**) showed comparable anti-*Mtb* activity with glycine-substituted hydrazide compounds, suggesting that unsubstituted or small alkyl group containing amino acids have a negative impact toward antituberculosis activity (Tables 7).

Remarkably, two compounds showed no activity against *Mtb* strains (**84d**) and (**86e**), which are 3,5-dinitrobenzene-substituted glycine and phenylalanine brominated hydrazides, respectively. This could be due to these compounds having no penetration of the cell membrane, therefore not being able to reach the target in *Mtb*. Another reason might be because the bromide is unfavourable in the *meta* and *para* position in the hydrazide fragment of the molecules, decreasing the binding affinity (Table 7). Likewise, a noticeable increase in the MIC values observed with compounds **87d**, **88c** and **88d** in which bromide hydrazide is present (Figure 69). The binding affinity for compounds can be identified through labelling the compound. This process involves attach a

fluorescent tag to the compound, this facilitates visualisation using a fluorescence microscope. Utilise a fluorescence microscope for examining the samples to measure the fluorescence intensity to determine the amount of compound linked to the target¹⁵⁵.

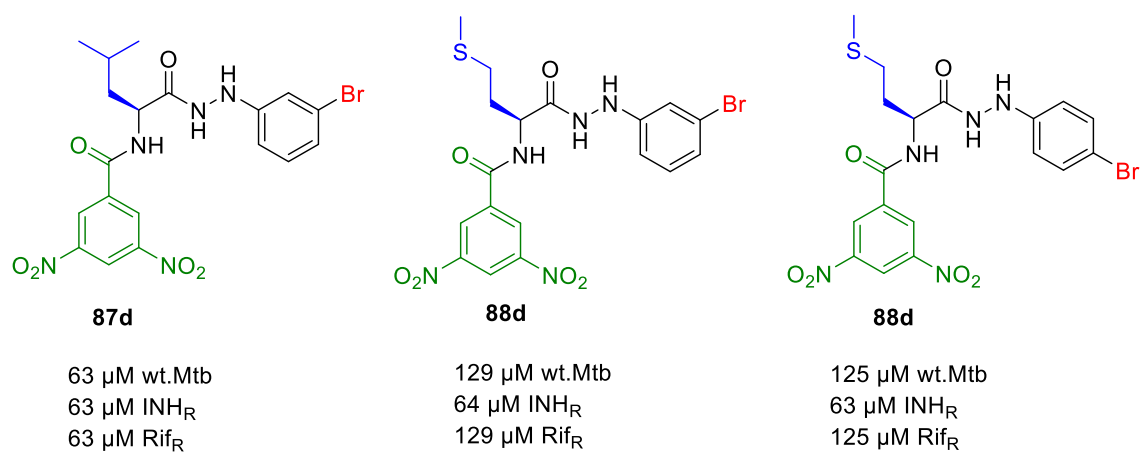
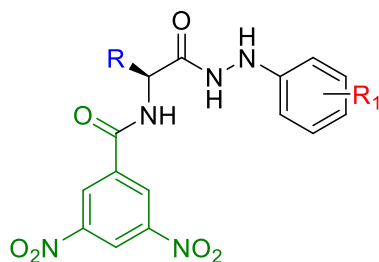


Figure 69: Significant loss of antituberculosis activity among of the *meta* and *para* substituted hydrazide 3,5 dinitrobenzene.

The MIC results (Table 7) indicated that the 3,5-dinitrobenzene substituted homophenylalanine-2-hydrazide **89c** had considerable antituberculosis action against sensitive, mono-resistant, and double-resistant *Mtb* strains, with a MIC value of 2 μ M. This indicated outstanding inhibition of the mycobacterial growth, and therefore, the applicability of this compound to be a hit compound to combat tuberculosis disease.

Overall, the 3,5-dinitrobenzene scaffolds have a definite impact on the anti-*Mtb* activity shown for most of the compounds, suggesting that this core is essential for activity. Moreover, a widely accepted and commonly used concept suggests that the reduction of nitro compounds leads to the formation of toxic intermediates, such as nitroso and superoxide species. Subsequently, the reduced nitro species form covalent bonds with DNA, leading to nuclear impairment and the death of cells¹⁴⁶. Therefore, we have explored the toxicity of the selected examples of the 3,5-dinitrobenzene substituted amino acid hydrazide compounds using viability cell assay of a mammalian cell line (Table 8).



84a - 89g

Entry	R	R ₁	Survivability %
84a	Gly	4-Br	55
86d	Phe	3-Br	42
86g	Phe	3-CF ₃	51
87a	Leu	3-Cl	15
87b	Leu	4-Cl	74
87d	Leu	3-Br	98
87e	Leu	4-Br	39
87f	Leu	2-CF ₃	9
87g	Leu	3-CF ₃	33
88a	Met	4-Cl	44
88b	Met	2-Br	36
88c	Met	3-Br	29
88d	Met	4-Br	76
88e	Met	2-CF ₃	68
88f	Met	3-CF ₃	45
89d	Hph	3-Br	24
89e	HPh	4-Br	9
89f	Hph	2-CF ₃	79
89g	Hph	3-CF ₃	109

Table 8: Results of selected examples examined for mammalian cytotoxicity assay, survivability percentage at (50 μ M), cell type= Human NCI-H460 lung carcinoma cells to the agents were determined using MTT assay, cell numbers= 2000, MIC and MTT assays were done by Dr A. Brown.

Guided by this, the data showed considerable toxicity as low percentage of viable cells observed with most of the 3,5-dinitro substituted amino acid compounds **84 – 89 g**, most likely due to the presence of the dinitro group within these molecules. For instance, compounds from **84a – 89g** (Table 8) showed a high percentage of toxicity (9 %) such as in compound **87f** and **89e** obtained at 50 μ M, suggesting their limited applicability of these compounds as future drug candidates. It is highly likely that the mechanism of action, which involves oxidative stress, can account for the high toxicity of this series of compounds against mammalian cells.

Upon analysis, compounds **89f**, **89g**, **87d**, **88d**, **84a**, **87b** and **86g** demonstrated reduced toxicity as seen by the significant percentage of viable mammalian cells. In addition, their MIC values were found to be high ranging between 30 μ M to 125 μ M, indicating that these agents may not be able to penetrate the cell wall. However, compounds **89e**, **87f**, and **87a** exhibited strong cytotoxic activity, (9 % and 15 %) respectively, of viable cell survived (Table 8).

To summarise, as explained earlier (*cf.* Chapter 1 and 2), this research focused on identifying compounds that are effective against tuberculosis disease using the scaffold hopping approach. In this Chapter, 3,5-dinitrobenzene substituted amino acid hydrazide compounds were successfully synthesized and SAR evaluated employing wild type, mono resistant, and double resistant Mycobacterial strains. Results supported antituberculosis efficacy of most of these compounds. However, cytotoxicity data of these compounds found them to be extremely toxic to mammalian cells. Consequently, we intend to proceed with the scaffold hopping method to investigate the impact of a nitrogen-containing compound and its coupling with the amino acid hydrazide moiety, to produce and study the structure-activity relationship (SAR). Therefore, the following chapter will discuss the synthesis of the 4-nitroimidazole and NBD-Cl scaffolds additional to the unsuccessful attempts to coupling these moieties with *N*-amino acid hydrazide framework.

4. Chapter4: Attempts to synthesise of 4-nitroimidazole and NBD scaffolds substituted amino acid hydrazide compounds.

4.1 Introduction

In the previous Chapter, compounds of 3,5-dinitrobenzene substituted amino acid hydrazides were investigated as potential antituberculosis agents, evaluated for SAR and their cytotoxicity. Anti-bacterial activity was demonstrated, but there were concerns regarding their cytotoxicity. Consequently, an investigation of various nitrogenous chemical scaffolds and their impact on anti-TB activity was conducted.

The chosen pharmacophores comprised a 4-nitroimidazole compound in the known anti-TB medication Pretomanid **31** and 4-chloro-7-nitro-1,2,3-benzoxadiazole (NBD-Cl) **46**, an analogue of our existing 4-chlorobenzoxa-[2,1,3]-diazole scaffold (*cf.* Chapter 1, Section 1.7).

Pretomanid is an oral anti-mycobacterial medication belonging to the class of bicyclic nitroimidazoxazine compounds. It consists of a nitroimidazole pyran A/B ring, an ether link to a hydrophobic side chain. This drug exhibits therapeutic activity against both replicating and non-replicating bacilli. Pretomanid **31**, which is a compound based on the nitroimidazole, is highly effective against both drug-sensitive and drug-resistant *Mtb* isolates. The structure-activity relationship (SAR) analysis revealed that the nitro group was essential for achieving high activity alongside the stereochemistry in determining the activity (Figure 70)¹⁵⁶.

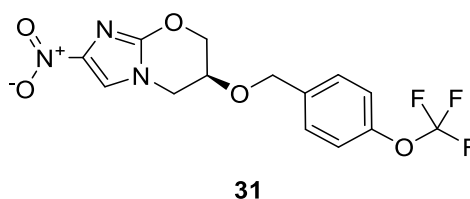


Figure 70: Chemical structure of Pretomanid

In connection with the project aim of discovering novel anti-TB agents to tackle TB disease and address the emergent rise in MDR and XDR TB, the synthesise of 4-nitroimidazole pharmacophore present in the Pretomanid drug was planned. This pharmacophore will be coupled with amino acid hydrazides to create the 4-nitroimidazole substituted amino acid hydrazide compound **89**, which will

subsequently be evaluated for its anti-TB activity using the REMA assay. Consequently, the synthesis of the 4-nitroimidazole scaffold and the attempted synthesis of the 4-nitroimidazole substituted amino acid hydrazide molecule **89** will be discussed in the subsequent sections (Figure 71).

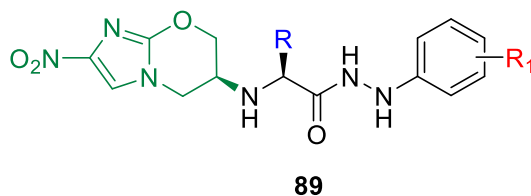
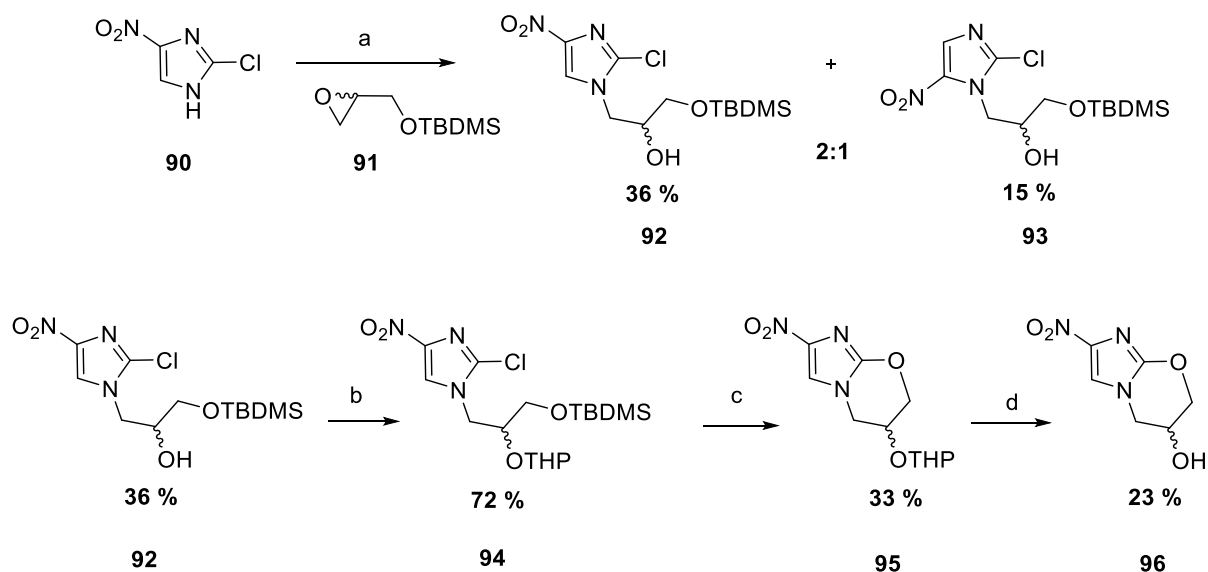


Figure 71: Structure of the 4- imidazole substituted amino acid hydrazide compound **89**.

4.2 Synthesis of the 4-nitroimidazole precursor.

As mentioned earlier, to explore the incorporation of nitro groups using the scaffold hopping approach, attention turned to the 4-nitroimidazole pharmacophore from the Pretomanid scaffold. For the synthesis of the 4-nitroimidazole moiety, literature approach to develop a suitable coupling partner for the amino acid hydrazides was followed¹⁵⁷. To begin, the epoxide **91** was reacted with the 4-nitroimidazole **90** to produce a regioisomeric combination of alcohols **92** and **93** in a ratio of 2:1. Flash chromatography was able to separate the two isomers allowing the desired major isomer **92** to be taken forward. THP protection of 4-nitroimidazole **94** followed by cyclisation with TBAF yields the bicyclic molecule **95**. Finally, deprotection of the alcohol with acetic acids yielded the free alcohol **96** in good overall yield (Scheme 8).



Scheme 8; Reagents and conditions. (a) **91**, K₂CO₃, EtOH, reflux, 70 °C, 20 h; (b) DHP, PPTS, CH₂Cl₂, rt, 2d, (c) TBAF, THF, rt, 18 h; (d) AcOH, THF, H₂O 60 °C, 18 h (%) percentage yield.

After deprotection of the THP group, the product was triturated using *n*-hexane to produce a white solid **96** with the structure confirmed by ¹H NMR showing the six protons including a singlet proton in the 4-nitroimidazole ring observed at 8.20 ppm, in addition to the five protons in the oxazolin ring obtained as doublet of doublets (dd) peaks observed at 4.30 and 4.08 ppm and doublet of doublets (dd) peaks at 3.61 and 3.53 ppm. In addition to the chiral proton observed around 4.01 ppm shows as a multiplet, this data matches the literature source^{157, 158}. Therefore, alcohol **96** was used in the coupling reaction to introduce the hydrazide moiety to synthesise the 4-nitroimidazole substituted amino acid hydrazide compound **89**.

4.3 Attempts to synthesise the 4-nitroimidazole amino acid hydrazide compounds

4.3.1 Introduction

To synthesise the 4-nitroimidazole substituted amino acid hydrazide compounds, it was necessary to convert the free alcohol group of **96** to a good leaving group. There are several synthetic methods to accomplish this objective. One method employs an S_N2 reaction by converting the alcohol to a good leaving group, such as *p*-toluenesulfonyl or methanesulfonyl (Figure 72A)¹⁵⁹. Likewise, a Mitsunobu reaction is a highly effective reaction in organic synthesis that transforms the

hydroxyl group to an alkoxyphosphonium ion to make it susceptible to a nucleophilic substitution in a one-pot reaction (Figure 72B)¹⁶⁰.

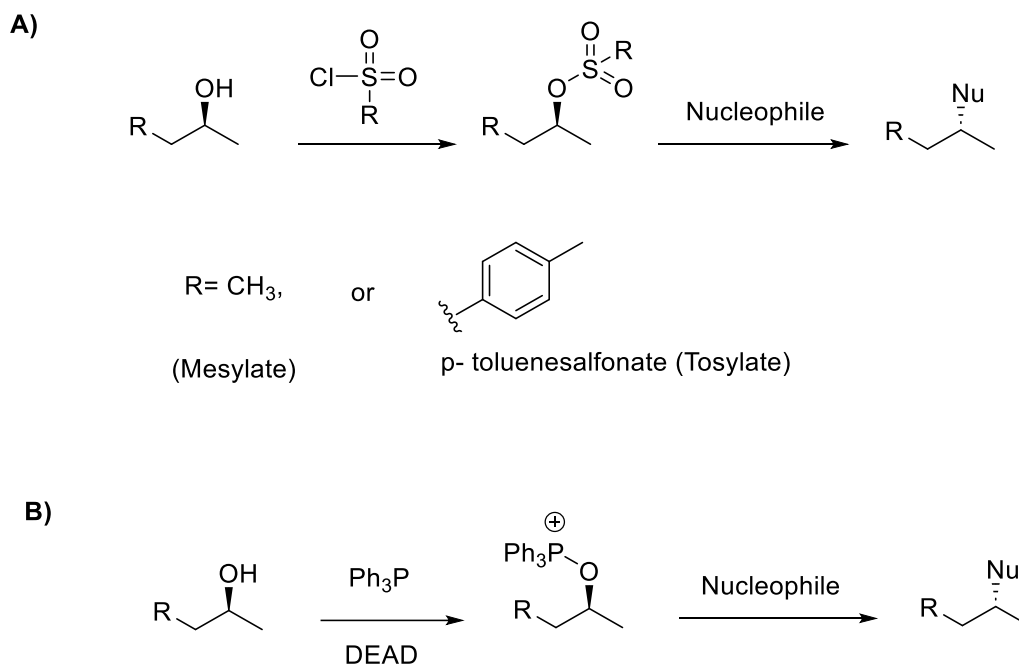
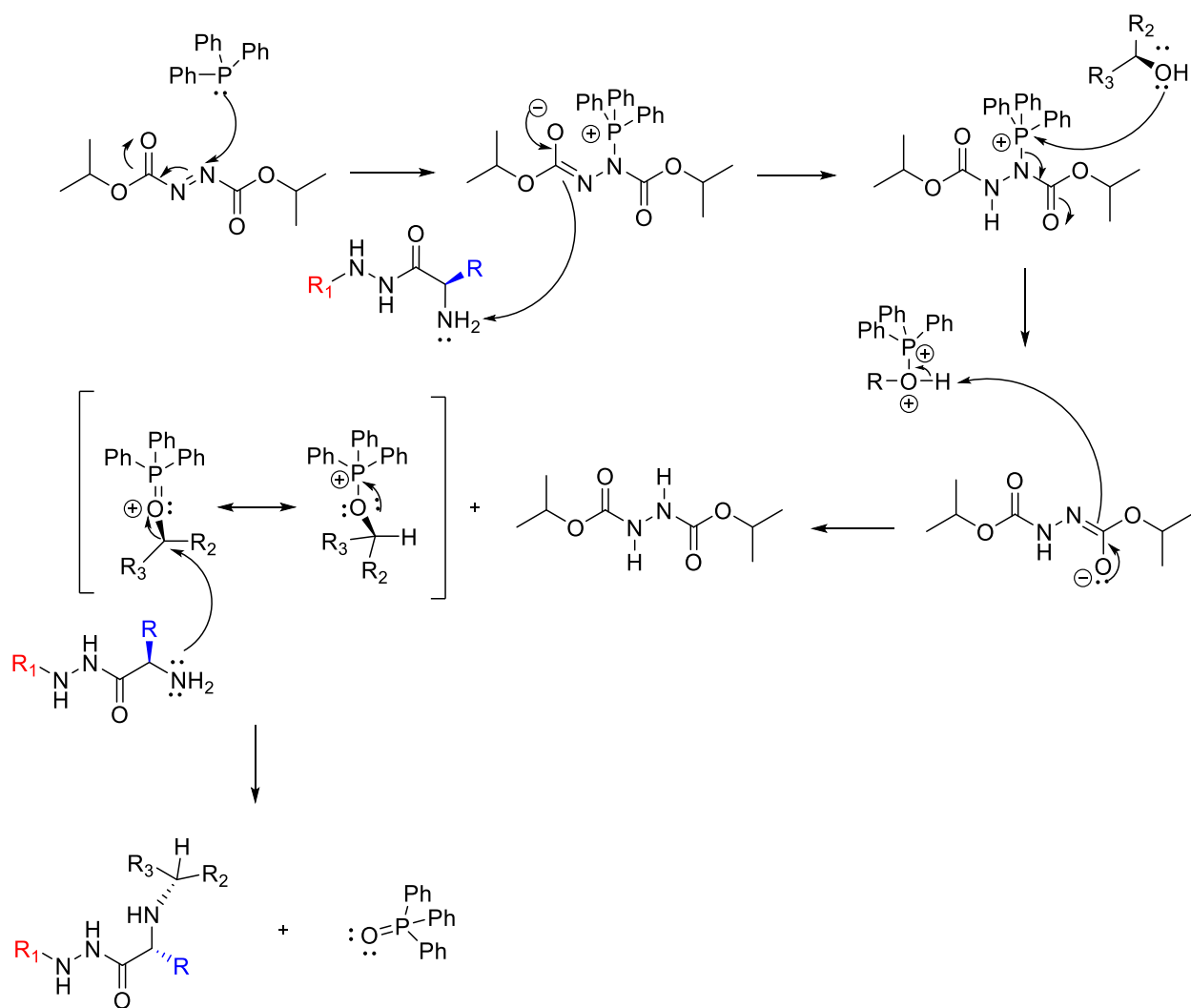


Figure 72: A). Schematic representation of the conversion of alcohol to good leaving group sulfonate. B) Conversion of alcohol into alkoxyphosphonium ion susceptible to nucleophilic substitution in Mitsunobu reaction.

Therefore, these techniques were used due to their mildness, selectivity, and efficiency in producing the target molecules.

4.3.2 Mitsunobu reaction

The use of a Mitsunobu reaction was explored, with triphenylphosphine and DIAD reacting to produce a triphenylphosphonium intermediate, which is then attacked by an alcohol group. The procedure is completed by substituting the activated phosphonium with a carboxylate, mercaptyl, or in this instance the *N*-amino acid hydrazide (Scheme 9)¹⁶¹.



Scheme 9: Mitsunobu reaction mechanism in which activating the alcohol oxygen as a leaving group to allow substitution with the amino acid hydrazide molecule¹⁶¹.

In the initial attempt to synthesise a 4-nitroimidazole substituted amino acid hydrazide compound involved the use of triphenylphosphine (PPh₃) and diisopropyl azodicarboxylate (DIAD). Thus, the alcohol **96** was dissolved and deprotected amino acid hydrazide **55** with triphenylphosphine and DIPEA as a base in THF, then the mixture cooled in an ice bath before adding the DIAD reagent slowly with stirring at room temperature for several hours. The reaction was monitored by TLC, showing the disappearance of the starting material and the formation of multiple new products after 3 h. Analysis of the ¹H NMR of the crude mixture showed the formation of a highly complex product with no signals for the desired product **89** (Figure 73).

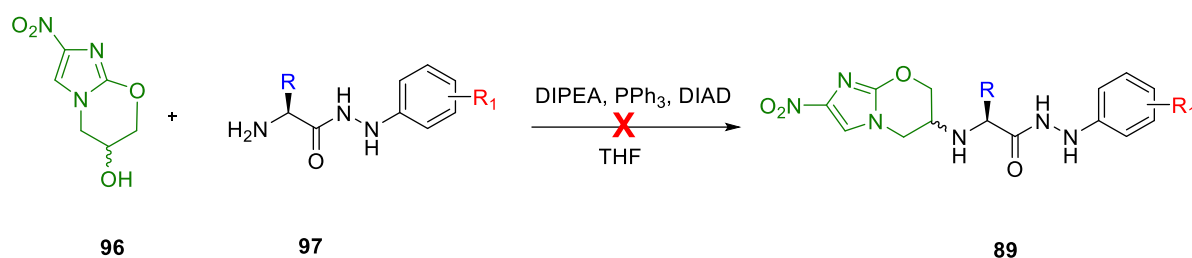


Figure 73: Schematic representation of Mitsunobu reaction.

Another Mitsunobu reaction attempt involved changing the order of addition for the reagents¹⁶², consequently, the diisopropyl azodicarboxylate (DIAD) was added to the stirring mixture of the triphenylphosphine in tetrahydrofuran, the reaction mixture was cooled to 0 °C before the addition of the 1 equivalent of the alcohol **96** and the amino acid hydrazide **97**. The reaction mixture was stirred for 3 to 4 hours whereupon TLC showed the disappearance of the starting material but with multiple products formed. The ¹H NMR spectrum of the crude product showed no signals for the intended product **89** leading to the conclusion that this reaction was unsuccessful.

Another attempt focused on increasing the equivalency of the nucleophile in the reaction, therefore, 1.5 equivalent of the amino acid hydrazide **97** was added to 1 equivalent of the alcohol **96**, then they were suspended in the THF at 0 °C. Following that, the triphenylphosphine was added then the dropwise addition of the DIAD reagent. The reaction mixture was stirred for several hours with the TLC showing multiple products, supported by the ¹H NMR spectrum presenting a complex mixture suggesting the reaction did not work.

Accordingly, our efforts to achieve success through the Mitsunobu reaction appeared to be ineffective. Consequently, we made the following attempt to convert the OH group into a good leaving group using a tosylation reaction.

4.3.2 Tosylation reaction

The toluenesulfonyl group, often known as the tosyl group (Ts or Tos), is a univalent functional group in the field of organic chemistry¹⁶³.

In this attempt, 1 eq. of the 4-nitroimidazole alcohol **96** was treated with 1. eq. of tosyl chloride in the presence of pyridine at room temperature for several hours. However, ¹H NMR analysis of the crude material did not show signals

corresponding to the anticipated product **98**, but signals for the starting material indicating that the reaction had not worked (Figure 74).

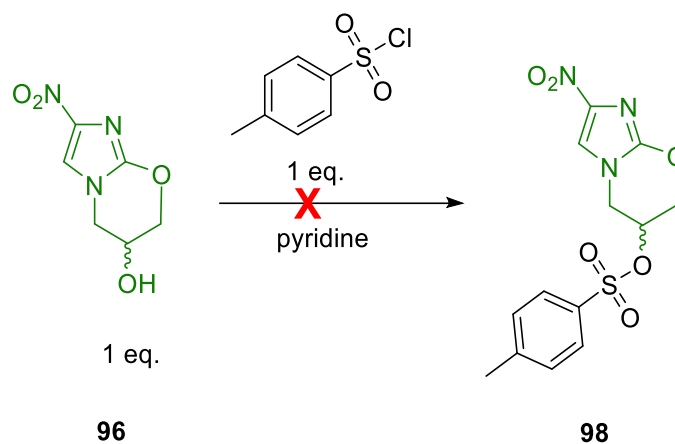


Figure 74: Converting alcohol **96** to toluene-4-sulphonic acid ester group which is good leaving group in the intended product **98**.

In another attempt, the 4-nitroimidazole alcohol **96** was dissolved in DCM and cooled to 5 °C, then, *p*-toluene sulphonyl chloride was added followed by pyridine¹⁶⁴. The reaction was stirred at room temperature for several hours until the disappearance of the starting material by TLC. After an aqueous workup, ¹H NMR analysis revealed a complex mixture of products had formed with no evidence for the desired product.

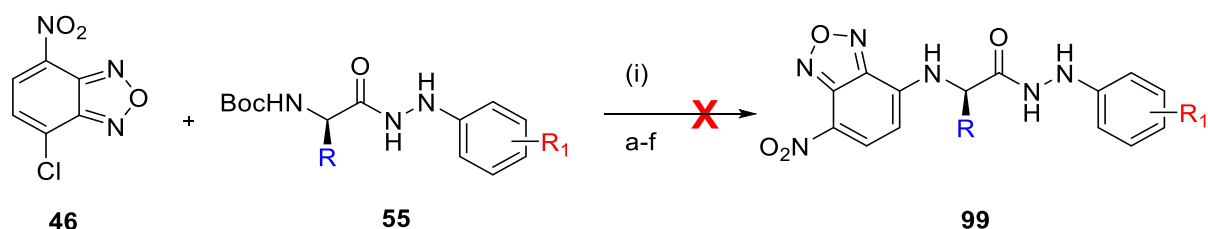
Due to the challenges encountered in the production of 4-nitroimidazole substituted amino acid hydrazides **89**, we shifted our focus towards 4-chloro-7-nitrobenzofurazan (NBD-Cl).

4.4 Reaction of the NBD-Cl with amino acid hydrazide compound

To address the issue of MDR and XDR TB following our project aim (Chapter 1, Section 1.7), an investigation of a nitrogenous molecule and explore its potential coupling with the amino acid hydrazide moiety was conducted. In this section, the commercially available 7-nitrobenzo-2,1,3-oxadiazole chloride (NBD-Cl) compound was applied. The goal of this investigation is to evaluate the antituberculosis activity of the NBD-substituted amino acid hydrazide compounds using the REMA assay, which will enable the generation of a structure-activity relationship (SAR) study.

The 7-nitrobenzo-2,1,3-oxadiazole (NBD) compound, developed in the late 1960s, is an excellent fluorescent label and has been commonly used in biology for a wide range of imaging agents, peptide, lipid, biotin, carbohydrate, protein and other labelling. The synthetic strategy to introduce the NBD molecule is typically carried out by a S_NAr reaction. An amine, either primary or secondary, reacts with the corresponding halide, either chloride or fluoride, to form the intensely fluorescent product^{165,166}.

The attempt to produce the desired NBD substituted amino acid hydrazide compound **99** (Scheme 10) involved using the nucleophilic aromatic substitution reaction in which the chloride is attacked with amine of the amino acid hydrazide **55**.



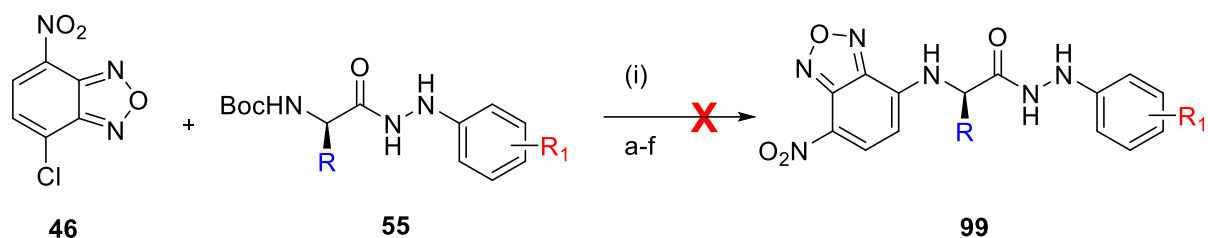
Scheme 10: reaction of the NBD-Cl with amino acid hydrazide compound to produce the NBD-Cl amino acid hydrazide containing product **99**. (i) 4N HCl in dioxan. (a-f) reaction condition listed in Table 1.

In this attempt, 1 equiv. of the NBD-Cl and 1.1 amino acid hydrazide reacted in presence of (0.1 M) phosphate saline buffer (PSB) in ethanol,¹⁶⁷ the mixture stirring at room temperature for several hours, the TLC showing formation of the new product, the ¹H NMR crude analysis showed the starting material. As polar protic solvent was used in this reaction, therefore, this might result in high solvation effect that weaken the nucleophilicity of the amine,¹⁶⁸ thus the nucleophilic aromatic substitution reaction was not take place. Furthermore, the potential for a hydrolysis reaction due to the ethanol employed in this reaction may occur; however, the ethyl signals are not evident in the crude HNMR spectrum.

Consequently, in another attempts, polar aprotic solvents that lack the acidic hydrogen have been used. These solvents such as dimethylformamide, acetonitrile and tetrahydrofuran may result in weak solvation effect thus would increase the reactivity of the nucleophile. In this reaction, 1 equiv. of the NBD-Cl was treated with 1.2 equiv. amino acid hydrazide in presence of the 3 equiv. of

base at room temperature ¹⁶⁹ (Table 1). The reaction was monitored by TLC, showing the disappearance of the starting material and the formation of a new product. Analysis of the ¹H NMR of the crude mixture showed the complex mixture formed.

Another attempt involves using of the tetrabutylammonium iodide (TBAI) reagent as catalyst to increase the reactivity of the chloride in the NBD-Cl compound toward the nucleophilic attack of the amine, therefore, 1.1 equiv. of the NBD-Cl and 1.2 equiv. of the amino acid hydrazide was reacted in the presence of the TBAI in DMF, the ¹H NMR of the crude revealed presence of the starting material suggesting that the reaction was not take place (Table 9).



Reagent	Time/h	Reaction outcome
a) 0.1 M phosphate buffer saline, EtOH, 1:1 v/v	3	starting material
b) Et ₃ N, THF, r.t	4	complex mixture obtained
c) DIPEA, DMF, r.t	3	complex mixture obtained
d) Et ₃ N, Acetonitrile	4	complex mixture obtained
e) Et ₃ N, DMF, r.t	5	complex mixture obtained
f) TBAI, DMF, r.t	Overnight	starting material

Table 9: Attempts to synthesis NBD-Cl substituted amino acid hydrazide compound **99**, (i) 4N HCl in dioxan.

Having discussed the attempts to synthesise the amino acid hydrazide substituted 4-nitroimidazole or NBD-Cl scaffolds, this thesis is going to draw a conclusion and propose possibilities for further research.

4.5 Conclusion and Future work

4.5.1 Thesis Conclusion

As previously mentioned in Chapter 1, the prevalence of tuberculosis (TB) disease is increasing, and the complexity is exacerbated by the spread of multidrug-resistant (MDR) and extensively drug-resistant (XDR) strains. Despite

the growing number of research efforts to identify new antibiotics, combating antibiotic-resistant TB infections remains an enormous challenge.¹³¹ This project aimed to identify a new agent that can effectively combat the proliferation of *Mtb*. Therefore, the scaffold hopping strategy was employed as the methodology for this study. In Chapter 2, the synthesis and evaluation of the structure-activity relationship (SAR) of the imidazo[1,2 a] pyridine substituted amino acid hydrazide compound are conducted utilising the REMA assay. The compound exhibited enhanced selectivity towards the monoresistant strain, but with limited anti-TB efficacy. In particular, the imidazo[1, 2a] pyridine containing unsubstituted amino acid side chain has been the best for among this compound library, in addition to the presence of the trifluoromethyl group in *meta* position of the phenyl hydrazine fragment such as compound **61a**. Furthermore, in Chapter 3, synthesis and evaluation of the structure-activity relationship (SAR) for 3,5-dinitrobenzene substituted amino acid hydrazide compounds using the REMA assay was conducted. The biological results showed that these compounds exhibited a remarkable anti-TB activity, exceeding the previous imidazo[1,2 a] pyridine library of compounds. Low MIC results was found with agents such as **89c**, **68b**, and **89a**. Those compounds have high Log P values (4.17), suggesting that this characteristic increases the inhibitory activity against the *Mtb*. Furthermore, a cytotoxicity assay was conducted on a selected example of this series, demonstrating the presence of significant toxicity in certain examples such as **89e**, **87f**, and **87a** while other compounds seemed acceptable such as **89f**, **89g**, **87d**, **88d**, and **86g**. Following that, we decided to focus our study on the examination of one nitrogenous-containing moiety, such as the 4-nitroimidazole scaffold, in the Pretomanid medication and NBD-Cl. Unfortunately, this objective was not achieved, therefore more experiments should be done in this area of research. Finally, this research participates in the field of discovering anti-TB agents and this can be a starting point for a more in-depth drug-to-target identification project.

4.5.2 Future work and additional studies

4.5.2.1 Synthesis of NBD-substituted amino acid hydrazide compound using alkyl ester amino acid.

Following an unsuccessful attempt to coupling the NBD-Cl with the hydrazide moiety (*cf.* Chapter 4, Section 4.4), the intention was shifted to employ the free amine amino acid in place of the amino acid hydrazide molecule. The reaction involved substitution of the good leaving group, chloride in the NBD-Cl **46** compound and replaced by the free amine of the amino acid **100** compounds utilising S_NAr reaction in the presence of base. This may lead to the NBD substituted amino acid alkyl ester compound **101**, which will undergo ester hydrolysis reaction. This would allow the coupling of the carboxylic acid in **102** with the phenyl hydrazine **103** to produce the NBD- amino acid hydrazide-containing compound **104** (Figure 75).

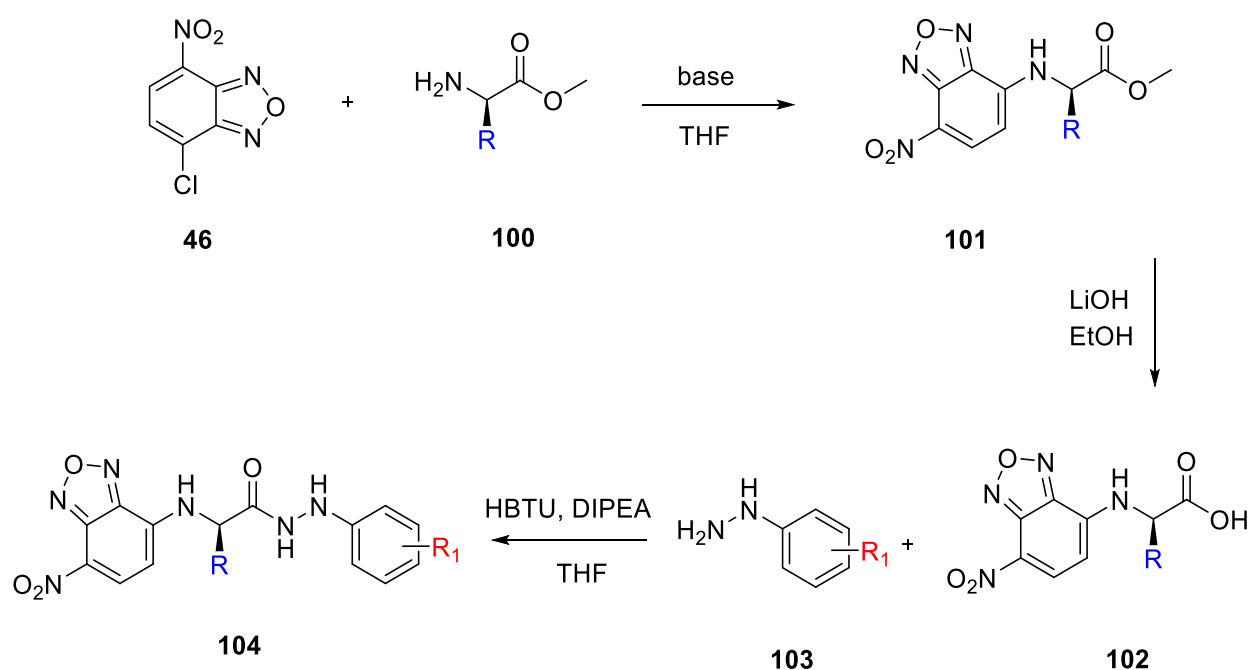


Figure 75: Schematic representation for synthesis of the NBD-Cl substituted amino acid hydrazide **104** using alkyl ester amino acid compound **100**. R= H or CH₃, R₁= substituted phenyl hydrazine.

In this reaction, one equivalent of the methyl ester glycine **105** was used and reacted with one equivalent NBD-Cl **46** in the presence of base and THF as a solvent, the reaction was monitored by TLC, the starting material was consumed and multiple products were observed, following an aqueous workup, the ¹H NMR showing starting material with no traces of the desired product **106** (Figure 76).

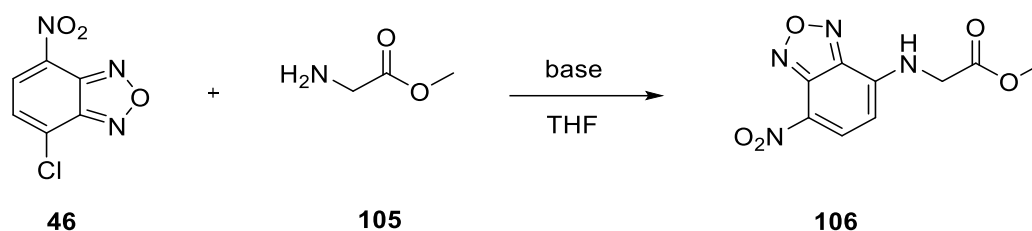


Figure 76: Synthesis of the NBD-Cl **46** substituted amino acid hydrazide using methyl ester of glycine amino acid **105**.

4.5.2.2 Synthesis of adamantyl substituted amino acid hydrazide compounds.

Currently, the adamantane moiety is commonly incorporated into existing active medicines to enhance their lipophilicity and enhance their pharmacological effects¹⁷⁰. New TB drug candidate SQ109 **12** (*cf.* Chapter 1, Section 1.4.2.4) has a unique mode of action and has been well tolerated and safe in Phase I and early Phase II clinical trials. SQ109 is a potent therapeutic candidate for treating *Mtb* with an MIC value being 0.3 – 0.6 μ M (Figure 77).

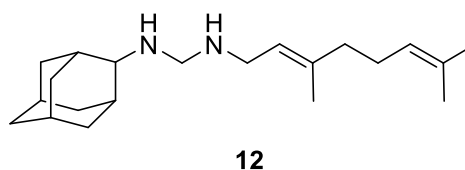
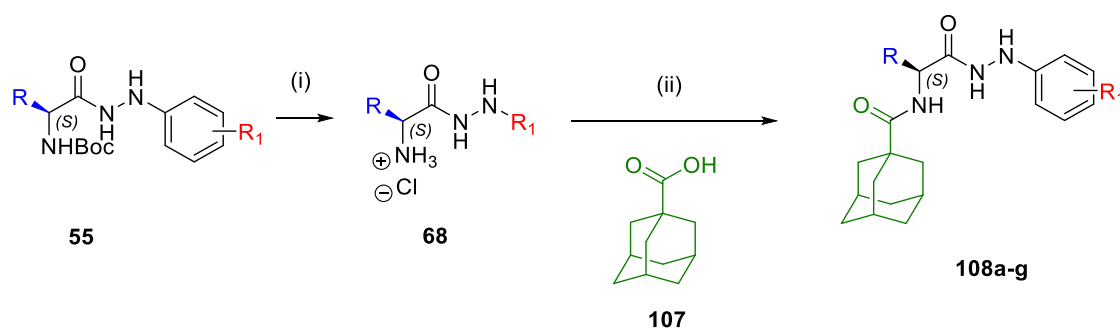


Figure 77: Chemical structure of the SQ109 **12** drug bearing an adamantane moiety.

As stated previously, we utilized the scaffold hopping approach in our research to discover new agents for treating drug-resistant forms of tuberculosis in both forms, MDR-TB and XDR-TB (Chapter 1, Section 1.7), therefore the synthesis of the adamantyl substituted amino acid hydrazide compounds was employed. The synthesis followed a coupling reaction between the commercially available 1-adamantyl carboxylic acid scaffold **107** and the *N*-amino acid hydrazide moiety to produce the corresponding compounds **108a-g** in modest yields (Scheme 11).



Scheme 11: synthesis of the adamantly substituted amino acid hydrazide compounds **108a-g**.

Their identity was confirmed chemically by ^1H NMR, ^{13}C NMR, IR and mass spectrometric analysis. To evaluate the antituberculosis activity, compounds **108a-g** were tested against sensitive and resistant strains of *Mtb*. Unfortunately, there was low inhibitory activity in sensitive and drug-resistant strains of *Mtb* at the maximum tested concentration (64 $\mu\text{g/mL}$) (Table 10).

Entry	R	R ₁	Yield (%)	WT (μM)	INH ^R (μM)	RIF/INH ^R (μM)	RIF/INH ^R (μM)
108a	Gly	4-CF ₃	49	-	-	177	177
108b	Ala	3-Cl	65	-	-	-	-
108c	Ala	4-CF ₃	38	-	-	-	-
108d	Phe	4-CF ₃	32	-	143	-	-
108e	Met	4-CF ₃	26	-	-	-	-
108f	Leu	4-CF ₃	20	-	-	-	-
108g	Ile	4-CF ₃	42	-	-	-	-

Table 10: MIC results for adamantly substituted amino acid hydrazide compounds against *Mtb* bacterial strains.

4.5.2.3 *In vivo* phenotypic screening.

The 3,5-dinitrobenzene substituted amino acid hydrazide compounds, observed to have the highest anti-TB activity such as compounds **89c**, **89a**, and **86a**, now need to be assessed in animal models to determine their anti-*Mtb* efficacy *in vivo*. The existing methodology entails the quantification of bacteria within the lungs by the utilisation of a colony-forming unit (Cfu) assay. However, the prolonged duration of these assays can be related to the slow proliferation of *Mycobacterium tuberculosis*¹⁷¹. Therefore, fluorescence assay tomography (FAT) can be performed to detect fluorescent *Mtb* cells in the lungs and then the resulting

image can be analysed and correlated with data obtained from a colony-forming unit (Cfu) assay¹⁷¹.

4.5.2.4 Evaluation of the Q203 analogues for anti-cancer and anti-proliferation activity.

Researchers have explored several non-oncology drugs for their possible antitumor effects. These include drugs having diverse applications, such as antiviral, anti-inflammatory, antipsychotic, antibacterial, and antifungal treatments¹⁷². For instance, Cerulenin is a fungal metabolite and a specific inhibitor of fatty acid synthase (FASN), which has shown a potential anticancer activity¹⁷³.

Consequently, although the low antituberculosis activity of the Q203 analogues, (*cf.* Chapter 2, Section 2.6.2) compounds **71a**, **72b**, **74f**, and **75c** exhibited high cytotoxicity effect, therefore, these compounds can be assessed for their anti-cancer and anti-proliferation activity. This evaluation will help determine their effectiveness and potential enhancement for existing chemotherapeutic agents.

Chapter 5. Experimental section.

5. General Experimental information.

5.1 Analysis

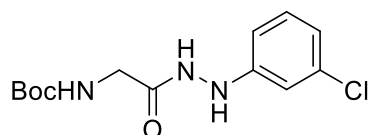
All reactions were carried out under a nitrogen atmosphere in glassware dried in an oven overnight (>75 °C) or under a high vacuum by a heat gun unless otherwise stated. 40-60 pet. ether refers to the fraction of petroleum ether boiling between 40 and 60 °C and was redistilled before use. Ether refers to diethyl ether. Solvents were obtained dry from Sigma or another appropriate chemical supplier and used as supplied. In cases where mixtures of solvents were utilised, the ratios refer to the volumes used. Reagents were used as supplied unless otherwise stated. Flash chromatography was carried out using silica gel 40-63 μ 60 Å. Analytical thin layer chromatography (TLC) was performed using precoated aluminium or glass-backed plates (silica gel 60 Å F₂₅₄) and visualised by UV radiation at 254 nm, or by staining with phosphomolybdic acid in ethanol or potassium permanganate in water. All melting points were determined using a Gallenkamp melting point apparatus and are uncorrected. Gas chromatography was carried out on a Hewlett-Packard 5890 Series II fitted with a 25 m column. Detection was by flame ionisation. Infrared spectra were recorded using a Diamond ATR (attenuated total reflection) accessory (Golden Gate) or as a solution in chloroform *via* transmission IR cells on a Bruker Tension 5 spectrometer. ¹H NMR spectra were recorded in CDCl₃ on Varian Mercury 200, Varian Unity-300, Varian VXR-400 or Varian Inova-500 instruments and are reported as follows; chemical shift δ (ppm) (number of protons, multiplicity, coupling constant *J* (Hz), assignment). Residual protic solvent CHCl₃ ($\delta_{\text{H}} = 7.26$) or DMSO ($\delta_{\text{H}} = 2.50$) were used as the internal reference. ¹³C NMR spectra were recorded using the central resonance of CDCl₃ ($\delta_{\text{C}} = 77.0$ ppm) or DMSO ($\delta_{\text{C}} = 39.5$ ppm) as the internal reference. All chemical shifts are quoted in parts per million relatives to tetramethylsilane ($\delta_{\text{H}} = 0.00$ ppm) and coupling constants are given in Hertz to the nearest 1 Hz. Assignment of spectra were carried out using COSY, HSQC, HMBC and NOESY experiments. Gas chromatography-mass spectra (EI) were obtained using a Thermo TRACE mass spectrometer. Electrospray mass spectra (ES) were obtained on a Micromass LCT mass spectrometer. High resolution mass spectra were obtained using a Thermo LTQ mass spectrometer (ES) at Newcastle University.

Chapter 5. Experimental section.

5.1.1 Synthesis of N-protected Hydrazides – General Procedure

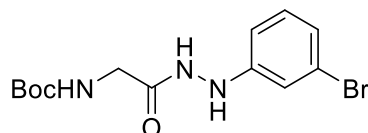
Firstly, *N*-protected amino acid (1 equiv.) was dissolved in THF (5 mL) under a nitrogen atmosphere at room temperature and treated with DIPEA (1.5 equiv.) followed by HBTU (1.2 equiv.). After that, substituted phenyl hydrazine (1.1 equiv.) was added at room temperature and stirring for 5 hours. Reaction mixed with Et₂O (10 mL) and distilled water (5 mL). After separation of the two phases the organic layer washed again with distilled water (5 mL × 3 mL) followed by a wash with sat. aq. NH₄Cl (6 mL) then sat. aq. NaHCO₃ (6 mL) followed by brine (8 mL). Organic layer dried over MgSO₄, filtered, evaporated and dried in *vacuo* achieving the desired *N*-Boc hydrazides **61a - 67f**.

***tert*-Butyl (2-(2-(3-chlorophenyl)hydrazinyl)-2-oxoethyl)carbamate 61a**



Following the general procedure outlined, *N*-Boc-glycine (0.23 g, 1.32 mmol) and 3-chlorophenylhydrazine hydrochloride (0.28 g, 1.58 mmol) were transformed following work up with EtOAc into the title compound which was isolated as a light yellow solid (0.19 g, 59 %); R_f 0.39 (DCM/EtOH/NH₃ 200:8:1); δ_H (700 MHz, CDCl₃) 8.43 (1H, s, CONH₂), 7.11 (1H, t, *J* 7, Ar-*H*), 6.84 (1H, dd, *J* 7, 1, Ar-*H*), 6.79 (1H, t, *J* 1, Ar-*H*), 6.67 (1H, dd, *J* 7, 2, Ar-*H*), 6.22 (1H, s, CONH₂) 5.38 (1H, s, NHCH₂), 3.88 (1H, d, *J* 5, NHCH₂), 1.47 (9H, s, C(CH₃)₃).

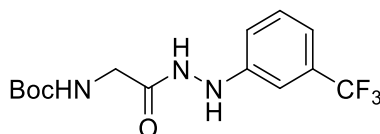
***tert*-Butyl (2-(2-(3-bromophenyl)hydrazinyl)-2-oxoethyl)carbamate 61b**



Following the general procedure outlined, *N*-Boc-glycine (0.23 g, 1.32 mmol) and 3-bromophenylhydrazine hydrochloride (0.28 g, 1.58 mmol) were transformed following work up with EtOAc into the title compound which was isolated as a pale yellow solid (0.21 g, 47 %); R_f 0.39 (DCM/EtOH/NH₃ 200:8:1); δ_H (700 MHz, CDCl₃) 8.43 (1H, s, CONH₂), 7.11 (1H, t, *J* 7, Ar-*CH*), 6.84 (1H, dd, *J* 7, 1, Ar-*CH*), 6.79 (1H, t, *J* 1, Ar-*CH*), 6.67 (1H, dd, *J* 7, 2, Ar-*CH*), 6.22 (1H, s, CONH₂) 5.38 (1H, s, NHCH₂), 3.88 (1H, d, *J* 5, NHCH₂), 1.47 (9H, s, C(CH₃)₃).

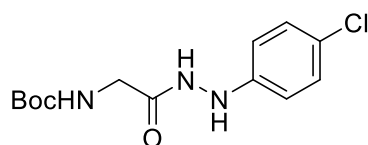
Chapter 5. Experimental section.

***tert*-Butyl (2-oxo-2-(2-(3-(trifluoromethyl)phenyl)hydrazineyl)ethyl) carbamate 61c**



Following the general procedure outlined, *N*-Boc-glycine (0.40 g, 2.28 mmol) and 3-trifluoromethylphenylhydrazine hydrochloride (0.53 g, 2.51 mmol) were transformed following work up with Et₂O into the title compound which was isolated as an orange solid (0.33 g, 70 %); R_f 0.44 (*n*-hex/EtOAc 4:1); δ_H (300 MHz, CDCl₃) 8.68 (1H, s, CONH₂), 7.25 (1H, d, *J* 7, Ar-*H*), 7.10 (1H, d, *J* 7, Ar-*H*), 7.00 (1H, s, Ar-*H*), 6.94 (1H, dd, *J* 8, 2, Ar-*H*), 5.48 (1H, s, BocNHCH₂), 3.88 (2H, d, *J* 5, BocNHCH₂), 1.44 (9H, s, (CH₃)₃CO);

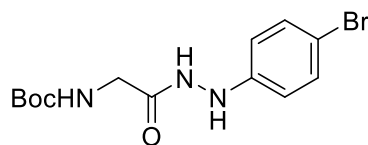
***tert*-Butyl-(2-(2-(4-chlorophenyl)hydrazinyl)-2-oxoethyl)carbamate 61d**



Following the general procedure outlined, *N*-Boc-glycine (0.20 g, 1.14 mmol) and 4-chlorophenylhydrazine hydrochloride (0.25 g, 1.37 mmol) were transformed following trituration with Et₂O into the title compound which was isolated as a white solid (0.18 g, 40 %) R_f 0.34 (*n*-hex/EtOAc 4:1); δ_H (300 MHz, CDCl₃) 8.45 (1H, bs, CONH₂), 7.15 – 7.13 (2H, d, *J* 8, Ar-*H*), 6.73 – 6.71 (2H, d, *J* 8, Ar-*H*), 6.25 (1H, bs, Ar-NH), 5.41 (1H, b, BocNHCH₂), 3.86 (2H, d, *J* 5, BocNHCH₂), 1.46 (9H, s, (CH₃)₃CO).

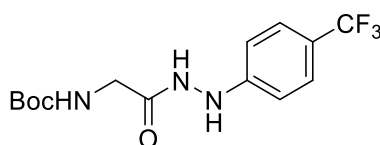
Chapter 5. Experimental section.

***tert*-Butyl (2-oxo-2-(2-(4-(bromophenyl)hydrazineyl)ethyl) carbamate 61e**



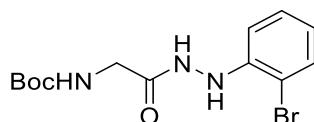
Following the general procedure outlined, *N*-Boc-glycine (0.20 g, 1.14 mmol) and 4-bromophenylhydrazine hydrochloride (0.25 g, 1.37 mmol) were transformed following trituration with Et₂O into the title compound which was isolated as a white solid (0.32 g, 88 %) R_f 0.30 (DCM/EtOH/NH₃ 200:8:1; (300 MHz, CDCl₃) δ_H 8.45 (1H, s, CONHNH), 7.15 – 7.13 (2H, d, *J* 8, Ar-*H*), 6.73 – 6.71 (2H, d, *J* 8, Ar-*H*), 6.25 (1H, s, Ar-NH), 5.41 (1H, s, BocNHCH₂), 3.86 (2H, d, *J* 5, BocNHCH₂), 1.46 (9H, s, (CH₃)₃CO).

***tert*-Butyl (2-oxo-2-(2-(4-(trifluoromethyl)phenyl)hydrazineyl)ethyl) carbamate 61f**



Following the general procedure outlined, *N*-Boc-glycine (0.50 g, 2.90 mmol) and 4-trifluorophenylhydrazine hydrochloride (0.61 g, 3.50 mmol) were transformed following trituration with Et₂O into the title compound which was isolated as a white solid (0.32 g, 50 %); δ_H (700 MHz, DMSO-*d*₆) 9.78 (1H, s, CONHNH), 8.32 (1H, s, CONHNH), 7.40 (2H, d, *J* 9, Ar-*H*), 7.07 (1H, t, *J* 6, BocNH), 6.78 (2H, d, *J* 9, Ar-*H*), 3.60 (2H, d, *J* 6, NHCH₂), 1.37 (9H, s, (CH₃)₃CO);

***tert*-Butyl (2-(2-(2-bromophenyl)hydrazineyl)-2-oxoethyl)carbamate 61A**

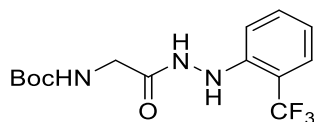


Following the general procedure outlined, *N*-Boc-glycine (0.40 g, 2.28 mmol) and 2-bromophenylhydrazine hydrochloride (0.56 g, 2.51 mmol) were transformed following work up with Et₂O into the title compound which was isolated as a yellow oil (0.39 g, 50 %) δ_H (300 MHz, CDCl₃) 8.52 (1H, s, CONHNH), 7.43 (1H, m, Ar-*H*), 7.16 (1H, td, *J* 8, Ar-*H*), 6.85 (1H, m, Ar-*H*), 6.77 (1H, td, *J* 7,1, Ar-*H*), 6.39

Chapter 5. Experimental section.

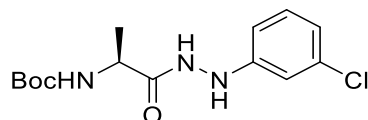
(1H, bd, J 3, Ar-NH), 5.45 (1H, s, BocNHCH₂), 3.88 (2H, d, J 6, BocNHCH₂), 1.45 (9H, s, (CH₃)₃CO);

tert-Butyl (2-oxo-2-(2-(2-(trifluoromethyl)phenyl)hydrazineyl)ethyl) carbamate 61B



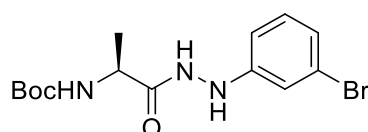
Following the general procedure outlined, *N*-Boc-glycine (0.40 g, 2.28 mmol) and 2-trifluoromethylphenylhydrazine hydrochloride (0.53 g, 2.51 mmol) were transformed following trituration with DCM into the title compound which was isolated as white yellowish solid (0.17 g, 22%); R_f 0.46 (*n*-hex/EtOAc 4:1); δ_H (300 MHz, CDCl₃) 8.23 (1H, s, CONH₂), 7.52 (1H, d, J 7, Ar-*H*), 7.41 (1H, t, J , Ar-*H*), 7.02 (1H, d, J 8, Ar-*H*), 6.99 (1H, t, J 7, Ar-*H*), 6.52 (1H, s, Ar-NH), 5.26 (1H, t, J 6, BocNHCH₂), 3.92 (2H, d, J 6, BocNHCH₂), 1.47 (9H, s, (CH₃)₃CO);

tert-Butyl (S)-(1-(2-(3-chlorophenyl)hydrazineyl)-1-oxopropan-2-yl) carbamate 62a



Following the general procedure outlined, *N*-Boc-*L*-alanine (0.25 g, 1.32 mmol) and 3-chlorophenylhydrazine hydrochloride (0.28 g, 1.56 mmol) were transformed following trituration with DCM into the title compound which was isolated as a white solid (0.34 g, 64 %); R_f 0.19 (DCM:EtOH:NH₃ 200:8:1); δ_H (300 MHz, CDCl₃) 8.52 (1H, s, CONH₂), 7.12 (1H, t, J 7, Ar-*H*), 6.85 (1H, d, J 7, Ar-*H*), 6.80 (1H, s, Ar-*H*), 6.70 (1H, d, J 7, Ar-*H*), 5.15 (1H, s, NHCH(CH₃)), 4.30 (1H, m, NHCHCH₃), 1.48 (9H, s, (CH₃)₃CO), 1.40 (3H, d, J 7, NHCH(CH₃));

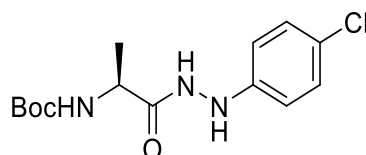
tert-butyl (S)-(1-(2-(3-bromophenyl)hydrazineyl)-1-oxopropan-2-yl)carbamate 62b



Chapter 5. Experimental section.

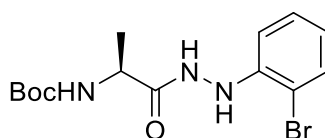
Following the general procedure outlined, *N*-Boc-*L*-alanine (0.25 g, 1.32 mmol) and 3-bromophenylhydrazine hydrochloride (0.28 g, 1.56 mmol) were transformed following trituration with DCM into the title compound which was isolated as white solid (0.20 g, 38 %); R_f 0.19 (DCM:EtOH:NH₃ 200:8:1); δ_H (300 MHz, CDCl₃) 8.52 (1H, s, CONHNH), 7.12 (1H, t, *J* 7, Ar-*H*), 6.85 (1H, d, *J* 7, Ar-*H*), 6.80 (1H, s, Ar-*H*), 6.70 (1H, d, *J* 7, Ar-*H*), 5.15 (1H, s, NHCH(CH₃)), 4.30 (1H, m, NHCHCH₃), 1.48 (9H, s, (CH₃)₃CO), 1.40 (3H, d, *J* 7, NHCH(CH₃));

tert-butyl (S)-(1-(2-(4-chlorophenyl)hydrazineyl)-1-oxopropan-2-yl) carbamate 62d



Following the general procedure outlined, *N*-Boc-*L*-alanine (0.10 g, 0.53 mmol) and 4-chlorophenylhydrazine hydrochloride (0.10 g, 0.53 mmol) were transformed following trituration with Et₂O into the title compound which was isolated as an yellow solid (0.19 g, 74 %); δ_H (300 MHz, CDCl₃) 8.68 (1H, s, CONHNH), 7.11 – 7.09 (2H, m, Ar-*H*), 6.69 – 6.67 (2H, m, Ar-*H*), 6.80 (1H, s, Ar-*H*), 6.70 (1H, d, *J* 7, Ar-*H*), 5.27 (1H, s, NHCHCH₃), 4.28 (1H, m, NHCHCH₃), 1.44 (9H, s, (CH₃)₃CO), 1.35 (3H, d, *J* 7, NHCHCH₃);

tert-Butyl (S)-(1-(2-(2-bromophenyl)hydrazineyl)-1-oxopropan-2-yl) carbamate 62A

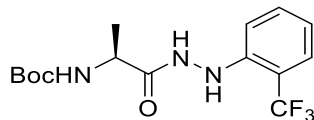


Following the general procedure outlined, *N*-Boc-*L*-alanine (0.20 g, 1.06 mmol) and 2-bromophenylhydrazine hydrochloride (0.28 g, 1.27 mmol) were transformed into the title compound which was isolated as a light orange solid (0.32 g, 84%); δ_H (700 MHz, CDCl₃) 8.66 (1H, s, CONHNH), 7.41 (1H, dd, *J* 8, 1, Ar-*H*), 7.14 (1H, m, Ar-*H*), 6.83 (1H, dd, *J* 8, 1, Ar-*H*), 6.73 (1H, m, Ar-*H*), 6.39

Chapter 5. Experimental section.

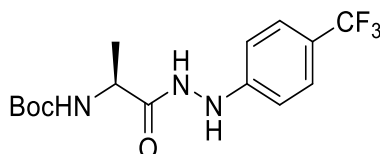
(1H, d, *J* 3 Ar-NH), 5.24 (1H, d, *J* 6, BocNHCH), 4.33 (1H, m, BocNHCH), 1.44 (9H, s, (CH₃)₃CO) 1.39 (3H, d, *J* 7, NHCHCH₃);

***tert*-Butyl (S)-(1-oxo-1-(2-(2-(trifluoromethyl)phenyl)hydrazineyl)propan-2-yl)carbamate 62B**



Following the general procedure outlined, *N*-Boc-*L*-alanine (0.40 g, 2.11 mmol) and 2-trifluoromethylphenylhydrazine hydrochloride (0.49 g, 2.33 mmol) were transformed following work up with Et₂O into the title compound which was isolated as a yellow gummy solid (0.52 g, 71 %); R_f 0.32 (DCM/EtOH/NH₃ 200:6:1); δ_H (300 MHz, CDCl₃) 8.47 (1H, s, CONHNH), 7.50 (1H, d, *J* 7, Ar-*H*), 7.38 (1H, t, *J* 7, Ar-*H*), 7.00 (1H, d, *J* 8, Ar-*H*), 6.97 (1H, t, *J* 7, Ar-*H*), 6.53 (1H, s, Ar-NH), 5.16 (1H, d, *J* 7, BocNHCH), 4.34 (1H, m, BocNHCH), 1.46 (9H, s, (CH₃)₃CO), 1.43 (3H, d, *J* 7, BocNHCHCH₃);

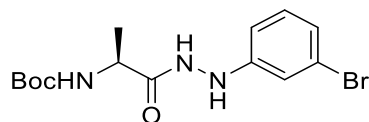
***tert*-Butyl (S)-(1-oxo-1-(2-(4-(trifluoromethyl)phenyl)hydrazineyl)propan-2-yl)carbamate 62f**



Following the general procedure outlined, *N*-Boc-*L*-alanine (0.25 g, 1.32 mmol) and 4-trifluorophenyl hydrazine hydrochloride (0.30 g, 1.75 mmol) were transformed following flash chromatography (DCM/EtOH/NH₃ 200:8:1) into the title compound as a dark brown solid (0.17 g, 46 %); R_f 0.37 (DCM/EtOH/NH₃ [200:8:1]); δ_H (300 MHz, CDCl₃) 8.50 (1H, s, CONHNH), 7.46 (2H, d, *J* 8, Ar-*H*), 6.87 (2H, d, *J* 8, Ar-*H*), 6.34 (1H, s, NH), 5.07 (1H, d, *J* 6, CONHNH), 4.40 (1H, m, CH₃CH), 1.50 (9H, s, (CH₃)₃CO), 1.43 (3H, d, *J* 7, CH₃CH);

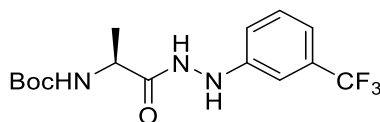
***tert*-Butyl (S)-(1-(2-(3-bromophenyl)hydrazineyl)-1-oxopropan-2-yl)carbamate 62b**

Chapter 5. Experimental section.



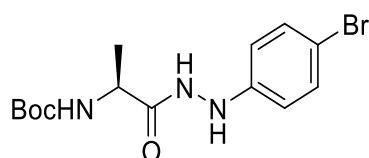
Following the general procedure outlined, *N*-Boc-*L*-alanine (0.40 g, 2.11 mmol) and 3-bromophenylhydrazine hydrochloride (0.52 g, 2.33 mmol) were transformed following work up with Et₂O into the title compound which was isolated as an orange gummy solid (0.34 g, 58 %); δ_{H} (300 MHz, CDCl₃) 8.73 (1H, s, CONHNH), 7.01 (1H, s, Ar-*H*), 6.97 (1H, t, *J* 1, Ar-*H*), 6.91 (1H, t, *J* 1, Ar-*H*), 6.69 (1H, m, Ar-*H*), 6.35 (1H, d, *J* 3, Ar-NH), 5.33 (1H, m, BocNHCH), 4.29 (1H, t, *J* 7, BocNHCH), 1.45 (9H, s, (CH₃)₃CO) 1.37 (3H, d, *J* 7, NHCHCH₃);

***tert*-Butyl (S)-(1-oxo-1-(2-(3-(trifluoromethyl)phenyl)hydrazineyl)propan-2-yl)carbamate 62c**



Following the general procedure outlined, *N*-Boc-*L*-alanine (0.40 g, 2.11 mmol) and 3-trifluoromethylphenylhydrazine hydrochloride (0.49 g, 2.33 mmol) were transformed following work up with Et₂O into the title compound which was isolated as a yellow solid (0.51 g, 69%); R_f 0.28 (DCM/EtOH/NH₃ 200:6:1); δ_{H} (300 MHz, CDCl₃) 8.61 (1H, s, CONHNH), 7.30 (1H, t, *J* 7, Ar-*H*), 7.12 (1H, d, *J* 7, Ar-*H*), 7.01 (1H, s, Ar-*H*), 6.96 (1H, dd, *J* 8, 2, Ar-*H*), 6.37 (1H, s, Ar-NH), 5.16 (1H, bd, *J* 7, BocNHCH), 4.32 (1H, m, BocNHCH), 1.45 (9H, s, (CH₃)₃CO), 1.40 (3H, d, *J* 7, BocNHCHCH₃);

***tert*-Butyl (S)-(1-(2-(4-bromophenyl)hydrazineyl)-1-oxopropan-2-yl)carbamate 62e**

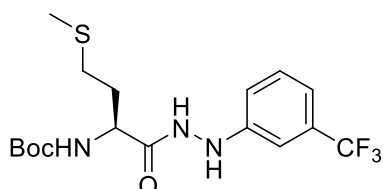


Following the general procedure outlined, *N*-Boc-*L*-alanine (0.40 g, 2.11 mmol) and 4-bromophenylhydrazine hydrochloride (0.52 g, 2.33 mmol) were transformed following flash column chromatography (DCM/EtOH/NH₃ 200:6:1)

Chapter 5. Experimental section.

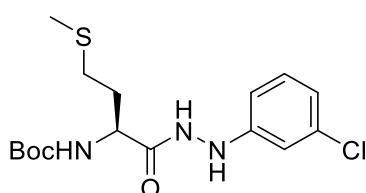
into the title compound which was isolated as a brown oil (0.41 g, 78 %); δ_{H} (300 MHz, CDCl_3) 8.43 (1H, s, CONH₂), 7.30 – 7.27 (2H, d, *J* 9, Ar-*H*), 6.69 – 6.66 (2H, d, *J* 8, Ar-*H*), 6.15 (1H, s, CONH₂), 5.12 (1H, d, *J* 7, BocNHCH), 4.28 (1H, m, BocNHCH), 1.46 (9H, s, $(\text{CH}_3)_3\text{CO}$), 1.39 (3H, d, *J* 7, BocNHCHCH₃);

***tert*-Butyl (S)-(4-(methylthio)-1-oxo-1-(2-(3-(trifluoromethyl)phenyl)hydrazineyl)butan-2-yl)carbamate 63c**



Following the general procedure outlined, *N*-Boc-*L*-methionine (0.40 g, 1.60 mmol) and 3-trifluoromethylphenylhydrazine hydrochloride (0.38 g, 1.77 mmol) were transformed following work up with Et_2O into the title compound which was isolated as a white solid (0.43 g, 64%); δ_{H} (300 MHz, CDCl_3) 8.82 (1H, s, CONH₂), 7.29 (1H, t, *J* 7, Ar-*H*), 7.11 (1H, d, *J* 7, Ar-*H*), 7.02 (1H, s, Ar-*H*), 6.96 (1H, d, *J* 8, Ar-*H*), 6.46 (1H, bs, Ar-NH), 5.42 (1H, d, *J* 8, BocNHCH), 4.47 (1H, q, *J* 7, BocNHCH), 2.57 (2H, t, *J* 7, $\text{CH}_2\text{CH}_2\text{S}$), 2.17 (1H, m, CHCH_2S), 2.08 (3H, s, $\text{CH}_2\text{CH}_2\text{SCH}_3$), 2.00 (1H, m, CHCH_2S), 1.45 (9H, s, $(\text{CH}_3)_3\text{CO}$);

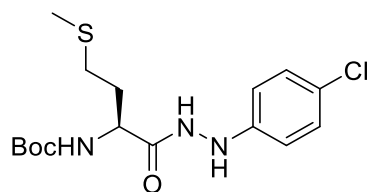
***tert*-Butyl (S)-(1-(2-(3-chlorophenyl)hydrazinyl)-4-(methylthio)-1-oxobutan-2-yl)carbamate 63a**



Following the general procedure outlined, *N*-Boc-*L*-methionine (0.20 g, 0.80 mmol) and 3-chlorophenylhydrazine hydrochloride (0.13 g, 0.88 mmol) were transformed following flash chromatography (*n* hexane/ EtOAc [2:1]) into the title compound which was isolated as a pale yellow solid (0.43 g, 82 %); δ_{H} (300 MHz, CDCl_3) 8.73 (1H, s, CONH₂), 7.10 (1H, t, *J* 8, Ar-*H*), 6.85 (1H, d, *J* 8, Ar-*H*), 6.80 (1H, s, Ar-*H*), 6.67 (1H, d, *J* 8, Ar-*H*), 6.34 (1H, s, Ar-NH), 5.42 (1H, d, *J* 8, BocNHCH), 4.43 (1H, q, *J* 7, BocNHCH), 2.57 (2H, t, *J* 7, $\text{CH}_2\text{CH}_2\text{S}$), 2.13 – 2.09 (5H, m, $\text{CH}_2\text{CH}_2\text{SCH}_3$), 1.47 (9H, s, $(\text{CH}_3)_3\text{CO}$);

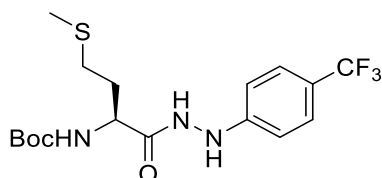
Chapter 5. Experimental section.

***tert*-Butyl (S)-(1-(2-(4-chlorophenyl)hydrazineyl)-4-(methylthio)-1-oxobutan-2-yl)carbamate 63d**



Following the general procedure outlined, *N*-Boc-*L*-methionine (0.20 g, 0.80 mmol) and 4-chlorophenylhydrazine hydrochloride (0.13 g, 0.88 mmol) were transformed following trituration with Et₂O into the title compound which was isolated as an orange gum (0.32 g, 74 %); δ_{H} (300 MHz, CDCl₃) 8.58 (1H, s, CONH₂), 7.15 – 7.13 (2H, d, *J* 8, Ar-*H*), 6.74 – 6.72 (2H, d, *J* 8, Ar-*H*), 6.24 (1H, s, Ar-*H*), 5.34 (1H, s, BocNHCH), 4.39 (1H, m, BocNHCH), 2.57 (2H, m, CH₂CH₂S), 2.13 – 2.06 (4H, m, CHHCH₂S, CH₂CH₂SCH₃), 1.97 (1H, m, CHHCH₂S), 1.45 (9H, s, (CH₃)₃CO);

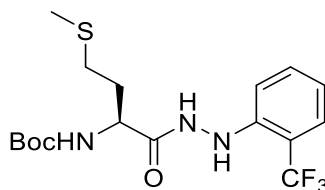
***tert*-Butyl (S)-(4-(methylthio)-1-oxo-1-(2-(4-(trifluoromethyl)phenyl)hydrazineyl)butan-2-yl)carbamate 63f**



Following the general procedure outlined, *N*-Boc-*L*-methionine (0.20 g, 0.80 mmol) and 4-trifluoromethylphenylhydrazine hydrochloride (0.19 g, 0.88 mmol) were transformed following trituration with DCM into the title compound which was isolated as a white solid (0.14 g, 44 %); δ_{H} (300 MHz, CDCl₃) 8.82 (1H, s, CONH₂), 7.41 (2H, d, *J* 8, Ar-*H*), 6.81 (2H, d, *J* 8, Ar-*H*), 6.53 (1H, s, Ar-*H*), 5.43 (1H, d, *J* 8, BocNHCH), 4.44 (1H, q, *J* 7, BocNHCH), 2.56 (2H, t, *J* 7, CH₂CH₂S), 2.09 - 2.14 (5H, m, CH₂CH₂SCH₃), 1.49 (9H, s, (CH₃)₃CO);

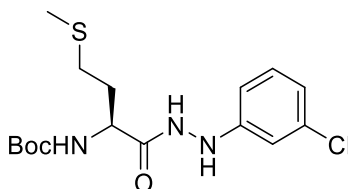
Chapter 5. Experimental section.

***tert*-Butyl (S)-(4-(methylthio)-1-oxo-1-(2-(2-(trifluoromethyl)phenyl)hydrazineyl)butan-2-yl)carbamate 63A**



Following the general procedure outlined, *N*-Boc-*L*-methionine (0.40 g, 1.60 mmol) and 2-trifluoromethylphenylhydrazine hydrochloride (0.38 g, 1.77 mmol) were transformed following work up with Et₂O into the title compound which was isolated as a light orange solid (0.33 g, 50 %); δ_{H} (300 MHz, CDCl₃) 8.95 (1H, s, CONH₂), 7.38 (1H, d, *J* 7, Ar-*H*), 7.23 (1H, m, Ar-*H*), 6.89 (1H, d, *J* 8, Ar-*H*), 6.81 (1H, t, *J* 7, Ar-*H*), 6.50 (1H, s, Ar-NH), 5.54 (1H, d, *J* 8, BocNHCH), 4.47 (1H, m, BocNHCH), 2.51 (2H, t, *J* 7, CH₂CH₂S), 2.00 (3H, s, CH₂CH₂SCH₃), 1.94 (2H, m, CH₂CH₂S), 1.35 (9H, s, (CH₃)₃CO);

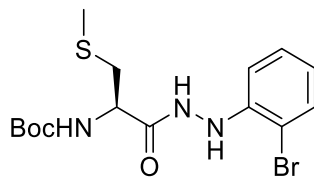
***tert*-Butyl (S)-(1-(2-(3-chlorophenyl)hydrazineyl)-4-(methylthio)-1-oxobutan-2-yl)carbamate 63a**



Following the general procedure outlined, *N*-Boc-*L*-methionine (0.30 g, 1.20 mmol) and 3-chlorophenylhydrazine hydrochloride (0.25 g, 1.32 mmol) were transformed following work up with Et₂O into the title compound which was isolated as a pale yellow solid (0.38 g, 82 %); δ_{H} (300 MHz, CDCl₃) 8.70 (1H, s, CONH₂), 7.03 (3H, m, Ar-*H*), 6.70 (1H, m, Ar-*H*), 6.30 (1H, d, *J* 4, Ar-*H*), 5.38 (1H, d, *J* 8, BocNHCH), 4.40 (1H, q, *J* 8, BocNHCH), 2.55 (2H, t, *J* 7, CH₂CH₂S), 2.09 (3H, s, CH₂CH₂SCH₃), 1.93 (2H, m, CH₂CH₂S), 1.46 (9H, s, (CH₃)₃CO);

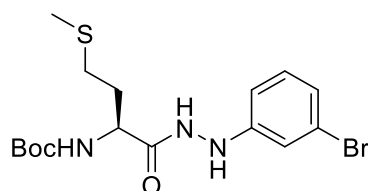
Chapter 5. Experimental section.

***tert*-Butyl (S)-(1-(2-(2-bromophenyl)hydrazineyl)-4-(methylthio)-1-oxobutan-2-yl)carbamate 63B**



Following the general procedure outlined, *N*-Boc-*L*-methionine (0.30 g, 1.20 mmol) and 2-bromophenylhydrazine hydrochloride (0.26 g, 1.33 mmol) were transformed following trituration with Et₂O into the title compound which was isolated as a light brown solid (0.25 g, 54 %); R_f 0.38 (DCM/EtOH/NH₃ 200:6:1); δ_H (300 MHz, CDCl₃) 8.77 (1H, bs, CONH₂), 7.26 (1H, dd, *J* 7, 1, Ar-*H*), 7.12 (1H, td, *J* 7, 1, Ar-*H*), 6.86 (1H, dd, *J* 8, 1, Ar-*H*), 6.80 (1H, dd, *J* 7, 1, Ar-*H*), 6.48 (1H, bd, *J* 3, Ar-NH), 5.45 (1H, bd, *J* 8, BocNHCH), 4.47 (1H, m, BocNHCH), 2.58 (2H, t, *J* 7, CH₂CH₂S), 2.09 (3H, s, CH₂CH₂SCH₃), 2.01 (2H, m, CH₂CH₂S), 1.44 (9H, s, (CH₃)₃CO);

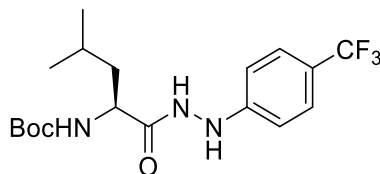
***tert*-Butyl (S)-(1-(2-(3-bromophenyl)hydrazineyl)-4-(methylthio)-1-oxobutan-2-yl)carbamate 63e**



Following the general procedure outlined, *N*-Boc-*L*-methionine (0.30 g, 1.20 mmol) and 3-bromophenylhydrazine hydrochloride (0.25 g, 1.32 mmol) were transformed following work up with Et₂O into the title compound which was isolated as a white solid (0.27 g, 59 %); R_f; δ_H (300 MHz, CDCl₃) 8.70 (1H, s, CONH₂), 7.03 (3H, m, Ar-*H*), 6.70 (1H, m, Ar-*H*), 6.30 (1H, bd, *J* 4, Ar-*H*), 5.38 (1H, bd, *J* 8, BocNHCH), 4.40 (1H, q, *J* 8, BocNHCH), 2.55 (2H, t, *J* 7, CH₂CH₂S), 2.09 (3H, s, CH₂CH₂SCH₃), 1.93 (2H, m, CH₂CH₂S), 1.46 (9H, s, (CH₃)₃CO);

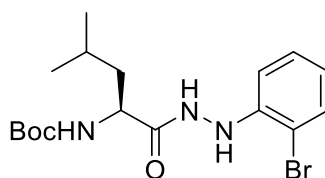
Chapter 5. Experimental section.

***tert*-Butyl (S)-(4-methyl-1-oxo-1-(2-(4-(trifluoromethyl)phenyl)hydrazineyl)pentan-2-yl)carbamate 64f**



Following the general procedure outlined, *N*-Boc-*L*-leucine (0.40 g, 1.73 mmol) and 4-trifluoromethylphenylhydrazine hydrochloride (0.40 g, 1.90 mmol) were transformed following work up with Et₂O into the title compound which was isolated as a yellow gummy solid (0.40 g, 82 %); δ_{H} (300 MHz, CDCl₃) 8.84 (1H, s, CONH₂), 7.39 – 7.37 (2H, d, *J* 8, Ar-*H*), 6.79 – 6.77 (2H, d, *J* 8, Ar-*H*), 5.20 (1H, d, *J* 8, BocNHCH), 4.27 (1H, m, BocNHCH), 1.68 – 1.53 (3H, m, CH₂CH(CH₃)₂, CH₂CH(CH₃)₂), 1.45 (9H, s, (CH₃)₃CO), 0.93 – 0.88 (6H, t, *J* 6, CH₂CH(CH₃)₂);

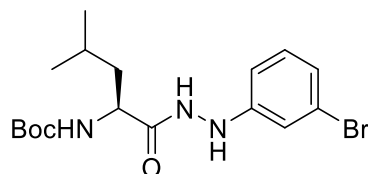
***tert*-Butyl (S)-(1-(2-(2-bromophenyl)hydrazineyl)-4-methyl-1-oxopentan-2-yl)carbamate 64A**



Following the general procedure outlined, *N*-Boc-*L*-leucine (0.40 g, 1.73 mmol) and 2-bromophenylhydrazine hydrochloride (0.43 g, 1.90 mmol) were transformed following trituration with DCM into the title compound which was isolated as an light orange solid (0.32 g, 46 %); δ_{H} (300 MHz, CDCl₃) 8.30 (1H, s, CONH₂), 7.44 (1H, dd, *J* 7,1, Ar-*H*), 6.18 (1H, dt, *J* 8, 1, Ar-*H*), 6.86 (1H, dd, *J* 8,1, Ar-*H*), 6.78 (1H, td, *J* 7,1, Ar-*H*), 6.40 (1H, d, *J* 3, CONH₂), 4.97 (1H, d, *J* 8, BocNHCH), 4.24 (1H, m, BocNHCH), 1.74 – 1.67 (3H, m, CH₂CH(CH₃)₂, CH₂CH(CH₃)₂), 1.47 (9H, s, (CH₃)₃CO), 0.98 – 0.96 (3H, d, *J* 6, CH₂CH(CH₃)₂), 0.95 – 0.93 (3H, d, *J* 6, CH₂CH(CH₃)₂);

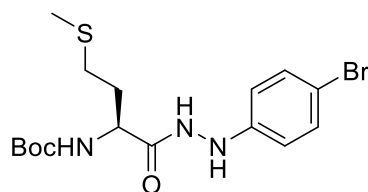
Chapter 5. Experimental section.

***tert*-Butyl (S)-(1-(2-(3-bromophenyl)hydrazineyl)-4-methyl-1-oxopentan-2-yl)carbamate 64b**



Following the general procedure outlined, *N*-Boc-*L*-leucine (0.40 g, 1.73 mmol) and 3-bromophenylhydrazine hydrochloride (0.43 g, 1.90 mmol) were transformed following trituration with Et₂O into the title compound which was isolated as a light orange solid (0.18 g, 38 %); δ_{H} (300 MHz, CDCl₃) 8.43 (1H, s, CONHNH), 7.04 (1H, d, *J* 7, Ar-*H*), 7.01 (1H, t, *J* 1, Ar-*H*), 6.95 (1H, t, *J* 1, Ar-*H*), 6.73 (1H, dt, *J* 7,1, Ar-*H*), 5.02 (1H, d, *J* 8, BocNHCH), 4.25 (1H, m, BocNHCH), 1.71 – 1.66 (2H, m, CHHCH(CH₃)₂, CH₂CH(CH₃)₂), 1.55 (1H, m, CHHCH(CH₃)₂), 1.47 (9H, s, (CH₃)₃CO), 0.97 – 0.95 (3H, d, *J* 6, CH₂CH(CH₃)₂), 0.94 – 0.92 (3H, d, *J* 6, CH₂CH(CH₃)₂);

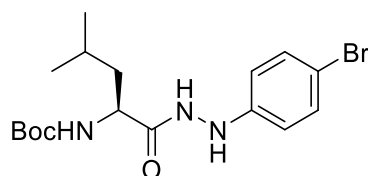
***tert*-Butyl (S)-(1-(2-(4-bromophenyl)hydrazineyl)-4-(methylthio)-1-oxobutan-2-yl)carbamate**



Following the general procedure outlined, *N*-Boc-*L*-methionine (0.40 g, 1.60 mmol) and 4-bromophenylhydrazine hydrochloride (0.39 g, 1.77 mmol) were transformed following work up with Et₂O into the title compound which was isolated as a brown gummy solid (0.28 g, 57 %); δ_{H} (300 MHz, CDCl₃) 8.63 (1H, s, CONHNH), 7.21 – 7.18 (2H, d, *J* 8, Ar-*H*), 6.60 – 6.57 (2H, d, *J* 8, Ar-*H*), 5.35 (1H, d, *J* 8, BocNHCH), 4.34 (1H, m, BocNHCH), 2.48 (2H, t, *J* 7, CH₂CH₂S), 2.07 (1H, m, CHHCH₂S), 2.01 (3H, s, CH₂CH₂SCH₃), 1.92 (1H, m, CHHCH₂S), 1.38 (9H, s, (CH₃)₃CO);

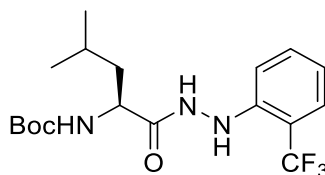
***tert*-Butyl (S)-(1-(2-(4-bromophenyl)hydrazineyl)-4-methyl-1-oxopentan-2-yl)carbamate 64e**

Chapter 5. Experimental section.



Following the general procedure outlined, *N*-Boc-*L*-leucine (0.40 g, 1.73 mmol) and 4-bromophenylhydrazine hydrochloride (0.43 g, 1.90 mmol) were transformed following trituration with Et₂O into the title compound which was isolated as a light orange solid (0.41 g, 57 %); R_f 0.53 (DCM/EtOH/NH₃ 200:6:1); δ_H (300 MHz, CDCl₃) 8.66 (1H, s, CONH₂), 7.26 – 7.24 (2H, d, *J* 8, Ar-*H*), 6.66 – 6.63 (2H, d, *J* 8, Ar-*H*), 6.24 (1H, s, CONHNH), 5.16 (1H, d, *J* 8, BocNHCH), 4.24 (1H, m, BocNHCH), 1.68 – 1.57 (2H, m, CHHCH(CH₃)₂, CH₂CH(CH₃)₂), 1.53 (1H, m, CHHCH(CH₃)₂), 1.45 (9H, s, (CH₃)₃CO), 0.94 – 0.89 (6H, t, *J* 6, CH₂CH(CH₃)₂);

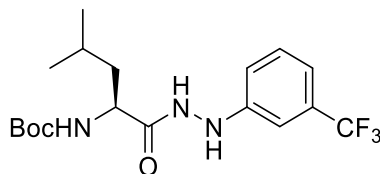
tert-Butyl (S)-(4-methyl-1-oxo-1-(2-(2-(trifluoromethyl)phenyl)hydrazineyl)pentan-2-yl)carbamate 64B



Following the general procedure outlined, *N*-Boc-*L*-leucine (0.40 g, 1.73 mmol) and 2-trifluoromethylphenylhydrazine hydrochloride (0.40 g, 1.90 mmol) were transformed following flash column chromatography (DCM/EtOH/NH₃ 200:8:1) into the title compound which was isolated as a yellow oil (0.29 g, 43 %); δ_H (300 MHz, CDCl₃) 9.18 (1H, s, CONH₂), 7.36 – 7.31 (2H, t, *J* 8, Ar-*H*), 7.16 (1H, t, *J* 8, Ar-*H*), 6.87 (1H, d, *J* 8, Ar-*H*), 6.49 (1H, bs, CONHNH), 5.50 (1H, d, *J* 8, BocNHCH), 4.34 (1H, m, BocNHCH), 1.59 – 1.47 (3H, m, CH₂CH(CH₃)₂, CH₂CH(CH₃)₂), 1.33 (9H, s, (CH₃)₃CO), 0.84 – 0.80 (6H, t, *J* 5, CH₂CH(CH₃)₂);

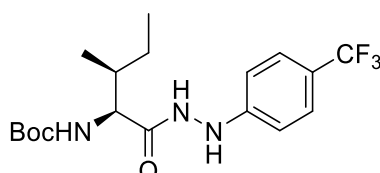
Chapter 5. Experimental section.

***tert*-Butyl (S)-(4-methyl-1-oxo-1-(2-(3-(trifluoromethyl)phenyl)hydrazineyl)pentan-2-yl)carbamate 64c**



Following the general procedure outlined, *N*-Boc-*L*-leucine (0.40 g, 1.73 mmol) and 3-trifluoromethylphenylhydrazine hydrochloride (0.40 g, 1.90 mmol) were transformed following work up with Et₂O into the title compound which was isolated as a yellow oil (0.41 g, 72 %); δ_{H} (300 MHz, CDCl₃) 8.93 (1H, s, CONH₂), 7.15 (1H, d, *J* 7, Ar-*H*), 7.01 (1H, d, *J* 7, Ar-*H*), 6.92 (1H, s, Ar-*H*), 6.84 (1H, dd, *J* 7, 1, Ar-*H*), 6.46 (1H, s, CONH₂), 5.18 (1H, d, *J* 8, BocNHCH), 4.26 (1H, m, BocNHCH), 1.57 – 1.51 (2H, m, CHHCH(CH₃)₂, CH₂CH(CH₃)₂), 1.45 (1H, m, CHHCH(CH₃)₂), 1.35 (9H, s, (CH₃)₃CO), 0.84 (3H, d, *J* 6, CH₂CH(CH₃)₂), 0.81 (3H, d, *J* 6, CH₂CH(CH₃)₂);

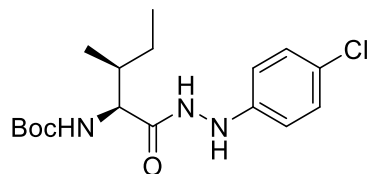
***tert*-butyl ((2S,3S)-3-methyl-1-oxo-1-(2-(4-(trifluoromethyl)phenyl)hydrazineyl)pentan-2-yl)carbamate 65f**



Following the general procedure outlined, *N*-Boc-*L*-isoleucine (0.40 g, 1.73 mmol) and 4-trifluoromethylphenylhydrazine hydrochloride (0.40 g, 1.90 mmol) were transformed following trituration with Et₂O into the title compound which was isolated as a yellow gummy solid (0.37 g, 51 %); δ_{H} (300 MHz, CDCl₃) 8.47 (1H, d, *J* 4, CONH₂), 7.44 (2H, d, *J* 9, Ar-*H*), 6.84 (2H, d, *J* 9, Ar-*H*), 6.42 (1H, d, *J* 9, BocNHCH), 5.16 (1H, d, *J* 9, BocNHCH), 4.01 (1H, m, BocNHCH), 1.57 (1H, m, CH(CH₃)CH(CH₃)), 1.46 (9H, s, (CH₃)₃CO), 1.28 – 1.05 (1H, m, CH(CH₃)CH(CH₃)), 0.96 – 0.90 (6H, m, CH(CH₃)CH(CH₃));

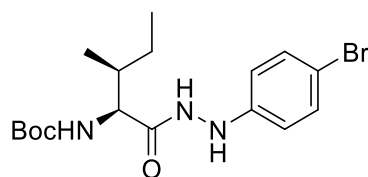
Chapter 5. Experimental section.

tert-butyl ((2S,3S)-1-(2-(4-chlorophenyl)hydrazineyl)-3-methyl-1-oxopentan-2-yl)carbamate 65d



Following the general procedure outlined, *N*-Boc-*L*-isoleucine (0.40 g, 1.73 mmol) and 4-chlorophenylhydrazine hydrochloride (0.40 g, 1.90 mmol) were transformed into the title compound which was isolated as a white solid (0.23 g, 41 %); δ_{H} (300 MHz, CDCl_3) 7.96 (1H, d, *J* 4, CONH₂), 7.19 – 7.14 (2H, d, *J* 9, Ar-*H*), 6.80 – 6.74 (2H, d, *J* 9, Ar-*H*), 6.09 (1H, d, *J* 9, BocNHCH), 4.98 (1H, d, *J* 9, BocNHCH), 3.99 – 3.90 (1H, m, CH(CH₃)CH(CH₃)), 1.47 (9H, s, (CH₃)₃CO), 1.26 – 1.11 (1H, m, CH(CH₃)CH(CH₃)), 0.99 – 0.89 (6H, m, CH(CH₃)CH(CH₃)),

tert-butyl ((2S,3S)-1-(2-(4-bromophenyl)hydrazineyl)-3-methyl-1-oxopentan-2-yl)carbamate 65e

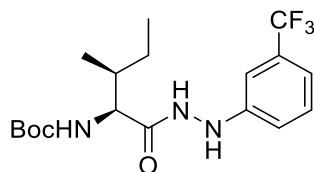


Following the general procedure outlined, *N*-Boc-*L*-isoleucine (0.40 g, 1.73 mmol) and 4-bromophenylhydrazine hydrochloride (0.40 g, 1.90 mmol) were transformed following trituration with Et₂O into the title compound which was isolated as an orange solid (0.43 g, 65 %); δ_{H} (300 MHz, CDCl_3) 8.06 (1H, d, *J* 4, CONH₂), 7.35 (2H, d, *J* 9, Ar-*H*), 6.78 (2H, d, *J* 9, Ar-*H*), 5.04 (1H, d, *J* 9, BocNHCH), 3.96 (1H, d, *J* 9, BocNHCH), 1.90 (1H, m, CH(CH₃)CH(CH₃)), 1.49 (9H, s, (CH₃)₃CO), 1.29 – 1.13 (1H, m, CH(CH₃)CH(CH₃)), 1.01 – 0.91 (6H, m, CH(CH₃)CH(CH₃));

Chapter 5. Experimental section.

tert-butyl

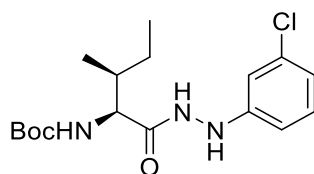
((2S,3S)-3-methyl-1-oxo-1-(2-(3-(trifluoromethyl)phenyl)hydrazineyl)pentan-2-yl)carbamate 65c



Following the general procedure outlined, *N*-Boc-*L*-isoleucine (0.40 g, 1.73 mmol) and 3-trifluoromethylphenylhydrazine hydrochloride (0.40 g, 1.90 mmol) were transformed into the title compound which was isolated as a yellow white solid (0.43 g, 74 %); δ_{H} (300 MHz, CDCl_3) 8.06 (1H, d, J 3.0, CONHNH), 7.31 (1H, t, J 8, Ar-H), 7.17 – 6.97 (3H, m, Ar-H), 6.23 (1H, d, J 4, Ar-H), 5.00 (1H, dd, J 7, 3, BocNHCH), 4.04 – 3.96 (1H, m, BocNHCH), 1.45 (9H, s, $(\text{CH}_3)_3\text{CO}$), 1.26 – 1.10 (2H, m, $\text{CH}(\text{CH}_3)\text{CH}(\text{CH}_3)$), 0.98 - 0.93 (6H, td, J 7, 7, $\text{CH}(\text{CH}_3)\text{CH}(\text{CH}_3)$);

tert-butyl

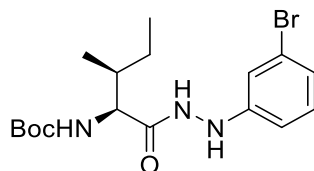
((2S,3S)-1-(2-(3-chlorophenyl)hydrazineyl)-3-methyl-1-oxopentan-2-yl)carbamate 65a



Following the general procedure outlined, *N*-Boc-*L*-isoleucine (0.40 g, 1.73 mmol) and 3-chlorophenylhydrazine hydrochloride (0.40 g, 1.90 mmol) were transformed into the title compound which was isolated as a yellow gummy solid (0.37 g, 52 %); R_f 0.38; δ_{H} (300 MHz, CDCl_3) 9.18 (s, 1H, s, CONHNH), 7.04 (1H, dd, J 20., 8.0, Ar -H), 6.77 (2H, d, J 11, Ar-H), 6.62 (1H, d, J 8, Ar-H), 5.54 (1H, d, J 9, BocNHCH), 4.08 (1H, t, J 9, BocNHCH), 1.88 – 1.69 (1H, m, $\text{CH}(\text{CH}_3)\text{CH}(\text{CH}_3)$), 1.43 (9H, s, $(\text{CH}_3)_3\text{CO}$), 1.13 (1H, t, J 7, $\text{CH}(\text{CH}_3)\text{CH}(\text{CH}_3)$), 0.86 (6H, dd, J 18.0, 7.0, $\text{CH}(\text{CH}_3)\text{CH}(\text{CH}_3)$);

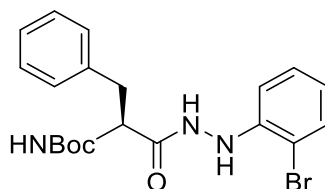
Chapter 5. Experimental section.

tert-butyl ((2*S*,3*S*)-1-(2-(3-bromophenyl)hydrazineyl)-3-methyl-1-oxopentane-2-yl)carbamate **65b**



Following the general procedure outlined, *N*-Boc-*L*-isoleucine (0.40 g, 1.73 mmol) and 3-bromophenylhydrazine hydrochloride (0.40 g, 1.90 mmol) were transformed following work up with Et₂O into the title compound which was isolated as a orange solid (0.41 g, 65 %); δ_{H} (300 MHz, CDCl₃) 8.99 (s, 1H, s, CONHNH), 7.00 (1H, dd, *J* 20., 8.0, Ar -*H*), 6.81 (2H, d, *J* 11, Ar-*H*), 6.60 (1H, d, *J* 8, Ar-*H*), 5.38 (1H, d, *J* 9, BocNHCH), 3.99 (1H, t, *J* 9, BocNHCH), 1.88 – 1.69 (1H, m, CH(CH₃)CH(CH₃)), 1.42 (9H, s, (CH₃)₃CO), 1.10 (1H, t, *J* 7, CH(CH₃)CH(CH₃)), 0.86 (6H, dd, *J* 18, 7, CH(CH₃)CH(CH₃));

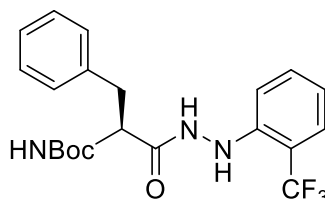
tert-Butyl (*S*)-(1-(2-(2-chlorophenyl)hydrazineyl)-1-oxo-3-phenylpropan-2-yl)carbamate **66A**



Following the general procedure outlined, *N*-Boc-*L*-phenylalanine (0.30 g, 1.13 mmol) and 2-bromophenylhydrazine hydrochloride (0.22 g, 1.24 mmol) were transformed following work up with Et₂O into the title compound which was isolated as a light brown gummy solid (0.41 g, 93 %); δ_{H} (300 MHz, CDCl₃) 7.82 (1H, s, CONHNH), 7.33 – 7.29 (2H, m, Ar-*H*), 7.25 – 7.21 (3H, m, Ar-*H*), 7.04 (1H, t, *J* 7, Ar-*H*), 6.82 (1H, td, *J* 7, 1, Ar-*H*), 6.43 (1H, d, *J* 7, Ar-*H*), 6.33 (1H, bd, *J* 3, Ar-NH), 5.08 (1H, d, *J* 8, BocNHCH), 4.48 (1H, q, *J* 7, BocNHCH), 3.12 (2H, d, *J* 7, Ar-CH₂), 1.44 (9H, s, (CH₃)₃CO);

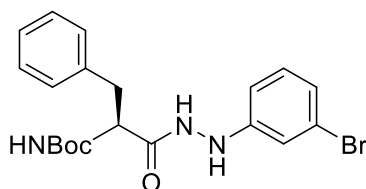
Chapter 5. Experimental section.

***tert*-Butyl (S)-(1-(2-(2-trifluoromethylphenyl)hydrazineyl)-1-oxo-3-phenylpropan-2-yl)carbamate 66B**



Following the general procedure outlined, *N*-Boc-*L*-phenylalanine (0.40 g, 1.51 mmol) and 2-trifluoromethylphenylhydrazine hydrochloride (0.37 g, 1.66 mmol) were transformed following work up with Et₂O into the title compound which was isolated as a brown solid (0.47 g, 72 %); δ_{H} (300 MHz, CDCl₃) 8.62 (1H, s, CONH₂), 7.36 (1H, d, *J* 7, Ar-*H*), 7.27 – 7.24 (2H, m, Ar-*H*), 7.20 – 7.17 (2H, m, Ar-*H*), 7.01 (1H, t, *J* 7, Ar-*H*), 6.69 (1H, t, *J* 7, Ar-*H*), 6.31 (2H, m, Ar-*H*), 5.47 (1H, d, *J* 8, BocNHCH), 4.62 (1H, m, BocNHCH), 3.07 (2H, d, *J* 6, Ar-CH₂), 1.37 (9H, s, (CH₃)₃CO);

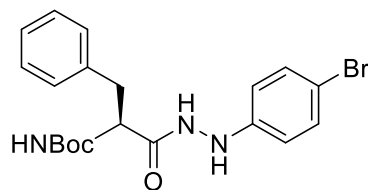
***tert*-Butyl (S)-(1-(2-(3-bromophenyl)hydrazineyl)-1-oxo-3-phenylpropan-2-yl)carbamate 66b**



Following the general procedure outlined, *N*-Boc-*L*-phenylalanine (0.33 g, 1.23 mmol) and 3-bromophenylhydrazine hydrochloride (0.25 g, 1.35 mmol) were transformed following work up with Et₂O into the title compound which was isolated as a pale orange solid (0.41 g, 79 %); δ_{H} (300 MHz, CDCl₃) 8.07 (1H, s, CONH₂), 7.29 (5H, m, Ar-*H*), 7.19 (2H, dd, *J* 7, 2, Ar-*H*), 6.97 (2H, d, *J* 4, Ar-*H*), 6.81 (1H, s, Ar-*H*), 6.49 (1H, s, Ar-NH), 5.15 (1H, d, *J* 8, BocNHCH), 4.45 (1H, q, *J* 7, BocNHCH), 3.07 (2H, t, *J* 7, Ar-CH₂), 1.43 (9H, s, (CH₃)₃CO);

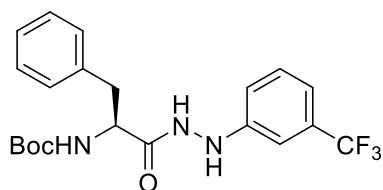
***tert*-Butyl (S)-(1-(2-(4-bromophenyl)hydrazineyl)-1-oxo-3-phenylpropan-2-yl)carbamate 66e**

Chapter 5. Experimental section.



Following the general procedure outlined, *N*-Boc-*L*-phenylalanine (0.40 g, 1.51 mmol) and 4-bromophenylhydrazine hydrochloride (0.37 g, 1.66 mmol) were transformed following trituration with Et₂O into the title compound which was isolated as an orange solid (0.37 g, 56 %); δ_{H} (300 MHz, CDCl₃) 8.22 (1H, s, CONHNH), 7.32 – 7.28 (3H, m, Ar-*H*), 7.23 – 7.18 (4H, m, Ar-*H*), 6.41 – 6.38 (2H, d, *J* 8, Ar-*H*), 5.27 (1H, d, *J* 8, BocNHCH), 4.62 (1H, q, *J* 7, BocNHCH), 3.08 (2H, d, *J* 7, Ar-CH₂), 1.44 (9H, s, (CH₃)₃CO);

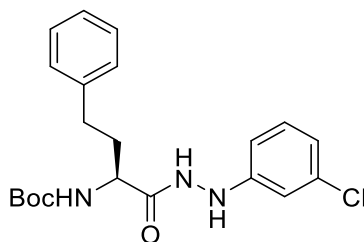
***tert*-Butyl (S)-(1-oxo-3-phenyl-1-(2-(3-(trifluoromethyl)phenyl)hydrazineyl)propan-2-yl)carbamate 66c**



Following the general procedure outlined, *N*-Boc-*L*-phenylalanine (0.40 g, 1.51 mmol) and 3-trifluoromethylphenylhydrazine hydrochloride (0.35 g, 1.66 mmol) were transformed following work up with Et₂O into the title compound which was isolated as a yellow solid (0.48 g, 76 %); δ_{H} (300 MHz, CDCl₃) 8.13 (1H, s, CONHNH), 7.23 – 7.17 (3H, m, Ar-*H*), 7.15 – 7.10 (3H, m, Ar-*H*), 7.03 (1H, d, *J* 7, Ar-*H*), 6.85 (1H, s, Ar-*H*), 6.63 (1H, d, *J* 7, Ar-*H*), 5.12 (1H, s, BocNHCH), 4.45 (1H, q, *J* 7, BocNHCH), 3.02 (2H, dd, *J* 7, 3, Ar-CH₂), 1.35 (9H, s, (CH₃)₃CO);

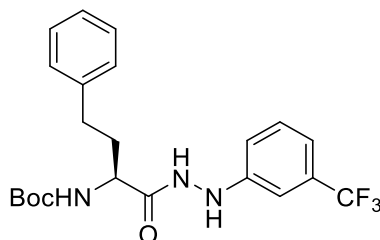
Chapter 5. Experimental section.

tert-Butyl (S)-(1-(2-(3-chlorophenyl)hydrazinyl)-1-oxo-4-phenylbutan-2-yl)carbamate 67a



Following the general procedure outlined, *N*-Boc-*L*-homophenylalanine (0.40 g, 1.43 mmol) and 3-chlorophenylhydrazine hydrochloride (0.28 g, 1.58 mmol) were transformed following trituration with Et₂O into the title compound which was isolated as a light orange solid (0.28 g, 82 %); δ_{H} (300 MHz, CDCl₃) 8.58 (1H, s, CONHNH), 7.27 – 7.25 (2H, m, Ar-*H*), 7.21 (1H, m, Ar-*H*), 7.15 – 7.12 (2H, m, Ar-*H*), 7.06 (1H, t, *J* 8, Ar-*H*), 6.83 (1H, m, Ar-*H*), 6.77 (1H, t, *J* 2, Ar-*H*), 6.66 (1H, m, Ar-*H*), 5.27 (1H, d, *J* 8, CONHCH), 4.20 (1H, m, CONHCH), 2.69 (2H, t, *J* 8, CH₂CH₂-Phe), 2.19 (1H, m, CH₂CH₂Phe), 1.98 (1H, m, CH₂CH₂Phe), 1.46 (9H, s, (CH₃)₃CO);

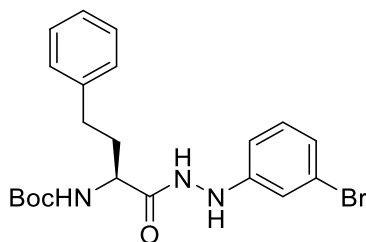
tert-butyl (S)-(1-oxo-4-phenyl-1-(2-(3-(trifluoromethyl)phenyl)hydrazineyl)butan-2-yl)carbamate 67c



Following the general procedure outlined, *N*-Boc-*L*-homophenylalanine (0.40 g, 1.43 mmol) and 3-trifluoromethylphenylhydrazine hydrochloride (0.28 g, 1.58 mmol) were transformed into the title compound which was isolated as a yellow solid (0.28 g, 48 %); δ_{H} (300 MHz, CDCl₃) 9.01 (1H, s, CONHNH), 7.21 (5H, dtd, *J* 16, 7, 2, Ar-*H*), 7.08 (3H, m, Ar-*H*), 7.01 (2H, m, Ar-*H*), 6.87 (1H, m, Ar-*H*), 6.56 (1H, s, Ar-*H*), 5.48 (1H, d, *J* 8, CONHCH), 4.27 (1H, m, CONHCH), 2.61 (2H, t, *J* 8, CH₂CH₂-Phe), 2.19 (1H, m, CH₂CH₂-Phe), 1.46 (9H, s, (CH₃)₃CO);

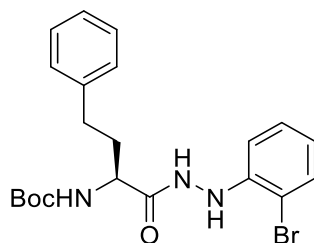
Chapter 5. Experimental section.

tert-butyl (S)-(1-(2-(3-bromophenyl)hydrazineyl)-1-oxo-4-phenylbutan-2-yl)carbamate 67b



Following the general procedure outlined, *N*-Boc-*L*-homophenylalanine (0.40 g, 1.43 mmol) and 3-bromophenylhydrazine hydrochloride (0.28 g, 1.58 mmol) were transformed into the title compound which was isolated as a light brown solid (0.31 g, 59 %); δ_{H} (300 MHz, CDCl_3) 8.58 (1H, s, CONHNH), 7.27 – 7.25 (2H, m, Ar-*H*), 7.21 (1H, m, Ar-*H*), 7.15 – 7.12 (2H, m, Ar-*H*), 7.06 (1H, t, *J* 8, Ar-*H*), 6.83 (1H, m, Ar-*H*), 6.77 (1H, t, *J* 2, Ar-*H*), 6.66 (1H, m, Ar-*H*), 5.27 (1H, b, *J* 8, CONHCH), 4.20 (1H, m, CONHCH), 2.69 (2H, t, *J* 8, CH_2CH_2 -Phe), 2.19 (1H, m, CH_2CH_2 -Phe), 1.46 (9H, s, $(\text{CH}_3)_3\text{CO}$);

tert-butyl (S)-(1-(2-(2-bromophenyl)hydrazineyl)-1-oxo-4-phenylbutan-2-yl)carbamate 67A

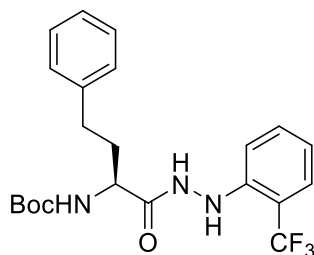


Following the general procedure outlined, *N*-Boc-*L*-homophenylalanine (0.40 g, 1.43 mmol) and 2-bromophenylhydrazine hydrochloride (0.28 g, 1.58 mmol) were transformed following trituration with DCM into the title compound which was isolated as a light orange solid (0.28 g, 48 %); δ_{H} (300 MHz, CDCl_3) 8.58 (1H, s, CONHNH), 7.27 – 7.25 (2H, m, Ar-*H*), 7.21 (1H, m, Ar-*H*), 7.15 – 7.12 (2H, m, Ar-*H*), 7.06 (1H, t, *J* 8, Ar-*H*), 6.83 (1H, m, Ar-*H*), 6.77 (1H, t, *J* 2, Ar-*H*), 6.66 (1H, m, Ar-*H*), 5.27 (1H, bd, *J* 8, CONHCH), 4.20 (1H, m, CONHCH), 2.69 (2H, t, *J* 8, CH_2CH_2 -Phe), 2.19 (2H, m, CH_2CH_2 -Phe), 1.46 (9H, s, $(\text{CH}_3)_3\text{CO}$);

Chapter 5. Experimental section.

tert-butyl

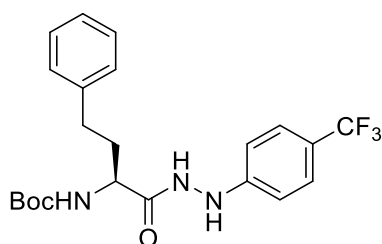
(S)-(1-oxo-4-phenyl-1-(2-(2-(trifluoromethyl)phenyl)hydrazineyl)butan-2-yl)carbamate 67B



Following the general procedure outlined, *N*-Boc-*L*-homophenylalanine (0.40 g, 1.43 mmol) and 2-trifluoromethylphenylhydrazine hydrochloride (0.28 g, 1.58 mmol) were transformed following trituration with Et₂O into the title compound which was isolated as a light yellow solid (0.38 g, 65 %); δ_{H} (300 MHz, CDCl₃) 9.15 (1H, d, *J* 4, CONHNH), 7.28 (2H, d, *J* 8, Ar-*H*), 7.15 (1H, t, *J* 2, Ar-*H*), 7.14 – 7.04 (2H, m, Ar-*H*), 7.04 – 6.98 (2H, m, Ar-*H*), 6.82 (1H, d, *J* 8, Ar-*H*), 6.69 (1H, t, *J* 7, Ar-*H*), 6.45 (1H, dd, *J* 4, 2, Ar-*H*), 5.71 (1H, d, *J* 9, CONHCH), 4.24 (1H, q, *J* 8, CONHCH), 2.55 (2H, m, CH₂CH₂-Phe), 1.92 – 1.78 (2H, m, CH₂CH₂-Phe), 1.32 (9H, s, (CH₃)₃CO);

tert-butyl

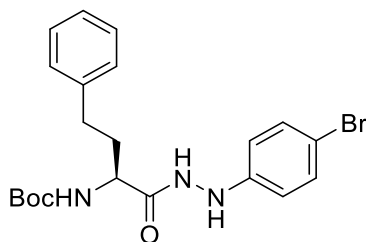
(S)-(1-oxo-4-phenyl-1-(2-(4-(trifluoromethyl)phenyl)hydrazineyl)butan-2-yl)carbamate 67f



Following the general procedure outlined, *N*-Boc-*L*-homophenylalanine (0.40 g, 1.43 mmol) and 4-trifluoromethylphenylhydrazine hydrochloride (0.28 g, 1.58 mmol) were transformed following trituration with DCM into the title compound which was isolated as a white solid (0.31 g, 55 %); δ_{H} (300 MHz, CDCl₃) 8.91 (1H, s, CONHNH), 7.46 – 7.32 (4H, m, Ar-*H*), 7.29 – 7.13 (5H, m, Ar-*H*), 7.13 – 7.07 (2H, m, Ar-*H*), 6.77 (2H, m, Ar-*H*), 5.44 (1H, d, *J* 8.0, CONHCH), 4.28 (1H, d, *J* 8, CONHCH), 2.71 (2H, m, CH₂CH₂Phe), 2.17 (1H, m, CH₂CH₂Phe), 1.44 (9H, s, (CH₃)₃CO);

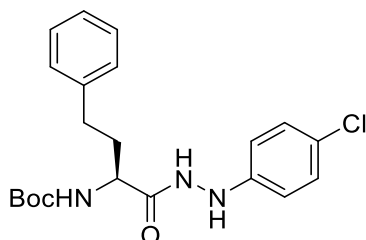
Chapter 5. Experimental section.

tert-butyl (S)-(1-(2-(4-bromophenyl)hydrazineyl)-1-oxo-4-phenylbutan-2-yl)carbamate 67e



Following the general procedure outlined, *N*-Boc-*L*-homophenylalanine (0.40 g, 1.43 mmol) and 4-bromophenylhydrazine hydrochloride (0.28 g, 1.58 mmol) were transformed following trituration with Et₂O into the title compound which was isolated as yellowish white solid (0.38 g, 70 %); δ_{H} (300 MHz, CDCl₃) 8.76 (1H, s, CONH₂), 7.34 – 7.21 (4H, m, Ar-*H*), 7.19 (2H, d, *J* 6, Ar-*H*), 7.09 (2H, d, *J* 7, Ar-*H*), 6.68 – 6.49 (2H, m, Ar-*H*), 5.40 (1H, d, *J* 8.0, CONHCH), 4.22 (1H, d, *J* 7, CONHCH), 2.09 (2H, m, CH₂CH₂Phe), 2.00 – 1.79 (1H, m, CH₂CH₂Phe), 1.44 (9H, s, (CH₃)₃CO);

tert-butyl (S)-(1-(2-(4-chlorophenyl)hydrazineyl)-1-oxo-4-phenylbutan-2-yl)carbamate 67a



Following the general procedure outlined, *N*-Boc-*L*-homophenylalanine (0.40 g, 1.43 mmol) and 4-chlorophenylhydrazine hydrochloride (0.28 g, 1.58 mmol) were transformed following trituration with DCM into the title compound which was isolated as a white solid (0.42 g, 82%); δ_{H} (300 MHz, CDCl₃) δ_{H} (300 MHz, CDCl₃) 8.76 (1H, s, CONH₂), 7.34 – 7.21 (4H, m, Ar-*H*), 7.19 (2H, d, *J* 6, Ar-*H*), 7.09 (2H, d, *J* 7, Ar-*H*), 6.68 – 6.49 (2H, m, Ar-*H*), 5.40 (1H, d, *J* 8.0, CONHCH), 4.22 (1H, d, *J* 7, CONHCH), 2.09 (2H, m, CH₂CH₂Phe), 2.00 – 1.79 (1H, m, CH₂CH₂Phe), 1.44 (9H, s, (CH₃)₃CO);

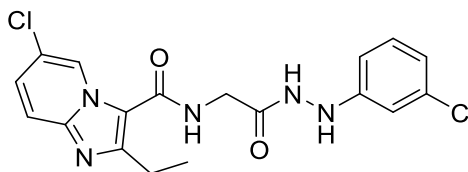
Chapter 5. Experimental section.

5.1.2 General procedure for synthesis of imidazo[1,2 a] pyridine substituted amino acid hydrazide compounds

The *N*-Boc amino acid hydrazides (1.20 equiv.) were dissolved in 4 M HCl solution in dioxane (3 mL) and stirred at room temperature. After 90 minutes the mixture was evaporated, dried *in vacuo* and precipitated using (EtOH / Et₂O). Then the precipitate was directly used in the next step without further purification. The resulting solid (1 equiv.) was dissolved in THF (3 mL) and diisopropylethylamine (3 equiv.) was added followed followed by (2-(1H-benzotriazol-1-yl)-1,1,3,3-tetramethyluronium hexafluorophosphate HBTU (1.20 equiv.). After stirring for 10 minutes at room temperature, the solution was treated with 6-chloro imidazo[1, 2a] pyridine-3-carboxylic acid (1.20 equiv.) and continued stirring for 4 hours. Then, reaction mixed with EtOAc (10 mL) and distilled water (5 mL). After separation of the two phases the organic layer washed again with distilled water (5 mL × 3 mL) followed by a wash with sat. aq. NH₄Cl (6 mL) then sat. aq. NaHCO₃ (6 mL) followed by brine (10 mL). The organic layer dried over MgSO₄, filtered, evaporated and dried *in vacuo*. The product was purified by trituration with (Et₂O or DCM) or through flash column chromatography (*n*-hexane/EtOAc [2:1]); (DCM/EtOH/NH₃ [600:8:1], [200:6:1]) to afford the desired compounds **69a** - **75f**;

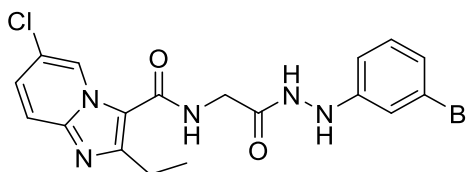
Chapter 5. Experimental section.

6-chloro-*N*-(2-(2-(3-chlorophenyl)hydrazineyl)-2-oxoethyl)-2-ethylimidazo[1,2-*a*]pyridine-3-carboxamide **69a**



Following the general procedure outlined, *tert*-butyl (2-(2-(3-chlorophenyl)hydrazineyl)-2-oxoethyl)carbamate **61a** (0.10 g, 0.30 mmol), was transformed following flush column chromatography to afford the title compound as yellow oil (0.05 g, 35 %); R_f 0.50 (*n*-hexane/EtOAc [2:1]); m.p. 240 – 241 °C ; ν_{\max} 2972, 1627, 1569, 1474, 1342, 914, 721 cm^{-1} ; δ_H (300 MHz, DMSO- d_6) 9.9 (1H, d, J 2, CONHNH), 9.2 (1H, dd, J 2, 0.9, Ar-*H*), 8.3 – 8.0 (1H, m, CONH), 8.1 (1H, d, J 2, CONHNH), 7.7 (1H, dd, J 10, 0.8, Ar-*H*), 7.5 (1H, dd, J 10, 2, Ar-*H*), 7.2 – 7.1 (1H, s, Ar-*H*), 6.9 (1H, t, J 2, Ar-*H*) 6.8 – 6.7 (2H, m, Ar-*H*), 4.0 (2H, d, J 6, CONHCH₂), 3.0 (2H, q, J 8, CH₂CH₃), 1.3 (3H, t, J 8, CH₂CH₃); δ_C (75 MHz, DMSO- d_6) 196.4 (CONHNH), 161.6 (CONH), 151.88 (*ipso*-Ar-C), 151.32 (*ipso*-Ar-C), 143.8 (*ipso*-Ar-C), 134.1 (*ipso*-Ar-C), 130.6 (*ipso*-Ar-C), 127.7 (Ar-C), 125.5 (Ar-C), 120.2 (*ipso*-Ar-C), 118.3 (Ar-C), 117.6 (Ar-C), 111.9 (Ar-C), 111.5 (Ar-C), 42.1 (CONHCH₂), 22.3 (CH₂CH₃), 13.5 (CH₂CH₃); m/z (ES⁺) 406 ([^{35,35}Cl]MH⁺), 408 ([^{35,37}Cl]MH⁺); HRMS (ES⁺) Found [^{35,35}Cl]MH⁺, 406.0544 (C₁₈H₁₈^{35,35}Cl₂N₅O₂ requires 406.0838);

N-(2-(2-(3-bromophenyl)hydrazineyl)-2-oxoethyl)-6-chloro-2-ethylimidazo[1,2-*a*]pyridine-3-carboxamide **69b**

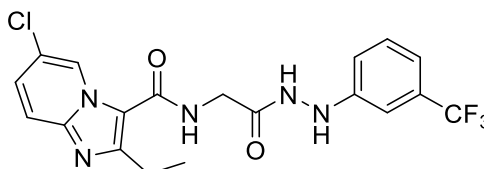


Following the general procedure outlined, *tert*-butyl (2-(2-(3-bromophenyl)hydrazineyl)-2-oxoethyl)carbamate **61b** (1.0 g, 0.3 mmol), was transformed following trituration with diethyl ether to afford the titled compounds as pale orange solid (0.07 g, 51 %); R_f 0.35 (DCM/EtOH/NH₃ [200:6:1]); m.p. 229

Chapter 5. Experimental section.

– 230 °C ; ν_{\max} 3263, 1751, 1664, 1612, 1526, 1511, 1487, 1417, 1394, 1374, 1328, 1291, 1189, 1158, 1108, 1066, 1013, 1000, 924, 897, 838 cm^{-1} ; δ_{H} (300 MHz, DMSO- d_6) 9.9 (1H, d, J 2, CONH NH), 9.2 (1H, dd, J 2, 0.9, Ar- H), 8.3 – 8.0 (1H, m, CONH), 8.1 (1H, d, J 2, CONH NH), 7.7 (1H, dd, J 10, 0.8, Ar- H), 7.5 (1H, dd, J 10, 2, Ar- H), 7.2 – 7.1 (1H, s, Ar- H), 6.9 (1H, t, J 2, Ar- H) 6.8 – 6.7 (2H, m, Ar- H), 4.0 (2H, d, J 6, CONH CH_2), 3.0 (2H, q, J 8, CH_2CH_3), 1.3 (3H, t, J 8, CH_2CH_3); δ_{C} (75 MHz, DMSO- d_6), 196.4 (CONH NH), 161.6 (CONH) 151.88 (*ipso*-Ar-C), 151.32 (*ipso*-Ar-C), 143.8 (*ipso*-Ar-C) 134.1 (*ipso*-Ar-C), 130.6 (*ipso*-Ar-C), 127.7 (*ipso*-Ar-C), 125.5 (Ar-C), 120.2 (*ipso*-Ar-C), 118 (Ar-C), 117.6 (Ar-C), 111.9 (Ar-C), 111.5 (Ar-C), 42.1 (NH CH_2CO), 22.3 (CH_2CH_3), 13.5 (CH_2CH_3); m/z (ES $^+$) 451 (^{35}Cl , ^{79}Br] MH^+), 453 (^{35}Cl , ^{81}Br] MH^+), 453 (^{37}Cl , ^{79}Br] MH^+); HRMS (ES $^+$) Found ^{35}Cl , ^{79}Br] MH^+ , 451.0330 ($\text{C}_{18}\text{H}_{18}^{79}\text{Br}^{35}\text{ClN}_5\text{O}_2$ requires 451.0411);

6-chloro-2-ethyl-*N*-(2-oxo-2-(2-(3-(trifluoromethyl)phenyl)hydrazineyl)ethyl)imidazo[1,2-*a*]pyridine-3-carboxamide 69c

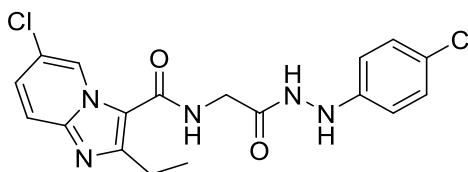


Following the general procedure outlined, *tert*-butyl (2-oxo-2-(2-(3-(trifluoromethyl)phenyl)hydrazineyl)ethyl)carbamate **61c** (0.10 g, 0.30 mmol) was transformed following flush column chromatography to produce a pale white solid (0.07 g, 50 %); R_f 0.56 (DCM/EtOH/ NH_3 [200:6:1]); m.p. 238 – 240 °C ; ν_{\max} 3448, 3263, 1751, 1664, 1612, 1526, 1511, 1487, 1417, 1394, 1374, 1328, 1291, 1189, 1158, 1108, 1066, 1013, 1000, 924, 897, 838 cm^{-1} ; δ_{H} (300 MHz, DMSO- d_6) 9.99 (1H, d, J 3, CONH NH), 9.17 (1H, dd, J 2, 0.9, Ar- H) 8.28 – 8.24 (2H, m, Ar- H), 7.68 (1H, dd, J 10, 0.8, Ar- H), 7.46 (1H, dd, J 10, 2, Ar- H), 7.40 – 7.33 (1H, m, Ar- H), 7.11 (1H, t, J 2, Ar- H), 7.08 – 6.99 (2H, m, Ar- H), 4.05 (2H, d, J 5, CONH CH_2), 3.02 (2H, d, J 8, CH_2CH_3), 1.34 – 1.27 (3H, t, J 8, CH_2CH_3); δ_{C} (75 MHz, DMSO- d_6) 196.5 (CONH NH), 161.6 (CONH), 151.8 (*ipso*-Ar-C), 150.5

Chapter 5. Experimental section.

(*ipso*-Ar-C), 143.8 (*ipso*-Ar-C), 130.1 (*ipso*-Ar-C), 127.6 (Ar-C), 125.5 (*ipso*-Ar-C), 122.7 (Ar-C), 120.2 (*ipso*-Ar-C), 119.7 (Ar-C), 117.6 (Ar-C), 116.4 (Ar-C), 115.9 (Ar-C), 115.7 (Ar-C), 108.4 (*ipso*-Ar-C), 42.1 (CONHCH₂), 22.3 (CH₂CH₃), 13.4 (CH₂CH₃); δ_F (282 MHz, DMSO-d₆) -61.25 (3F, s, CF₃); m/z (ES⁺) 440 ([³⁵Cl]MH⁺) 442 ([³⁷Cl]MH⁺); HRMS (ES⁺) Found [³⁵Cl]MH⁺, 440.0605 (C₁₉H₁₈³⁵ClF₃N₅O₂ requires 440.1101);

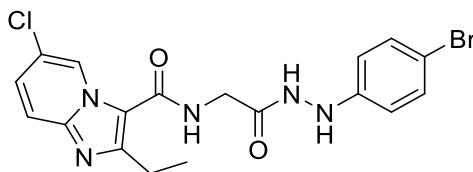
6-chloro-N-(2-(2-(4-chlorophenyl)hydrazineyl)-2-oxoethyl)-2-ethylimidazo[1,2-a]pyridine-3-carboxamide **69d**



Following the general procedure outlined, *tert*-butyl(2-oxo-2-(2-(4-chlorophenyl)hydrazineyl)ethyl)carbamate **61d** (0.1 g, 0.3 mmol), was transformed trituration by diethyl ether to produce the titled compound as white solid (0.05 g, 33 %); R_f 0.45 (*n*-hexane/EtOAc[2:1]); m.p. 239 – 240 °C; ν_{max} 3255, 2933, 1673, 1626, 1509, 1487, 1389, 1207, 1090, 1046, 820, 728, 556 cm⁻¹; δ_H (300 MHz, DMSO-d₆) 9.90 (1H, d, J 3, CONH₂), 9.11 (1H, dd, J 2, 0.8, Ar-H) 8.27 (1H, m, CONH) 7.97 (1H, d, J 3, CONHNH), 7.67 (1H, dd, J 9.5, 0.8, Ar-H), 7.46 (1H, dd, J 10, 2, Ar-H), 7.18 (2H, m, Ar-H), 6.86 (2H, m, Ar-H), 4.04 (2H, d, J 6, CONHCH₂), 3.00 (2H, q, J 8, CH₂CH₃), 1.30 (3H, t, J 8, CH₂CH₃); δ_C (75 MHz, DMSO-d₆) 169 (CONHNH), 161.5 (CONH), 151.7 (*ipso*-Ar-C), 148.7 (*ipso*-Ar-C), 143.8 (*ipso*-Ar-C), 128.8 (Ar-C), 127.6 (Ar-C), 125.4 (Ar-C), 122.3 (*ipso*-Ar-C), 120.2 (*ipso*-Ar-C), 117 (Ar-C), 116.2 (*ipso*-Ar-C), 114.2 (Ar-C), 41.9 (CONHCH₂), 22.2 (CH₂CH₃), 13.5 (CH₂CH₃); m/z (ES⁺) 406 ([^{35,35}Cl]MH⁺), 408 ([^{35,37}Cl]MH⁺); HRMS (ES⁺) Found [^{35,35}Cl]MH⁺ 406.0544 (C₁₈H₁₇^{35,35}Cl₂N₅O₂ requires 406.0383);

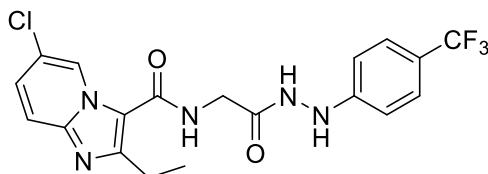
Chapter 5. Experimental section.

N-(2-(2-(4-bromophenyl)hydrazineyl)-2-oxoethyl)-6-chloro-2-ethylimidazo[1,2-*a*]pyridine-3-carboxamide **69e**



Following the general procedure outlined, *tert*-butyl (2-(2-(4-bromophenyl)hydrazineyl)-2-oxoethyl)carbamate **61e** (1.0 g, 0.3 mmol), was transformed following trituration to afford titled compound as pale yellow solid (0.07 g, 51 %). R_f 0.35 (DCM/EtOH [200:6]); m.p. 220 – 226 °C; ν_{max} 3255, 2933, 1673, 1626, 1509, 1487, 1389, 1207, 1090, 1046, 820, 728, 556 cm^{-1} ; δ_H (300 MHz, DMSO- d_6) 9.90 (1H, d, J 3, CONH NH), 9.11 (1H, dd, J 2, 0.8, Ar- H) 8.27 (1H, m, CONH) 7.97 (1H, d, J 3, CONH NH), 7.67 (1H, dd, J 9.5, 0.8, Ar- H), 7.46 (1H, dd, J 10, 2, Ar- H), 7.18 (2H, m, Ar- H), 6.86 (2H, m, Ar- H), 4.04 (2H, d, J 6, CONH CH_2), 3.00 (2H, q, J 8, CH_2CH_3), 1.30 (3H, t, J 8, CH_2CH_3); δ_C (75 MHz, DMSO- d_6) 169 (CONH NH), 161.5 (CONH), 151.7 (*ipso*-Ar-C), 148.7 (*ipso*-Ar-C), 143.8 (*ipso*-Ar-C), 128.8 (Ar-C), 127.6 (Ar-C), 125.4 (Ar-C), 122.3 (*ipso*-Ar-C), 120.2 (*ipso*-Ar-C), 117 (Ar-C), 116.2 (*ipso*-Ar-C), 114.2 (Ar-C), 41.9 (CONH CH_2), 22.2 (CH_2CH_3), 13.5 (CH_2CH_3); m/z (ES $^+$) 449 ([^{35}Cl , ^{79}Br]MH $^+$), 451 ([^{35}Cl , ^{81}Br]MH $^+$), 451 ([^{37}Cl , ^{79}Br]MH $^+$), 453 ([^{37}Cl , ^{81}Br]MH $^+$); HRMS Found [^{35}Cl , ^{79}Br]MH $^+$, 449.9824 (C $_{18}$ H $_{18}$ ^{79}Br ^{35}Cl N $_5$ O $_2$ requires 450.0332);

6-chloro-2-ethyl-*N*-(2-oxo-2-(2-(4-(trifluoromethyl)phenyl)hydrazineyl)ethyl)imidazo[1,2-*a*]pyridine-3-carboxamide **69f**

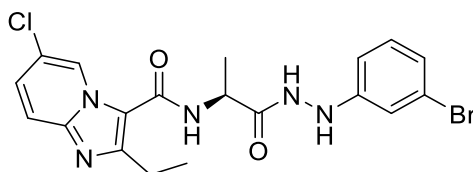


Following the general procedure outlined, *tert*-butyl (2-oxo-2-(2-(4-(trifluoromethyl)phenyl)hydrazineyl)ethyl)carbamate **61f** (0.10 g, 0.30 mmol), was transformed following trituration with Et $_2$ O to obtain the titled compound as pale white solid (0.07 g, 51 %); R_f 0.35 (*n*-hexane/EtOAc [2:1]); m.p. 235 – 237 °C;

Chapter 5. Experimental section.

ν_{\max} 2972, 1959, 1641, 1610, 1595, 1485, 1390, 1214, 1125, 1049, 815, 755, 685, 535, 430 cm^{-1} ; δ_{H} (300 MHz, DMSO- d_6) 10.02 (1H, s, CONHNNH), 9.12 (1H, d, J 2, Ar-H), 8.34 (1H, t, J 6, CONH) 7.70 (1H, d, J 10, Ar-H), 7.58 (1H, d, J 9, Ar-H), 7.53 – 7.44 (3H, m, Ar-H), 6.89 (2H, d, J 9, Ar-H), 4.05 (2H, d, J 6, CONHCH $_2$), 3.09 – 2.92 (2H, q, J 8, CH $_2$ CH $_3$), 1.29 (3H, t, J 8, CH $_2$ CH $_3$); δ_{C} (75 MHz, DMSO- d_6) 169.4 (CONHNNH), 161.3 (CONH), 152.9 (*ipso*-Ar-C), 143.4 (*ipso*-Ar-C), 128.2 (Ar-C), 126.52 (Ar-C), 126.46 (Ar-C) 125.5 (Ar-C), 120.5 (*ipso*-Ar-C) 117.3 (Ar-C), 116.3 (*ipso*-Ar-C), 112.0 (Ar-C), 41.9 (CONHCH $_2$), 21.9 (CH $_2$ CH $_3$), 13.5 (CH $_2$ CH $_3$); m/z (ES $^+$) 440 ([^{35}Cl]MH $^+$); HRMS (ES $^+$) Found [^{35}Cl]MH $^+$ 440.0809 (C $_{19}$ H $_{18}$ ^{35}Cl F $_3$ N $_5$ O $_2$ requires 440.1011);

(S)-N-(1-(2-(3-bromophenyl)hydrazineyl)-1-oxopropan-2-yl)-6-chloro-2-ethylimidazo[1,2-a]pyridine-3-carboxamide 70b

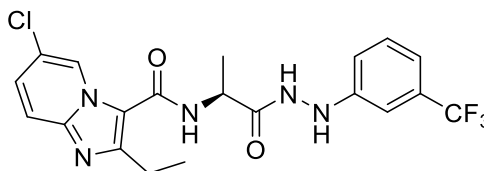


Following the general procedure outlined, *tert*-butyl (S)-1-(2-(3-bromophenyl)hydrazineyl)-1-oxopropan-2-yl)carbamate **62b** (0.1 g, 0.3 mmol), was transformed following trituration with DCM to obtain the titled compound as white solid (0.03 g, 19 %); R_f 0.40 (*n*-hexane/EtOAc [4;1]); m.p. 250 – 265 $^{\circ}\text{C}$; ν_{\max} 3026, 1642, 1595, 1486, 1390, 1214, 813, 771 cm^{-1} ; δ_{H} (300 MHz, DMSO- d_6) 10.01 (1H, d, J 2, CONHNNH), 9.10 (1H, dd, J 2, 0.9, Ar-H), 8.38 (1H, m, CONH), 7.73 (1H, d, J 9, Ar-H), 7.56 (1H, dd, J 10, 2, Ar-H), 7.09 (1H, t, J 8, Ar-H), 6.99 (1H, t, J 2, Ar-H), 6.86 (1H, dd, J 7, 2, Ar-H), 6.76 (1H, dd, J 8, 2, Ar-H), 4.57 (1H, p, J 7, CONHCH), 3.00 (2H, q, J 8, CH $_2$ CH $_3$), 1.47 (3H, d, J 7, CONHCH(CH $_3$)), 1.28 (3H, t, J 8, CH $_2$ CH $_3$); δ_{C} (75 MHz, DMSO- d_6) 172.7 (CONHNNH), 160.7 (CONH), 151.4 (*ipso*-Ar-C), 143 (*ipso*-Ar-C), 131.0 (Ar-C), 128.6 (Ar-C), 125.4 (Ar-C), 122.7 (*ipso*-Ar-C), 121.2 (Ar-C), 120.7 (*ipso*-Ar-C), 117.1 (Ar-C), 116.4 (*ipso*-Ar-C), 114.8 (Ar-C), 111.7 (Ar-C), 48.4 (CO NHCH(CH $_3$)) 21.8 (CH $_2$ CH $_3$), 18.1 (CONHCH(CH $_3$)), 13.4 (CH $_2$ CH $_3$); m/z (ES $^+$) 464 ([^{35}Cl , ^{79}Br]MH $^+$), 466 ([^{35}Cl ,

Chapter 5. Experimental section.

$^{81}\text{Br}[\text{MH}^+)$, 466 (^{37}Cl , $^{79}\text{Br}[\text{MH}^+)$, 468 (^{37}Cl , $^{81}\text{Br}[\text{MH}^+)$; HRMS (ES⁺) Found [^{35}Cl , $^{79}\text{Br}[\text{MH}^+$, 464.0211 (C₁₉H₂₀⁷⁹Br³⁵ClN₅O₂ requires 464.0489);

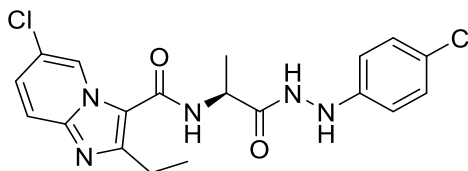
(S)-6-chloro-2-ethyl-N-(1-oxo-1-(2-(3-(trifluoromethyl)phenyl)hydrazineyl)propan-2-yl)imidazo[1,2-a]pyridine-3-carboxamide 70c



Following the general procedure outlined, *tert*-butyl (S)-(1-oxo-1-(2-(3-(trifluoromethyl)phenyl)hydrazineyl)propan-2-yl)carbamate **62c** (0.10 g, 0.30 mmol), was transformed following trituration using DCM to obtain the titled compound as pale yellow solid (0.04 g, 33 %); R_f 0.43 (*n*-hexane/EtOAc [2:1]); m.p. 250 – 251 °C; ν_{max} 3258, 2978, 1666, 1608, 1538, 1492, 1455, 1417, 1394, 1370, 1317, 1269, 1248, 1218, 1159, 1139, 1075, 1044, 993, 950, 850, 802 cm⁻¹; δ_{H} (300 MHz, DMSO- d₆) δ_{H} (300 MHz, DMSO-d₆) 10.06 (1H, d, *J* 2, CONH₂), 9.03 (1H, dd, *J* 2, 0.9, Ar-H), 8.28 (1H, m, CONH), 7.68 (1H, dd, *J* 10, 0.8, Ar-H), 7.46 (1H, dd, *J* 10, 2, Ar-H), 7.37 (1H, t, *J* 8, Ar-H), 7.05 (3H, dd, *J* 16, 8, Ar-H), 4.57 (1H, q, *J* 7, CONHCH), 3.00 (2H, q, *J* 8, CH₂CH₃), 1.47 (3H, d, *J* 7, CONHCH(CH₃)), 1.28 (3H, t, *J* 8, CH₂CH₃); δ_{C} (75 MHz, DMSO-d₆) 172.8 (CONH₂), 161.1 (CONH), 150.9 (*ipso*-Ar-C), 151.3 (*ipso*-Ar-C), 143.7 (*ipso*-Ar-C), 134.1 (*ipso*-Ar-C), 130.7 (Ar-C), 127.3 (Ar-C), 125.1 (Ar-C), 120.0 (*ipso*-Ar-C), 117.7 (Ar-C), 116.3 (Ar-C), 115.0 (Ar-C), 48.4 (NHCH(CH₃)CO), 22.2 (CH₂CH₃), 18.1 (NHCH(CH₃)CO), 13.4 (CH₂CH₃); δ_{C} (75 MHz, DMSO-d₆) 172.7 (CONH₂), 160.7 (CONH), 151.4 (*ipso*-Ar-C), 143 (*ipso*-Ar-C), 131 (*ipso*-Ar-C), 128.6 (Ar-C), 125.5 (Ar-C), 122.7 (Ar-C), 121.2 (Ar-C), 120.7 (*ipso*-Ar-C), 117.1 (*ipso*-Ar-C), 116.4 (Ar-C), 114.8 (*ipso*-Ar-C), 111.7 (Ar-C), 48.4 (NHCH(CH₃)CO) 21.8 (CH₂CH₃), 18.1 (NHCH(CH₃)CO), 13.4 (CH₂CH₃); δ_{F} (376 MHz, DMSO-d₆) -61.25 (3F, s, CF₃); *m/z* (ES⁺) 454 ($^{35}\text{Cl}[\text{MH}^+)$; HRMS (ES⁺) Found [$^{35}\text{Cl}[\text{MH}^+$, 454.0850 (C₂₀H₂₀³⁵ClF₃N₅O₂ requires 454.1258);

Chapter 5. Experimental section.

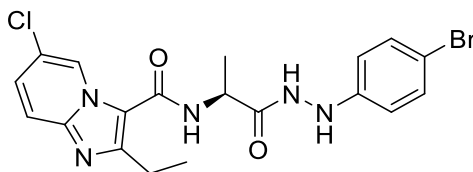
(S)-6-chloro-N-(1-(2-(4-chlorophenyl)hydrazineyl)-1-oxopropan-2-yl)-2-ethylimidazo[1,2-a]pyridine-3-carboxamide 70d



Following the general procedure outlined, *tert*-butyl (S)-(1-(2-(4-chlorophenyl)hydrazineyl)-1-oxopropan-2-yl)carbamate **62d** (0.10 g, 0.3 mmol), was transformed followed by flush column chromatography to obtain the titled compound as a white solid (0.03 g, 22 %); R_f 0.45 (*n*-hexane/EtOAc [2:1]); m.p. 230 – 234 °C; ν_{\max} 3258, 2978, 1666, 1608, 1605, 1538, 1492, 1455, 1417, 1394, 1370, 1317, 1269, 1248, 1218, 1159, 1139, 1110, 1075, 1044, 993, 950, 906, 850, 802 cm^{-1} ; δ_H (300 MHz, DMSO- d_6) 9.98 (1H, d, J 3, CONHNH), 9.05 – 8.98 (1H, m, Ar-*H*), 8.29 (1H, d, J 7, CONH), 8.00 (1H, d, J 3, CONHNH), 7.68 (1H, dd, J 10, 0.9, Ar-*H*), 7.46 (1H, dd, J 10, 2, Ar-*H*), 7.23 – 7.12 (2H, d, J 9, Ar-*H*), 6.85 – 6.74 (2H, d, J 9, Ar-*H*), 4.58 (1H, t, J 7, CONHCH(CH_3)), 2.99 (2H, q, J 8, CH_2CH_3), 1.45 (3H, d, J 7, CONHCH(CH_3)), 1.28 (3H, t, J 8, CH_2CH_3); δ_C (75 MHz, DMSO- d_6) 172.7 (CONHNH), 160.9 (CONH), 151.5 (*ipso*-Ar-C), 148.8 (*ipso*-Ar-C), 143.5 (*ipso*-Ar-C), 128.9 (Ar-C), 127.7 (*ipso*-Ar-C), 125.2 (Ar-C), 122.2 (*ipso*-Ar-C), 120.1 (*ipso*-Ar-C), 117.7 (Ar-C), 116.4 (*ipso*-Ar-C), 114.1 (Ar-C), 48.2 (CONHCH(CH_3)), 22.2 (CH_2CH_3), 18.3 (CONHCH(CH_3)), 13.5 (CH_2CH_3); m/z (ES⁺) 420 ([^{35,35}Cl]MH⁺), 422 ([^{35,37}Cl]MH⁺); HRMS (ES⁺) Found [^{35,35}Cl]MH⁺, 420.0781 (C₁₉H₂₀^{35,35}Cl₂N₅O₂ requires 420.0994);

Chapter 5. Experimental section.

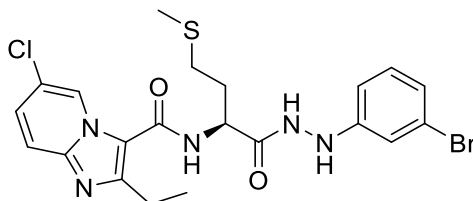
(S)-N-(1-(2-(4-bromophenyl)hydrazineyl)-1-oxopropan-2-yl)-6-chloro-2-ethylimidazo[1,2-a]pyridine-3-carboxamide 70e



Following the general procedure outlined, *tert*-butyl (S)-(1-(2-(4-bromophenyl)hydrazineyl)-1-oxopropan-2-yl)carbamate **62e** (0.1 g, 0.3 mmol), was transformed followed by flush column chromatography to obtain the titled compound as faint yellow solid (0.08 g, 59 %); R_f 0.56 (*n*-hexane/EtOAc [2:1]); m.p. 247 – 249 °C; ν_{\max} 3258, 2978, 1666, 1608, 1605, 1538, 1492, 1455, 1417, 1394, 1370, 1317, 1269, 1248, 1218, 1159, 1139, 1110, 1075, 1044, 993, 950, 906, 850, 802 cm^{-1} ; δ_H (300 MHz, DMSO- d_6) 9.98 (1H, d, J 3, CONH NH), 9.05 – 8.98 (1H, m, Ar- H), 8.29 (1H, d, J 7, CONH), 8.00 (1H, d, J 3, CONH NH), 7.68 (1H, dd, J 10, 0.9, Ar- H), 7.46 (1H, dd, J 10, 2, Ar- H), 7.23 – 7.12 (2H, d, J 9, Ar- H), 6.85 – 6.74 (2H, d, J 9, Ar- H), 4.58 (1H, t, J 7, CONHCH(CH_3)), 2.99 (2H, q, J 8, CH_2CH_3), 1.45 (3H, d, J 7, CONHCH(CH_3)), 1.28 (3H, t, J 8, CH_2CH_3); δ_C (75 MHz, DMSO- d_6) 172.7 (CONH NH), 160.9 (CONH), 151.5 (*ipso*-Ar-C), 148.8 (*ipso*-Ar-C), 143.5 (*ipso*-Ar-C), 128.9 (Ar-C), 127.7 (*ipso*-Ar-C), 125.2 (Ar-C), 122.2 (*ipso*-Ar-C), 120.1 (*ipso*-Ar-C), 117.7 (Ar-C), 116.4 (*ipso*-Ar-C), 114.1 (Ar-C), 48.2 (CONHCH(CH_3)), 22.2 (CH_2CH_3) 18.3 (CONHCH(CH_3)), 13.5 (CH_2CH_3); m/z (ES^+) 464 ($[^{35}\text{Cl}, ^{79}\text{Br}]\text{MH}^+$), 466 ($[^{35}\text{Cl}, ^{81}\text{Br}]\text{MH}^+$), 466 ($[^{37}\text{Cl}, ^{79}\text{Br}]\text{MH}^+$), 468 ($[^{37}\text{Cl}, ^{81}\text{Br}]\text{MH}^+$); HRMS (ES^+) Found $[^{35}\text{Cl}, ^{79}\text{Br}]\text{MH}^+$, 464.0222 ($\text{C}_{19}\text{H}_{20}^{79}\text{Br}^{35}\text{ClN}_5\text{O}_2$ requires 464.0489);

Chapter 5. Experimental section.

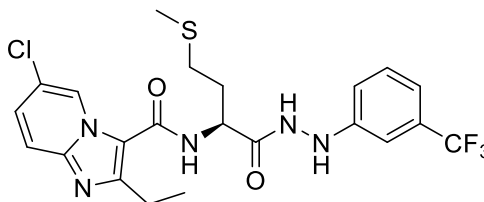
(S)-N-(1-(2-(3-bromophenyl)hydrazineyl)-4-(methylthio)-1-oxobutan-2-yl)-6-chloro-2-ethylimidazo[1,2-a]pyridine-3-carboxamide 71b



Following the general procedure outlined, *tert*-butyl(S)-(4-(methylthio)-1-oxo-1-(2-(3-(bromophenyl)hydrazineyl)butan-2-yl)carbamate **63b** (0.10 g, 0.30 mmol), was transformed following trituration by DCM to produce titled compound as (0.06 g, 48 %); R_f 0.46 (DCM/EtOH [200;6]); m.p. 245 -247 °C ; ν_{max} 3334, 2916, 1666, 1603, 1519, 1489, 1417, 1396, 1341, 1305, 1288, 1212, 1151, 1120, 1048, 998, 963, 872, 847, 814 cm⁻¹; δ_H (300 MHz, DMSO-d₆) 10.05 (1H, d, *J* 2, CONHNH), 9.04 (1H, d, *J* 2, Ar-*H*), 8.41 (1H, d, *J* 7, CONH), 8.15 (1H, d, *J* 2, CONHNH), 7.70 (1H, d, *J* 9, Ar-*H*), 7.48 (1H, dd, *J* 9, 2, Ar-*H*), 7.16 (1H, t, *J* 6, Ar-*H*), 6.86 (1H, s, Ar-*H*), 6.76-6.68 (2H, m, Ar-*H*), 4.59 (1H, q, *J* 7, NHCH(CH₂CH₂SCH₃)), 3.00 (2H, q, *J* 7, CH₂CH₃), 2.68-2.56 (2H, m, NHCH(CH₂CH₂SCH₃)), 2.12-2.06 (5H, m, NHCH(CH₂CH₂SCH₃)), 1.28 (3H, t, *J* 7, CH₂CH₃); δ_C (75 MHz, DMSO-d₆) 172.0 (CONHNH), 161.6 (CONH), 152.0 (*ipso*-Ar-C), 151.3 (*ipso*-Ar-C), 143.8 (*ipso*-Ar-C), 134.1 (*ipso*-Ar-C), 130.7 (Ar-C), 127.6 (Ar-C), 125.3 (Ar-C), 120.1 (*ipso*-Ar-C), 118.3 (*ipso*-Ar-C), 117.7 (Ar-C), 116.4 (*ipso*-Ar-C), 112.0 (Ar-C), 111.4 (Ar-C), 52.0 (NHCH(CH₂CH₂SCH₃)), 31.2 (NHCH(CH₂CH₂SCH₃)), 31.1 (NHCH(CH₂CH₂SCH₃)), 22.3 (CH₂CH₃), 15.1 (NHCH(CH₂CH₂SCH₃)), 13.6 (CH₂CH₃); *m/z* (ES⁺) 524 ([³⁵Cl, ⁷⁹Br]MH⁺), 526 ([³⁵Cl, ⁸¹Br]MH⁺), 526 ([³⁷Cl, ⁷⁹Br]MH⁺), 528 ([³⁷Cl, ⁸¹Br]MH⁺); HRMS (ES⁺) Found [³⁵Cl, ⁷⁹Br]MH⁺, 526.0501 (C₂₁H₂₄⁷⁹Br³⁵ClN₅O₂S requires 524.0532);

Chapter 5. Experimental section.

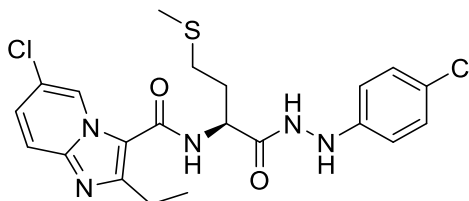
(S)-6-chloro-2-ethyl-N-(4-(methylthio)-1-oxo-1-(2-(3-(trifluoromethyl)phenyl)hydrazineyl)butan-2-yl)imidazo[1,2-a]pyridine-3-carboxamide 71c



Following the general procedure outlined, *tert*-butyl(S)-(4-(methylthio)-1-oxo-1-(2-(3-(trifluoromethyl)phenyl)hydrazineyl)butan-2-yl)carbamate **63c** (0.10 g, 0.30 mmol), was transformed following flush column chromatography to produce the titled compound as a pale white solid (0.04 g, 29 %); R_f 0.46 (DCM/EtOH [200;6]); m.p. 248 – 250 °C; ν_{\max} 3334, 2916, 1666, 1603, 1519, 1489, 1417, 1396, 1341, 1305, 1288, 1212, 1151, 1120, 1048, 998, 963, 872, 847, 814 cm^{-1} ; δ_{H} (300 MHz, DMSO- d_6) 10.13 (1H, d, J 2, CONHNH), 8.98 (1H, d, J 3.0, Ar- H), 8.29 (1H, d, J 2, CONHNH), 7.67 (1H, d, J 7, CONH), 7.49 – 7.44 (1H, m, Ar- H), 7.37 (2H, t, J 8, Ar- H), 7.05 (3H, dd, J 15, 8, Ar- H), 4.61 (1H, q, J 7, NHCH(CH₂CH₂SCH₃)), 3.01 (2H, q, J 8, CH₂CH₃), 2.71 – 2.56 (2H, m, NHCH(CH₂CH₂SCH₃)), 2.11 (5H, m, NHCH(CH₂CH₂SCH₃)), 1.27 (3H, t, J 8, CH₂CH₃); δ_{C} (75 MHz, DMSO- d_6) 171.9 (CONHNH), 161.6 (CONH), 151.9 (*ipso*-Ar-C), 150.4 (*ipso*-Ar-C), 143.7 (*ipso*-Ar-C), 130.1 (Ar-C), 127.6 (Ar-C), 125.2 (Ar-C), 120.1 (*ipso*-Ar-C), 117.7 (Ar-C), 116.4 (*ipso*-Ar-C), 115 (Ar-C), 108.3 (Ar-C), 52.1 (NHCH(CH₂CH₂SCH₃)), 31.2 (NHCH(CH₂CH₂SCH₃)), 30.4 (NHCH(CH₂CH₂SCH₃)), 22.3 (CH₂CH₃), 15 (NHCH(CH₂CH₂SCH₃)), 13.6 (CH₂CH₃); m/z (ES⁺) 514 ([³⁵Cl]MH⁺); HRMS (ES⁺) Found [³⁵Cl]MH⁺, 514.0823 (C₂₂H₂₄³⁵ClF₃N₅O₂S requires 514.1291);

Chapter 5. Experimental section.

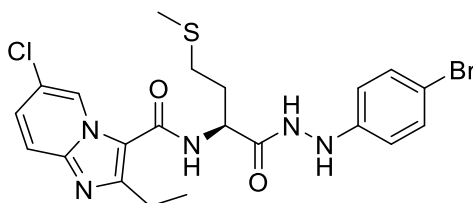
(S)-6-chloro-N-(1-(2-(4-chlorophenyl)hydrazineyl)-4-(methylthio)-1-oxobutan-2-yl)-2-ethylimidazo[1,2-a]pyridine-3-carboxamide 71d



Following the general procedure outlined, *tert*-butyl (S)-(1-(2-(4-chlorophenyl)hydrazineyl)-4-(methylthio)-1-oxobutan-2-yl)carbamate **63d** (0.10 g, 0.30 mmol), was transformed followed by trituration with DCM to produce the titled compound as a white solid (0.05 g, 35 %); R_f 0.46 (DCM/EtOH [200:6]); m.p. 226 – 227 °C; ν_{\max} 3248, 1664, 1612, 1526, 1487, 1417, 1394, 1374, 1328, 1291, 1189, 1158, 1108, 1066, 1013, 1000, 924, 897, 838 cm^{-1} ; δ_H (300 MHz, DMSO- d_6) 10.05 (1H, d, J 2, CONHNH), 8.96 (1H, d, J 2, Ar- H), 8.38 (1H, d, J 7, CONH), 8.02 (1H, d, J 2, CONHNH), 7.68 (1H, d, J 9 Ar- H), 7.47 (1H, dd, J 9, 2, Ar- H), 7.23 – 7.14 (2H, d, J 8, Ar- H), 6.85 – 6.76 (2H, d, J 8.7, Ar- H), 4.63 (1H, q, J 7, NHCH(CH₂CH₂SCH₃)), 3.00 (2H, q, J 7, CH₂CH₃), 2.62 (2H, q, J 7, NHCH(CH₂CH₂SCH₃)), 2.11 (5H, m, NHCH(CH₂CH₂SCH₃)), 1.28 (3H, t, J 7, CH₂CH₃); δ_C (75 MHz, DMSO- d_6) 171.8 (CONHNH) 161.5 (CONH), 151.8 (*ipso*-Ar-C), 148.7 (*ipso*-Ar-C), 143.7 (*ipso*-Ar-C), 128.9 (*ipso*-Ar-C), 127.5 (Ar-C), 125.2 (Ar-C), 122.3 (Ar-C), 120.02 (*ipso*-Ar-C), 117.7 (Ar-C), 116.5 (*ipso*-Ar-C), 114.2 (Ar-C), 51.9 (NHCH(CH₂CH₂SCH₃)), 31.3 (NHCH(CH₂CH₂SCH₃)), 30.4 (NHCH(CH₂CH₂SCH₃)), 22.2 (CH₂CH₃), 15.1 (NHCH(CH₂CH₂SCH₃)), 13.6 (CH₂CH₃); m/z (ES⁺) 480 ([^{35,35}Cl]MH⁺), 482 ([^{35,37}Cl]MH⁺); HRMS (ES⁺) Found [^{35,35}Cl]MH⁺ 480.0581 (C₂₁H₂₄^{35,35}Cl₂N₅O₂S requires 480.1028);

Chapter 5. Experimental section.

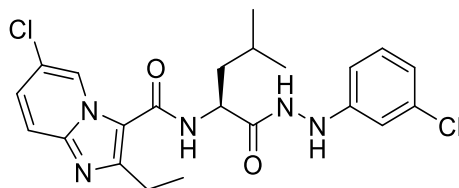
(S)-N-(1-(2-(4-bromophenyl)hydrazineyl)-4-(methylthio)-1-oxobutan-2-yl)-6-chloro-2-ethylimidazo[1,2-a]pyridine-3-carboxamide 71e



Following the general procedure outlined, *tert*-butyl (S)-(1-(2-(4-bromophenyl)hydrazineyl)-4-(methylthio)-1-oxobutan-2-yl)carbamate **63e** (0.10 g, 0.30 mmol), was transformed followed by trituration with diethyl ether to produce the titled compound as orange gummy solid (0.08 g, 51 %); R_f 0.44 (*n*-hexane/EtOAc [4:1]); m.p. 254 – 255 °C; ν_{max} 3248, 1664, 1612, 1526, 1487, 1417, 1394, 1374, 1328, 1291, 1189, 1158, 1108, 1066, 1013, 1000, 924, 897, 838 cm^{-1} ; δ_H (300 MHz, DMSO- d_6) 10.05 (1H, d, J 2, CONH NH), 8.96 (1H, d, J 2, Ar- H), 8.38 (1H, d, J 7, CONH), 8.02 (1H, d, J 2, CONH NH), 7.68 (1H, d, J 9, Ar- H), 7.47 (1H, dd, J 9, 2, Ar- H), 7.23 – 7.14 (2H, d, J 8, Ar- H), 6.85 – 6.76 (2H, d, J 8.7, Ar- H), 4.63 (1H, q, J 7, NHCH(CH $_2$ CH $_2$ SCH $_3$)), 3.00 (2H, q, J 7, CH $_2$ CH $_3$), 2.62 (2H, q, J 7, NHCH(CH $_2$ CH $_2$ SCH $_3$)), 2.11 (5H, m, NHCH(CH $_2$ CH $_2$ SCH $_3$)), 1.28 (3H, t, J 7, CH $_2$ CH $_3$); δ_C (75 MHz, DMSO- d_6) 171.8 (CONH NH) 161.5 (CONH), 151.8 (*ipso*-Ar-C), 148.7 (*ipso*-Ar-C), 143.7 (*ipso*-Ar-C), 128.9 (*ipso*-Ar-C), 127.5 (Ar-C), 125.2 (Ar-C), 122.3 (Ar-C), 120.02 (*ipso*-Ar-C), 117.7 (Ar-C), 116.5 (*ipso*-Ar-C), 114.2 (Ar-C), 51.9 (NHCH(CH $_2$ CH $_2$ SCH $_3$)), 31.3 (NHCH(CH $_2$ CH $_2$ SCH $_3$)), 30.4 (NHCH(CH $_2$ CH $_2$ SCH $_3$)), 22.2 (CH $_2$ CH $_3$), 15.1 (NHCH(CH $_2$ CH $_2$ SCH $_3$)), 13.6 (CH $_2$ CH $_3$); m/z (ES $^+$) 524 ([^{35}Cl , ^{79}Br]MH $^+$), 526 ([^{35}Cl , ^{81}Br]MH $^+$), 526 ([^{37}Cl , ^{79}Br]MH $^+$), 528 ([^{37}Cl , ^{81}Br]MH $^+$); HRMS (ES $^+$) Found [^{35}Cl , ^{79}Br]MH $^+$, 524.0558 (C $_{21}$ H $_{24}$ ^{79}Br ^{35}Cl N $_5$ O $_2$ S requires 524.0522);

Chapter 5. Experimental section.

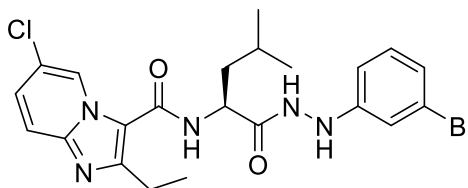
(S)-6-chloro-N-(1-(2-(3-chlorophenyl)hydrazineyl)-4-methyl-1-oxopentan-2-yl)-2-ethylimidazo[1,2-a]pyridine-3-carboxamide 72a



Following the general procedure outlined, *tert*-butyl (S)-(1-(2-(3-chlorophenyl)hydrazineyl)-4-methyl-1-oxopentan-2-yl)carbamate **64a** (0.10 g, 0.26 mmol) was transformed following trituration with Et₂O yielding pure product (0.09 g, 67 %. R_f 0.43, (*n*-hexane;EtOAc; [2:1]); m.p. 267 – 269 °C ; ν_{max} 3231, 2968, 1667, 1612, 1598, 1527, 1492, 1417, 1395, 1321, 1289, 1103, 1070, 1050, 1103, 996, 870, 854, 810, 780, 741, 676, 603, 536, 471 cm⁻¹; δ_H (300 MHz, DMSO-d₆) 10.08 (1H, d, *J* 3, CONH₂), 9.02 (1H, dd, *J* 2, 0.9, Ar-H), 8.35 (1H, d, *J* 8, CONH), 8.13 (1H, d, *J* 2, CONH₂), 7.68 (1H, dd, *J* 10, 0.9 Ar-H), 7.47 (1H, dd, *J* 10, 2, Ar-H), 7.15 (1H, t, *J* 8, Ar-H), 6.87 (1H, t, *J* 2, Ar-H), 6.72 (2H, dd, *J* 8, 2, Ar-H), 4.56 – 4.46 (1H, m, CONHCH₂CH(CH₃)₂), 3.00 (2H, q, *J* 8, CH₂CH₃), 1.85 - 1.54 (3H, m, CONHCH₂CH(CH₃)₂), 1.26 (3H, t, *J* 8, CH₂CH₃), 0.98 (6H, dd, *J* 10.3, 6.1 CONHCH₂CH(CH₃)₂); δ_C (75 MHz, DMSO-d₆) 172.6 (CONH₂), 161.4 (CONH), 152.0 (*ipso*-Ar-C), 151.4 (*ipso*-Ar-C), 143.7 (*ipso*-Ar-C), 134.1 (*ipso*-Ar-C), 130.6 (Ar-C), 127.6 (Ar-C), 125.1 (Ar-C), 120. (*ipso*-Ar-C), 118.2 (Ar-C), 117.7 (Ar-C), 116.4 (Ar-C), 111.9 (Ar-C), 111.4 (Ar-C), 51.3 (CONHCH₂CH(CH₃)₂), 25.01 (CONHCH₂CH(CH₃)) 23.5 (CONHCH₂CH(CH₃)₂), 22.3 (CH₂CH₃), 21.9 (CONHCH₂CH(CH₃)₂), 13.6.(CH₂CH₃); *m/z* (ES⁺) 462 ([^{35,35}Cl]MH⁺), 464 ([^{35,37}Cl]MH⁺) ; HRMS (ES⁺) Found [^{35,35}Cl]MH⁺, 462.1229 (C₂₂H₂₆^{35,35}Cl₂N₅O₂ requires 462.1464);

Chapter 5. Experimental section.

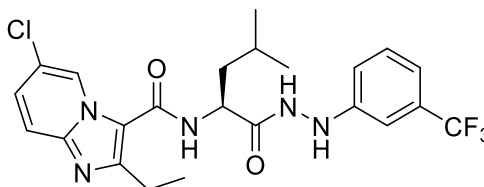
(S)-N-(1-(2-(3-bromophenyl)hydrazineyl)-4-methyl-1-oxopentan-2-yl)-6-chloro-2-ethylimidazo[1,2-a]pyridine-3-carboxamide 72b



Following the general procedure outlined, *tert*-butyl (S)-(1-(2-(3-bromophenyl)hydrazineyl)-4-methyl-1-oxopentan-2-yl)carbamate **64b** (0.10 g, 0.26 mmol) was transformed following trituration with Et₂O yielding pure product. R_f 0.43, (*n*.hexane; EtOAc; [2:1]); m.p. 260 – 261 °C ; ν_{max} 3231, 1667, 1613, 1598, 1493, 1417, 1395, 1321, 1219, 1123, 1103, 993 cm⁻¹; δ_H (300 MHz, DMSO-d₆) 10.08 (1H, d, *J* 2, CONH₂NH), 9.02 (1H, dd, *J* 2, 0.9, Ar-*H*), 8.35 (1H, d, *J* 8, CONH), 8.13 (1H, d, *J* 2, CONHNH), 7.68 (1H, dd, *J* 10, 0.9 Ar-*H*), 7.47 (1H, dd, *J* 10, 2, Ar-*H*), 7.15 (1H, t, *J* 8, Ar-*H*), 6.87 (1H, t, *J* 2, Ar-*H*), 6.72 (2H, dd, *J* 8, 2, Ar-*H*), 4.56 – 4.46 (1H, m, CONHCHCH₂CH(CH₃)₂), 3.00 (2H, q, *J* 8, CH₂CH₃), 1.85 - 1.54 (3H, m, CONHCHCH₂CH(CH₃)₂), 1.26 (3H, t, *J* 8, CH₂CH₃), 0.98 (6H, dd, *J* 10, 6. CONHCHCH₂CH(CH₃)₂); δ_C (75 MHz, DMSO-d₆) 172.6 (CONHNH), 161.4 (CONH), 152.0 (*ipso*-Ar-C), 151.4 (*ipso*-Ar-C), 143.7 (*ipso*-Ar-C), 134.1 (*ipso*-Ar-C), 131 (Ar-C), 127.6 (Ar-C), 124.8 (Ar-C), 121.0. (Ar-C), 117.7 (Ar-C), 116.4 (Ar-C), 114.9 (Ar-C), 111.7 (Ar-C), 51.3 (CONHCHCH₂CH(CH₃)₂), 25.0 (CONHCHCH₂CH(CH₃)) 23.5 (CONHCHCH₂CH(CH₃)₂), 22.3 (CH₂CH₃), 21.9 (CONHCHCH₂CH(CH₃)₂), 13.6 (CH₂CH₃); *m/z* (ES⁺) 506 ([³⁵Cl, ⁷⁹Br]MH⁺), 508 ([³⁵Cl, ⁸¹Br]MH⁺), 508 ([³⁷Cl, ⁷⁹Br]MH⁺), 510 ([³⁷Cl, ⁸¹Br]MH⁺); HRMS (ES⁺) Found [³⁵Cl⁷⁹Br]MH⁺, 506.0687 (C₂₂H₂₆⁷⁹Br³⁵ClN₅O₂ requires 506.0958);

Chapter 5. Experimental section.

(S)-6-chloro-2-ethyl-N-(4-methyl-1-oxo-1-(2-(3-(trifluoromethyl)phenyl)hydrazineyl)pentan-2-yl)imidazo[1,2-a]pyridine-3-carboxamide 72c

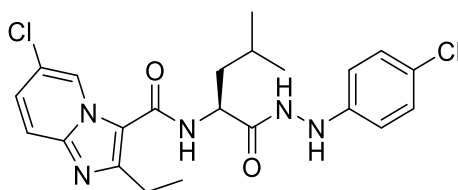


Following the general procedure outlined, *tert*-butyl (S)-(4-methyl-1-oxo-1-(2-(3-(trifluoromethyl)phenyl)hydrazineyl)pentan-2-yl)carbamate **64c** (0.10 g, 0.26 mmol) was deprotected using (2 ml) of 4N HCl dioxane stirred under N₂ for 90 min. The solvent was removed under reduced pressure. EtOH and Et₂O were added, and precipitation was formed, then evaporated the solvent under reduced pressure and carried out product to the next step. The deprotected Leucine-3-trifluorophenyl hydrazide (0.10 g, 0.26 mmol) was dissolved in 5 ml THF in 25 ml round bottom flask at rt as solvent stir under N₂ atmosphere. The 6-chloro imidazo[1,2] pyridine 2-ethyl 3-carboxylic acid (0.07 g, mmol) and diisopropylethylamine (0.09 ml, 0.52 mmol), followed by (2-(1H-benzotriazol-1-yl)-1,1,3,3-tetramethyluronium hexafluorophosphate HBTU (0.12 g, 0.31 mmol) were added. The mixture was stirred for 4 hr. Then the mixture was extracted by EtOAc. The organic layer was washed with sat. aq. NaHCO₃ (5 ml), sat. aq. NH₄Cl (5 ml), dist.H₂O (10 ml) and brine (10 ml). The organic layer was dried with MgSO₄, filtered, evaporated under a reduced pressure to obtain a yellow solid. This was purified by trituration with DCM yielding pure product as a white solid (0.07 g, 51%); R_f 0.37 (*n* hexane; EtOAc; [1:1]); m.p. 270 – 271 °C ; ν_{\max} 3378, 3287, 2982, 2902, 2166, 2140, 2025, 1968, 1727, 1669, 1522, 1392, 1280, 1222, 1161, 1103, 1069, 997, 932 cm⁻¹; δ_{H} (300 MHz, DMSO-d₆) 10.15 (1H, d, *J* 3, CONH₂), 8.97 (1H, d, *J* 2, Ar-H), 8.32 (1H, d, *J* 9, CONH), 7.68 (1H, d, *J* 10, Ar-H), 7.45 (1H, dd, *J* 10, 2, Ar-H), 7.36 (1H, t, *J* 8, Ar-H), 7.09 – 7.00 (3H, m, Ar-H), 4.62 – 4.48 (1H, m, CONHCH(CH₂CH(CH₃)₂)), 3.00 (2H, q, *J* 8, CH₂CH₃), 1.88 – 1.63 (3H, m, CONHCH(CH₂CH(CH₃)₂)), 1.26 (3H, t, *J* 8, CH₂CH₃), 1.04 – 0.93 (6H, m, CONHCH(CH₂CH(CH₃)₂)); δ_{C} (75 MHz, DMSO-d₆) 172.7 (CONH₂), 161.4 (CONH), 151.9 (*ipso*-Ar-C), 150.5 (*ipso*-Ar-C), 143.7 (*ipso*-Ar-

Chapter 5. Experimental section.

C), 130.1 (Ar-C), 127.5 (Ar-C), 126.7 (Ar-C), 124.9 (Ar-C), 123.1 (ipso-Ar-C), 120.1 (*ipso*-Ar-C), 117.7 (Ar-C), 116.4 (Ar-C), 114.9 (Ar-C), 108.3 (Ar-C), 51.2 (CONHCH(CH₂CH(CH₃)₂), 25.0 (CONHCH(CH₂CH(CH₃)₂), 23.4 (CONHCH(CH₂CH(CH₃)₂), 22.3 (CH₂CH₃), 21.9 (CONHCH(CH₂CH(CH₃)₂), 13.6 (CH₂CH₃); *m/z* (ES⁺) 496 ([³⁵Cl]MH⁺); HRMS (ES⁺) Found [³⁵Cl]MH⁺ 496.1470 (C₂₃H₂₆³⁵ClF₃N₅O₂ requires 496.1727);

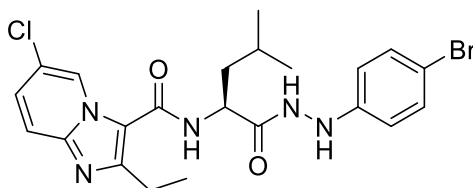
(S)-6-chloro-N-(1-(2-(4-chlorophenyl)hydrazineyl)-4-methyl-1-oxopentan-2-yl)-2-ethylimidazo[1,2-a]pyridine-3-carboxamide 72d



Following the general procedure outlined, *tert*-butyl (S)-(1-(2-(4-chlorophenyl)hydrazineyl)-4-methyl-1-oxopentan-2-yl)carbamate **64d** (0.20 g, 0.60 mmol) was transported trituration with Et₂O yielding the titled compound as pure white solid (0.15 g, 76 %); R_f 0.43 (*n*-hexane: EtOAc [2:1]); m.p. 265 – 267 °C *v*_{max} 3250, 1665, 1598, 1530, 1489, 1393, 1372, 1334, 1319, 1225, 1116, 1130, 910, 845, 828, 799, 762, 649, 579, 506 cm⁻¹; δ_H (300 MHz, DMSO-d₆) 10.06 (1H, d, *J* 3, CONHNH), 8.93 (1H, d, *J* 2, Ar-H), 8.34 (1H, d, *J* 8, CONH), 8.01 (1H, d, *J* 3, CONHNH), 7.68 (1H, d, *J* 10, Ar-H), 7.46 (1H, dd, *J* 10, 2, Ar-H), 7.23 – 7.13 (2H, d, *J* 8, Ar-H), 6.84 – 6.76 (2H, d, *J* 8, Ar-H), 4.63 – 4.48 (1H, m, NHCHCH₂CH(CH₃)₂), 2.98 (2H, q, *J* 8, CH₂CH₃), 1.82 – 1.55 (3H, m, NHCHCH₂CH(CH₃)), 1.26 (3H, t, *J* 8, CH₂CH₃), 1.03 – 0.91 (6H, m, NHCHCH₂CH(CH₃)); δ_C (75 MHz, DMSO-d₆) 172.5 (CONHNH), 161.4 (CONH), 151.7 (*ipso*-Ar-C), 148.8 (*ipso*-Ar-C), 143.7 (*ipso*-Ar-C), 128.8 (Ar-C), 127.5 (*ipso*-Ar-C), 125.0 (*ipso*-Ar-C), 122.2 (Ar-C), 120.0 (*ipso*-Ar-C), 117.7 (Ar-C), 116.5 (Ar-C), 114.2 (Ar-C), 51.1 (NHCHCH₂), 25.0 (CH₂CH(CH₃)₂), 23.5 (CH₂CH(CH₃)₂), 22.5 (CH₂CH₃), 21.9 (CH₂CH(CH₃)₂), 13.6 (CH₂CH₃); *m/z* (ES⁺) 462 ([^{35,35}Cl]MH⁺), 464 ([^{35,37}Cl]MH⁺); HRMS (ES⁺) Found [^{35,35}Cl]MH⁺, 462.1093 (C₂₂H₂₆^{35,35}Cl₂N₅O₂ requires 462.1464);

Chapter 5. Experimental section.

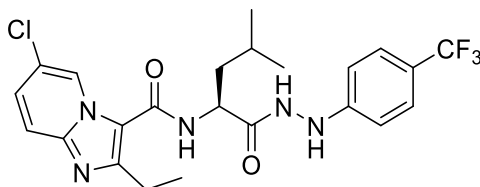
(S)-N-(1-(2-(4-bromophenyl)hydrazineyl)-4-methyl-1-oxopentan-2-yl)-6-chloro-2-ethylimidazo[1,2-a]pyridine-3-carboxamide 72e



Following the general procedure outlined, *tert*-butyl (S)-(1-(2-(4-bromophenyl)hydrazineyl)-4-methyl-1-oxopentan-2-yl)carbamate **64e** (0.20 g, 0.60 mmol) was transported following trituration with Et₂O yielding pure white solid (0.15 g, 76 %); R_f 0.43 (*n*-hexane: EtOAc [2:1]); m.p. 265 – 267 °C ν_{\max} 3250, 1665, 1598, 1530, 1489, 1393, 1372, 1334, 1319, 1225, 1116, 1130, 910, 845, 828, 799, 762, 649, 579, 506 cm⁻¹; δ_{H} (300 MHz, DMSO-d₆) 10.06 (1H, d, *J* 3, CONHNH), 8.93 (1H, d, *J* 2, Ar-H), 8.34 (1H, d, *J* 8, CONH), 8.01 (1H, d, *J* 3, CONHNH), 7.68 (1H, d, *J* 10, Ar-H), 7.46 (1H, dd, *J* 10, 2, Ar-H), 7.23 – 7.13 (2H, d, *J* 8, Ar-H), 6.84 – 6.76 (2H, d, *J* 8, Ar-H), 4.63 – 4.48 (1H, m, NHCHCH₂CH(CH₃)₂), 2.98 (2H, q, *J* 8, CH₂CH₃), 1.82 – 1.55 (3H, m, NHCHCH₂CH(CH₃)), 1.26 (3H, t, *J* 8, CH₂CH₃), 1.03 – 0.91 (6H, m, NHCHCH₂CH(CH₃)); δ_{C} (75 MHz, DMSO-d₆) 172.5 (CONHNH), 161.4 (CONH), 151.7 (*ipso*-Ar-C), 148.8 (*ipso*-Ar-C), 143.7 (*ipso*-Ar-C), 128.8 (Ar-C), 127.5 (Ar-C), 125.0 (Ar-C), 120.0 (*ipso*-Ar-C), 117.7 (Ar-C), 116.5 (*ipso*-Ar-C), 114.2 (Ar-C), 51.1 (NHCHCH₂CH(CH₃)₂), 25.0 (NHCHCH₂CH(CH₃)₂), 23.5 (NHCHCH₂CH(CH₃)₂), 22.5 (CH₂CH₃), 21.9 (NHCHCH₂CH(CH₃)₂) 13.6 (CH₂CH₃); *m/z* (ES⁺) 506 ([³⁵Cl, ⁷⁹Br]MH⁺), 508 ([³⁵Cl, ⁸¹Br]MH⁺), 508 ([³⁷Cl, ⁷⁹Br]MH⁺), 510 ([³⁷Cl, ⁸¹Br]MH⁺), HRMS (ES⁺) Found [³⁵Cl, ⁷⁹Br]MH⁺, 506.0676 (C₂₂H₂₆⁷⁹Br³⁵ClN₅O₂ requires 506.0958);

Chapter 5. Experimental section.

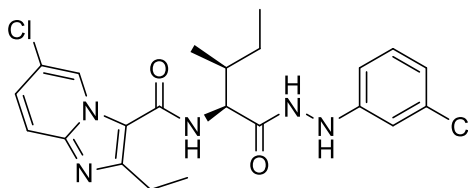
(S)-6-chloro-2-ethyl-N-(4-methyl-1-oxo-1-(2-(4-(trifluoromethyl)phenyl)hydrazineyl)pentan-2-yl)imidazo[1,2-a]pyridine-3-carboxamide 72f



Following the general procedure outlined, *tert*-butyl (S)-(4-methyl-1-oxo-1-(2-(4-(trifluoromethyl)phenyl)hydrazineyl)pentan-2-yl)carbamate **64f** (0.10 g, 0.26 mmol) was transformed following trituration with Et₂O yielding pure product as white solid (0.04 g, 28 %); R_f 0.50 (*n*-hexane;EtOAc; [2:1]); m.p. 260 - 261 °C ; ν_{\max} 3248, 1664, 1612, 1526, 1487, 1417, 1394, 1374, 1328, 1291, 1189, 1158, 1108, 1066, 1013, 1000, 924, 897, 838 cm⁻¹. δ_{H} (300 MHz, DMSO-d₆), 10.17 (1H, d, *J* 2, CONH₂NH), 8.93 (1H, m, Ar-*H*), 8.48 (1H, m, CONHNH), 8.40 (1H, d, *J* 8, CONH), 7.68 (1H, d, *J* 9, Ar-*H*), 7.47 (3H, m, Ar-*H*), 6.92 (2H, d, *J* 8, Ar-*H*), 4.57 (1H, m, CONHCH), 2.98 (2H, q, *J* 8, CH₂CH₃), 1.81 - 1.57 (3H, m, NHCHCH₂CH(CH₃)₂), 1.26 (3H, t, *J* 8, CH₂CH₃), 1.02 - 0.94 (6H, m, NHCHCH₂CH(CH₃)₂). δ_{C} (75 MHz, DMSO-d₆), 172.5 (CONHNH), 161.5 (CONH), 152.0 (*ipso*-Ar-C), 151.7 (*ipso*-Ar-C), 148.8 (*ipso*-Ar-C), 143.6 (*ipso*-Ar-C), 127.5 (Ar-C), 126.6 (Ar-C), 124.6 (Ar-C), 120.0 (*ipso*-Ar-C), 117.8 (Ar-C), 116.5 (*ipso*-Ar-C), 112.0 (Ar-C), 51.2 (NHCHCH₂CH(CH₃)₂), 25.0 (NHCHCH₂CH(CH₃)₂), 23.5 (NHCHCH₂CH(CH₃)₂), 22.2 (CH₂CH₃), 21.9 (NHCHCH₂CH(CH₃)₂), 13.6 (CH₂CH₃); *m/z* (ES⁺) 469 ([³⁵Cl]MH⁺), 470 ([³⁷Cl]MH⁺); HRMS (ES⁺) Found [³⁵Cl]MH⁺, 496.1335 (C₂₃H₂₆³⁵ClF₃N₅O₂ requires 496.1682);

Chapter 5. Experimental section.

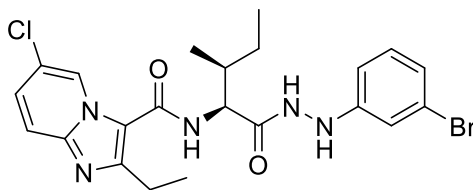
6-chloro-*N*-((2*S*,3*S*)-1-(2-(3-chlorophenyl)hydrazineyl)-3-methyl-1-oxopentan-2-yl)-2-ethylimidazo[1,2-*a*]pyridine-3-carboxamide 73a



Following the general procedure outlined, *tert*-butyl ((2*S*,3*S*)-1-(2-(3-chlorophenyl)hydrazineyl)-3-methyl-1-oxopentan-2-yl)carbamate **65a** (0.10 g, 0.40 mmol) were transformed following trituration with Et₂O yielding pure product as a white solid (0.08 g, 60 %); R_f 0.35 (*n*-hexane; EtOAc [2:1]); m.p. 269 – 270 °C; ν_{\max} 3242, 2966, 1661, 1597, 1530, 1489, 1393, 1220, 227, 1070, 993, 846, 802, 755, 679, 577, 479 cm⁻¹. δ_{H} (300 MHz, DMSO-*d*₆) 10.09 (1H, s, CONHNH), 9.02 (1H, d, *J* 2, Ar-*H*), 8.20 (1H, d, *J* 8, CONH), 7.68 (1H, d, *J* 9, Ar-*H*), 7.50 (1H, dd, *J* 10, 2, Ar-*H*), 7.15 (1H, t, *J* 8, Ar-*H*), 6.87 (1H, d, *J* 2, Ar-*H*), 6.73 (2H, dd, *J* 9, 6, Ar-*H*), 4.37 (1H, t, *J* 8, CONHCH(CH₂CH₃CH₂(CH₃))), 3.00 (2H, q, *J* 8, CH₂CH₃), 2.05 – 1.95 (1H, m, CONHCH(CH₂CH₃CH₂(CH₃))), 1.67 – 1.58 (2H, m, CONHCH(CH₂CH₃CH₂(CH₃))), 1.27 (3H, t, *J* 8, CH₂CH₃), 1.00 (3H, d, *J* 6.8, CONHCH(CH₂CH₃CH₂(CH₃))), 0.92 (3H, t, *J* 7, CONHCH(CH₂CH₃CH₂(CH₃))); δ_{C} (75 MHz, DMSO- *d*₆) 171.7 (CONHNH) 161.4 (CONH), 151.4 (*ipso*-Ar-C) 134.1 (*ipso*-Ar-C), 130.6 (*ipso*-Ar-C), 127.8 (Ar-C), 125.0 (Ar-C), 120.4 (*ipso*-Ar-C), 118.3 (Ar-C), 117.7 (Ar-C), 111.9 (Ar-C), 111.5 (Ar-C), 56.9 (CONHCHCH₂CH₃CH₂(CH₃)), 36.0 (CONHCHCH₂CH₃CH₂(CH₃)), 25.3 (CONHCHCH₂CH₃CH₂(CH₃)), 22.3 (CH₂CH₃), 16.02 (CONHCHCH₂CH₃CH₂(CH₃)), 13.6 (CH₂CH₃), 11.1 (CONHCHCH₂CH₃CH₂(CH₃)); *m/z* (ES⁺) 462 ([^{35,35}Cl]MH⁺), 464 ([^{35,37}Cl]MH⁺); HRMS (ES⁺) Found [^{35,35}Cl]MH⁺, 462.1099 (C₂₂H₂₆^{35,35}Cl₂N₅O₂ requires 462.1419);

Chapter 5. Experimental section.

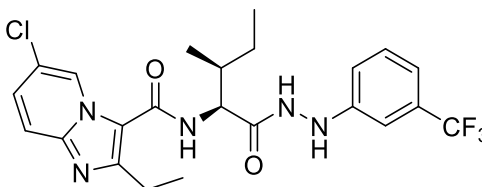
***N*-((2*S*,3*S*)-1-(2-(3-bromophenyl)hydrazineyl)-3-methyl-1-oxopentan-2-yl)-6-chloro-2-ethylimidazo[1,2-*a*]pyridine-3-carboxamide 73b**



Following the general procedure outlined, *tert*-butyl ((2*S*,3*S*)-1-(2-(3-bromophenyl)hydrazineyl)-3-methyl-1-oxopentan-2-yl)carbamate **65b** (0.10 g, 0.4 mmol) were transformed following triturated with DCM to produce the title product as faint brown solid (0.05 g, 37 %); R_f 0.36 (*n*.hexane; EtOAc; [4:1]); m.p. 262 – 263 °C ; ν_{max} 3242, 2966, 1661, 1597, 1530, 1489, 1393, 1224, 1227, 1070, 993 cm^{-1} ; δ_H (300 MHz, DMSO- d_6) 10.09 (1H, s, CONHNH), 9.02 (1H, d, J 2, Ar-*H*), 8.20 (1H, d, J 8, CONH), 7.68 (1H, d, J 9, Ar-*H*), 7.50 (1H, dd, J 10, 2, Ar-*H*), 7.15 (1H, t, J 8, Ar-*H*), 6.87 (1H, d, J 2, Ar-*H*), 6.73 (2H, dd, J 9, 6, Ar-*H*), 4.37 (1H, t, J 8, CONHCHCHCH₃CH₂(CH₃)), 3.00 (2H, q, J 8, CH₂CH₃), 2.05 – 1.95 (1H, m, CONHCHCHCH₃CH₂(CH₃)), 1.67 – 1.58 (2H, m, CONHCHCHCH₃CH₂(CH₃)), 1.27 (3H, t, J 8, CH₂CH₃), 1.00 (3H, d, J 6.8, CONHCHCHCH₃CH₂(CH₃)), 0.92 (3H, t, J 7, CONHCHCHCH₃CH₂(CH₃)); δ_C (75 MHz, DMSO- d_6) 171.7 (CONHNH) 161.4 (CONH), 151.4, (*ipso*-Ar-C) 134.1(*ipso*-Ar-C), 130.6 (*ipso*-Ar-C), 127.8 (*ipso*-Ar-C), 125.0 (*ipso*-Ar-C), 120.4 (Ar-C), 118.3 (Ar-C), 117.7 (Ar-C), 111.9 (Ar-C), 111.5 (Ar-C), 56.9 (CONHCHCHCH₃CH₂(CH₃)), 36.0 (CONHCHCHCH₃CH₂(CH₃)) , 25.3 (CONHCHCHCH₃CH₂(CH₃)), 22.3 (CH₂CH₃), 16.02 (CONHCHCHCH₃CH₂(CH₃)) , 13.6 (CH₂CH₃), 11.1 (CONHCHCHCH₃CH₂(CH₃)); m/z (ES⁺) 506 ([³⁵Cl, ⁷⁹Br]MH⁺), 508 ([³⁵Cl, ⁸¹Br]MH⁺), 508 ([³⁷Cl, ⁷⁹Br]MH⁺), 510 ([³⁷Cl, ⁸¹Br]MH⁺, HRMS (ES⁺) Found, ([³⁵Cl, ⁷⁹Br]MH⁺, 506.0690 (C₂₂H₂₆⁷⁹Br³⁵ClN₅O₂ requires 506.0958);

Chapter 5. Experimental section.

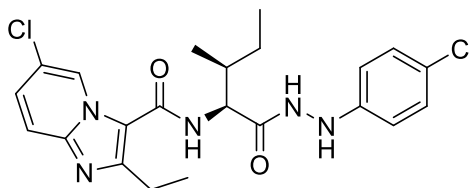
6-chloro-2-ethyl-*N*-((2*S*,3*S*)-3-methyl-1-oxo-1-(2-(3-(trifluoromethyl)phenyl)hydrazineyl)pentan-2-yl)imidazo[1,2-*a*]pyridine-3-carboxamide 73c



Following the general procedure outlined, *tert*-butyl ((2*S*,3*S*)-1-(2-(3-trifluorophenyl) hydrazineyl)-3-methyl-1-oxopentan-2-yl)carbamate **65c** (0.10 g, 0.4 mmol) were transformed to obtain the titled compound as a faint orange solid (0.04 g, 36 %) R_f 0.63 (*n*-hexane;EtOAc;[1:1]). m.p. 270 – 273 °C ; ν_{max} 3249, 1670, 1602, 1490, 1393, 1335, 1164, 1216, 1112, 1065, 993, 842, 763, 724, 801, 694, 557, 467 cm^{-1} ; δ_H (300 MHz, DMSO- d_6) 10.16 (1H, d, J 2, CONHNH), 8.96 (1H, dd, J 2, 0.9, Ar-*H*), 8.34 (1H, d, J 2, CONHNH), 8.15 (1H, d, J 8, CONH), 7.69 (1H, dd, J 10, 0.8 Ar-*H*), 7.48 – 7.32 (2H, m, Ar-*H*), 7.10 – 6.98 (3H, m, Ar-*H*), 4.41 (1H, t, J 8, CONHCH(CHCH₃CH₂(CH₃))), 3.00 (2H, q, J 8, CH₂CH₃), 2.00 – 1.95 (1H, m, CONHCH(CHCH₃CH₂(CH₃))), 1.67 – 1.58 (2H, m, CONHCH(CHCH₃CH₂(CH₃))), 1.27 (3H, t, J 8, CH₂CH₃), 1.01 (3H, d, J 7, CONHCH(CHCH₃CH₂(CH₃))), 0.92 (3H, t, J 7 CONHCH(CHCH₃CH₂(CH₃))); δ_C (75 MHz, DMSO- d_6) 171.7 (CONHNH) 161.4 (CONH), 152 (*ipso*-Ar-C), 150.5 (*ipso*-Ar-C), 143.7 (*ipso*-Ar-C), 130.1 (Ar-C), 127.6 (Ar-C), 124.9 (Ar-C), 120.2 (*ipso*-Ar-C), 117.7 (Ar-C), 116.5 (Ar-C), 108.3 (Ar-C), 56.9 (CONHCH(CHCH₃CH₂(CH₃))), 36.2 (CONHCH(CHCH₃CH₂(CH₃))), 25.3 (CONHCH(CHCH₃CH₂(CH₃))), 22.4 (CH₂CH₃), 16.0 (CONHCH(CHCH₃CH₂(CH₃))), 13.6 (CH₂CH₃), 11.1 (CONHCH(CHCH₃CH₂(CH₃))); m/z (ES⁺) 496 ([³⁵Cl]MH⁺); HRMS (ES⁺) Found [³⁵Cl]MH⁺ 496.1477 (C₂₃H₂₆³⁵ClF₃N₅O₂ requires 497.1619);

Chapter 5. Experimental section.

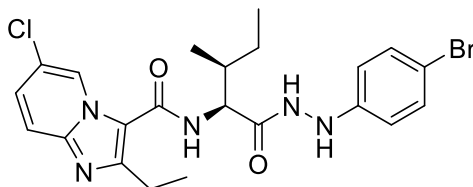
6-chloro-*N*-((2*S*,3*S*)-1-(2-(4-chlorophenyl)hydrazineyl)-3-methyl-1-oxopentan-2-yl)-2-ethylimidazo[1,2-*a*]pyridine-3-carboxamide 73d



Following the general procedure outlined, *tert*-butyl ((2*S*,3*S*)-1-(2-(4-chlorophenyl)hydrazineyl)-3-methyl-1-oxopentan-2-yl)carbamate **65d** (0.12 g, 0.31 mmol) was transformed following trituration with Et₂O to afford the titled compound as pale white solid (0.05 g, 40 %); R_f 0.43 (*n*-hexane/EtOAc [4:1]) m.p. 277- 287 °C ; ν_{\max} 3434, 1655, 1608, 1536, 1488, 1392, 1220, 1120, 1070. 810, 780, 675 cm⁻¹; δ_{H} (300 MHz, DMSO-*d*₆) 10.09 (1H, d, *J* 3, CONHNH), 8.92 (1H, dd, *J* 2, 0.8, Ar-*H*), 8.22 (1H, d, *J* 8, CONH), 8.08 (1H, d, *J* , 3, CONHNH), 7.69 (1H, d, *J* 10, Ar-*H*), 7.47 (1H, dd, *J* 10, 2, Ar-*H*), 7.29 (2H, d, *J* 9, Ar-*H*), 6.78 (2H, d, *J* 9 Ar-*H*), 4.40 (1H,, m, CONHCH(CHCH₃CH₂(CH₃)), 2.97 (2H, q, *J* 8, CH₂CH₃), 2.00 – 1.85 (1H, m, CONHCH(CHCH₃CH₂(CH₃)), 1.59 (2H, m, CONHCH(CHCH₃CH₂(CH₃)), 1.27 (3H, t, *J* 8, CH₂CH₃), 0.99 (3H, d, *J* 7, CONHCH(CHCH₃CH₂(CH₃)), 0.92 (3H, t, *J* 8, CONHCH(CHCH₃CH₂(CH₃)); δ_{C} (75 MHz, DMSO-*d*₆) 171.7 (CONHNH), 161.4 (CONH), 151.8 (*ipso*-Ar-C), 143.7 (*ipso*-Ar-C), 131.7 (Ar-C), 130.3 (*ipso*-Ar-C), 127.5 (Ar-C), 114.8 (Ar-C) 56.7 (CONHCH(CHCH₃CH₂(CH₃)), 36.0 (CONHCH(CHCH₃CH₂(CH₃)), 31.2 (CONHCH(CHCH₃CH₂(CH₃)), 22.3 (CH₂CH₃), 13.6 (CH₂CH₃), 11.1 (CONHCH(CHCH₃CH₂(CH₃)); *m/z* (ES⁺) 462 ([^{35,35}Cl]MH⁺), 464 ([^{35,37}Cl]MH⁺); HRMS (ES⁺) Found [^{35,35}Cl]MH⁺, 462.1206 (C₂₂H₂₆^{35,35}Cl₂N₅O₂ requires 462.1419);

Chapter 5. Experimental section.

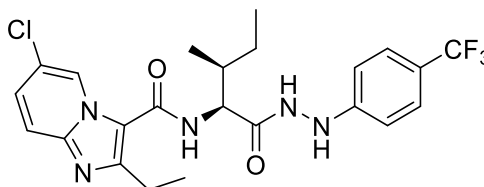
N*-((2*S*,3*S*)-1-(2-(4-bromophenyl)hydrazineyl)-3-methyl-1-oxopentan-2-yl)-6-chloro-2-ethylimidazo[1,2-*a*]pyridine-3-carboxamide **73e*



Following the general procedure outlined, *tert*-butyl ((2*S*,3*S*)-1-(2-(4-bromophenyl)hydrazineyl)-3-methyl-1-oxopentan-2-yl)carbamate **65e** (0.12 g, 0.31 mmol) was transformed following flush column chromatography to afford the titled compound as yellowish white solid (0.05 g, 40 %); R_f 0.34 (*n*-hexane/EtOAc [4;1]); m.p. 281- 284 °C ; ν_{max} 3434, 1655, 1608, 1536, 1488, 1392, 1220, 1120, 1070. 810, 780, 675 cm^{-1} ; δ_H (300 MHz, DMSO- d_6) 10.09 (1H, d, J 3, CONHNH), 8.92 (1H, dd, J 2, 0.8, Ar-*H*), 8.22 (1H, d, J 8, CONH), 8.08 (1H, d, J 3, CONHNH), 7.69 (1H, d, J 10, Ar-*H*), 7.47 (1H, dd, J 10, 2, Ar-*H*), 7.29 (2H, d, J 9, Ar-*H*), 6.78 (2H, d, J 9 Ar-*H*), 4.40 (1H, m, CONHCH(CHCH₃CH₂(CH₃))), 2.97 (2H, q, J 8, CH₂CH₃), 2.00 – 1.85 (1H, m, CONHCH(CHCH₃CH₂(CH₃))), 1.59 (2H, m, CONHCH(CHCH₃CH₂(CH₃))), 1.27 (3H, t, J 8, CH₂CH₃), 0.99 (3H, d, J 7, CONHCH(CHCH₃CH₂(CH₃))), 0.92 (3H, t, J 8, CONHCH(CHCH₃CH₂(CH₃))); δ_C (75 MHz, DMSO- d_6) 171.7 (CONHNH), 161.4 (CONH), 151.8 (*ipso*-Ar-C), 143.7 (*ipso*-Ar-C), 131.7 (Ar-C), 130.3 (*ipso*-Ar-C), 127.5 (Ar-C), 114.8 (Ar-C) 56.7 (CONHCH(CHCH₃CH₂(CH₃))), 36.0 (CONHCH(CHCH₃CH₂(CH₃))), 31.2 (CONHCH(CHCH₃CH₂(CH₃))), 22.3 (CH₂CH₃), 13.6 (CH₂CH₃), 11.1 (CONHCH(CHCH₃CH₂(CH₃))); m/z (ES⁺) 506 ([³⁵Cl, ⁷⁹Br]MH⁺), 508 ([³⁵Cl, ⁸¹Br]MH⁺), 508 ([³⁷Cl, ⁷⁹Br]MH⁺), 510 ([³⁷Cl, ⁸¹Br]MH⁺, HRMS (ES⁺) Found, ([³⁵Cl, ⁷⁹Br]MH⁺, 506.0690 (C₂₂H₂₆⁷⁹Br³⁵ClN₅O₂ requires 506.0958);

Chapter 5. Experimental section.

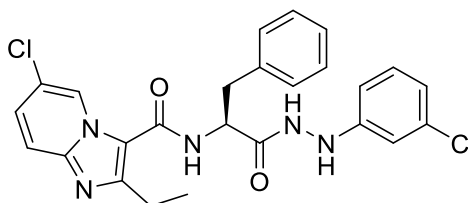
6-chloro-2-ethyl-N-((2S,3S)-3-methyl-1-oxo-1-(2-(4-(trifluoromethyl)phenyl)hydrazineyl)pentan-2-yl)imidazo[1,2-a]pyridine-3-carboxamide 73f



Following the general procedure outlined, *tert*-butyl ((2S,3S)-3-methyl-1-oxo-1-(2-(4-(trifluoromethyl)phenyl)hydrazineyl)pentan-2-yl)carbamate **65f** (0.12 g, 0.31 mmol) was transformed following trituration with Et₂O to afford the titled compound as white solid (0.05 g, 29 %); R_f 0.53 (*n*-hexane/EtOAc [2:1]); m.p. 277 – 278 °C ; ν_{max}, 3249, 1604, 1532, 1493, 1393, 1218, 1163, 1050, 933, 842, 763, 724, 801 cm⁻¹; δ_H (300 MHz, DMSO-d₆) 10.19 (1H, d, *J* 2, CONH₂), 8.92 (1H, d, *J* 2, Ar-H), 8.52 (1H, d, *J* 2, CONH₂), 8.27 (1H, d, *J* 8, CONH), 7.70 (1H, s, Ar-H), 7.46 (3H, dd, *J* 9, 2, Ar-H), 6.93 (2H, d, *J* 9, Ar-H), 4.37 (1H, t, *J* 8, CONHCHCHCH₃CH₂(CH₃)), 2.97 (2H, q, *J* 8, CH₂CH₃), 2.06 – 1.90 (1H, m, CONHCHCHCH₃CH₂(CH₃)), 1.67 – 1.56 (1H, m, CONHCHCHCH₃CH₂(CH₃)), 1.26 (3H, t, *J* 8, CH₂CH₃), 0.99 (3H, d, *J* 7, CONHCHCHCH₃CH₂(CH₃)), 0.95 – 0.88 (3H, m, CONHCHCHCH₃CH₂(CH₃)); δ_C (75 MHz, DMSO- d₆) 171.8 (CONH₂), 161.5 (CONH), 153.0 (*ipso*-Ar-C), 151.8 (*ipso*-Ar-C), 143.7 (*ipso*-Ar-C), 127.5 (*ipso*-Ar-C), 126.5 (Ar-C), 124.8 (Ar-C), 120.2 (*ipso*-Ar-C), 117.8 (Ar-C), 112.1 (Ar-C), 57 (CONHCHCHCH₃CH₂(CH₃)), 35.9 (CONHCHCHCH₃CH₂(CH₃)), 25.34 (CONHCHCHCH₃CH₂(CH₃)), 22.3 (CH₂CH₃), 16.0 (CONHCHCHCH₃CH₂(CH₃)), 13.6 (CH₂CH₃), 11.0 (CONHCHCHCH₃CH₂(CH₃)); *m/z* (ES⁺) 496 ([³⁵Cl]MH⁺); HRMS (ES⁺) Found [³⁵Cl]MH⁺, 496.1361 (C₂₃H₂₆³⁵ClF₃N₅O₂ requires 496.1727);

Chapter 5. Experimental section.

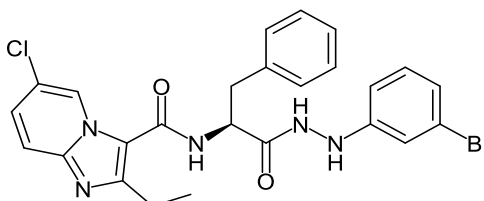
(S)-6-chloro-N-(1-(2-(3-chlorophenyl)hydrazineyl)-1-oxo-3-phenylpropan-2-yl)-2-ethylimidazo[1,2-a]pyridine-3-carboxamide 74a



Following the general procedure outlined, *tert*-butyl (S)-(1-(2-(3-chlorophenyl)hydrazineyl)-1-oxo-3-phenylpropan-2-yl)carbamate **66a** (0.10 g, 0.4 mmol) was transformed following flush column chromatography to produce faint yellow oil (0.05 g, 36 %); R_f 0.51 (*n*-hexane;EtOAc;[2:1]); m.p. 275 – 278 °C ; ν_{\max} 3249, 1665, 1613, 1596, 1496, 1398, 1324, 1232, 1210, 1123, 1074, 995, 809, 755 cm^{-1} ; δ_H (300 MHz, DMSO- d_6) 10.13 (1H, d, J 2, CONHNH), 8.86 (1H, d, J 2, Ar-H), 8.36 (1H, d, J 8, CONH), 8.16 (1H, d, J 2, CONHNH), 7.64 (1H, dd, J 10, 0.7, Ar-H), 7.46 – 7.22 (7H, m, Ar-H), 7.15 (1H, t, J 8, Ar-H), 6.87 (1H, t, J 2, Ar-H), 6.76 – 6.65 (2H, m, Ar-H), 4.76 (1H, m, CONHCHCH₂Ph), 3.24 – 3.02 (2H, m, CONHCHCH₂Ph), 2.82 – 2.58 (2H, m, CH₂CH₃), 1.05 (3H, t, J 8, CH₂CH₃); δ_C (75 MHz, DMSO- d_6) 171.8 (CONHNH), 161.4 (CONH), 152.1 (*ipso*-Ar-C), 151.2 (*ipso*-Ar-C), 143.7 (*ipso*-Ar-C), 138.2 (*ipso*-Ar-C), 134.1(*ipso*-Ar-C), 130.6 (Ar-C), 129.7 (Ar-C), 128.7 (Ar-C), 127.6 (Ar-C), 127.0 (Ar-C), 125.0 (Ar-C), 120.1 (*ipso*-Ar-C), 118.3 (Ar-C), 117.6 (Ar-C), 116.2 (*ipso*-Ar-C), 111.9 (Ar-C), 111.5 (Ar-C), 54.7 (CONHCHCH₂Ph), 37.2 (CONHCHCH₂Ph), 22.1 (CH₂CH₃) , 13.4 (CH₂CH₃); m/z (ES⁺) 496 ([^{35,35}Cl]MH⁺), 498 ([^{35,37}Cl]MH⁺); HRMS (ES⁺) Found [^{35,35}Cl]MH⁺, 496.1029 (C₂₅H₂₄^{35,35}Cl₂N₅O₂ requires 496.1307);

Chapter 5. Experimental section.

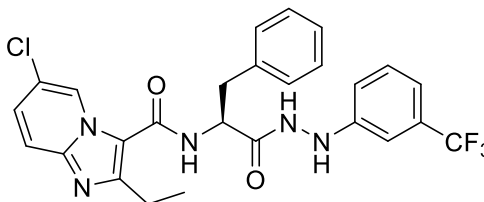
(S)-N-(1-(2-(3-bromophenyl)hydrazineyl)-1-oxo-3-phenylpropan-2-yl)-6-chloro-2-ethylimidazo[1,2-a]pyridine-3-carboxamide 74b



Following the general procedure outlined, *tert*-butyl (S)-(1-(2-(3-bromophenyl)hydrazineyl)-1-oxo-3-phenylpropan-2-yl)carbamate **66b** (0.10 g, 0.30 mmol) was transformed following flush column chromatography (DCM/EtOH/NH₃ [200:8:1]) to produce the titled compound as colourless oil (0.06 g, 48 %); R_f 0.47 (*n*-hexane;EtOAc;[2:1]); m.p. 270 – 275 °C ; ν_{\max} 3259, 2985, 1727, 1654, 1610, 1531, 1494, 1395, 1331, 1232, 1211, 1166, 1067, 997, 990 cm⁻¹; δ_{H} (300 MHz, DMSO-d₆) 10.13 (1H, d, *J* 2, CONHNH), 8.86 (1H, d, *J* 2, Ar-H), 8.36 (1H, d, *J* 8, CONH), 8.16 (1H, d, *J* 2, CONHNNH), 7.64 (1H, dd, *J* 10, 0.7, Ar-H), 7.46 – 7.22 (7H, m, Ar-H), 7.15 (1H, t, *J* 8, Ar-H), 6.87 (1H, t, *J* 2, Ar-H), 6.76 – 6.65 (2H, m, Ar-H), 4.76 (1H, m, CONHCHCH₂Ph), 3.24 – 3.02 (2H, m, CONHCHCH₂Ph), 2.82 – 2.58 (2H, m, CH₂CH₃), 1.05 (3H, t, *J* 8, CH₂CH₃); δ_{C} (75 MHz, DMSO- d₆) 171.8 (CONHNNH), 161.4 (CONH), 152.1 (*ipso*-Ar-C), 151.2 (*ipso*-Ar-C), 143.7 (*ipso*-Ar-C), 138.2 (*ipso*-Ar-C), 134.1(*ipso*-Ar-C), 130.6 (Ar-C), 129.7 (Ar-C), 128.7 (Ar-C), 127.6 (Ar-C), 127.0 (Ar-C), 125.0 (Ar-C), 120.1 (*ipso*-Ar-C), 118.3 (Ar-C), 117.6 (Ar-C), 116.2 (*ipso*-Ar-C), 111.9 (Ar-C), 111.5 (Ar-C), 54.7 (CONHCHCH₂Ph), 37.2 (CONHCHCH₂Ph), 22.1 (CH₂CH₃) , 13.4 (CH₂CH₃); *m/z* (ES⁺) 540 ([³⁵Cl, ⁷⁹Br]MH⁺), 542 ([³⁵Cl, ⁸¹Br]MH⁺), 542 ([³⁷Cl, ⁷⁹Br]MH⁺), 544 ([³⁷Cl, ⁸¹Br]MH⁺); HRMS (ES⁺) Found [³⁵Cl, ⁷⁹Br]MH⁺, 540.0264 (C₂₅H₂₄⁷⁹Br³⁵ClN₅O₂ requires 540.0802);

Chapter 5. Experimental section.

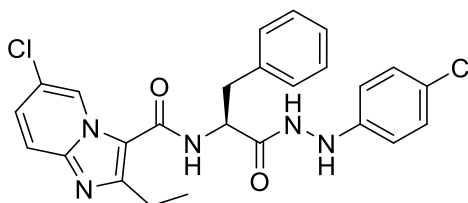
(S)-6-chloro-2-ethyl-N-(1-oxo-3-phenyl-1-(2-(4-(trifluoromethyl)phenyl)hydrazineyl)propan-2-yl)imidazo[1,2-a]pyridine-3-carboxamide 74c



Following the general procedure outlined, *tert*-butyl (S)-(1-oxo-3-phenyl-1-(2-(3-(trifluoromethyl)phenyl)hydrazineyl)propan-2-yl)carbamate **66c** (0.10 g, 0.24 mmol) was transformed following flush column chromatography (*n*-hexane;EtOAc [4:1]) to afforded the titled compound as faint yellow oil (0.05 g, 36 %); R_f 0.36 (*n*.hexane;EtOAc;[2:1]); m.p. 285 – 286 °C ; ν_{max} 3247, 1666, 1611, 1520, 1491, 1395, 1335, 1282, 1255, 1168, 1060, 1115, 995,, 850 cm^{-1} ; δ_H (300 MHz, DMSO- d_6) 10.21 (1H, d, J 2, CONHNH), 8.81 (1H, dd, J 2, 0.8, Ar- H), 8.40 – 8.31 (1H, m, CONH), 7.64 (1H, dd, J 10, 0.8, Ar- H), 7.47 – 7.21 (6 H, m, Ar- H), 7.12 (1H, d, J 2, Ar- H), 7.06 – 6.97 (2H, m, Ar- H), 4.87 – 4.69 (1H, m, CONHCHCH₂Ph), 3.28 – 3.02 (2H, m, CONHCHCH₂Ph), 2.81 – 2.57 (2H, m, CH₂CH₃), 1.05 (t, J 8, CH₂CH₃); δ_C (75 MHz, DMSO- d_6) 171.8 (CONHNH), 161.4 (CONH), 152.1 (*ipso*-Ar-C), 151.2 (*ipso*-Ar-C), 143.7 (*ipso*-Ar-C), 138.2 (*ipso*-Ar-C), 134.1(*ipso*-Ar-C), 130.6 (Ar-C), 129.7 (Ar-C), 128.8 (Ar-C), 127.5 (Ar-C), 127.0 (Ar-C), 125.0 (Ar-C), 120.0 (*ipso*-Ar-C), 117.6 (Ar-C), 116.34 (Ar-C), 116.26 (*ipso*-Ar-C), 114.9 (Ar-C), 108.5 (Ar-C) 54.7 (CONHCHCH₂Ph), 37.2 (CONHCHCH₂Ph), 22.1 (CH₂CH₃) , 13.4 (CH₂CH₃); m/z (ES⁺) 530 ([³⁵Cl]MH⁺); HRMS (ES⁺) Found [³⁵Cl]MH⁺, 530.1299 (C₂₆H₂₄³⁵ClF₃N₅O₆ require 530.1571)

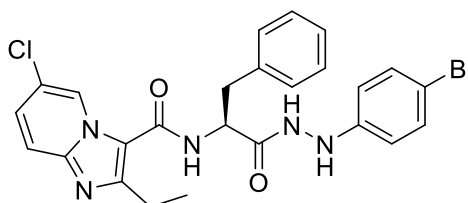
Chapter 5. Experimental section.

(S)-6-chloro-N-(1-(2-(4-chlorophenyl)hydrazineyl)-1-oxo-3-phenylpropan-2-yl)-2-ethylimidazo[1,2-a]pyridine-3-carboxamide 74d



Following the general procedure outlined, *tert*-butyl (S)-(1-(2-(4-chlorophenyl)hydrazineyl)-1-oxo-3-phenylpropan-2-yl)carbamate **66d** (0.10 g, 0.4 mmol) was transformed following with trituration by Et₂O to produce the titled compound as white solid (0.04 g, 40 %); R_f 0.66 (*n*.hexane;EtOAc; [2:1]); m.p. 277- 279 °C ; ν_{\max} d_H (300 MHz, DMSO-d₆) 10.10 (1H, d, *J* 2, CONH₂), 8.76 – 8.71 (1H, m, Ar-*H*), 8.39 (1H, d, *J* 8, CONH), 8.05 (1H, d, *J* 2, CONH₂), 7.64 (1H, d, *J* 10, Ar-*H*), 7.46 – 7.22 (5H, m, Ar-*H*), 7.14 (2H, d, *J* 9, Ar-*H*), 6.73 (2H, d, *J* 9, Ar-*H*), 4.82 – 4.74 (1H, m, CONHCHCH₂Ph), 3.25 – 2.98 (2H, m, CONHCHCH₂Ph), 2.81 – 2.61 (2H, m, CH₂CH₃), 1.07 (3H, t, *J* 8, CH₂CH₃); δ_c (75 MHz, DMSO- d₆) 171.6 (CONH₂), 161.3 (CONH), 155.7 (*ipso*-Ar-C), 151.8 (*ipso*-Ar-C), 148.6 (*ipso*-Ar-C), 143.6 (*ipso*-Ar-C) 138.2 (*ipso*-Ar-C), 129.7 (Ar-C), 128.8 (Ar-C), 124.9 (Ar-C), 122.2 (Ar-C), 120.1 (*ipso*-Ar-C), 116.4 (Ar-C), 114.2 (Ar-C), 112.4 (Ar-C) 54.4 (CONHCHCH₂Ph), 37.4 (CONHCHCH₂Ph) ,22 (CH₂CH₃), 13.44 (CH₂CH₃); *m/z* (ES⁺) 496 ([^{35,35}Cl]MH⁺), 498 ([^{35,37}Cl]MH⁺), HRMS (ES⁺) Found [^{35,35}Cl]MH⁺, 496.1048 [^{35,35}Cl]MH⁺ (C₂₅H₂₄^{35,35}Cl₂N₅O₂ requires 496.1370);

(S)-N-(1-(2-(4-bromophenyl)hydrazineyl)-1-oxo-3-phenylpropan-2-yl)-6-chloro-2-ethylimidazo[1,2-a]pyridine-3-carboxamide 74e

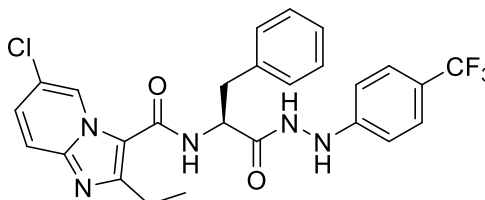


Following the general procedure outlined, *tert*-butyl (S)-(1-(2-(4-bromophenyl)hydrazineyl)-1-oxo-3-phenylpropan-2-yl)carbamate **66e** (0.10 g, 0.4 mmol) was transformed to obtain the titled compound as faint orange solid

Chapter 5. Experimental section.

(0.07 g, 53 %); R_f 0.45 (*n*-hexane;EtOAc;[2:1]); m.p. 278 – 281 °C ; ν_{max} δ_H (300 MHz, DMSO- d_6) 10.10 (1H, d, J 2, CONHNNH), 8.76 – 8.71 (1H, m, Ar-*H*), 8.39 (1H, d, J 8, CONH), 8.05 (1H, d, J 2, CONHNNH), 7.64 (1H, d, J 10, Ar-*H*), 7.46 – 7.22 (5H, m, Ar-*H*), 7.14 (2H, d, J 9, Ar-*H*), 6.73 (2H, d, J 9, Ar-*H*), 4.82 – 4.74 (1H, m, CONHCHCH₂Ph), 3.25 – 2.98 (2H, m, CH₂CH₃), 2.81 – 2.61 (2H, m, CONHCH(CH₂Ph)), 1.07 (3H, t, J 8, CH₂CH₃); δ_C (75 MHz, DMSO- d_6) 171.6 (CONHNNH), 161.3 (CONH), 155.7 (*ipso*-Ar-C), 151.8 (*ipso*-Ar-C), 148.6 (*ipso*-Ar-C), 143.6 (*ipso*-Ar-C) 138.2 (*ipso*-Ar-C), 129.7 (Ar-C), 128.8 (Ar-C), 124.9 (Ar-C), 122.2 (Ar-C), 120.1 (*ipso*-Ar-C), 116.4 (Ar-C), 114.2 (Ar-C), 112.4 (Ar-C) 54.4 (CONHCHCH₂Ph), 37.4 (CONHCHCH₂Ph), 22 (CH₂CH₃), 13.5 (CH₂CH₃); m/z (ES⁺) 540 ([³⁵Cl, ⁷⁹Br]MH⁺), 542 ([³⁵Cl, ⁸¹Br]MH⁺), 542 ([³⁷Cl, ⁷⁹Br]MH⁺), 544 ([³⁷Cl, ⁸¹Br]MH⁺), HRMS (ES⁺) Found [³⁵Cl, ⁷⁹Br]MH⁺, 540.0264 (C₂₅H₂₄⁷⁹Br³⁵ClN₅O₂ requires 540.0802);

(S)-6-chloro-2-ethyl-N-(1-oxo-3-phenyl-1-(2-(3-(trifluoromethyl)phenyl)hydrazineyl)propan-2-yl)imidazo[1,2-a]pyridine-3-carboxamide 74f

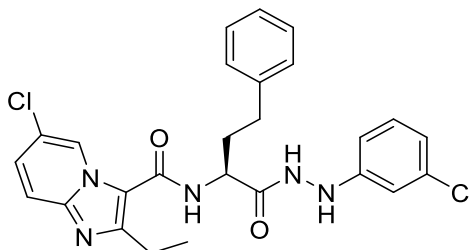


Following the general procedure outlined, *tert*-butyl (S)-(1-oxo-3-phenyl-1-(2-(4-(trifluoromethyl)phenyl)hydrazineyl)propan-2-yl)carbamate **66f** (0.10 g, 0.24 mmol) was transformed following trituration by Et₂O to obtain the titled product as white solid. (0.05 g, 40 %); R_f 0.53 (*n*-hexane/EtOAc 2:1); m.p. 270- 271 °C ; ν_{max} 3290, 1667, 1531, 1395, 1333, 1218, 1159, 1067, 810 cm⁻¹; δ_H (300 MHz, DMSO- d_6) 10.23 (1H, d, J 2 ,CONHNNH), 8.76 (1H, d, J 1.3, Ar-*H*), 8.51 (1H, d, J 2,CONHNNH), 8.44 (1H, d, J 8, CONH), 7.64 (1H, dd, J 10, 0.9, Ar-*H*), 7.48 – 7.26 (7H, m, Ar-*H*), 6.85 (2H, d, J 8, Ar-*H*), 4.84 – 4.75 (1H, m, CONHCHCH₂Ph), 3.27 – 3.19 (2H, m, CONHCHCH₂Ph), 2.81 – 2.63 (2H, m, CH₂CH₃), 1.10 – 1.04 (3H, m, CH₂CH₃); δ_C (75 MHz, DMSO- d_6) 171.7 (CONHNNH), 161.4 (CONH), 152.8 (*ipso*-Ar-C), 151.9 (*ipso*-Ar-C), 143.7 (*ipso*-Ar-C), 138.2 (*ipso*-Ar-C), 129.7 (*ipso*-Ar-C), 128.8 (Ar-C), 127.5 (*ipso*-Ar-C), 127.0 (Ar-C), 126.5 (Ar-C), 124.9 (Ar-C),

Chapter 5. Experimental section.

120.0 (*ipso*-Ar-C), 117.7 (Ar-C), 116.4 (Ar-C), 112.1 (Ar-C), 54.5 (CONHCHCH₂Ph), 37.3 (CONHCHCH₂Ph) 22.0 (CH₂CH₃), 13.4 (CH₂CH₃); *m/z* (ES⁺) 530 ([³⁵Cl]MH⁺); HRMS (ES⁺) Found [³⁵Cl]MH⁺, 530.1251 (C₂₆H₂₄³⁵ClF₃N₅O₆ require 530.1571);

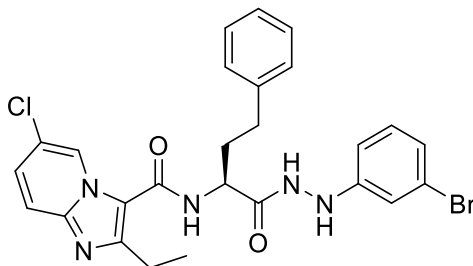
(S)-6-chloro-N-(1-(2-(3-chlorophenyl)hydrazineyl)-1-oxo-4-phenylbutan-2-yl)-2-ethylimidazo[1,2-a]pyridine-3-carboxamide 75a



Following the general procedure outlined, *tert*-butyl (S)-(1-(2-(3-chlorophenyl)hydrazineyl)-1-oxo-4-phenylbutan-2-yl)carbamate **67a** (0.10 g, 0.4 mmol) was transformed following trituration with Et₂O to produce the titled product as white solid (0.07 g, 51 %); R_f 0.55 (*n*.hexane; EtOAc;[2:1]); m.p. 280 -284 °C ; ν_{\max} 3300, 3285, 1658, 1598, 1528, 1492, 1381, 1322, 1293, 1228, 1123, 1073, 1049, 994 cm⁻¹; δ_{H} (300 MHz, DMSO- d₆) 10.05 (1H, d, *J* 2, CONH₂NH), 9.05 (1H, dd, *J* 2, 0.9, Ar-*H*), 8.42 (1H, d, *J* 8, CONH), 8.14 (1H, d, *J* 2, CONH₂NH), 7.69 (1H, dd, *J* 10, 0.8, Ar-*H*), 7.48 (1H, dd, *J* 10, 2, Ar-*H*), 7.38 – 7.18 (5H, m, Ar-*H*), 7.22 – 7.09 (1H, m, Ar-*H*), 6.86 (1H, t, *J* 2, Ar-*H*), 6.72 (2H, dd, *J* 8, 2, Ar-*H*), 4.49 (1H, q, *J* 8, CONHCH(CH₂CH₂Ph)), 3.07 (2H, q, *J* 8, CH₂CH₃), 2.76 (2H, m, CONHCH(CH₂CH₂Ph)) 2.2 (2H, m, CONHCH(CH₂CH₂Ph)), 1.27, (3H, t, *J* 8, CH₂CH₃); δ_{C} (75 MHz, DMSO-d₆) 172.1 (CONH₂NH), 161.5 (CONH), 151.9 (*ipso*-Ar-C), 151.3 (*ipso*-Ar-C), 143.9 (*ipso*-Ar-C), 141.5 (*ipso*-Ar-C), 134.1(*ipso*-Ar-C), 130.7 (*ipso*-Ar-C), 128.8 (Ar-C), 127.6 (Ar-C), 126.5 (Ar-C), 125.3 (Ar-C), 120.1 (*ipso*-Ar-C), 118.3 (Ar-C), 117.7 (Ar-C), 116.4 (Ar-C), 111.9), 111.4(Ar-C), 52.6 (CONHCH(CH₂CH₂Ph)), 33.5 (CONHCH(CH₂CH₂Ph)), 32.3 (CONHCH(CH₂CH₂Ph)), 22.3 (CH₂CH₃), 13.6 (CH₂CH₃); *m/z*; (ES⁺) 510 ([^{35,35}Cl]MH⁺), 512 ([^{35,37}Cl]MH⁺), HRMS (ES⁺) Found [^{35,35}Cl]MH⁺, 510.1184 (C₂₆H₂₆^{35,35}Cl₂N₅O₂ requires 510.1464);

Chapter 5. Experimental section.

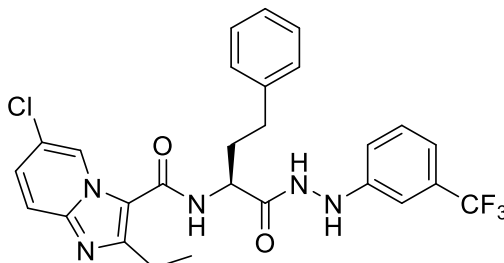
(S)-N-(1-(2-(3-bromophenyl)hydrazineyl)-1-oxo-4-phenylbutan-2-yl)-6-chloro-2-ethylimidazo[1,2-a]pyridine-3-carboxamide 75b



Following the general procedure outlined, *tert*-butyl (S)-(1-(2-(3-bromophenyl)hydrazineyl)-1-oxo-4-phenylbutan-2-yl)carbamate **67b** (0.10 g, 0.40 mmol) was transformed to obtain the titled compound as a light orange solid (0.06 g, 60 %) R_f 0.32 (*n*.hexane;EtOAc;[2:1]). m.p. 280- 284 °C ; ν_{max} 3300, 3285, 1658, 1598, 1528, 1492, 1381, 1322, 1293, 1228, 1123, 1073, 1049, 994 cm^{-1} ; δ_H (300 MHz, DMSO- d_6) 10.05 (1H, d, J 2, CONH NH), 9.05 (1H, dd, J 2, 0.9, Ar- H), 8.42 (1H, d, J 8, CONH), 8.14 (1H, d, J 2, CONH NH), 7.69 (1H, dd, J 10, 0.8, Ar- H), 7.48 (1H, dd, J 10, 2, Ar- H), 7.38 – 7.18 (5H, m, Ar- H), 7.22 – 7.09 (1H, m, Ar- H), 6.86 (1H, t, J 2, Ar- H), 6.72 (2H, dd, J 8, 2, Ar- H), 4.49 (1H, q, J 8, CONHCH(CH_2CH_2Ph)), 3.07 (2H, q, J 8, CH_2CH_3), 2.76 (2H, m, CONHCH(CH_2CH_2Ph)) 2.2 (2H, m, CONHCH(CH_2CH_2Ph)), 1.27, (3H, t, J 8, CH_2CH_3); δ_C (75 MHz, DMSO- d_6) 172.1 (CONH NH), 161.5 (CONH), 151.9 (*ipso*-Ar-C), 151.3 (*ipso*-Ar-C), 143.9 (*ipso*-Ar-C), 141.5 (*ipso*-Ar-C), 134.1(*ipso*-Ar-C), 130.7 (*ipso*-Ar-C), 128.8 (Ar-C), 127.6 (Ar-C), 126.5 (Ar-C), 125.3 (Ar-C), 120.1 (*ipso*-Ar-C), 118.3 (Ar-C), 117.7 (Ar-C), 116.4 (Ar-C), 111.9), 111.4(Ar-C), 52.6 (CONHCH(CH_2CH_2Ph)), 33.5 (CONHCH(CH_2CH_2Ph)), 32.3 (CONHCH(CH_2CH_2Ph)), 22.3 (CH_2CH_3), 13.6 (CH_2CH_3); m/z (ES $^+$) 554 ([^{35}Cl , ^{79}Br]MH $^+$), 556 ([^{35}Cl , ^{81}Br]MH $^+$), 556 ([^{37}Cl , ^{79}Br]MH $^+$) 558 ([^{37}Cl , ^{81}Br]MH $^+$), HRMS (ES $^+$) Found [^{35}Cl , ^{79}Br]MH $^+$, 545.0973 (C $_{26}$ H $_{26}$ ^{79}Br ^{35}Cl N $_5$ O $_2$ requires 545.0958);

Chapter 5. Experimental section.

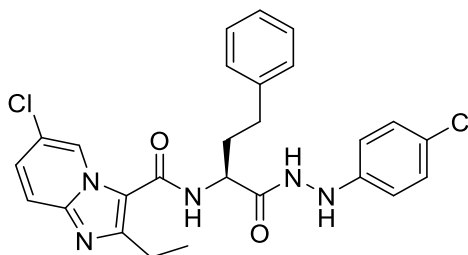
(S)-6-chloro-2-ethyl-N-(1-oxo-4-phenyl-1-(2-(3-(trifluoromethyl)phenyl)hydrazineyl)butan-2-yl)imidazo[1,2-a]pyridine-3-carboxamide 75c



Following the general procedure outlined, *tert*-butyl (S)-(1-oxo-4-phenyl-1-(2-(3-(trifluoromethyl)phenyl)hydrazineyl)butan-2-yl)carbamate **67c** (0.10 g, 0.40 mmol) was transformed following trituration with DCM to produce the titled compound as white solid (0.05 g, 37 %); R_f 0.36 (*n*.hexane;EtOAc; [2:1]); m.p. 268 – 270 °C ; ν_{max} 3258, 1666, 1602, 1491, 1395, 1339, 1334, 1395, 1228, 1168, 1112, 1069, 832, 696, 55 cm^{-1} ; d_H (300 MHz, DMSO- d_6) 10.13 (1H, d, J 2, CONHNNH), 9.00 (1H, d, J 2, Ar- H), 8.42 (1H, d, J 8, CONH), 8.30 (1H, d, J 2, CONHNNH), 7.69 (1H, d, J 10, Ar- H), 7.49 – 7.38 (1H, m, Ar- H), 7.28 (6H, ,m, Ar- H), 7.05 (3H, m, Ar- H), 4.51 (1H, q, J 8, CONHCH(CH₂CH₂Ph)), 3.06 (2H, q, J 8, CH₂CH₃), 2.88 – 2.66 (2H, m, CONHCH(CH₂CH₂Ph)), 2.15 (2H, m, CONHCH(CH₂CH₂Ph)), 1.30 (3H, t, J 8 ,CH₂CH₃); d_C (75 MHz, DMSO- d_6) 172.2 (CONHNNH), 161.5 (CONH) 151.9 (*ipso*-Ar-C), 150.4 (*ipso*-Ar-C), 143.6 (*ipso*-Ar-C), 141.5 (*ipso*-Ar-C), 130.1 (Ar-C), 128.7 (*ipso*-Ar-C), 127.6 (Ar-C), 126.5 (Ar-C), 125.22 (Ar-C), 120.07 (*ipso*-Ar-C), 117.7 (Ar-C), 116.42 (*ipso*-Ar-C), 116.36 (Ar-C), 114.95 (Ar-C), 52.64 (CONHCH(CH₂CH₂Ph)), 33.53 (CONHCH(CH₂CH₂Ph)), 32.33 (CONHCH(CH₂CH₂Ph)) 22.32 (CH₂CH₃), 13.62 (CH₂CH₃); m/z (ES⁺) 544 ([³⁵Cl]MH⁺); HRMS (ES⁺) Found [³⁵Cl]MH⁺; 544.1443 (C₂₇H₂₆³⁵ClF₃N₅O₂ requires 544.1682);

Chapter 5. Experimental section.

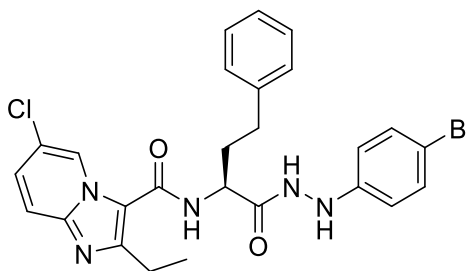
(S)-6-chloro-N-(1-(2-(4-chlorophenyl)hydrazineyl)-1-oxo-4-phenylbutan-2-yl)-2-ethylimidazo[1,2-a]pyridine-3-carboxamide 75d



Following the general procedure outlined, *tert*-butyl (S)-(1-(2-(4-chlorophenyl)hydrazineyl)-1-oxo-4-phenylbutan-2-yl)carbamate **67d** (0.12 g, 0.31 mmol) was transformed following flush column chromatography to obtain the titled compound as a white solid (0.04 g, 33 %); R_f 0.34 ((DCM/EtOH; [200;4]); m.p. 278 - 280 °C ; ν_{max} 3273, 2933, 1673, 1626, 1509, 1487, 1389, 1321, 1203, 1090, 1011, 1064, 820, 728, 556, 490 cm^{-1} ; δ_H (300 MHz, DMSO- d_6) 10.05 (1H, d, J 3, CONHNNH), 8.97 (1H, d, J 2, Ar- H), 8.43 (1H, d, J 8, CONH), 8.02 (1H, d, J 3, CONHNNH), 7.69 (1H, d, J 10, Ar- H), 7.47 (1H, dd, J 10, 2, Ar- H), 7.36 – 7.14 (7H, m, Ar- H), 6.85 – 6.76 (2H, m, Ar- H), 4.53 (1H, q, J 8, CONHCH(CH₂CH₂Ph)), 3.04 (2H, q, J 8, CH₂CH₃), 2.76 (2H, CONHCH(CH₂CH₂Ph)), 2.16 (2H, m, CONHCH(CH₂CH₂Ph)), 1.30 (3H, t, J 8, CH₂CH₃); δ_C (75 MHz, DMSO- d_6) 172.2 (CONHNNH), 161.4 (CONH), 151.7 (*ipso*-Ar-C), 148.8 (*ipso*-Ar-C), 141.4 (*ipso*-Ar-C), 128.8 (Ar-C), 126.5 (Ar-C), 125.2 (*ipso*-Ar-C), 122.3 (*ipso*-Ar-C), 120.0 (*ipso*-Ar-C), 117.7 (Ar-C), 114.8 (Ar-C), 52.5 (CONHCH(CH₂CH₂Ph)), 33.6 (CONHCH(CH₂CH₂Ph)), 32.3 (CONHCH(CH₂CH₂Ph)), 22.3 (CH₂CH₃), 13.8 (CH₂CH₃); m/z (ES⁺) 510 ([^{35,35}Cl]MH⁺), 512 ([^{35,37}Cl]MH⁺); HRMS (ES⁺) Found [^{35,35}Cl]MH⁺, 510.1202 (C₂₆H₂₆^{35,35}Cl₂N₅O₂ requires 510.1464);

Chapter 5. Experimental section.

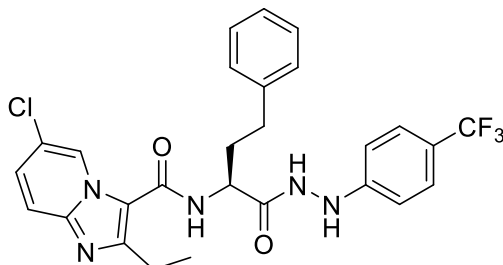
(S)-N-(1-(2-(4-bromophenyl)hydrazineyl)-1-oxo-4-phenylbutan-2-yl)-6-chloro-2-ethylimidazo[1,2-a]pyridine-3-carboxamide 75e



Following the general procedure outlined, *tert*-butyl (S)-(1-(2-(4-bromophenyl)hydrazineyl)-1-oxo-4-phenylbutan-2-yl)carbamate **67e** (0.12 g, 0.31 mmol) was transformed following trituration with Et₂O to produce the titled compound as pale-yellow solid; (0.08 g, 63 %) R_f 0.46 (*n*-hexane/EtOAc [2:1]); m.p. 278- 280 °C; ν_{\max} 3273, 2933, 1673, 1626, 1509, 1487, 1389, 1321, 1203, 1090, 1011, 1064, 820, 728, 556, 490 cm⁻¹; δ_{H} (300 MHz, DMSO-d₆) 10.05 (1H, d, *J* 3, CONHNH), 8.97 (1H, d, *J* 2, Ar-*H*), 8.43 (1H, d, *J* 8, CONH), 8.02 (1H, d, *J* 3, CONHNH), 7.69 (1H, d, *J* 10, Ar-*H*), 7.47 (1H, dd, *J* 10, 2, Ar-*H*), 7.36 – 7.14 (7H, m, Ar-*H*), 6.85 – 6.76 (2H, m, Ar-*H*), 4.53 (1H, q, *J* 8, CONHCH(CH₂CH₂Ph)), 3.04 (2H, q, *J* 8, CH₂CH₃), 2.76 (2H, CONHCH(CH₂CH₂Ph)), 2.16 (2H, m, CONHCH(CH₂CH₂Ph)), 1.30 (3H, t, *J* 8, CH₂CH₃); δ_{C} (75 MHz, DMSO-d₆) 172.2 (CONHNH), 161.4 (CONH), 151.7 (*ipso*-Ar-C), 148.8 (*ipso*-Ar-C), 141.4 (*ipso*-Ar-C), 128.8 (Ar-C), 126.5 (Ar-C) 125.2 (*ipso*-Ar-C), 122.3 (*ipso*-Ar-C), 120.0 (*ipso*-Ar-C), 117.7 (Ar-C), 114.8 (Ar-C), 52.5 (CONHCH(CH₂CH₂Ph)), 33.6 (CONHCH(CH₂CH₂Ph)), 32.3 (CONHCH(CH₂CH₂Ph)), 22.3 (CH₂CH₃), 13.8 (CH₂CH₃); *m/z* (ES⁺) 554 ([³⁵Cl,⁷⁹Br]MH⁺), 556 ([³⁵Cl, ⁸¹Br]MH⁺), 556 ([³⁷Cl,⁷⁹Br]MH⁺), 558 ([³⁷Cl,⁸¹Br]MH⁺); HRMS (ES⁺) Found [³⁵Cl⁷⁹Br]MH⁺, 554.0649 (C₂₆H₂₆⁷⁹Br³⁵ClN₅O₂ requires 555.0958);

Chapter 5. Experimental section.

(S)-6-chloro-2-ethyl-N-(1-oxo-4-phenyl-1-(2-(4-(trifluoromethyl)phenyl)hydrazineyl)butan-2-yl)imidazo[1,2-a]pyridine-3-carboxamide 75f



Following the general procedure outlined, *tert*-butyl (S)-(1-oxo-4-phenyl-1-(2-(4-(trifluoromethyl)phenyl)hydrazineyl)butan-2-yl)carbamate **67f** (0.10 g, 0.4 mmol) was transformed following flush column chromatography to produce the above compound as faint yellow oil (0.07 g, 66 %); R_f 0.36 (*n*-hexane; EtOAc; [2:1]); m.p. 265 -368 °C ; ν_{\max} 3270, 1664, 1610, 1324, 1220, 1162, 1105, 1066, 832, 696, 557 cm^{-1} ; δ_{H} (300 MHz, DMSO- d_6) 10.17 (1H, d, J 3, CONH NH), 8.97 (1H, d, J 2, Ar- H), 8.43 (1H, d, J 8, Ar- H) 8.03 (1H, d, J 3, CONH NH), 7.69 (1H, d, J 10, Ar- H), 7.47 (1H, dd, J 10, 2, Ar- H), 7.35 – 7.15 (7H, m, Ar- H), 6.80 (2H, d, J 9, Ar- H), 4.53 (1H, q, J 8, CONHCH($\text{CH}_2\text{CH}_2\text{Ph}$)), 3.05 (2H, q, J 8, CH_2CH_3), 2.85 – 2.64 (2H, m, CONHCH($\text{CH}_2\text{CH}_2\text{Ph}$)), 2.20 – 2.07 (2H, m, CONHCH($\text{CH}_2\text{CH}_2\text{Ph}$)), 1.31 (3H, t, J 8, CH_2CH_3); δ_{C} (75 MHz, DMSO- d_6) 172, (CONH NH), 161.4 (CONH), 151.7 (*ipso*-Ar-C), 148.8 (*ipso*-Ar-C), 143.7 (*ipso*-Ar-C), 141.6 (*ipso*-Ar-C), 128.8 (Ar-C), 127.5 (Ar-C), 126.5 (Ar-C), 125.2 (Ar-C), 122.23 (Ar-C), 120.02 (*ipso*-Ar-C), 117.7 (Ar-C), 116.5 (Ar-C), 114.2 (Ar-C), 52.5 (CONHCH($\text{CH}_2\text{CH}_2\text{Ph}$)), 33.6 (CONHCH($\text{CH}_2\text{CH}_2\text{Ph}$)), 32.3 (CONHCH($\text{CH}_2\text{CH}_2\text{Ph}$)), 22.3 (CH_2CH_3), 13.7 (CH_2CH_3); m/z (ES $^+$) 544 ([^{35}Cl]MH $^+$); HRMS (ES $^+$) Found [^{35}Cl]MH $^+$; 544.1443 (C $_{27}$ H $_{26}$ ^{35}Cl F $_3$ N $_5$ O $_2$ requires 544.1682);

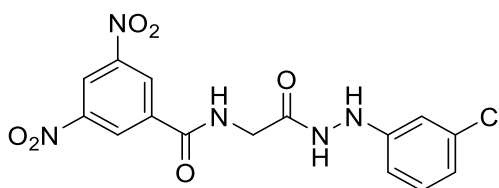
Chapter 5. Experimental section.

5.1.3 General procedure for synthesis of 3,5-dinitrobenzene substituted amino acid hydrazide compounds.

The *N*-Boc amino acid hydrazide (1.20 equiv.) was dissolved in 4 N HCl solution in dioxane (2 mL) and stirred at room temperature for 90 minutes. After that, the solvent was evaporated, dried *in vacuo* and precipitated using (EtOH / Et₂O). The precipitate was directly used in the next step without further purification. Therefore, the resulting deprotected amino acid hydrazide solid (1 equiv.) was dissolved in THF (3 mL). Then, diisopropylethylamine (3 equiv.) was added followed by (2-(1H-benzotriazol-1-yl)-1,1,3,3-tetramethyluronium hexafluorophosphate HBTU (1.20 equiv.). The mixture was stirred for 10 minutes at room temperature, then the solution was treated with 3,5-dinitrobenzoic acid (1.20 equiv.) and continued stirring for 4 hours. After that, the reaction mixed with ethyl acetate (10 mL) and distilled water (5 mL). After separation of the two phases the organic layer washed again with distilled water (5 mL × 3 mL) followed by a wash with sat. aq. NH₄Cl (6 mL) then sat. aq. NaHCO₃ (6 mL) followed by brine (10 mL). Organic layer dried over MgSO₄, filtered, evaporated and dried *in vacuo*. The product was purified by trituration with (Et₂O or DCM) or through flash chromatography (*n*-hexane/EtOAc [2:1]); (DCM/EtOH/NH₃ [600:8:1], [200:6:1]) afforded the desired compounds **84a – 89h**.

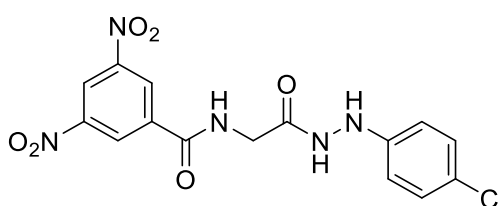
Chapter 5. Experimental section.

***N*-(2-(2-(3-chlorophenyl)hydrazineyl)-2-oxoethyl)-3,5-dinitrobenzamide 84a**



Following the general standard procedure, *tert*-butyl (2-(2-(3-chlorophenyl)hydrazineyl)-2-oxoethyl)carbamate **61a** (0.11 g, 0.37 mmol) was transformed following flush column chromatography (*n*-hexane/EtOAc) [4:1] to produce the titled product as yellow solid (0.07 g, 46 %); R_f 0.31 (DCM/EtOH/NH₃ [200:6:1]); m.p. 90 - 91 °C; ν_{max} 3303, 3101, 1594, 1488, 1249, 1092, 1010, 1092, 918, 822; δ_H (300 MHz, DMSO-*d*₆) 9.98 (1H, d, J 2, CONHNH), 9.68 (1H, t, J 6, CONH), 9.11 (2H, d, J 2, Ar-*H*), 8.99 (1H, t, J 2, Ar-*H*), 8.06 (1H, d, J 2, CONHNH), 7.09 (1H, t, J 8.0, Ar-*H*), 6.92 (1H, t, J 2, Ar-*H*), 6.85 (1H, dt, J 8, 1, Ar-*H*), 6.74 (1H, dt, J 8, Ar-*H*), 4.06 (1H, d, J 6, CONHCH₂); δ_C (75 MHz, DMSO-*d*₆) 168.9 (CONHNH), 163.5 (CONH), 151.4 (*ipso*-Ar-C), 148.6 (*ipso*-Ar-C), 137.1 (*ipso*-Ar-C), 131.1 (Ar-C), 128.9 (Ar-C), 122.6 (Ar-C), 121.5 (Ar-C), 121.3 (Ar-C), 114.8 (Ar-C), 111.7 (Ar-C), 42.5 (CONHCH₂); m/z (ES⁺) 394 ([³⁵Cl]MH⁺), 396 ([³⁷Cl]MH⁺); HRMS (ES⁺) Found [³⁵Cl]MH⁺, 394.0536 (C₁₅H₁₃³⁵ClN₅O₆ require 394.0555);

***N*-(2-(2-(4-chlorophenyl)hydrazineyl)-2-oxoethyl)-3,5-dinitrobenzamide 84b**



Following the general standard procedure, *tert*-butyl (2-(2-(4-chlorophenyl)hydrazineyl)-2-oxoethyl)carbamate **61d** (0.10 g, 0.33 mmol) was transformed following flush column chromatography (*n*-hexane/EtOAc) [3:1] to produce the titled product as a light yellow solid (0.03 g, 26 %); R_f 0.47 (DCM/EtOH/NH₂ [200:6:1]); m.p. 90 - 92 °C; ν_{max} 3272, 1630, 1549, 1423, 1249, 1097, 1010, 748, 699 cm⁻¹; δ_H (700 MHz, DMSO-*d*₆) 9.98 (1H, d, J 2, CONHNH), 9.67 (1H, t, J 6, CONH), 9.08 (2H, d, J 2, Ar-*H*), 8.98 (1H, d, J 2, Ar-*H*), 7.95 (1H,

Chapter 5. Experimental section.

d, *J* 2, CONHNH), 7.20 (2H, d, *J* 9, Ar-*H*), 6.75 (2H, d, *J* 9, Ar-*H*), 4.04 (2H, d, *J* 6, CONHCH₂); δ_c (700 MHz, DMSO-d₆) 168.3 (CONHNH), 162.9 (CONH), 148.6 (*ipso*-Ar-C), 136.5 (*ipso*-Ar-C), 128.3.1 (Ar-C), 127.6 (Ar-C), 121.7 (Ar-C), 120.9 (Ar-C), 113.6 (Ar-C), 42.5 (CONHCH₂) 168.8 (CONHNH), 163.4 (CONH), 148.6 (*ipso*-Ar-C), 148.6 (*ipso*-Ar-C), 137.1 (*ipso*-Ar-C), 128.9 (Ar-C), 128.2 (Ar-C), 122.2 (Ar-C), 121.5 (Ar-C), 114.1 (Ar-C), 42.4 (CONHCH₂).; *m/z* (ES⁺) 394 ([³⁵Cl]MH⁺), 396 ([³⁷Cl]MH⁺); HRMS (ES⁺) Found [³⁵Cl]MH⁺, 394.0536 (C₁₅H₁₃³⁵ClN₅O₆ require 394.0554);

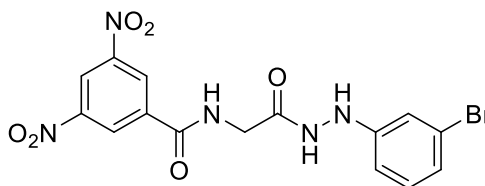
***N*-(2-(2-(2-bromophenyl)hydrazineyl)-2-oxoethyl)-3,5-dinitrobenzamide 84c**



Following the general standard procedure, *tert*-butyl (2-(2-(2-bromophenyl)hydrazineyl)-2-oxoethyl)carbamate **61A** (0.10 g, 0.29 mmol) was transformed following trituration with Et₂O to produce the titled compound as yellow solid (0.07 g, 58 %); R_f 0.53 (DCM/EtOH/NH₃ [200:6:1]); m.p. 91 -94 °C ; ν_{\max} 3290, 1667, 1531, 1395, 1333, 1218, 1159, 1067, 810 cm⁻¹; δ_H (300 MHz, DMSO-d₆) 10.13 (1H, d, *J* 2, CONHNH), 9.68 (1H, t, *J* 6, CONH), 9.10 (2H, d, *J* 2, Ar-*H*), 8.99 (1H, t, *J* 2, Ar-*H*), 7.44 (1H, dd, *J* 8, 2, Ar-*H*), 7.25 (1H, s, CONHNH), 7.20 (1H, m, Ar-*H*), 6.87 (1H, dd, *J* 8., 2, Ar-*H*), 6.71 (1H, td, *J* 8, 2, Ar-*H*), 4.08 (2H, d, *J* 6 ,CONHCH₂). δ_c (75 MHz, DMSO-d₆) 168.8 (CONHNH), 163.5 (CONH), 148.6 (*ipso*-Ar-C), 145.9 (*ipso*-Ar-C), 136.7 (*ipso*-Ar-C), 132.8 (Ar-C), 128.7 (Ar-C), 128.2 (Ar-C), 121.5 (Ar-C) 120.7 (Ar-C), 113.8 (Ar-C), 107.4 (*ipso*-Ar-C), 42.4 (CONHCH₂) ; *m/z* (ES⁺) 438 ([⁷⁹Br]MH⁺), 440 ([⁸¹Br]MH⁺); HRMS (ES⁺) Found [⁷⁹Br]MH⁺, 438.0034 (C₁₅H₁₃⁷⁹BrN₅O₆ require 438.0049);

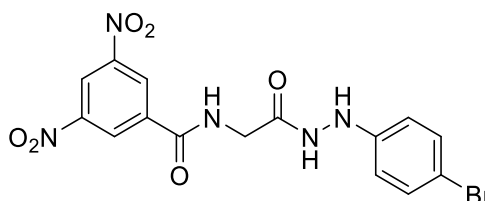
Chapter 5. Experimental section.

N-(2-(2-(3-bromophenyl)hydrazineyl)-2-oxoethyl)-3,5-dinitrobenzamide 84d



Following the general standard procedure, *tert*-butyl (2-(2-(3-bromophenyl)hydrazineyl)-2-oxoethyl)carbamate **61b** (0.10 g, 0.29 mmol) was transformed following flush column chromatography (*n*-hexane/EtOAc) [4:1] to produce the titled compound as yellow gummy solid (0.07 g, 57 %); R_f 0.31 (DCM/EtOH [200:6]); m.p. 94 -95 °C; ν_{max} 3282, 1682, 1599, 1477, 1248, 1151, 1044, 992, 864, 768, 434 cm^{-1} ; δ_H (300 MHz, DMSO- d_6) 9.98 (1H, d, J 2, CONHNH), 9.68 (1H, t, J 6, CONH), 9.11 (2H, d, J 2, Ar-H), 8.99 (1H, t, J 2, Ar-H), 8.06 (1H, d, J 2, CONHNH), 7.09 (1H, t, J 8, Ar-H), 6.92 (1H, t, J 2, Ar-H), 6.85 (1H, dt, J 8, 1, Ar-H), 6.74 (1H, dt, J 8, 1, Ar-H), 4.06 (1H, d, J 6, CONHCH $_2$); δ_C (75 MHz, DMSO- d_6) 168.9 (CONHNH), 163.5 (CONH), 151.4 (*ipso*-Ar-C), 148.6 (*ipso*-Ar-C), 137.1 (*ipso*-Ar-C), 131.1 (Ar-C), 128.9 (Ar-C), 122.6 (*ipso*-Ar-C), 121.5 (Ar-C), 121.3 (Ar-C), 114.8 (Ar-C), 111.7 (Ar-C), 42.5 (CONHCH $_2$); m/z (ES $^+$) 438 ([^{79}Br]MH $^+$), 440 ([^{81}Br]MH $^+$); HRMS (ES $^+$) Found [^{79}Br]MH $^+$, 438.0804 (C $_{15}H_{13}^{79}BrN_5O_6$ require 438.0049);

N-(2-(2-(4-bromophenyl)hydrazineyl)-2-oxoethyl)-3,5-dinitrobenzamide 84e

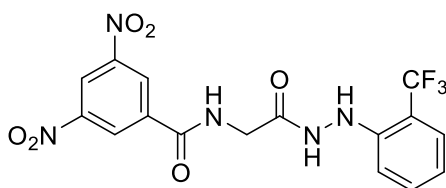


Following the general standard procedure, *tert*-butyl (2-(2-(4-bromophenyl)hydrazineyl)-2-oxoethyl)carbamate **61e** (0.09 g, 0.26 mmol) was transformed following flush column chromatography (*n*-hexane/EtOAc) [3:1] to produce the titled product as a light yellow solid (0.04 g, 37 %); R_f 0.32 (DCM/EtOH/NH $_2$ [200:6:1]); m.p. 90 - 92 °C; ν_{max} 3272, 1639, 1538, 1323, 1277, 1097, 1034, 748, 699 cm^{-1} ; δ_H (300 MHz, DMSO- d_6) 9.97 (1H, d, J 2, CONHNH),

Chapter 5. Experimental section.

9.66 (1H, t, *J* 6, CONH), 9.11 (2H, d, *J* 2, Ar-*H*), 8.99 (1H, d, *J* 2, Ar-*H*), 7.97 (1H, d, *J* 2, CONH), 7.19 (2H, d, *J* 9, Ar-*H*), 6.77 (2H, d, *J* 9, Ar-*H*), 4.06 (2H, d, *J* 6, CONHCH₂); δ_c (75 MHz, DMSO-d₆) 168.8 (CONH), 163.4 (CONH), 148.6 (*ipso*-Ar-C), 137.1 (*ipso*-Ar-C), 128.9 (Ar-C), 128.2 (Ar-C), 122.2 (*ipso*-Ar-C), 121.5 (Ar-C), 114.1 (Ar-C), 42.4 (CONHCH₂).; *m/z* (ES⁺) 438 ([⁷⁹Br]MH⁺), 440 ([⁸¹Br]MH⁺); HRMS (ES⁺) Found [⁷⁹Br]MH⁺, 438.0020 (C₁₅H₁₃⁷⁹BrN₅O₆ requires 438.0049);

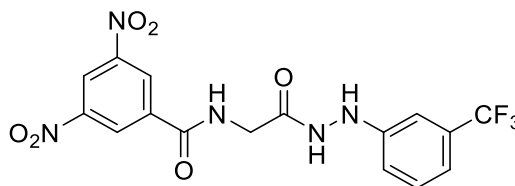
3,5-dinitro-*N*-(2-oxo-2-(2-(2-(trifluoromethyl)phenyl)hydrazineyl)ethyl)benzamide **84f**



Following the general standard procedure, *tert*-butyl (2-oxo-2-(2-(2-(trifluoromethyl)phenyl)hydrazineyl)ethyl)carbamate **61B** (0.10 g, 0.30 mmol) was transformed following trituration with Et₂O to produce titled compound as a light yellow solid (0.06 g, 49 %); R_f 0.34 (*n*-hexane/EtOAc) [3:1]; m.p. 89 - 91 °C; ν_{\max} 3087, 1664, 1529, 1345, 1271, 1095, 748 cm⁻¹; δ_H (300 MHz, DMSO-d₆) 10.14 (1H, d, *J* 2, CONH), 9.70 (1H, t, *J* 6, CONH), 9.10 (2H, d, *J* 2, Ar-*H*), 8.98 (1H, t, *J* 2, Ar-*H*), 7.53 (1H, s, CONH), 7.46 (2H, t, *J* 8, Ar-*H*), 7.03 (1H, d, *J* 8, Ar-*H*), 6.87 (1H, t, *J* 8, Ar-*H*), 4.08 (2H, d, *J* 6, CONHCH₂); δ_c (75 MHz, DMSO-d₆) 168.9 (CONH), 163.5 (CONH), 148.6 (*ipso*-Ar-C), 146.5 (*ipso*-Ar-C), 137.1 (*ipso*-Ar-C), 133.8 (Ar-C), 128.2 (Ar-C), 126.5 (*ipso*-Ar-CCF₃), 121.5 (Ar-C), 118.7 (Ar-C), 113.7 (Ar-C), 112.3 (*ipso*-Ar-C), 42.5 (CONHCH₂); δ_F (282 MHz, DMSO-d₆) -59.30 (3F, s, CF₃); *m/z* (ES⁺) 427 (MH⁺); HRMS (ES⁺) found MH⁺, 428.0579 (C₁₆H₁₃F₃N₅O₆ requires 428.0818);

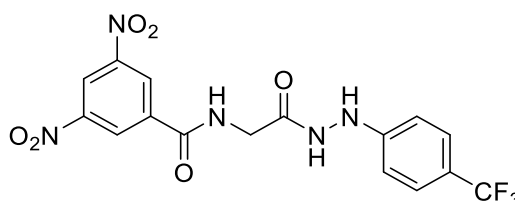
Chapter 5. Experimental section.

3,5-dinitro-*N*-(2-oxo-2-(2-(3-(trifluoromethyl)phenyl)hydrazineyl)ethyl)benzamide **84g**



Following the general standard procedure, *tert*-butyl (2-oxo-2-(2-(3-(trifluoromethyl)phenyl)hydrazineyl)ethyl)carbamate **61c** (0.10 g, 0.30 mmol) was transformed following flush column chromatography (DCM/EtOAc [3:1]) to produce titled compound as a yellow solid (0.06 g, 49 %); R_f 0.36 (DCM/EtOH/NH₃ [200:6:1]); m.p. 96 – 97 °C; ν_{max} 3322, 1629, 1533, 1344, 1167, 1065, 1109, 748, 699 cm⁻¹; δ_H (300 MHz, DMSO-*d*₆) 10.05 (1H, d, *J*2, CONHNH), 9.70 (1H, t, *J*6, CONH), 9.10 (2H, d, *J*2, Ar-*H*), 8.98 (1H, t, *J*2, Ar-*H*), 8.23 (1H, d, *J*2, CONHNH), 7.36 (1H, t, *J*8, Ar-*H*), 7.03 (2H, d, *J*5, Ar-*H*), 7.00 – 6.98 (1H, m, Ar-*H*), 4.06 (2H, d, *J*6, CONHCH₂) (75 MHz, DMSO-*d*₆) 169 (CONHNH), 163.5 (CONH), 150.33 (*ipso*-Ar-C), 148.6 (*ipso*-Ar-C), 137.1 (*ipso*-Ar-C), 130.2 (Ar-C), 128.2 (Ar-C), 121.4 (Ar-C), 116.3 (Ar-C) 114.9 (*ipso*-Ar-C), 108.4 (Ar-C) 42.5 (CONHCH₂); δ_F (282 MHz, DMSO-*d*₆) -59.29 (3F, s, CF₃); *m/z* (ES⁺) 427 (MH⁺); HRMS (ES⁺) found MH⁺, 428.0796 (C₁₆H₁₃F₃N₅O₆ requires 428.0818);

3,5-dinitro-*N*-(2-oxo-2-(2-(4-(trifluoromethyl)phenyl)hydrazineyl)ethyl)benzamide **84h**

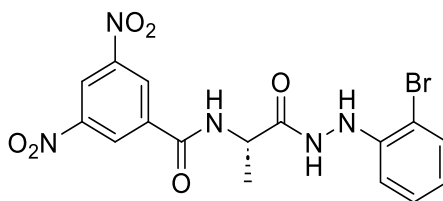


Following the general standard procedure, *tert*-butyl (2-oxo-2-(2-(4-(trifluoromethyl)phenyl)hydrazineyl)ethyl)carbamate **61f** (0.10 g, 0.30 mmol) was transformed following trituration with Et₂O to produce titled compound as a yellow solid (0.06 g, 49 %); R_f 0.36 (DCM/EtOH/NH₃ [200:6:1]); m.p. 95 – 96 °C; ν_{max} 3272, 1639, 1538, 1323, 1277, 1097, 1034, 748, 699 cm⁻¹; δ_H (300 MHz, DMSO-*d*₆) 10.09 – 10.06 (1H, m, CONHNH), 9.69 (1H, t, *J*6, CONH), 9.10 (2H, d, *J*

Chapter 5. Experimental section.

2.,Ar-H), 8.99 (1H, t, J 2, Ar-H), 8.42 (1H, s, CONHNNH), 7.47 (2H, d, J 9, Ar-H), 6.86 (2H, d, J 9 Ar-H), 4.08 (1H, d, J 6, CONHCH₂). δ_c (75 MHz, DMSO-d₆) 168.9 (CONHNNH), 163.5 (CONH), 152.8 (*ipso*-Ar-C) 148.6 (*ipso*-Ar-C), 137.1 (*ipso*-Ar-C), 128.2 (Ar-C), 126.6 (Ar-C), 121.5 (Ar-C), 118.9 (*ipso*-Ar-CCF₃), 111.0 (Ar-C). 42.4 (CONHCH₂); δ_F (282 MHz, DMSO-d₆) -61.30 (3F, s, CF₃); m/z (ES⁺) 428 (MH⁺); HRMS (ES⁺) found MH⁺, 428.0808 (C₁₆H₁₃F₃N₅O₆ requires 427.0812).

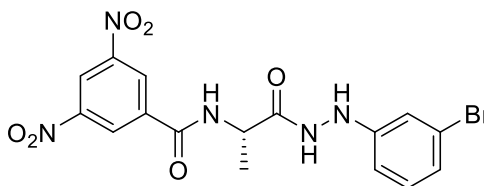
(S)-N-(1-(2-(2-bromophenyl)hydrazineyl)-1-oxopropan-2-yl)-3,5-dinitrobenzamide **85b**



Following the general standard procedure, *tert*-butyl (S)-(1-(2-(2-bromophenyl)hydrazineyl)-1-oxopropan-2-yl)carbamate **62A** (0.10 g, 0.28 mmol) was transformed to obtain the titled compound as yellow solid, (0.09 g, 68 %); R_f 0.65 (*n*-hexane/EtOAc) [2:1]; m.p. 101 - 102 °C; ν_{max} 2155, 1638, 1344, 1165, 1095, 728 cm⁻¹; δ_H (300 MHz, DMSO-d₆) 10.22 (1H, d, J 2, CONHNNH), 9.52 (1H, d, J 7, CONH), 9.19 (2H, d, J 2, Ar-H), 9.03 (1H, t, J 2., Ar-H), 7.49 (1H, dd, J 8, 1., Ar-H), 7.32 – 7.20 (1H, m, Ar-H), 6.91 (1H, dd, J 8., 2, Ar-H), 6.75 (1H, td, J 8, 2, Ar-H), 4.67 (1H, p, J 7, CONHCHCH₃), 1.54 (3H, d, J 7, CONHCHCH₃); δ_c (75 MHz, DMSO-d₆) 172.3 CONHNNH), 163 (CONH), 148.6 (*ipso*-Ar-C), 146. (*ipso*-Ar-C), 137.1 (*ipso*-Ar-C), 132.8 (Ar-C), 128.8 (Ar-C), 128.4 (*ipso*-Ar-C), 121.5 (Ar-C), 120.7 (*ipso*-Ar-C), 107.4 (Ar-C), 49.2 (CONHCHCH₃), 18.0 (CONHCHCH₃); m/z (ES⁺) 452 ([⁷⁹Br]MH⁺) 454 ([⁸¹Br]MH⁺); HRMS (ES⁺) found [⁷⁹Br] MH⁺, 452.2200 (C₁₆H₁₅⁷⁹BrN₅O₆ requires 452.0206);

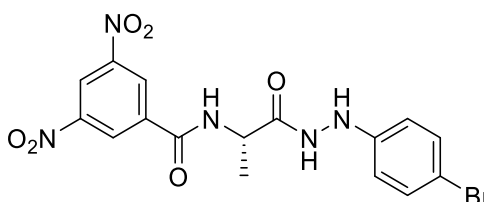
Chapter 5. Experimental section.

(S)-N-(1-(2-(3-bromophenyl)hydrazineyl)-1-oxopropan-2-yl)-3,5-dinitrobenzamide 85c



Following the general standard procedure, *tert*-butyl (S)-(1-(2-(3-bromophenyl)hydrazineyl)-1-oxopropan-2-yl)carbamate **62b** (0.10g, 0.28 mmol) was transformed to obtain the titled compound as pale-yellow solid, (0.06 g, 36 %); R_f 0.24 (*n*-hexane/EtOAc) [4:1]; m.p. 98 - 100 °C; ν_{max} 3267, 1683, 1642, 1536, 1476, 1341, 1283, 1224, 1069, 898, cm^{-1} ; δ_H (300 MHz, DMSO- d_6) 10.03 (1H, s, CONHNH), 9.47 (1H, d, *J* 7, CONH), 9.17 (2H, d, *J* 2, Ar-*H*), 8.99 (1H, m, Ar-*H*), 8.07 (1H, b, CONHNH), 7.11 (1H, t, *J* 8, Ar-*H*), 6.76 (1H, t, *J* 2, Ar-*H*), 6.73-6.66 (2H, m, Ar-*H*), 4.58 (1H, p, *J* 7 CONHCH(CH₃)), 1.48 (3H, d, *J* 7, CONHCH(CH₃)); δ_C (75 MHz, DMSO- d_6) 171.9 (CONHNH), 162.5 (CONH), 150.9 (*ipso*-Ar-C), 148.1 (*ipso*-Ar-C), 136.6 (*ipso*-Ar-C), 130.6 (Ar-C), 127.9 (Ar-C), 122.1 (Ar-C), 121.0 (Ar-C), 120.7 (Ar-C), 114.9 (Ar-C), 111.2 (Ar-C), 49.2 (CONHCH(CH₃)), 17.4 (CONHCH(CH₃)); m/z (ES⁺) 452 ([⁷⁹Br]MH⁺) 454 ([⁸¹Br]MH⁺); HRMS (ES⁺) found [⁷⁹Br] MH⁺, 452.2200 (C₁₆H₁₅⁷⁹BrN₅O₆ requires 452.0260);

(S)-N-(1-(2-(4-bromophenyl)hydrazineyl)-1-oxopropan-2-yl)-3,5-dinitrobenzamide 85d

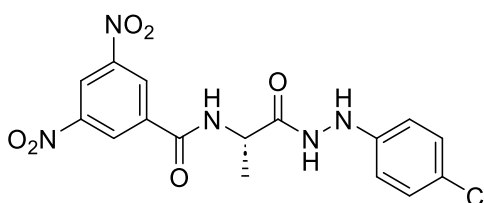


Following the general standard procedure, *tert*-butyl (S)-(1-(2-(4-bromophenyl)hydrazineyl)-1-oxopropan-2-yl)carbamate **62e** (0.10 g, 0.27 mmol) was transformed following trituration with Et₂O to produce the above compound (0.04 g, 37 %); R_f 0.56 (*n*-hexane/EtOAc) [2:1]; m.p. 107 - 109 °C; ν_{max} 3238, 1640, 1593, 1487, 1342, 1284, 1230, 1055, 959, cm^{-1} ; δ_H (300 MHz, DMSO- d_6)

Chapter 5. Experimental section.

10.01 (1H, d, J 3 CONHNH), 9.44 (1H, d, J 7, CONH), 9.13 (2H, d, J 2, Ar-H), 8.99 (1H, d, J 2, Ar-H), 7.98 (1H, d, J 2, CONHNH), 7.29 (2H, d, J 9, Ar-H), 6.70 (2H, d, J 8.8, Ar-H), 4.58 (1H, p, J 8, CONHCH(CH₃)), 1.47 (3H, d, J 7, CONHCH(CH₃)); δ_c (75 MHz, DMSO-d₆) 171.8 (CONHNH), 161.1 (CONH), 148.7 (*ipso*-Ar-C), 148.1 (*ipso*-Ar-C), 136.7 (*ipso*-Ar-C), 131.3 (Ar-C), 128.0 (Ar-C), 121.0 (Ar-C), 114.2 (Ar-C), 109.3 (*ipso*-Ar-C), 48.7 (CONHCH(CH₃)), 17.6 (CONHCH(CH₃)); m/z (ES⁺) 452 ([⁷⁹Br]MH⁺) 454 ([⁸¹Br]MH⁺); HRMS (ES⁺) found [⁷⁹Br]MH⁺, 452.2200 (C₁₆H₁₅⁷⁹BrN₅O₆ requires 452.0206);

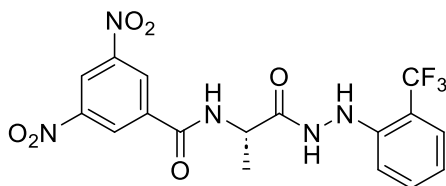
(S)-N-(1-(2-(4-chlorophenyl)hydrazineyl)-1-oxopropan-2-yl)-3,5-dinitrobenzamide 85a



Following the general standard procedure, *tert*-butyl (S)-(1-(2-(4-chlorophenyl)hydrazineyl)-1-oxopropan-2-yl)carbamate **62d** (0.12 g, 0.38 mmol) was transformed following trituration with Et₂O to produce the above compound (0.09 g, 56 %); R_f 0.34 (*n*-hexane/EtOAc) [3:1]; m.p. 100 - 102 °C; ν_{\max} 3302, 1635, 1536, 1487, 1341, 1284, 1230, 1055, 959 cm⁻¹; δ_H (300 MHz, DMSO-d₆) 10.00 (1H, d, J 3 CONHNH), 9.44 (1H, d, J 7, CONH), 9.13 (2H, d, J 2, Ar-H), 8.99 (1H, d, J 2, Ar-H), 7.98 (1H, d, J 2, CONHNH), 7.29 (2H, d, J 9, Ar-H), 6.70 (2H, d, J 8.8, Ar-H), 4.58 (1H, p, J 8, CONHCH(CH₃)), 1.47 (3H, d, J 7, CONHCH(CH₃)); δ_c (75 MHz, DMSO-d₆) 171.9 (CONHNH), 162.5 (CONH), 149.1 (*ipso*-Ar-C), 148.5 (*ipso*-Ar-C), 136.7 (*ipso*-Ar-C), 131.7 (Ar-C), 128.4 (Ar-C), 127.9 (Ar-C), 121.7 (Ar-C), 121.0 (Ar-C), 113.6 (*ipso*-Ar-C), 48.7 (CONHCH(CH₃)), 17.6 (CONHCH(CH₃)), m/z (ES⁺) 408 ([³⁵Cl]MH⁺), 410 ([³⁷Cl]MH⁺); HRMS (ES⁺) Found [³⁵Cl]MH⁺, 408.0000 (C₁₆H₁₅³⁵ClN₅O₆ require 408.0711);

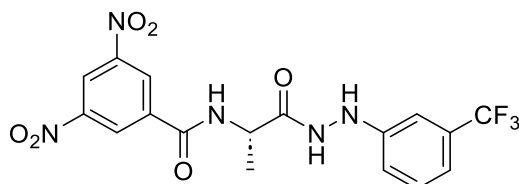
Chapter 5. Experimental section.

(S)-3,5-dinitro-N-(1-oxo-1-(2-(2-(trifluoromethyl)phenyl)hydrazineyl)propan-2-yl)benzamide 85e



Following the general standard procedure, *tert*-butyl (S)-(1-oxo-1-(2-(2-(trifluoromethyl)phenyl)hydrazineyl)propan-2-yl)carbamate **62B** (0.10 g, 0.29 mmol) was transformed following trituration with Et₂O to produce the above compound (0.03 g, 21 %); R_f 0.29 (*n*-hexane/EtOAc) [4:1]; m.p. 98 - 100 °C; ν_{\max} 3272, 1639, 1503, 1459, 1342, 1286, 1127, 1035, 940, 755, 645, cm⁻¹; δ_{H} (300 MHz, DMSO-d₆) 10.18 (1H, d, *J* 2, CONHNH), 9.48 (1H, d, *J* 7, CONH), 9.15 (2H, d, *J* 2, Ar-H), 8.99 (1H, t, *J* 2, Ar-H), 7.35 (1H, bs, CONHNH), 7.49 – 7.43 (2H, m, Ar-H), 7.03 (1H, d, *J* 8, Ar-H), 6.87 (1H, t, *J* 8, Ar-H), 4.62 (1H, p, *J* 7, CONHCH(CH₃)), 1.50 (3H, d, *J* 7, CONHCH(CH₃)).; δ_{C} (75 MHz, DMSO-d₆) 172.2 (CONHNH), 163.0 (CONH), 148.5 (*ipso*-Ar-C), 146.6 (*ipso*-Ar-C), 137.1 (*ipso*-Ar-C), 133.8 (Ar-C), 128.4 (Ar-C), 126.4 (Ar-C), 123.0 (*ipso*-Ar-CCF₃), 121.4 (Ar-C), 118.6 (Ar-C), 113.6 (*ipso*-Ar-C), 49.2 (CONHCH(CH₃)), 17.9 (CONHCH(CH₃)). δ_{F} (282 MHz, DMSO-d₆) -59.30 (3F, s, CF₃); *m/z* (ES⁺) 442 (MH⁺); HRMS (ES⁺) found MH⁺, 442.0731 (C₁₇H₁₅F₃N₅O₆ requires 442.0974);

(S)-3,5-dinitro-N-(1-oxo-1-(2-(3-(trifluoromethyl)phenyl)hydrazineyl)propan-2-yl)benzamide 85f

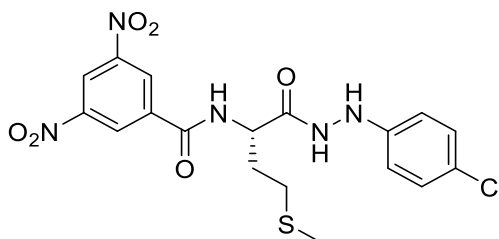


Following the general standard procedure, *tert*-butyl (S)-(1-oxo-1-(2-(3-(trifluoromethyl)phenyl)hydrazineyl)propan-2-yl)carbamate **62c** (0.10 g, 0.29 mmol) was transformed following trituration with Et₂O to produce the above compound (0.06 g, 43 %); R_f 0.32 (*n*-hexane/EtOAc) [4:1]; m.p. 103 - 105 °C; ν_{\max}

Chapter 5. Experimental section.

3280, 1638, 1540, 1344, 1127, 1070, 920, 785 cm^{-1} ; δ_{H} (300 MHz, DMSO- d_6) 10.11 (1H, d, J 2, CONHNNH), 9.48 (1H, d, J 7, CONH), 9.15 (2H, d, J 2, Ar-H), 8.99 (1H, t, J 2, Ar-H), 8.25 (1H, d, J 2, CONHNNH), 7.36 (1H, t, J 8, Ar-H), 7.06 – 6.94 (3H, m, Ar-H), 4.57 (1H, p, J 7, CONHCH(CH_3)), 1.49 (3H, d, J 7, CONHCH(CH_3)). δ_{C} (75 MHz, DMSO- d_6) 172.5 (CONHNNH), 163.0 (CONH), 150.4 (*ipso*-Ar-C), 148.6 (*ipso*-Ar-C), 137.0 (*ipso*-Ar-C), 130.2 (Ar-C), 128.4 (Ar-C), 121.5 (Ar-C), 115.3 (*ipso*-Ar- CCF_3), 108 (Ar-C), 49.3 (CONHCH(CH_3)), 17.8 (CONHCH(CH_3)); δ_{F} (282 MHz, DMSO- d_6) -61.35 (3F, s, CF_3); m/z (ES^+) 442 (MH^+); HRMS (ES^+) found MH^+ , 442.0734 ($\text{C}_{17}\text{H}_{15}\text{F}_3\text{N}_5\text{O}_6$ requires 442.0930);

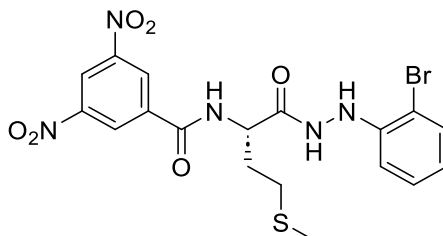
(S)-N-(1-(2-(4-chlorophenyl)hydrazineyl)-4-(methylthio)-1-oxobutan-2-yl)-3,5-dinitrobenzamide 88a



Following the general standard procedure, *tert*-butyl (S)-1-(2-(4-chlorophenyl)hydrazineyl)-4-(methylthio)-1-oxobutan-2-yl)carbamate **63d** (0.10 g, 0.28 mmol) was transformed following flush column chromatography using DCM/EtOH [200:4] produce the tilted compound as light yellow solid (0.09 g, 68 %); R_f 0.56 (DCM/EtOH/ NH_3) [200:3:1]; m.p. 90 - 92°C; ν_{max} 3269, 1654, 1537, 1478, 1341, 1320, 1073, 915, 822 cm^{-1} ; δ_{H} (300 MHz, DMSO- d_6) 10.10 (1H, d, J 3, CONHNNH), 9.43 (1H, d, J 7, CONH), 9.15 (2H, d, J 2, Ar-H), 8.99 (1H, t, J 2, Ar-H), 8.00 (1H, d, J 3, CONHNNH), 7.28 (2H, d, J 9, Ar-H), 6.69 (2H, d, J 9, Ar-H), 4.72 – 4.63 (1H, m, CONHCH($\text{CH}_2\text{CH}_2\text{SCH}_3$)) – 2.51 (2H, m, CONHCH($\text{CH}_2\text{CH}_2\text{SCH}_3$)), 2.10 (5H, m, CONHCH($\text{CH}_2\text{CH}_2\text{SCH}_3$)). δ_{C} (75 MHz, DMSO- d_6) 171.3 (CONHNNH), 163.3 (CONH), 149.1 (*ipso*-Ar-C), 148.5 (*ipso*-Ar-C), 137.1 (*ipso*-Ar-C), 131.7 (*ipso*-Ar-C), 128.5 (Ar-C), 121.4 (Ar-C), 114.6 (Ar-C), 109.8 (*ipso*-Ar-C), 52.7, (CONHCH($\text{CH}_2\text{CH}_2\text{SCH}_3$)), 31.3 ((CONHCH($\text{CH}_2\text{CH}_2\text{SCH}_3$)), 30.4 (CONHCH($\text{CH}_2\text{CH}_2\text{SCH}_3$)), 15.1 (CONHCH($\text{CH}_2\text{CH}_2\text{SCH}_3$)); m/z (ES^+) 468 ($[^{35}\text{Cl}]\text{MH}^+$) 470 ($[^{37}\text{Cl}]\text{MH}^+$); HRMS (ES^+) found $[^{35}\text{Cl}]\text{MH}^+$, 468.0760 ($\text{C}_{18}\text{H}_{19}^{35}\text{ClN}_5\text{O}_6\text{S}$ requires 468.0745);

Chapter 5. Experimental section.

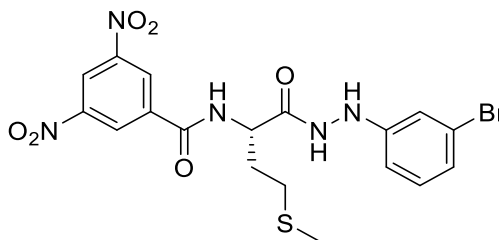
(S)-N-(1-(2-(2-bromophenyl)hydrazineyl)-4-(methylthio)-1-oxobutan-2-yl)-3,5-dinitrobenzamide 88b



Following the general standard procedure, *tert*-butyl (S)-(1-(2-(2-bromophenyl)hydrazineyl)-4-(methylthio)-1-oxobutan-2-yl)carbamate **63A** (0.20 g, 0.48 mmol) was transformed following trituration with Et₂O to produce the above compound as light orange solid (0.12 g, 49 %); R_f 0.23 (DCM/EtOH) [200:3]; m.p. 125 - 126 °C; ν_{\max} 3260, 1644, 1593, 1430, 1312, 1226, 1163, 1023, 915 cm⁻¹; δ_{H} (300 MHz, DMSO-d₆) 10.24 (1H, d, *J* 2, CONHNH), 9.44 (1H, d, *J* 7, CONH), 9.15 (2H, d, *J* 2, Ar-*H*), 8.98 (1H, d, *J* 2, Ar-*H*), 7.44 (1H, d, *J* 8, CONHNH), 7.28 (1H, s, Ar-*H*), 7.21 (1H, t, *J* 8, Ar-*H*), 6.85 – 6.81 (1H, m, Ar-*H*), 6.70 (1H, t, *J* 8, Ar-*H*), 4.69 (1H, q, *J* 8, CONHCH(CH₂CH₂SCH₃)), 2.62 (2H, m, CONHCH(CH₂CH₂SCH₃)), 2.10 (5H, m, CONHCH(CH₂CH₂SCH₃)); δ_{C} (75 MHz, DMSO-d₆) 170.8 (CONHNH), 162.9 (CONH), 148.1 (*ipso*-Ar-C), 145.5 (*ipso*-Ar-C), 136.6 (*ipso*-Ar-C), 132.3 (Ar-C) 128.3 (Ar-C), 128.0 (Ar-C), 121.0 (Ar-C), 120.2 (Ar-C), 113.0 (Ar-C), 107.0 (*ipso*-Ar-C), 52.3 (CONHCH(CH₂CH₂SCH₃)), 30.8 (CONHCH(CH₂CH₂SCH₃)), 29.8 (CONHCH(CH₂CH₂SCH₃)), 14.1 (CONHCH(CH₂CH₂SCH₃)); *m/z* (ES⁺) 512 ([⁷⁹Br]MH⁺) 514 ([⁸¹Br]MH⁺); HRMS (ES⁺) found [⁷⁹Br] MH⁺ 512.0204, (C₁₈H₁₉⁷⁹BrN₅O₆S requires 512.0239);

Chapter 5. Experimental section.

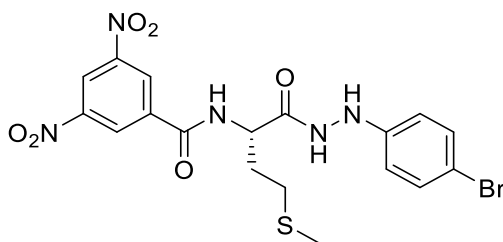
(S)-N-(1-(2-(3-bromophenyl)hydrazineyl)-4-(methylthio)-1-oxobutan-2-yl)-3,5-dinitrobenzamide 88c



Following the general standard procedure, *tert*-butyl (S)-(1-(2-(3-bromophenyl)hydrazineyl)-4-(methylthio)-1-oxobutan-2-yl)carbamate **63b** (0.10 g, 0.25 mmol) was transformed following trituration with Et₂O to produce the above compound as light orange solid (0.09 g, 69 %); R_f 0.32 (DCM/EtOH/NH₃) [200:3:1]; m.p. 127 - 129 °C; ν_{\max} 3259, 3071, 1649, 1640, 1596, 1536, 1476, 1341, 1340, 1320, 1076, 1041, 918, 847 cm⁻¹; δ_{H} (300 MHz, DMSO-d₆) 10.12 (1H, s, CONHNH), 9.44 (1H, d, *J* 7, CONH), 9.15 (2H, d, *J* 2, Ar-*H*), 8.99 (1H, dd, *J* 2, Ar-*H*), 8.10 (1H, s, CONHNH), 7.15 (1H, t, *J* 8, Ar-*H*), 6.78–6.62 (3H, m, Ar-*H*), 4.68 (1H, m, CONHCH(CH₂CH₂SCH₃)), 2.74–2.53 (2H, m, CONHCH(CH₂CH₂SCH₃)), 2.19–2.04 (5H, m, CONHCH(CH₂CH₂SCH₃)); δ_{C} (75 MHz, DMSO-d₆) 171.8 (CONHNH), 170.0 (CONH), 151.4 (*ipso*-Ar-C), 131.1 (Ar-C), 128.5 (Ar-C), 122.5 (Ar-C), 121.2 (Ar-C), 114.8 (Ar-C), 111.6 (Ar-C), , 51.8 (CONHCH(CH₂CH₂SCH₃)), 30.1 (CONHCH(CH₂CH₂SCH₃)), 23.0 (CONHCH(CH₂CH₂SCH₃)), 15.1 (CONHCH(CH₂CH₂SCH₃)); *m/z* (ES⁺) 512 ([⁷⁹Br]MH⁺) 514 ([⁸¹Br]MH⁺); HRMS (ES⁺) found [⁷⁹Br] MH⁺ 512.0204, (C₁₈H₁₉⁷⁹BrN₅O₆S requires 512.0239);

Chapter 5. Experimental section.

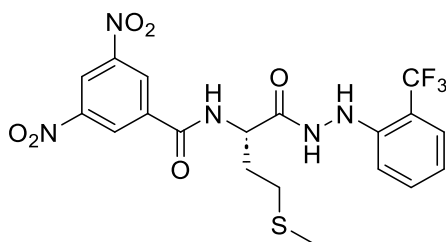
(S)-N-(1-(2-(4-bromophenyl)hydrazineyl)-4-(methylthio)-1-oxobutan-2-yl)-3,5-dinitrobenzamide 88d



Following the general standard procedure, *tert*-butyl (S)-(1-(2-(3-bromophenyl)hydrazineyl)-4-(methylthio)-1-oxobutan-2-yl)carbamate **63e** (0.10 g, 0.24 mmol) was transformed following trituration with Et₂O to produce the title compound as light orange solid (0.09 g, 69 %); R_f 0.32 (DCM/EtOH/NH₃) [200:3:1]; m.p. 90 - 92°C; ν_{\max} 3269, 1654, 1537, 1478, 1341, 1320, 1073, 915, 822 cm⁻¹; δ_{H} (300 MHz, DMSO-d₆) 10.10 (1H, d, *J* 3, CONHNH), 9.43 (1H, d, *J* 7, CONH), 9.15 (2H, d, *J* 2, Ar-H), 8.99 (1H, t, *J* 2, Ar-H), 8.00 (1H, d, *J* 3, CONHNH), 7.28 (2H, d, *J* 9, Ar-H), 6.69 (2H, d, *J* 9, Ar-H), 4.72 – 4.63 (1H, m, CONHCH(CH₂CH₂SCH₃)) – 2.51 (2H, m, CONHCH(CH₂CH₂SCH₃)), 2.10 (5H, m, CONHCH(CH₂CH₂SCH₃)). δ_{C} (75 MHz, DMSO-d₆) 171.3 (CONHNH), 163.3 (CONH), 149.1 (*ipso*-Ar-C), 148.5 (*ipso*-Ar-C), 137.1 (*ipso*-Ar-C), 131.7 (*ipso*-Ar-C), 128.5 (Ar-C), 121.4 (Ar-C), 114.6 (Ar-C), 109.8 (*ipso*-Ar-C), 52.7, (CONHCH(CH₂CH₂SCH₃)), 31.3 ((CONHCH(CH₂CH₂SCH₃)), 30.4 (CONHCH(CH₂CH₂SCH₃)), 15.1 (CONHCH(CH₂CH₂SCH₃)), *m/z* (ES⁺) 512 ([⁷⁹Br]MH⁺) 512 ([⁸¹Br]MH⁺) 514; HRMS (ES⁺) found [⁷⁹Br] MH⁺ 512.0249, (C₁₈H₁₉⁷⁹BrN₅O₆S requires 512.0239);

Chapter 5. Experimental section.

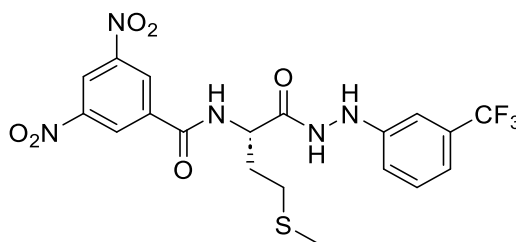
(S)-N-(4-(methylthio)-1-oxo-1-(2-phenylhydrazineyl)butan-2-yl)-3,5-dinitrobenzamide 88e



Following the general standard procedure, *tert*-butyl (S)-4-(4-(methylthio)-1-oxo-1-(2-(2-(trifluoromethyl)phenyl)hydrazineyl)butan-2-yl)carbamate **63B** (0.13 g, 0.31 mmol) was transformed following trituration with Et₂O to produce the above compound as light yellow solid (0.05 g, 35 %); R_f 0.34 (DCM/EtOH) [200:3]; m.p. 128 - 130 °C; ν_{\max} 3281, 1640, 1592, 1485, 1071, 914, 820, 700 cm⁻¹; δ_{H} (300 MHz, DMSO-d₆) 10.25 (1H, d, *J* 2., CONH₂), 9.45 (1H, d, *J* 7, CONH), 9.16 (2H, d, *J* 2. Ar-*H*), 8.99 (1H, t, *J* 2, Ar-*H*), 7.57 (1H, d, *J* 2, CONH₂), 7.53 – 7.40 (1H, m, Ar-*H*), 7.02 (1H, d, *J* 8, Ar-*H*), 6.87 (1H, t, *J* 8, Ar-*H*), 4.70 (1H, m, CONHCHCH₂CH₂(SCH₃)), 2.76 – 2.51 (2H, m, CONHCHCH₂CH₂(SCH₃)), 2.21 – 2.13 (5H, m, CONHCHCH₂CH₂(SCH₃)); δ_{C} (75 MHz, DMSO-d₆) 171.3 (CONH₂), 163.5 (CONH), 148.5 (*ipso*-Ar-C), 146.5 (*ipso*-Ar-C), 137.1 (*ipso*-Ar-C), 133.8 (Ar-C), 128.5 (Ar-C), 126.8 (Ar-C), 126.0 (*ipso*-Ar-CCF₃), 121.5 (Ar-C), 118.6 (Ar-C), 113.5 (Ar-C), 112.4 (*ipso*-Ar-C), 52.8 (NHCH(CH₂CH₂SCH₃)), 31.2 (NHCH(CH₂CH₂SCH₃)), 30.3 (CONHCH(CH₂CH₂SCH₃)), 15.0 (NHCH(CH₂CH₂SCH₃)); δ_{F} (282 MHz, DMSO-d₆) -60.75 (3F, s, CF₃); *m/z* (ES⁺) 502 (MH⁺); HRMS (ES⁺) found MH⁺, 502.1000 (C₁₉H₁₉F₃N₅O₆S requires 502.1008);

Chapter 5. Experimental section.

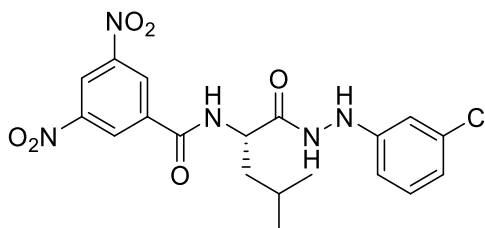
(S)-N-(4-(methylthio)-1-oxo-1-(2-(3-(trifluoromethyl)phenyl)hydrazineyl)butan-2-yl)-3,5-dinitrobenzamide 88f



Following the general standard procedure, *tert*-butyl (S)-4-(4-(methylthio)-1-oxo-1-(2-(3-(trifluoromethyl)phenyl)hydrazineyl)butan-2-yl)carbamate **63c** (0.12 g, 0.28 mmol) was transformed following trituration with DCM to produce the above compound as an yellowish white solid (0.09 g, 62 %); R_f 0.45 (n-hexane/EtOAc) [4:1]; m.p. 128 - 130 °C; ν_{max} 3281, 1640, 1592, 1485, 1071, 914, 820, 700 cm^{-1} ; δ_H (300 MHz, DMSO- d_6) 10.20 (1H, d, J 3, CONHNH), 9.46 (1H, d, J 7, CONH), 9.15 (2H, d, J 2, Ar-H), 8.99 (1H, t, J 2, Ar-H), 8.26 (1H, s, CONHNH), 7.36 (1H, t, J 8, Ar-H), 7.01 (3H, d, J 7, Ar-H), 4.66 (1H, q, J 7, CONHCH(CH₂CH₂SCH₃)), 2.70 - 2.55 (2H, m, CONHCH(CH₂CH₂SCH₃)), 2.10 (5H, m, CONHCH(CH₂CH₂SCH₃)). δ_C (75 MHz, DMSO- d_6) 171.5 (CONHNH), 163.4 (CONH), 150.3 (*ipso*-Ar-C), 148.6 (*ipso*-Ar-C), 136.9 (*ipso*-Ar-C), 130.2 (Ar-C), 128.4 (Ar-C), 121.5 (Ar-C), 116.3 (Ar-C), 52.8 (CONHCH(CH₂CH₂SCH₃)), 31.1 ((CONHCH(CH₂CH₂SCH₃)), 30.3 (CONHCH(CH₂CH₂SCH₃)), 15.02 ((CONHCH(CH₂CH₂SCH₃)); δ_F (282 MHz, DMSO- d_6) -59.29 (3F, s, CF₃); m/z (ES⁺) 502 (MH⁺); HRMS (ES⁺) found MH⁺, 502.1000 (C₁₉H₁₉F₃N₅O₆S requires 502.1008);

Chapter 5. Experimental section.

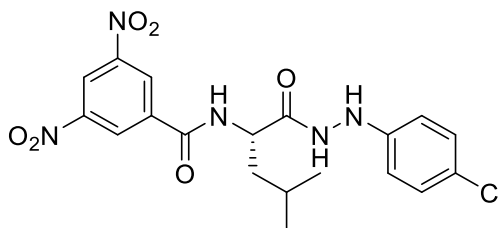
(S)-N-(1-(2-(3-chlorophenyl)hydrazineyl)-4-methyl-1-oxopentan-2-yl)-3,5-dinitrobenzamide 87a



Following the general standard procedure, *tert*-butyl (S)-(1-(2-(3-chlorophenyl)hydrazineyl)-4-methyl-1-oxopentan-2-yl)carbamate **64a** (0.13 g, 0.37 mmol) was transformed following trituration with Et₂O produce the above compound as white yellowish solid (0.08 g, 46 %); R_f 0.56 (*n*-hexane/EtOAc) [2:1]; m.p. 90 - 92 °C; ν_{\max} 3247, 1665, 1537, 1470, 1340, 1320, 1082, 916 cm⁻¹; δ_{H} (300 MHz, DMSO-d₆) 10.23 (1H, d, *J* 2, CONH₂), 9.42 (1H, d, *J* 7, CONH), 9.17 (2H, d, *J* 2, Ar-H), 8.99 (1H, t, *J* 2, Ar-H), 8.10 (1H, d, *J* 2, CONH₂), 7.08 (1H, t, *J* 8, Ar-H), 6.90 (1H, t, *J* 2, Ar-H), 6.89 – 6.79 (1H, m, Ar-H), 6.76 – 6.65 (1H, m, Ar-H), 4.68 – 4.55 (1H, m, CONHCH(CH₂CH(CH₃)₂)), 1.87 – 1.61 (2H, m, CONHCH(CH₂CH₂)₃), 0.99 (3H, d, *J* 6, CONHCH(CH₂CH₂)₃), 0.93 (3H, d, *J* 6, CONHCH(CH₂CH₂)₃); δ_{C} (75 MHz, DMSO-d₆) 172.1 (CONH₂), 163.1 (CONH), 148.6 (*ipso*-Ar-C), 136.9 (*ipso*-Ar-C), 130.4 (Ar-C), 130.1 (*ipso*-Ar-C), 129.0 (Ar-C), 128.4 (Ar-C), 126.7 (Ar-C), 121.5 (Ar-C), 116.4 (Ar-C), 115.0 (Ar-C), 108.3 (*ipso*-Ar-C), 51.9 (CONHCH(CH₂CH(CH₃)₂)), 24.8 ((CONHCH(CH₂CH(CH₃)₂)), 23.2 ((CONHCH(CH₂CH(CH₃)₂)), 22.0 ((CONHCH(CH₂CH(CH₃)₂)); *m/z* (ES⁺) 450 ([³⁵Cl]MH⁺) 452 ([³⁷Cl]MH⁺); HRMS (ES⁺) found [³⁵Cl] MH⁺, 450.1165 (C₁₉H₂₁³⁵ClN₅O₆ requires 450.1180);

Chapter 5. Experimental section.

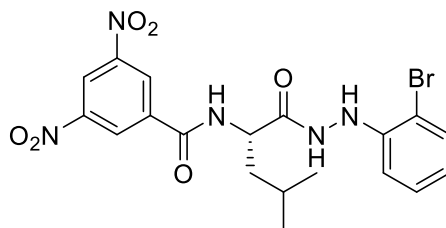
(S)-N-(1-(2-(4-chlorophenyl)hydrazineyl)-4-methyl-1-oxopentan-2-yl)-3,5-dinitrobenzamide 87b



Following the general standard procedure, *tert*-butyl (S)-(1-(2-(4-chlorophenyl)hydrazineyl)-4-methyl-1-oxopentan-2-yl)carbamate **64d** (0.09 g, 0.23 mmol) was transformed following trituration with Et₂O to afford the titled compound as faint yellow solid (0.07 g, 62 %); R_f 0.34 (DCM/EtOH) [2:/0.6]; m.p. 90 - 92 °C; ν_{\max} 3081, 1639 1530, 1490, 1320, 1087, 916, 818 cm⁻¹; δ_{H} (300 MHz, DMSO-d₆) 10.17 (1H, d, *J* 3, CONH₂NH), 9.46 (1H, d, *J* 8, CONH), 9.21 (2H, d, *J* 2, Ar-H), 9.05 (1H, t, *J* 2, Ar-H), 8.05 (1H, d, *J* 3, Ar-H), 7.29 (2H, d, *J* 8, Ar-H), 6.89 – 6.73 (2H, d *J* 8, Ar-H), 4.75 – 4.62 (1H, m, CONHCH(CH₂CH(CH₃)₂)), 1.95 – 1.64 (3H, m, CONHCH(CH₂CH(CH₃)₂)), 1.04 (3H, d, *J* 6, CONHCH(CH₂CH(CH₃)₂)), 0.98 (3H, d, *J* 6.0, CONHCH(CH₂CH(CH₃)₂)); δ_{C} (75 MHz, DMSO-d₆) 172 (CONH₂NH), 163.1 (CONH), 148.7 (*ipso*-Ar-H), 148.6 (*ipso*-Ar-H), 137.2 (*ipso*-Ar-H), 128.9 (Ar-H), 128.4 (Ar-H), 122.2 (*ipso*-Ar-H), 121.5 (Ar-H), 114.1 (Ar-H), 51.7 (CONHCH(CH₂CH(CH₃)₂)), 24.8 (CONHCH(CH₂CH(CH₃)₂)), 23.4 (CONHCH(CH₂CH(CH₃)₂)), 21.9 (CONHCH(CH₂CH(CH₃)₂)); *m/z* (ES⁺) 450 ([³⁵Cl]MH⁺) 452 ([³⁷Cl]MH⁺); HRMS (ES⁺) found [³⁵Cl] MH⁺, 450.1165 (C₁₉H₂₁³⁵ClN₅O₆ requires 450.1180);

Chapter 5. Experimental section.

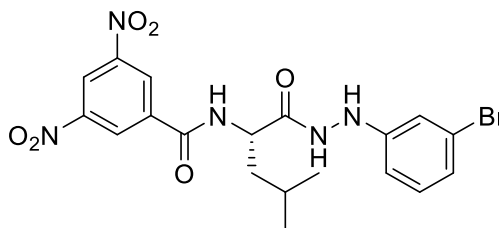
(S)-N-(1-(2-(2-bromophenyl)hydrazineyl)-4-methyl-1-oxopentan-2-yl)-3,5-dinitrobenzamide 87c



Following the general standard procedure, *tert*-butyl (S)-(1-(2-(2-bromophenyl)hydrazineyl)-4-methyl-1-oxopentan-2-yl)carbamate **64A** (0.10 g, 0.25 mmol) was transformed following flush column chromatography to produce the titled compound as faint yellow solid (0.09 g, 63 %); R_f 0.53 (DCM/EtOH/NH₃) [2:/0.6/0.01]; m.p. 90 - 93 °C; ν_{\max} 3259, 1644, 1536, 1341, 1076, 1022, 915, 747 cm⁻¹; δ_H (300 MHz, DMSO-d₆) 10.27 (1H, d, J 3, CONHNH), 9.42 (1H, d, J 8, CONH), 9.16 (2H, d, J 2, Ar-H), 8.98 (1H, t, J 2, Ar-H), 7.44 (1H, dd, J 8, 1, Ar-H), 7.26 (1H, d, J 3, CONHNH), 7.21 (1H, t, J 7, Ar-H), 6.82 (1H, dd, J 8, 2, Ar-H), 6.70 (1H, td, J 8, 2, Ar-H), 4.75 – 4.60 (1H, m, CONHCH(CH₂CH(CH₃)₂)), 1.91 – 1.60 (3H, m, CONHCH(CH₂CH(CH₃)₂)), 0.96 (6H, dd, J 16, 6, CONHCH(CH₂CH(CH₃)₂)); δ_C (75 MHz, DMSO-d₆) 171.9 (CONHNH), 163.2 (CONH), 148.6 (*ipso*-Ar-C), 146.0 (*ipso*-Ar-C), 137.0 (*ipso*-Ar-C), 132.8 (Ar-C), 128.8 (Ar-C), 128.4 (Ar-C), 121.5 (Ar-C), 120.7 (*ipso*-Ar-C), 113.6 (Ar-C), 107.4 (Ar-C), 51.7 (CONHCH(CH₂CH(CH₃)₂)), 24.8 (CONHCH(CH₂CH(CH₃)₂)), 23.4 (CONHCH(CH₂CH(CH₃)₂)), 21.9 (CONHCH(CH₂CH(CH₃)₂)); m/z (ES⁺) 494 ([⁷⁹Br]MH⁺) 496 ([⁸¹Br]MH⁺); HRMS (ES⁺) found [⁷⁹ Br] MH⁺, 494.0652 (C₁₉H₂₁⁷⁹BrN₅O₆ requires 494.0675);

Chapter 5. Experimental section.

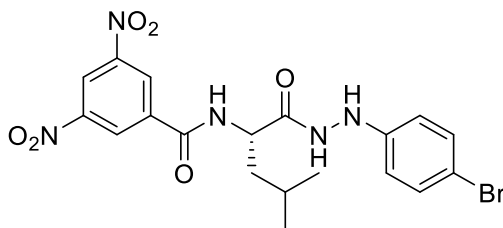
(S)-N-(1-(2-(3-bromophenyl)hydrazineyl)-4-methyl-1-oxopentan-2-yl)-3,5-dinitrobenzamide 87d



Following the general standard procedure, *tert*-butyl (S)-(1-(2-(3-bromophenyl)hydrazineyl)-4-methyl-1-oxopentan-2-yl)carbamate **64b** (0.10 g, 0.25 mmol) was transformed following trituration with Et₂O produce the above compound as white yellowish solid (0.06 g, 52 %); R_f 0.56 (DCM/EtOH/NH₃) [200:3:1]; m.p. 100-102 °C; ν_{\max} 3247, 1665, 1537, 1470, 1340, 1320, 1082, 916 cm⁻¹; δ_{H} (300 MHz, DMSO-d₆) 10.14 (1H, d, *J* 3, CONH₂), 9.42 (1H, d, *J* 7, CONH), 9.17 (2H, d, *J* 2, Ar-H), 8.99 (1H, t, *J* 2, Ar-H), 8.10 (1H, d, *J* 3, CONH₂), 7.08 (1H, t, *J* 8, Ar-H), 6.90 (1H, t, *J* 2, Ar-H), 6.89 – 6.79 (1H, m, Ar-H), 6.76 – 6.65 (1H, m, Ar-H), 4.68 – 4.55 (1H, m, CONHCH(CH₂CH(CH₃)₂)), 1.87 – 1.61 (2H, m, CONHCH(CH₂CH(CH₃)₂)), 0.99 (3H, d, *J* 6, CONHCH(CH₂CH(CH₃)₂)), 0.93 (3H, d, *J* 6, CONHCH(CH₂CH(CH₃)₂)); δ_{C} (75 MHz, DMSO-d₆) 172.1 (CONH₂), 163.1 (CONH), 148.6 (*ipso*-Ar-C), 136.9 (*ipso*-Ar-C), 130.4 (Ar-C), 130.1 (*ipso*-Ar-C), 129.0 (Ar-C), 128.4 (Ar-C), 126.7 (Ar-C), 121.5 (Ar-C), 116.4 (Ar-C), 115.0 (Ar-C), 108.3 (*ipso*-Ar-C), 51.9 (CONHCH(CH₂CH(CH₃)₂)), 24.8 ((CONHCH(CH₂CH(CH₃)₂)), 23.2 ((CONHCH(CH₂CH(CH₃)₂)), 22.0 ((CONHCH(CH₂CH(CH₃)₂)); *m/z* (ES⁺) 494 ([⁷⁹Br]MH⁺) 496 ([⁸¹Br]MH⁺); HRMS (ES⁺) found [⁷⁹Br] MH⁺, 494.0652 (C₁₉H₂₁⁷⁹BrN₅O₆ requires 494.0675);

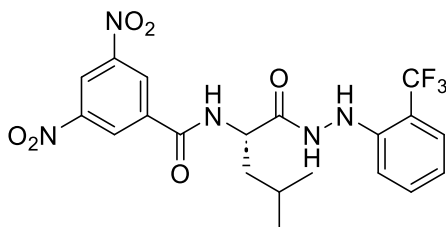
Chapter 5. Experimental section.

(S)-N-(1-(2-(4-bromophenyl)hydrazineyl)-4-methyl-1-oxopentan-2-yl)-3,5-dinitrobenzamide 87e



Following the general standard procedure, *tert*-butyl (S)-(1-(2-(4-bromophenyl)hydrazineyl)-4-methyl-1-oxopentan-2-yl)carbamate **64e** (0.09 g, 0.23 mmol) was transformed following trituration with Et₂O to produce the above compound as faint yellowish solid (0.07 g, 62 %); R_f 0.34 (DCM/EtOH) [200/6]; m.p. 90 - 92 °C; ν_{\max} 3266, 1643, 1533, 1354, 1170, 1095, 765, 646 cm⁻¹; δ_{H} (300 MHz, DMSO-d₆) 10.17 (1H, d, *J* 3, CONHNH), 9.46 (1H, d, *J* 8, CONH), 9.21 (2H, d, *J* 2, Ar-*H*), 9.05 (1H, t, *J* 2, Ar-*H*), 8.05 (1H, d, *J* 3, Ar-*H*), 7.29 (2H, d, *J* 8, Ar-*H*), 6.89 – 6.73 (2H, d *J* 8, Ar-*H*), 4.75 – 4.62 (1H, m, CONHCH(CH₂CH(CH₃)₂)), 1.95 – 1.64 (3H, m, CONHCH(CH₂CH(CH₃)₂)), 1.04 (3H, d, *J* 6, CONHCH(CH₂CH(CH₃)₂)), 0.98 (3H, d, *J* 6.0, CONHCH(CH₂CH(CH₃)₂)); δ_{C} (75 MHz, DMSO-d₆) 172 (CONHNH), 163.1 (CONH), 148.7 (*ipso*-Ar-*H*), 148.6 (*ipso*-Ar-*H*), 137.2 (*ipso*-Ar-*H*), 128.9 (Ar-*H*), 128.4 (Ar-*H*), 122.2 (*ipso*-Ar-*H*), 121.5 (Ar-*H*), 114.1 (Ar-*H*), 51.7 (CONHCH(CH₂CH(CH₃)₂)), 24.8 (CONHCH(CH₂CH(CH₃)₂)), 23.4 (CONHCH(CH₂CH(CH₃)₂)), 21.9 (CONHCH(CH₂CH(CH₃)₂)); *m/z* (ES⁺) 494 ([⁷⁹Br]MH⁺), 496 ([⁸¹Br]MH⁺); HRMS (ES⁺) found [⁷⁹Br] MH⁺, 494.0652 (C₁₉H₂₁⁷⁹BrN₅O₆ requires 494.0675);

(S)-N-(4-methyl-1-oxo-1-(2-(2-(trifluoromethyl)phenyl)hydrazineyl)pentan-2-yl)-3,5-dinitrobenzamide 87f

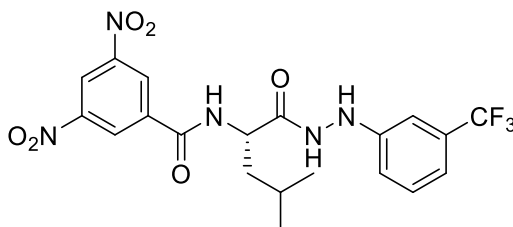


Following the general standard procedure, *tert*-butyl (S)-(4-methyl-1-oxo-1-(2-(2-(trifluoromethyl)phenyl)hydrazineyl)pentan-2-yl)carbamate **64B** (0.10 g, 0.26

Chapter 5. Experimental section.

mmol) was transformed following trituration with DCM to produce the titled compound as white yellowish solid (0.09 g, 70 %); R_f 0.56 (DCM/EtOH) [200:8]; m.p. 93 - 94 °C; ν_{max} 3276, 1668, 1593, 1455, 1323, 1155, 1075, 921, 743 cm^{-1} ; δ_H (300 MHz, DMSO- d_6) 10.20 (1H, d, J 2, CONHNH), 9.36 (1H, d, J 8, CONH), 9.09 (2H, d, J 2, Ar- H), 8.92 (1H, t, J 2, Ar- H), 7.49 (1H, s, CONHNH), 7.44 – 7.36 (2H, m, Ar- H), 4.68 – 4.54 (1H, m, CONHCH(CH₂CH(CH₃)₂)), 1.87 – 1.55 (3H, m, CONHCH(CH₂CH(CH₃)₂)), 0.89 (6H, dd, J 16, 6, CONHCH(CH₂CH(CH₃)₂)); δ_C (75 MHz, DMSO- d_6) 171.9 (CONHNH), 163.2 (CONH), 148.6 (*ipso*-Ar-C), 146.5 (*ipso*-Ar-C), 137.0 (*ipso*-Ar-C), 133.8 (Ar-C), 128.4 (Ar-C), 121.5 (*ipso*-Ar-CCF₃), 118.6 (Ar-C), 113.6 (*ipso*-Ar-C), 51.8 (CONHCH(CH₂CH(CH₃)₂)), 24.8 (CONHCH(CH₂CH(CH₃)₂)), 23.4 (CONHCH(CH₂CH(CH₃)₂)), 21.8 (CONHCH(CH₂CH(CH₃)₂)); δ_F (282 MHz, DMSO- d_6) -60.77 (3F, s, CF₃); m/z (ES⁺) 484 (MH⁺); HRMS (ES⁺) found MH⁺, 484.1451 (C₂₀H₂₁F₃N₅O₆ requires 484.1444);

(S)-N-(4-methyl-1-oxo-1-(2-(3-(trifluoromethyl)phenyl)hydrazineyl)pentan-2-yl)-3,5-dinitrobenzamide 87g

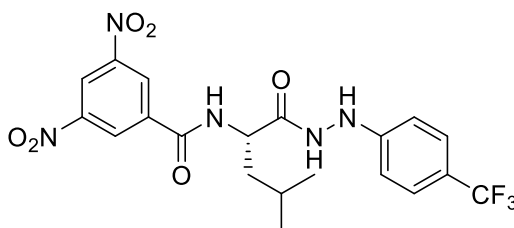


Following the general standard procedure, *tert*-butyl (S)-N-(4-methyl-1-oxo-1-(2-(3-(trifluoromethyl)phenyl)hydrazineyl)pentan-2-yl)carbamate **64c** (0.10 g, 0.26 mmol) was transformed following trituration with Et₂O produce the above compound as white yellowish solid (0.08 g, 46 %); R_f 0.43 (*n*-hexane/EtOAc) [1:2]; m.p. 90 - 92 °C; ν_{max} 3247, 1665, 1537, 1470, 1340, 1320, 1082, 916 cm^{-1} ; δ_H (300 MHz, DMSO- d_6) 10.14 (1H, d, J 2., CONHNH), 9.42 (1H, d, J 7, CONH), 9.16 (2H, d, J 2, Ar- H), 8.98 (1H, t, J 2, Ar- H), 8.11 (1H, d, J 2, CONHNH), 7.13 (1H, t, J 8, Ar- H), 6.74 (1H, t, J 2., Ar- H), 6.72 – 6.63 (2H, m, Ar- H), 4.69 – 4.56 (1H, m, CONHCH(CH₂CHCH₃)₂), 1.85 – 1.63 (3H, m, CONHCH(CH₂CHCH₃)₂), 0.96 (6H, dd, J 18, 6, CONHCH(CH₂CHCH₃)₂)); δ_C (75 MHz, DMSO- d_6) 172.0 (CONHNH) 163.2 (CONH), 151.3 (*ipso*-Ar-C)148.6

Chapter 5. Experimental section.

(*ipso*-Ar-C), 137.0 (*ipso*-Ar-C), 133.0 (Ar-C), 130.7 (*ipso*-Ar-C), 128.4 (Ar-C), 121.5 (Ar-C), 118.3 (Ar-C), 111.9 (Ar-C), 111.30 (*ipso*-Ar-C), 51.8 (CONHCH(CH₂CH(CH₃)₂)), 24.8 (CONHCH(CH₂CH(CH₃)₂)), 23.3 (CONHCH(CH₂CH(CH₃)₂)), 22.0 (CONHCH(CH₂CH(CH₃)₂)); *m/z* (ES⁺) 506 (M⁺Na⁺) 506; HRMS (ES⁺) found MNa⁺, 506.1256 (C₁₈H₁₉⁷⁹BrN₅O₆S requires 506.1258);

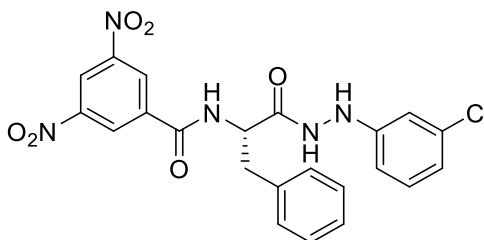
(S)-N-(4-methyl-1-oxo-1-(2-(4-(trifluoromethyl)phenyl)hydrazineyl)pentan-2-yl)-3,5-dinitrobenzamide 87h



Following the general standard procedure, *tert*-butyl (S)-(4-methyl-1-oxo-1-(2-(3-(trifluoromethyl)phenyl)hydrazineyl)pentan-2-yl)carbamate **64f** (0.10 g, 0.26 mmol) was transformed following trituration with Et₂O produce the above compound as white yellowish solid (0.08 g, 47 %); R_f 0.56 (DCM/EtOH) [2: 0.6]; m.p. 93 - 94 °C; ν_{\max} 1640, 1536, 1486, 1342, 1282, 749, 719, 699, 510 cm⁻¹; δ_{H} (300 MHz, DMSO-d₆) 10.23 (1H, s, CONHNH), 9.43 (1H, d, *J* 8, CONH), 9.17 (2H, d, *J* 2, Ar-H), 8.99 (1H, t, *J* 2., Ar-H), 8.46 (1H, s, CONHNH), 7.47 (2H, d, *J* 9, Ar-H), 6.83 (2H, d, *J* 9, Ar-H), 4.67 (1H, m, CONHCH(CH₂CHCH₃)₂), 1.90 – 1.62 (3H, m, CONHCH(CH₂CHCH₃)₂), 0.97 (6H, dd, *J* 16, 6, CONHCH(CH₂CHCH₃)₂); δ_{C} (75 MHz, DMSO-d₆) 172.1 (CONHNH), 163.1 (CONH), 152.8 (*ipso*-Ar-C), 148.6 (*ipso*-Ar-C), 137.0 (*ipso*-Ar-C), 128.4 (Ar-C), 127.2 (Ar-C), 126.6 (Ar-C), 121.4 (Ar-C), 118.8 (Ar-C), 118.5 (Ar-C), 111.9 (Ar-C), 51.8 (CONHCH(CH₂CH(CH₃)₂)), 24.8 (CONHCH(CH₂CH(CH₃)₂)), 23.4 (CONHCH(CH₂CH(CH₃)₂)), 21.83 (CONHCH(CH₂CH(CH₃)₂)); *m/z* (ES⁺) 484 (MH⁺); HRMS (ES⁺) found MH⁺, 848.1423 (C₂₀H₂₁F₃N₅O₆ requires 848.1444);

Chapter 5. Experimental section.

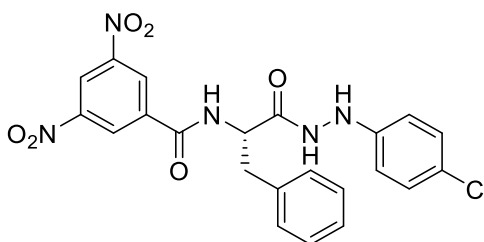
(S)-N-(1-(2-(3-chlorophenyl)hydrazineyl)-1-oxo-3-phenylpropan-2-yl)-3,5-dinitrobenzamide 86a



Following the general standard procedure, *tert*-butyl (S)-(1-(2-(3-chlorophenyl)hydrazineyl)-1-oxo-3-phenylpropan-2-yl)carbamate **66a** (0.12 g, 0.31 mmol) was transformed following flush column chromatography (DCM;EtOAc [3:1]) to produce the above compound as yellow solid (0.08 g, 54 %); R_f 0.50 (DCM/EtOH/NH₃ [200:6:1]); m.p. 110-112 °C; ν_{\max} 3227, 1672, 1641, 1538, 1341, 1076, 767, 699, 460 cm⁻¹; δ_H (300 MHz, DMSO-d₆) 10.16 (1H, s, CONHNH), 9.61 (1H, d, J 8, CONH), 9.06 (2H, d, J 2, Ar-H), 8.96 (1H, d, J 2, Ar-H), 7.31 (6H, m, Ar-H), 7.11 (1H, t, J 8, Ar-H), 6.74 – 6.66 (2H, m, Ar-H), 6.55 (1H, m, Ar-H), 4.93 – 4.82 (1H, m, CONHCH(CH₂Phe)), 3.23 – 3.11 (2H, m, CONHCH(CH₂Phe)); δ_C (75 MHz, DMSO-d₆) 171.1 (CONHNH), 163.1 (CONH), 151.1 (*ipso*-Ar-C), 148.6 (*ipso*-Ar-C), 138.0 (*ipso*-Ar-C), 136.9 (*ipso*-Ar-C), 133.9 (*ipso*-Ar-C), 130.8 (Ar-C), 129.6 (Ar-C), 128.8 (Ar-C), 128.2 (Ar-C), 127.0 (*ipso*-Ar-C), 121.5 (Ar-C), 118.4 (Ar-C), 111.9 (Ar-C), 111.2 (Ar-C), 54.7 (CONHCH(CH₂Phe)), 37.3 (CONHCH(CH₂Phe)); m/z (ES⁺) 484 ([³⁵Cl]MH⁺), 486 ([³⁷Cl]MH⁺); HRMS (ES⁺) found ([³⁵Cl]MH⁺) MH⁺, 484.1027(C₂₂H₂₀³⁵ClN₅O₆ requires 484.1024);

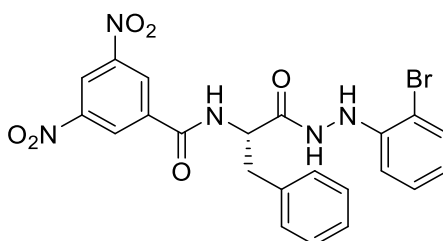
Chapter 5. Experimental section.

(S)-N-(1-(2-(4-chlorophenyl)hydrazineyl)-1-oxo-3-phenylpropan-2-yl)-3,5-dinitrobenzamide 86b



Following the general standard procedure, *tert*-butyl (S)-(1-(2-(4-chlorophenyl)hydrazineyl)-1-oxo-3-phenylpropan-2-yl)carbamate **66d** (0.05 g, 0.13 mmol) was transformed following trituration with DCM to produce the above compound as faint yellow solid (0.04 g, 60 %); R_f 0.54 (DCM/EtOH/NH₃ [200:6:1]); m.p. 106 -108 °C; ν_{max} 3264, 1728, 1627, 1537, 1472, 1341, 1155, 1077, 921, 765 cm⁻¹; δ_H (300 MHz, DMSO-d₆) 10.14 (1H, d, J 3, CONHNH), 9.59 (1H, d, J 8, CONH), 9.05 (2H, d, J 2, Ar-H), 8.96 (1H, t, J 2, Ar-H), 8.00 (1H, d, J 2, CONHNH), 7.43 – 7.23 (4H, m, Ar-H), 7.29 – 7.18 (1H, m, Ar-H), 7.23 – 7.06 (2H, m, Ar-H), 6.63 – 6.52 (2H, m, Ar-H), 4.96 – 4.83 (1H, m, CONHCH(CH₂Phe)), 3.23 (1H, dd, J 14, 6, CONHCH(CH₂Phe)), 3.11 (1H, dd, J 14, 10, CONHCH(CH₂Phe)); δ_C (75 MHz, DMSO-d₆) 171.0 (CONHNH), 163.0 (CONH), 148.6 (*ipso*-Ar-C), 148.5 (*ipso*-Ar-C), 138.0 (*ipso*-Ar-C), 136.9 (*ipso*-Ar-C), 129.7 (Ar-C), 128.9 (Ar-C), 128.8 (Ar-C), 128.2 (Ar-C), 127.0 (Ar-C), 122.2 (*ipso*-Ar-C), 121.5 (Ar-C), 114.1 (Ar-C), 54.5 (CONHCH(CH₂Ph), 37.5 (CONHCH(CH₂Phe)); m/z (ES⁺) 484 ([³⁵Cl]MH⁺), 486 ([³⁷Cl]MH⁺); HRMS (ES⁺) found ([³⁵Cl]MH⁺) MH⁺, 484.1027 (C₂₂H₂₀³⁵ClN₅O₆ requires 484.1024);

(S)-N-(1-(2-(2-bromophenyl)hydrazineyl)-1-oxo-3-phenylpropan-2-yl)-3,5-dinitrobenzamide 86c

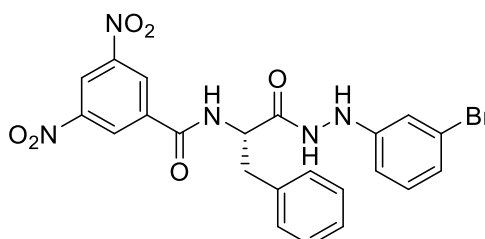


Following the general standard procedure, *tert*-butyl (S)-(1-(2-(2-bromophenyl)hydrazineyl)-1-oxo-3-phenylpropan-2-yl)carbamate **66A** (0.10 g,

Chapter 5. Experimental section.

0.23 mmol) was transformed following trituration with DCM to produce the titled compound as white yellowish solid (0.05 g, 44 %); R_f 0.56 (DCM/EtOH) [200: 6]; m.p. 93 - 94 °C; ν_{max} 1640, 1536, 1486, 1342, 1282, 749, 719, 699, 510 cm^{-1} ; δ_H (500 MHz, DMSO- d_6) 10.30 (1H, d, J 2, CONH NH), 9.60 (1H, d, J 8, CONH), 9.04 (3H, d, J 2, Ar-H), 8.94 (1H, t, J 2, Ar-H), 7.49 – 7.34 (6H, m, Ar-H), 7.27 (5H, dd, J 10, 8, Ar-H), 7.22 – 7.07 (3H, m, Ar-H), 6.73 – 6.62 (1H, m, Ar-H), 6.53 (2H, dd, J 8, 2, Ar-H), 4.99 – 4.85 (1H, m, CONHCH(CH_2 Phe)), 3.25 (1H, dd, J 12, 5, CONHCH(CH_2 Phe)), 3.10 (1H, dd, J 13, 10, CONHCH(CH_2 Phe)); δ_C (125 MHz, DMSO- d_6) 171 (CONH NH), 163 (CONH), 148.6 (*ipso*-Ar-C), 145.8 (*ipso*-Ar-C), 138.1 (*ipso*-Ar-C), 136.9 (*ipso*-Ar-C), 132.8 (*ipso*-Ar-C), 129.7 (Ar-C), 128.8 (Ar-C), 128.8 (Ar-C), 128.2 (Ar-C), 127.0 (Ar-C), 121.5 (Ar-C), 120.7 (Ar-C), 113.6 (Ar-C), 107.4 (Ar-C), 54.5 (CONHCH(CH_2 Phe)), 37.4 CONHCH(CH_2 Phe)); m/z (ES $^+$) m/z (ES $^+$) 528 ($[^{79}Br]MH^+$) 528 ($[^{81}Br]MH^+$); HRMS (ES $^+$) found $[^{79}Br] MH^+$, 528.0504, ($C_{22}H_{19}^{81}BrN_5O_6$ requires 528.0519);

(S)-N-(1-(2-(3-bromophenyl)hydrazineyl)-1-oxo-3-phenylpropan-2-yl)-3,5-dinitrobenzamide 86d

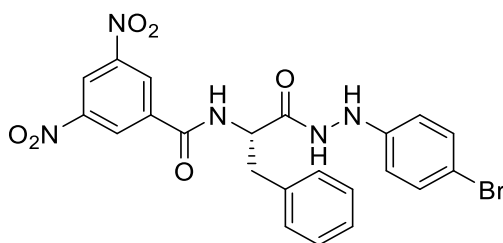


Following the general standard procedure, *tert*-butyl (S)-(1-(2-(3-bromophenyl)hydrazineyl)-1-oxo-3-phenylpropan-2-yl)carbamate **66b** (0.11 g, 0.25 mmol) was transformed following flush column chromatography (DCM;EtOH:NH $_3$ [200:6:1]) to produce the above compound as white yellowish solid (0.04 g, 31 %); R_f 0.63 (DCM/EtOH/NH $_3$ [200:6:1]); m.p. 107-109 °C; ν_{max} 3264, 1728, 1627, 1537, 1472, 1341, 1155, 1077, 921, 765 cm^{-1} ; δ_H (300 MHz, DMSO- d_6) 10.16 (1H, s, CONH NH), 9.61 (1H, d, J 8, CONH), 9.07 (2H, d, J 2, Ar-H), 8.95 (H, t, J 2, CONH NH), 8.11 (1H, s, Ar-H), 7.30 (7H, m, Ar-H), 7.04 (1H, t, J 8, Ar-H), 6.83 (2H, d, J 8, Ar-H), 6.58 (1H, d, J 7, Ar-H), 4.94 – 4.80 (1H, m, CONHCH(CH_2 Phe)), 3.29 – 3.04 (2H, m, CONHCH(CH_2 Phe)); δ_C (75 MHz, DMSO- d_6) 171.1 (CONH NH), 163.0 (CONH), 151.2 (*ipso*-Ar-C), 148.6 (*ipso*-Ar-

Chapter 5. Experimental section.

C), 138.0 (*ipso*-Ar-C), 136.9 (*ipso*-Ar-C), 131.1 (Ar-C), 129.6 (Ar-C), 128.8 (Ar-C), 128.2 (Ar-C), 127.0 (Ar-C), 122.5 (*ipso*-Ar-C), 121.5 (*ipso*-Ar-C), 121.3 (Ar-C), 114.8 (Ar-C), 111.6 (Ar-C), 54.7 (CONHCH(CH₂Phe)), 37.3 (CONHCH(CH₂Phe)); *m/z* (ES⁺) 528 ([⁷⁹Br]MH⁺) 530 ([⁸¹Br]MH⁺); HRMS (ES⁺) found [⁷⁹Br] MH⁺, 528.0522, (C₂₂H₁₉⁸¹BrN₅O₆ requires 528.0522);

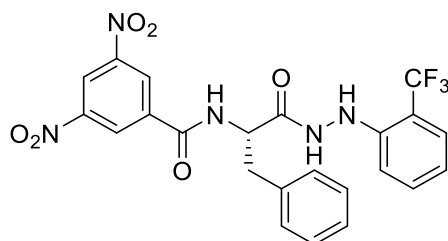
(S)-N-(1-(2-(4-bromophenyl)hydrazineyl)-1-oxo-3-phenylpropan-2-yl)-3,5-dinitrobenzamide 86e



Following the general standard procedure, *tert*-butyl (S)-1-(2-(4-bromophenyl)hydrazineyl)-1-oxo-3-phenylpropan-2-yl)carbamate **66e** (0.12 g, 0.31 mmol) was transformed following flush column chromatography (DCM;EtOAc [3:1]) to produce the above compound as yellow solid (0.08 g, 54 %); R_f 0.50 (DCM/EtOH/NH₃ [200:6:1]); m.p. 99 -101 °C; ν_{\max} 3282, 1728, 1627, 1537, 1472, 1341, 1155, 1077, 921, 765 cm⁻¹; δ_{H} (300 MHz, DMSO-d₆) 10.14 (1H, d, *J* 3, CONHNH), 9.59 (1H, d, *J* 8, CONH), 9.05 (2H, d, *J* 2, Ar-*H*), 8.96 (1H, t, *J* 2, Ar-*H*), 8.00 (1H, d, *J* 2, CONHNH), 7.43 – 7.23 (4H, m, Ar-*H*), 7.29 – 7.18 (1H, m, Ar-*H*), 7.23 – 7.06 (2H, m, Ar-*H*), 6.63 – 6.52 (2H, m, Ar-*H*), 4.96 – 4.83 (1H, m, CONHCH(CH₂Phe)), 3.23 (1H, dd, *J* 14, 6, CONHCH(CH₂Phe)), 3.11 (1H, dd, *J* 14, 10, CONHCH(CH₂Phe)); δ_{C} (75 MHz, DMSO-d₆) 171.0 (CONHNH), 163.0 (CONH), 148.6 (*ipso*-Ar-C), 148.5 (*ipso*-Ar-C), 138.0 (*ipso*-Ar-C), 136.9 (*ipso*-Ar-C), 129.7 (*ipso*-Ar-C), 128.9 (Ar-C), 128.8 (Ar-C), 128.2 (Ar-C), 127.0 (Ar-C), 122.2 (*ipso*-Ar-C), 121.5 (*ipso*-Ar-C), 114.1 (Ar-C), 54.5 (CONHCH(CH₂Ph), 37.5 (CONHCH(CH₂Phe)); *m/z* (ES⁺) 528 ([⁷⁹Br]MH⁺) 530 ([⁸¹Br]MH⁺); HRMS (ES⁺) found [⁷⁹Br] MH⁺, 528.0507, (C₂₂H₁₉⁸¹BrN₅O₆ requires 528.0519);

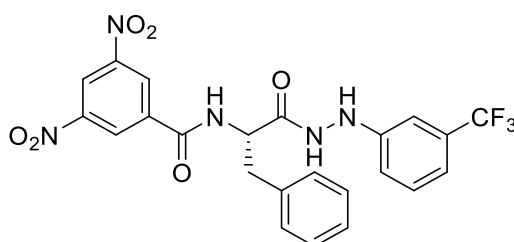
(S)-3,5-dinitro-N-(1-oxo-3-phenyl-1-(2-(2-(trifluoromethyl)phenyl)hydrazineyl)propan-2-yl)benzamide 86f

Chapter 5. Experimental section.



Following the general standard procedure, *tert*-butyl (S)-(1-oxo-3-phenyl-1-(2-(2-(trifluoromethyl)phenyl)hydrazineyl)propan-2-yl)carbamate **66B** (0.10 g, 0.26 mmol) was transformed following trituration with Et₂O to produce the titled compound as light orange solid (0.03 g, 45 %); R_f 0.56 (DCM/EtOH) [2: 0.6]; m.p. 93 - 94 °C; ν_{\max} 3260, 1629, 1540, 1343, 1181, 1034, 916 cm⁻¹; δ_{H} (300 MHz, DMSO-d₆) 10.33 (1H, d, *J* 2, CONHNH), 9.62 (1H, d, *J* 8, CONH), 9.05 (2H, d, *J* 2, Ar-*H*), 8.95 (1H, q, *J* 3, CONHNH), 7.56 (1H, s, Ar-*H*), 7.51 – 7.45 (1H, m, Ar-*H*), 7.44 – 7.21 (7H, m, Ar-*H*), 6.85 (1H, t, *J* 8, Ar-*H*), 6.69 (1H, d, *J* 8, Ar-*H*), 4.93 (1H, m, CONHCH(CH₂Ph)), 3.31 – 3.07 (2H, m, CONHCH(CH₂Ph)); δ_{C} (75 MHz, DMSO-d₆) 171.0 (CONHNH), 163.0 (CONH), 148.6 (*ipso*-Ar-C), 146.3 (*ipso*-Ar-C), 138.1 (*ipso*-Ar-C), 136.9 (*ipso*-Ar-C), 133.9 (*ipso*-Ar-C), 129.7 (*ipso*-Ar-C), 128.8 (Ar-C), 128.2 (Ar-C), 127.0 (Ar-C), 121.5 (Ar-C), 118.7 (Ar-C), 113.4 (Ar-C), 112.4 (*ipso*-Ar-C), 54.6 (CONHCH(CH₂ Phe)), 37.4 (CONHCH(CH₂ Phe)); *m/z* (ES⁺) 518 (MH⁺); HRMS (ES⁺) found MH⁺, 518.1290 (C₂₃H₁₉F₃N₅O₆ requires 518.1278);

(S)-3,5-dinitro-*N*-(1-oxo-3-phenyl-1-(2-(3-(trifluoromethyl)phenyl)hydrazineyl)propan-2-yl)benzamide **86g**

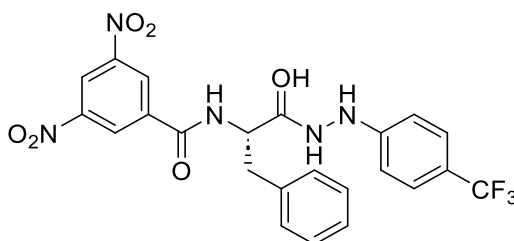


Following the general standard procedure, *tert*-butyl (S)-(1-oxo-3-phenyl-1-(2-(3-(trifluoromethyl)phenyl)hydrazineyl)propan-2-yl)carbamate **66c** (0.10 g, 0.24 mmol) was transformed following flush column chromatography (DCM;EtOH:NH₃ [200:6:1]) to produce the above compound as white yellowish solid (0.09 g, 72 %); R_f 0.27 (DCM/EtOH/NH₃ [200:6:1]); m.p. 102-105 °C; ν_{\max} 3276, 1668, 1593,

Chapter 5. Experimental section.

1455, 1323, 1155, 1075, 921, 743 cm^{-1} ; δ_{H} (300 MHz, DMSO- d_6) 10.25 (1H, d, J 2, CONH NH), 9.63 (1H, d, J 8, CONH), 9.06 (2H, d, J 2, Ar- H), 8.96 (1H, t, J 2, Ar- H), 8.28 (1H, d, J 2, CONH NH), 7.42 – 7.37 (2H, m, Ar- H), 7.35 – 7.19 (5H, m, Ar- H), 7.10 – 6.96 (3H, m, Ar- H), 6.84 (1H, d, J 8, Ar- H), 4.95 – 4.81 (1H, m, CONHCH(CH_2Ph)), 3.28 – 3.08 (2H, m, CONHCH(CH_2Ph)); δ_{C} (75 MHz, DMSO- d_6) 171.2 (CONH NH), 163.1 (CONH), 150.2 (*ipso*-Ar-C), 148.6 (*ipso*-Ar-C), 138.1 (*ipso*-Ar-C), 136.9 (*ipso*-Ar-C), 129.6 (Ar-C), 128.8 (Ar-C), 128.2 (Ar-C), 127.0 (Ar-C), 123.0 (Ar-C), 121.6 (*ipso*-Ar-C), 116.2 (Ar-C), 115.0 (*ipso*-Ar-C), 108.5 (Ar-C), 54.7 (CONHCH(CH_2Ph)), 37.3 (CONHCH(CH_2Ph)); δ_{F} (282 MHz, DMSO- d_6) -59.30 (3F, s, CF_3); m/z (ES^+) 518 (MH^+); HRMS (ES^+) found MH^+ , 518.1290 ($\text{C}_{23}\text{H}_{19}\text{F}_3\text{N}_5\text{O}_6$ requires 518.1287).

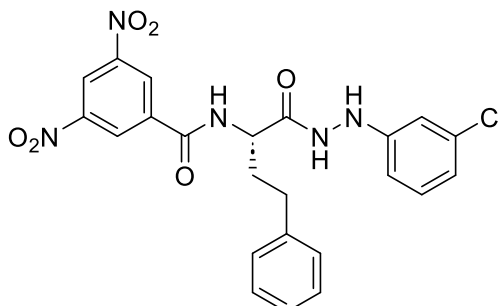
(S)-3,5-dinitro-*N*-(1-oxo-3-phenyl-1-(2-(4-(trifluoromethyl)phenyl)hydrazineyl)propan-2-yl)benzamide 86h



Following the general standard procedure, *tert*-butyl (S)-(1-oxo-3-phenyl-1-(2-(4-(trifluoromethyl)phenyl)hydrazineyl)propan-2-yl)carbamate **66f** (0.10 g, 0.24 mmol) was transformed following trituration with DCM to produce the titled compound as white yellowish solid (0.05 g, 43 %); R_f 0.53 (DCM/EtOH) [200:6]; m.p. 93 - 94 $^{\circ}\text{C}$; ν_{max} 3276, 1668, 1593, 1455, 1323, 1155, 1075, 921, 743 cm^{-1} ; δ_{H} (300 MHz, DMSO- d_6) 10.24 (1H, d, J 2, CONH NH), 9.05 (2H, d, J 2.1, Ar- H), 8.97 – 8.92 (1H, m, Ar- H), 8.46 (1H, d, J 2, CONH NH), 7.42 – 7.23 (7H, m, Ar- H), 6.66 (2H, d, J 9, Ar- H), 4.95 – 4.85 (1H, m, CONHCH(CH_2Phe)), 3.26 – 3.04 (2H, m, CONHCH(CH_2Phe)). δ_{C} (75 MHz, DMSO- d_6) 170.6 (CONH NH), 162.5 (CONH), 152.2 (*ipso*-Ar-C), 148.1 (*ipso*-Ar-C), 137.5 (*ipso*-Ar-C), 136.4 (*ipso*-Ar-C), 129.1 (Ar-C), 128.3 (Ar-C), 127.8 (*ipso*-Ar- CCF_3), 126.5 (Ar-C), 126.1 (Ar-C), 121.1 (*ipso*-Ar-C), 111.4 (Ar-C), 54.1 (CONHCH(CH_2Phe)), 37.0 CONHCH(CH_2Phe); δ_{F} (282 MHz, DMSO- d_6) -59.29 (3F, s, CF_3); m/z (ES^+) 518 (MH^+); HRMS (ES^+) found MH^+ , 518.1290 ($\text{C}_{23}\text{H}_{19}\text{F}_3\text{N}_5\text{O}_6$ requires 518.1287);

Chapter 5. Experimental section.

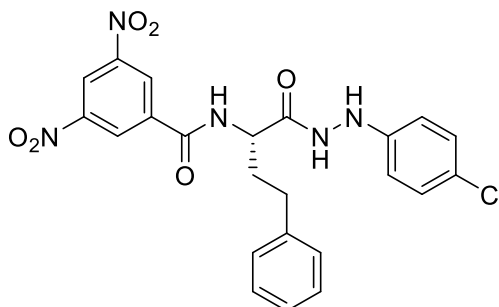
(S)-N-(1-(2-(3-chlorophenyl)hydrazineyl)-1-oxo-4-phenylbutan-2-yl)-3,5-dinitrobenzamide 89a



Following the general standard procedure, *tert*-butyl (S)-(1-(2-(3-chlorophenyl)hydrazineyl)-1-oxo-4-phenylbutan-2-yl)carbamate **67a** (0.10 g, 0.25 mmol) was transformed to obtain the titled compound as yellow white solid (0.10 g, 83 %); R_f 0.48 (n-hexane/EtOAc) [2:1]; m.p. 111 - 113 °C; ν_{\max} 3265, 1628, 1538, 1442, 1309, 1221, 1140, 1072, 991, 729, 570 cm^{-1} ; δ_H (300 MHz, DMSO- d_6) 10.11 (1H, d, J 2., CONH NH), 9.50 (1H, d, J 7, CONH), 9.17 (2H, d, J 2, Ar- H), 8.99 (1H, t, J 2, Ar- H), 8.11 (1H, d, J 2., CONH NH), 7.34 – 7.16 (6H, m, Ar- H), 7.07 (1H, t, J 8., Ar- H), 6.90 (1H, t, J 2., Ar- H), 6.86 – 6.81 (2H, m, Ar- H), 6.76 – 6.66 (2H, m, Ar- H), 4.53 (1H, q, J 7, CONHCH($\text{CH}_2\text{CH}_2\text{Phe}$)), 2.87 – 2.61 (2H, m, CONHCH($\text{CH}_2\text{CH}_2\text{Phe}$)), 2.16 (2H, q, J 8, CONHCH($\text{CH}_2\text{CH}_2\text{Phe}$)); δ_C (75 MHz, DMSO- d_6) 171.6 (CONH NH), 163.4 (CONH), 151.4 (*ipso*-Ar-C), 148.6 (*ipso*-Ar-C), 137.1 (*ipso*-Ar-C), 131.1 (*ipso*-Ar-C), 128.9 (Ar-C), 128.5 (Ar-C), 126.5 (Ar-C), 122.6 (Ar-C), 121.5 (Ar-C), 121.2 (Ar-C), 114.8 (Ar-C), 111.7 (Ar-C), 79.6 (Ar-C), 53.4 (CONHCH($\text{CH}_2\text{CH}_2\text{Phe}$)) 32.8 (CONHCH($\text{CH}_2\text{CH}_2\text{Phe}$)); 31.8 (CONHCH($\text{CH}_2\text{CH}_2\text{Phe}$)); m/z (ES $^+$) 498 ([^{35}Cl]MH $^+$) 500 ([^{37}Cl]MH $^+$); HRMS (ES $^+$) found [^{35}Cl] MH $^+$, 498.0875 (C $_{23}$ H $_{20}$ ^{35}Cl N $_5$ O $_6$ requires 498.1180);

Chapter 5. Experimental section.

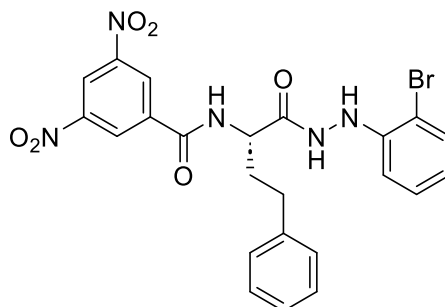
(S)-N-(1-(2-(4-chlorophenyl)hydrazineyl)-1-oxo-4-phenylbutan-2-yl)-3,5-dinitrobenzamide 89b



Following the general standard procedure, *tert*-butyl (S)-(1-(2-(4-chlorophenyl)hydrazineyl)-1-oxo-4-phenylbutan-2-yl)carbamate **67d** (0.10 g, 0.25 mmol) was transformed following flash column chromatography (DCM;EtOAc) [3:1] to produce the titled compound as white solid (0.08 g, 63 %); R_f 0.60 (*n*-hexane/EtOAc) [3:1]; m.p. 106 - 108 °C; ν_{\max} 3639, 1644, 1540, 1324, 1157, 1099, 917, 833 cm^{-1} ; δ_H (300 MHz, DMSO- d_6) 10.08 (1H, d, J 3 CONHNH), 9.47 (1H, d, J 8, CONH), 9.15 (2H, d, J 2, Ar-H), 8.99 (1H, t, J 2, Ar-H), 7.99 (1H, d, J 3, CONHNH), 7.33 – 7.18 (5H, m, Ar-H), 7.16 (2H, d, J 9, Ar-H), 6.72 (2H, d, J 9, Ar-H), 4.55 (1H, q, J 8, CONHCH(CH₂CH₂Phe)), 2.86 – 2.59 (2H, m, CONHCH(CH₂CH₂Phe)), 2.17 (2H, t, J 8, CONHCH(CH₂CH₂Phe)); δ_C (75 MHz, DMSO- d_6) 171.1 (CONHNH), 162.9; (CONH), 148.1 (*ipso*-Ar-C), 141.0 (*ipso*-Ar-C), 136.7 (*ipso*-Ar-C), 128.5 (Ar-C), 128.0 (Ar-C), 125.9 (Ar-C), 121.8 (Ar-C), 121.0 (*ipso*-Ar-C), 113.7 (Ar-C), 52.9 (CONHCH(CH₂CH₂Phe)), 33.0 (CONHCH(CH₂CH₂Phe)), 31.9 CONHCH(CH₂CH₂Phe)); m/z (ES⁺) 498 ([³⁵Cl]MH⁺) 500 ([³⁷Cl]MH⁺); HRMS (ES⁺) found [³⁵Cl] MH⁺, 498.1177 (C₂₃H₂₀³⁵ClN₅O₆ requires 498.1180);

Chapter 5. Experimental section.

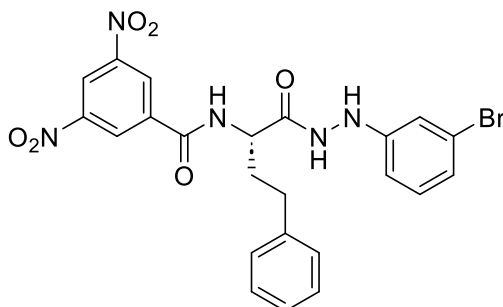
(S)-N-(1-(2-(2-bromophenyl)hydrazineyl)-1-oxo-4-phenylbutan-2-yl)-3,5-dinitrobenzamide 89c



Following the general standard procedure, *tert*-butyl (S)-1-(2-(2-bromophenyl)hydrazineyl)-1-oxo-4-phenylbutan-2-yl)carbamate **67A** (0.10 g, 0.22 mmol) was transformed following flush column chromatography (*n*-hexane;EtOAc) [3:1] to produce the titled compound as white solid (0.08 g, 63 %); R_f 0.56 (DCM/EtOH) [200: 6]; m.p. 93 - 94 °C; ν_{max} 3268, 1655, 1537, 1488, 1342, 744, 649, 494 cm^{-1} ; δ_H (300 MHz, DMSO- d_6) 10.24 (1H, d, J 2, CONHNH), 9.50 (1H, d, J 7, CONH), 9.16 (2H, d, J 2., Ar- H), 9.00 (1H, t, J 2, Ar- H), 7.44 (1H, dd, J 8, 1, Ar- H), 7.35 – 7.31 (5H, m, Ar- H), 7.24 (1H, m, CONHNH) 6.83 (1H, dd, J 8, 2, Ar- H), 6.69 (1H, ddd, J 8, 7, 2, Ar- H), 4.58 (1H, m, CONHCH(CH₂CH₂Phe)), 2.83 – 2.67 (2H, m, CONHCH(CH₂CH₂Phe)), 2.23 – 2.11 (2H, m, CONHCH(CH₂CH₂Phe)); δ_C (75 MHz, DMSO- d_6) 171.5 (CONHNH), 163.4 (CONH), 148.6 (*ipso*-Ar-C), 145.98 (*ipso*-Ar-C), 141.5 (*ipso*-Ar-C), 137.1 (*ipso*-Ar-C), 132.8 (Ar-C), 128.9 (Ar-C), 128.8 (*ipso*-Ar-C), 128.5 (Ar-C), 126.4 (Ar-C), 121.5 (Ar-C), 120.7 (Ar-C), 113.7 (Ar-C), 107.4 (*ipso*-Ar-C), 53.3 (CONHCH(CH₂CH₂Phe)), 33.4 (CONHCH(CH₂CH₂Phe)), 32.2 (CONHCH(CH₂CH₂Phe)); m/z (ES⁺) 564 ([⁷⁹Br]MNa⁺) 566 ([⁸¹Br]MNa⁺); HRMS (ES⁺) found [⁷⁹Br] MNa⁺, 564.0491 (C₂₃H₂₁⁷⁹BrN₅O₆ requires 564.0489);

Chapter 5. Experimental section.

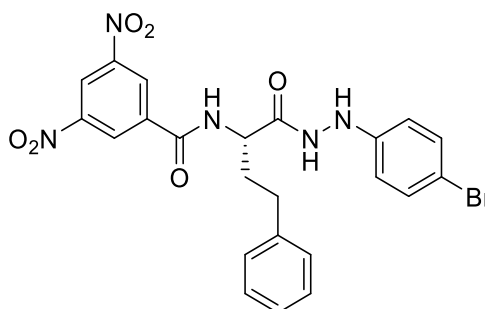
(S)-N-(1-(2-(3-bromophenyl)hydrazineyl)-1-oxo-4-phenylbutan-2-yl)-3,5-dinitrobenzamide 89d



Following the general standard procedure, *tert*-butyl (S)-(1-(2-(3-bromophenyl)hydrazineyl)-1-oxo-4-phenylbutan-2-yl)carbamate **67b** (0.13 g, 0.28 mmol) was transformed following flush column chromatography (*n*-hexane;EtOAc) [3:1] to produce the titled compound as white solid (0.08 g, 44 %); R_f 0.56 (DCM/EtOH) [200:6]; m.p. 112 - 114 °C; ν_{max} 3279, 1642, 1595, 1490, 1341, 1077, 915, 861, 769 cm^{-1} ; δ_H (300 MHz, DMSO- d_6) 10.11 (1H, d, J 2., CONHNH), 9.50 (1H, d, J 7, CONH), 9.17 (2H, d, J 2, Ar- H), 8.99 (1H, t, J 2, Ar- H), 8.11 (1H, d, J 2., CONHNH), 7.34 – 7.16 (6H, m, Ar- H), 7.07 (1H, t, J 8., Ar- H), 6.90 (1H, t, J 2., Ar- H), 6.86 – 6.81 (2H, m, Ar- H), 6.76 – 6.66 (2H, m, Ar- H), 4.53 (1H, q, J 7, CONHCH(CH₂CH₂Phe)), 2.87 – 2.61 (2H, m, CONHCH(CH₂CH₂Phe)), 2.16 (2H, q, J 8, CONHCH(CH₂CH₂Phe)). δ_C (75 MHz, DMSO- d_6) 171.6 (CONHNH), 163.4 (CONH), 151.4 (*ipso*-Ar-C), 148.6 (*ipso*-Ar-C), 137.1 (*ipso*-Ar-C), 131.1 (*ipso*-Ar-C), 128.9 (Ar-C), 128.5 (Ar-C), 126.5 (Ar-C), 122.6 (Ar-C), 121.5 (Ar-C), 121.2 (Ar-C), 114.8 (Ar-C), 111.7 (Ar-C), 79.6 (Ar-C), 53.4 (CONHCH(CH₂CH₂Phe));, 33.3 (CONHCH(CH₂CH₂Phe)); 32.3 (CONHCH(CH₂CH₂Phe)); m/z (ES⁺) 542 ([⁷⁹Br]MH⁺) 544 ([⁸¹Br]MH⁺), HRMS (ES⁺) found [⁷⁹Br] MH⁺, 544.0645, (C₂₃H₂₀⁷⁹BrN₅O₆ requires 544.0675);

Chapter 5. Experimental section.

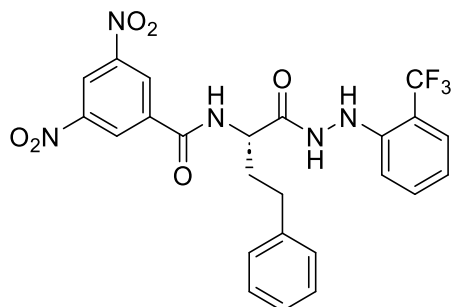
(S)-N-(1-(2-(4-bromophenyl)hydrazineyl)-1-oxo-4-phenylbutan-2-yl)-3,5-dinitrobenzamide 89e



Following the general standard procedure, *tert*-butyl (S)-(1-(2-(4-bromophenyl)hydrazineyl)-1-oxo-4-phenylbutan-2-yl)carbamate **67e** (0.10 g, 0.22 mmol) was transformed following flush column chromatography (*n*-hexane;EtOAc) [3:1] to produce the titled compound as white solid (0.08 g, 63 %); R_f 0.56 (DCM/EtOH) [200:6]; m.p. 112 - 114 °C; ν_{\max} 3283, 1640, 1537, 1485, 1342, 1070, 914, 820, 686 cm^{-1} ; δ_H (300 MHz, DMSO- d_6) 10.11 (1H, d, J 2., CONHNH), 9.50 (1H, d, J 7, CONH), 9.17 (2H, d, J 2, Ar- H), 8.99 (1H, t, J 2, Ar- H), 8.11 (1H, d, J 2., CONHNH), 7.34 – 7.16 (6H, m, Ar- H), 7.07 (1H, t, J 8., Ar- H), 6.90 (1H, t, J 2., Ar- H), 6.86 – 6.81 (2H, m, Ar- H), 6.76 – 6.66 (2H, m, Ar- H), 4.53 (1H, q, J 7, CONHCH(CH₂CH₂Phe)), 2.87 – 2.61 (2H, m, CONHCH(CH₂CH₂Phe)), 2.16 (2H, q, J 8, CONHCH(CH₂CH₂Phe)). δ_C (75 MHz, DMSO- d_6) 171.6 (CONHNH), 163.4 (CONH), 151.4 (*ipso*-Ar-C), 148.6 (*ipso*-Ar-C), 137.1 (*ipso*-Ar-C), 131.1 (*ipso*-Ar-C), 128.9 (Ar-C), 128.5 (Ar-C), 126.5 (Ar-C), 122.6 (Ar-C), 121.5 (Ar-C), 121.2 (Ar-C), 114.8 (Ar-C), 111.7 (Ar-C), 79.6 (Ar-C), 53.4 (CONHCH(CH₂CH₂Phe)) 33.3 (CONHCH(CH₂CH₂Phe)); 32.3 (CONHCH(CH₂CH₂Phe)); m/z (ES⁺) 542 ([⁷⁹ Br]MH⁺) 543 ([⁸¹ Br]MH⁺); HRMS (ES⁺) found [⁸¹ Br]MH⁺, 544.0645 (C₂₃H₂₀⁸¹BrN₅O₆ requires 544.0659);

Chapter 5. Experimental section.

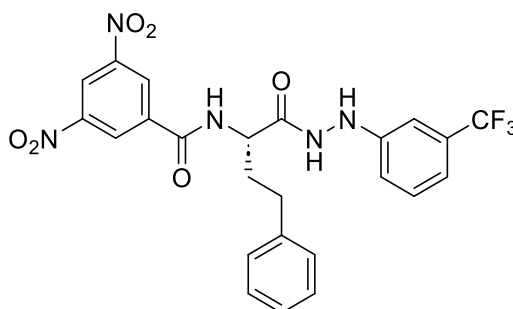
(S)-3,5-dinitro-N-(1-oxo-4-phenyl-1-(2-(2-(trifluoromethyl)phenyl)hydrazineyl)butan-2-yl)benzamide 89f



Following the general standard procedure, *tert*-butyl (S)-(1-oxo-4-phenyl-1-(2-(2-(trifluoromethyl)phenyl)hydrazineyl)butan-2-yl)carbamate **67B** (0.10 g, 0.23 mmol) was transformed following trituration with Et₂O to produce the titled compound as white solid (0.08 g, 62 %); R_f 0.56 (DCM/EtOH) [200:6]; m.p. 106 - 108 °C; ν_{\max} 3278, 1645, 1552, 1343, 1297, 1102, 820 cm⁻¹; δ_{H} (300 MHz, DMSO-d₆) 10.25 (1H, d, *J* 2, CONHNH), 9.51 (1H, d, *J* 7, CONH), 9.17 (2H, d, *J* 2, Ar-*H*), 9.00 (1H, t, *J* 2, Ar-*H*), 7.56 (1H, s, CONHNH), 7.46 (2H, dd, *J* 13, 8, Ar-*H*), 7.35 – 7.17 (5H, m, Ar-*H*), 7.01 (1H, d, *J* 8, Ar-*H*), 6.86 (1H, t, *J* 8, Ar-*H*), 4.64 – 4.53 (1H, m, CONHCH(CH₂CH₂Phe)), 2.86 – 2.69 (1H, m, CONHCH(CH₂CH₂Phe)), 2.30 – 2.12 (2H, m, CONHCH(CH₂CH₂Phe)); δ_{C} (75 MHz, DMSO-d₆) 171.5 (CONHNH) 163.4 (CONH), 148.6 (*ipso*-Ar-C), 146.5 (*ipso*-Ar-C), 141.5 (*ipso*-Ar-C), 137.1 (*ipso*-Ar-C), 133.8 (Ar-C), 128.8 (Ar-C), 128.5 (Ar-C), 126.4 (*ipso*-Ar-CCF₃), 121.5 (Ar-C), 118.6 (Ar-C), 113.5 (Ar-C), 112.4 (*ipso*-Ar-C), 53.4 (CONHCH(CH₂CH₂Phe)), 33.3 (CONHCH(CH₂CH₂Phe)), 32.2 (CONHCH(CH₂CH₂Phe)); *m/z* (ES⁺) 532 (MH⁺); HRMS (ES⁺) found MH⁺, 532.1432 (C₂₄H₂₁F₃N₅O₆ requires 532.1444);

Chapter 5. Experimental section.

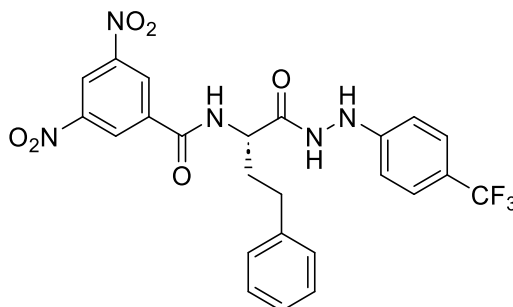
(S)-3,5-dinitro-N-(1-oxo-4-phenyl-1-(2-(3-(trifluoromethyl)phenyl)hydrazineyl)butan-2-yl)benzamide 89g



Following the general standard procedure, *tert*-butyl (S)-(1-oxo-4-phenyl-1-(2-(3-(trifluoromethyl)phenyl)hydrazineyl)butan-2-yl)carbamate **67c** (0.10 g, 0.23 mmol) was transformed following trituration with diethyl ether to produce the titled compound as light yellow solid (0.05 g, 44 %); R_f 0.45 (DCM/EtOH) [1:0.3]; m.p 113- 115 °C; ν_{max} 3275, 1651, 1538, 1445, 1275, 1119, 1067, 918, 718 cm^{-1} ; δ_H (300 MHz, DMSO- d_6) ; 10.20 (1H, d, J 2, CONHNH), 9.52 (1H, d, J 7, CONH), 9.17 (2H, d, J 2, Ar- H), 9.00 (1H, t, J 2, Ar- H), 8.28 (1H, d, J 2, CONHNH), 7.38 – 7.16 (7H, m, Ar- H), 7.04 – 6.96 (2H, m, Ar- H), 4.54 (1H, q, J 7, CONHCH(CH₂CH₂Phe)), 2.99 – 2.62 (2H, m, CONHCH(CH₂CH₂Phe)), 2.17 (2H, q, J 8, CONHCH(CH₂CH₂Phe)); δ_C (75 MHz, DMSO- d_6) 171.7 (CONHNH), 163.4 (CONH), 150.4 (*ipso*-Ar-C), 148.6 (*ipso*-Ar-C), 141.4 (*ipso*-Ar-C), 137.0 (*ipso*-Ar-C), 128.9 (Ar-C), 128.8 (Ar-C), 128.4 (Ar-C), 126.5 (*ipso*-Ar-CCF₃), 121.5 (Ar-C), 116.4 (Ar-C), 115.0 (Ar-C), 53.4 (CONHCH(CH₂CH₂Phe)), 33.2 (CONHCH(CH₂CH₂Phe)), 32.3 (CONHCH(CH₂CH₂Phe)); m/z (ES⁺) 532 (MH⁺); HRMS (ES⁺) found MH⁺, 532.1436 (C₂₄H₂₁F₃N₅O₆ requires 532.1444);

Chapter 5. Experimental section.

(S)-3,5-dinitro-N-(1-oxo-4-phenyl-1-(2-(4-(trifluoromethyl)phenyl)hydrazineyl)butan-2-yl)benzamide 89h



Following the general standard procedure, *tert*-butyl (S)-(1-oxo-4-phenyl-1-(2-(4-(trifluoromethyl)phenyl)hydrazineyl)butan-2-yl)carbamate **67f** (0.09 g, 0.20 mmol) was transformed following trituration with diethyl ether to produce the titled compound as yellow solid (0.05 g, 26 %); R_f 0.50 (*n*-hexane/EtOAc) [3:1]; m.p 113- 115 °C; ν_{max} 3275, 1644, 1537, 1342, 1158, 1066, 697 cm^{-1} ; δ_H (300 MHz, DMSO- d_6) ; 10.20 (1H, d, J 2, CONHNNH), 9.52 (1H, d, J 7, CONH), 9.17 (2H, d, J 2, Ar- H), 9.00 (1H, t, J 2, Ar- H), 8.28 (1H, d, J 2, CONHNNH), 7.38 – 7.16 (7H, m, Ar- H), 7.04 – 6.96 (2H, m, Ar- H), 4.54 (1H, q, J 7, CONHCH(CH₂CH₂Phe)), 2.99 – 2.62 (2H, m, CONHCH(CH₂CH₂Phe)), 2.17 (2H, q, J 8, CONHCH(CH₂CH₂Phe)). δ_C (75 MHz, DMSO- d_6) 171.7 (CONHNNH), 163.4 (CONH), 152.8 (*ipso*-Ar-C), 148.6 (*ipso*-Ar-C), 141.4 (*ipso*-Ar-C) 137.1 (*ipso*-Ar-C), 128.9 (*ipso*-Ar-CCF₃), 128.8 (Ar-C), 128.5 (Ar-C), 126.6 (Ar-C), 126.6 (Ar-C), 126.5 (Ar-C), 123.8 (Ar-C), 121.5 (Ar-C), 111.9 (*ipso*-Ar-C), 53.3 (CONHCH(CH₂CH₂Phe)), 33.4 (CONHCH(CH₂CH₂Phe)), 32.3 (CONHCH(CH₂CH₂Phe)); δ_F (282 MHz, DMSO- d_6) -59.29 (3F, s, CF₃); m/z (ES⁺) 554 (MNa⁺), HRMS (ES⁺) found MNa⁺, 554.1261 (C₂₄H₂₁F₃N₅O₆ requires 554.1258).

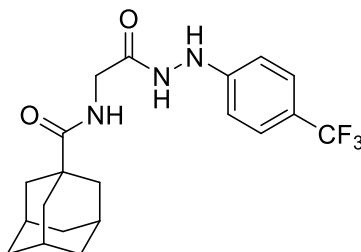
Chapter 5. Experimental section.

5.1.4 General procedure for synthesis of 1-admantyl substituted amino acid hydrazide compounds.

The *N*-Boc amino acid hydrazide (1.20 equiv.) was dissolved in 4 N HCl solution in dioxane (2 mL) and stirred at room temperature for 90 minutes. After that, the solvent was evaporated, dried *in vacuo* and precipitated using (EtOH / Et₂O). The precipitate was directly used in the next step without further purification. Therefore, the resulting deprotected amino acid hydrazide solid (1 equiv.) was dissolved in THF (3 mL). Then, diisopropylethylamine (3 equiv.) was added followed by (2-(1H-benzotriazol-1-yl)-1,1,3,3-tetramethyluronium hexafluorophosphate HBTU (1.20 equiv.). The mixture was stirred for 10 minutes at room temperature, then the solution was treated with 1-admantyl carboxylic acid (1.20 equiv.) and continued stirring for 4 hours. After that, the reaction mixed with ethyl acetate (10 mL) and distilled water (5 mL). After separation of the two phases the organic layer washed again with distilled water (5 mL × 3 mL) followed by a wash with sat. aq. NH₄Cl (6 mL) then sat. aq. NaHCO₃ (6 mL) followed by brine (10 mL). Organic layer dried over MgSO₄, filtered, evaporated and dried in *vacuo*. The product was purified by trituration with (Et₂O or DCM) or through flash chromatography (*n*-hexane/EtOAc [2:1]); (DCM/EtOH/NH₃ [600:8:1], [200:6:1]) afforded the desired compounds **108a – 108g**.

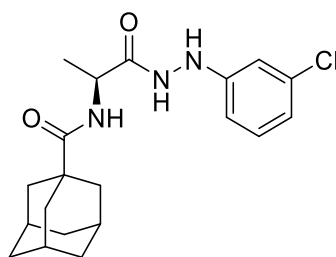
Chapter 5. Experimental section.

(3*r*,5*r*,7*r*)-N-(2-oxo-2-(2-(4-(trifluoromethyl)phenyl)hydrazineyl)ethyl)adamantane-1-carboxamide 108a



tert-butyl (2-oxo-2-(2-(4-(trifluoromethyl)phenyl)hydrazineyl)ethyl)carbamate (0.10 g, 0.30 mmol) **61f** was transformed following flush column chromatography to afford yellow oil (0.05 g, 38 %); R_f 0.42 (DCM/EtOH/NH₃ 200:8:1); m.p 252 – 253 °C; ν_{\max} 3089 2903, 1597, 1510, 1449, 1077, 766, 681, 486 cm⁻¹ δ_H (300 MHz, CDCl₃) 8.75 (1H, bs, CONH₂), 7.45 (2 H, d, J 9, Ar-*H*), 6.83 (2H, d, J 9, Ar-*H*), 6.49 (1H, bs, CONH₂), 6.26 (1H, s, CONHCH), 4.03 (2H, d, J 6, CONHCH₂), 2.06 - 1.62 (24H, m, Ar-*H*); m/z (ES⁺) 396 HRMS MH⁺, Found 396.1617 (C₂₀H₂₅F₃N₃O₂ requires 396.1899).

(3*S*,5*S*,7*S*)-N-((*S*)-1-(2-(3-chlorophenyl)hydrazineyl)-1-oxopropan-2-yl)adamantane-1-carboxamide 108b

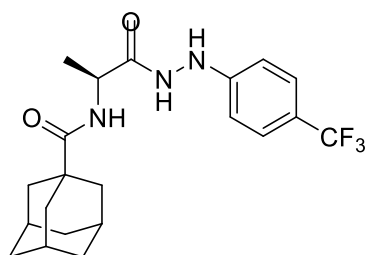


tert-butyl (*S*)-(1-(2-(3-chlorophenyl)hydrazineyl)-1-oxopropan-2-yl)carbamate (0.10 g, 0.32 mmol) **62a** was transformed to obtain the titled compound as dark orange oil. This was purified using flush column chromatography to afford faint yellow oil (0.04 g, 33 %); R_f 0.62 (*n*-hexane/EtOAc [4:1]); m.p 252 – 254 °C; ν_{\max} , 2903, 1597, 1510, 1449, 1077, 766, 681, 486 cm⁻¹; δ_H (300 MHz, CDCl₃) 9.23 (1H, d, J 4, CONH₂), 7.11 - 7.06 (1H, t, J 8, Ar-*H*), 6.83 – 6.80 (1H, m, Ar-*H*), 6.76 (1H, t, J 2, Ar-*H*), 6.65 (1H, dd, J 8, 2, Ar-*H*), 6.25 (1H, d, J 8, CONH), 6.18 (1H, d, J 4, CONH₂), 4.69 (1H, p, J 8, CONHCHCH₃), 2.03 – 1.62 (22H, m,

Chapter 5. Experimental section.

$C_{18}H_{16}$), 1.42 (3H, d, J 7, CONHCHCH₃); δ_C (75 MHz, CDCl₃) 178.9 (CONHNH), 172.2 (CONH) 149.2 (*ipso*-Ar-C), 135.0 (*ipso*-Ar-C), 120.9 (Ar-C), 113.3 (Ar-C), 111.8 (Ar-C), 45.1 (CONHCHCH₃), 39 (Ar-C), 36.4 (Ar-C), 28.0 (Ar-C), 17.8 (CONHCHCH₃); m/z (ES⁺) 376 ([³⁵Cl]MH⁺); HRMS (ES⁺) Found [^{35,35}Cl]MH⁺, 376.1471 (C₂₀H₂₆ClN₃O₂ requires 376.1792).

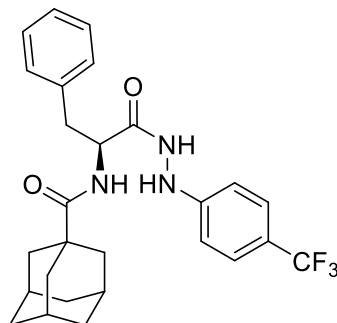
(3S,5S,7S)-N-((S)-1-oxo-1-(2-(4-(trifluoromethyl)phenyl)hydrazineyl)propan-2-yl)adamantane-1-carboxamide 108c



tert-butyl (S)-(1-oxo-1-(2-(4-(trifluoromethyl)phenyl)hydrazineyl)propan-2-yl)carbamate (0.10 g, 0.29 mmol) **62f** was transformed following flush column chromatography to afford yellow oil (0.05 g, 38 %); R_f 0.43 (DCM/EtOH/NH₃) ([200:8:1]); m.p. 255 – 259 °C; ν_{max} 2904, 1687, 1565, 1282, 1103, 959, 816, 740, 669, 529 cm⁻¹; δ_H (300 MHz, CDCl₃) 9.04 (1H, bs, CONHNH), 7.46 – 7.39 (3H, m, Ar-H), 6.85 – 6.78 (2H, m, Ar-H), 6.24 (1H, d, J 7, CONH), 4.65 (1H, p, J 7, (CONHCH(CH₃))), 2.09 – 1.61 (20H, m, Ar-H), 1.44 (3H, d, J 7, CONHCH(CH₃)); m/z (ES⁺) 410; HRMS (ES⁺) Found MH⁺, 410.1743 (C₂₁H₂₇F₃N₃O₂ requires 410.2055);

Chapter 5. Experimental section.

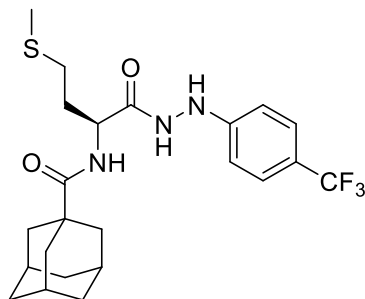
(3S,5S,7S)-N-((S)-1-oxo-3-phenyl-1-(2-(4-(trifluoromethyl)phenyl)hydrazineyl)propan-2-yl)adamantane-1-carboxamide 108d



tert-butyl(S)-(1-oxo-3-phenyl-1-(2-(4-(trifluoromethyl)phenyl)hydrazineyl)propan-2-yl)carbamate (0.10 g, 0.30 mmol) **66f** was transformed to obtain the titled compound as orang oil. This was purified using flush column chromatography to afford yellow oil (0.05 g, 38 %). R_f 0.42; m.p. 282 – 285 °C; ν_{\max} 3089, 2903, 1662, 1613, 1579, 1520, 1440, 1077, 766, 855, 681, 486 cm^{-1} ; δ_H (300 MHz, CDCl_3) 8.82 (1H, d, J 11, Ar-*H*), 7.47 – 7.08 (8H, m, Ar-*H*) 6.50 (2H, d, J 9, Ar-*H*), 6.31 – 6.18 (2H, m, Ar-*H*), 4.92 (1H, d, J 7, CONHCHCH₂Ph), 3.08 (2H, m, CONHCHCH₂Ph), 2.19 – 1.22 (28H, m, Ar-*H*); δ_C (75 MHz, CDCl_3) 178.9 (CONHNH), 171.7 (CONH), 150.3 (*ipso*-Ar-C) 135.9 (*ipso*-Ar-C), 129.4 (Ar-C) 128.8 (Ar-C), 127.2 (Ar-C), 126.4 (Ar-C), 112.7 (Ar-C), 52.5, CONHCHCH₂Ph), 40.7 (*ipso*-Ar-C), 38.9 (Ar-C), 37.9 (*ipso*-Ar-C), 36.2 (Ar-C) 27.9 (Ar-C); m/z (ES⁺) 486; HRMS (ES⁺) Found MH⁺, 486.2055 (C₂₇H₃₁F₃N₃O₂ requires 486.2368);

Chapter 5. Experimental section.

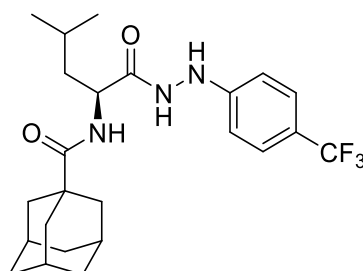
(3S,5S,7S)-N-((S)-4-(methylthio)-1-oxo-1-(2-(4-(trifluoromethyl)phenyl)hydrazineyl)butan-2-yl)adamantane-1-carboxamide carboxamide 108e



tert-butyl (S)-(4-(methylthio)-1-oxo-1-(2-(4-(trifluoromethyl)phenyl)hydrazineyl)butan-2-yl)carbamate (0.20 g, 0.50 mmol) **63f** was transformed to obtain the titled compound as dark oil. This was purified using flush column chromatography to afford the titled compound as yellow oil (0.09 g, 38 %); R_f 0.62 (DCM/EtOH/NH₃ [200:8:1]); m.p. 281 – 285 °C; ν_{max} 3089, 2903, 1676 1545, 1523, 1487, 1302, 1279, 1077, 967, 765, 681, 515 cm⁻¹; δ_H (300 MHz, CDCl₃) 9.23 (1H, d, J 4, CONHNH), 7.43 (2H, d, J 9, Ar-H), 6.81 (2H, d, J 9, Ar-H), 6.55 (1H, d, J 8, CONH), 6.43 (1H, d, J 4, CONHNNH), 4.88 – 4.77 (1H, m, CONHCHCH₂CH₂SCH), 2.62 – 2.53 (2H, m, CONHCHCH₂CH₂SCH₃), 2.12 (3H, d, J 0.7, CONHCHCH₂CH₂SCH₃), 2.03 (2H, d, J 8, CH₂CH₂SCH₃), 1.86 -1.61 (20H, m, Ar-H); δ_C (75 MHz, CDCl₃) 179.2 (CONHNNH), 171.9 (CONH), 150.6 (*ipso*-Ar-C), 126.6 (*ipso*-Ar-C), 112.8 (Ar-C), 50.6 (CONHCHCH₂CH₂SCH₃), 40.8 (*ipso*-Ar-C), 39.1(Ar-C), 38.7 (*ipso*-Ar-C), 36.3 (Ar-C), 30.8 (CONHCHCH₂CH₂SCH₃), 30.2 (CONHCHCH₂CH₂SCH₃) 27.9 (Ar-C), 15.6 (CONHCHCH₂CH₂SCH₃); m/z (ES⁺) 470; HRMS (ES⁺) Found MH⁺, 470.1772 (C₂₃H₃₁F₃N₃O₂S requires 470.2089);

Chapter 5. Experimental section.

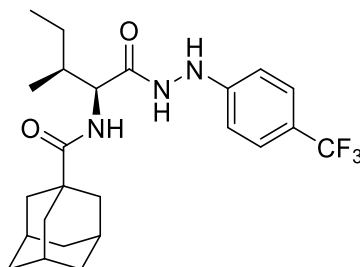
(3S,5S,7S)-N-((S)-4-methyl-1-oxo-1-(2-(4-(trifluoromethyl)phenyl)hydrazineyl)pentan-2-yl)adamantane-1-carboxamide 108f



tert-butyl (S)-(4-methyl-1-oxo-1-(2-(4-(trifluoromethyl)phenyl)hydrazineyl)pentan-2-yl)carbamate (0.10 g, 0.26 mmol) **64f** was transformed following flush column chromatography to afford clear oil (0.04 g, 33 %); R_f 0.34 (DCM/EtOH/NH₃ [200:8:1]); m.p 257- 260 °C ; ν_{\max} 3071, 1635, 1115, 1066, 836, 587 cm⁻¹; δ_H (300 MHz, CDCl₃) 9.14 (1H, d, J 4, CONH₂), 7.45 – 7.38 (2H, d, J 8, Ar-*H*), 6.84 – 6.75 (2H, d, J 8, Ar-*H*), 6.32 (1H, d, J 4, CONH₂), 6.05 (1H, d, J 8, CONH), 4.68 (1H, m, CONHCH(CH₂CH(CH₃)₂)), 2.01 (3H, h, J 3, Ar-*H*), 1.82 (6H, d, J 3, Ar-*H*), 1.78 – 1.56 (11H, m, Ar-*H*), 0.95 (6H, dd, J 16, 6, CONHCH(CH₂CH(CH₃)₂)); δ_C (75 MHz, CDCl₃) 178.9 (CONH₂), 172.5 (CONH), 150.7 (*ipso*-Ar-C), 126.5 (Ar-C), 112.7 (Ar-C), 49.6 (CONHCH(CH₂CH(CH₃)₂)), 40.7 (*ipso*-Ar-C), 40.3 (CONHCH(CH₂CH(CH₃)₂)), 39.1 (Ar-C), 36.3 (Ar-C), 28.2 (Ar-C), 24.9 (CONHCH(CH₂CH(CH₃)₂)), 22.7 (CONHCH(CH₂CH(CH₃)₂)) 22.3 (CONHCH(CH₂CH(CH₃)₂)); δ_F (282 MHz, DMSO-*d*₆) -59.30 (3F, s, CF₃); m/z (ES⁺) 452 (MH⁺); HRMS (ES⁺) Found MH⁺, 452.2151 (C₂₄H₃₃F₃N₃O₂ requires 452.2525).

Chapter 5. Experimental section.

(3S,5S,7S)-N-((2S,3S)-3-methyl-1-oxo-1-(2-(4-(trifluoromethyl)phenyl)hydrazineyl)pentan-2-yl)adamantane-1-carboxamide 108g



tert-butyl ((2S,3S)-3-methyl-1-oxo-1-(2-(4-(trifluoromethyl)phenyl)hydrazineyl)pentan-2-yl)carbamate (0.10 g, 0.32 mmol) **65f** was transformed following flash column chromatography to afford light yellow oil (0.04 g, 33 %); R_f 0.34 (DCM/EtOH/NH₃ [200:8:1]); m.p. 270 - 247 °C; ν_{max} 3250, 2906, 1671, 1631, 1322, 1158, 1055, 910, 835, 588 cm⁻¹; d_H (300 MHz, CDCl₃) 9.61 (1H, d, J 4, CONHNH), 7.40 (2H, d, J 9, Ar-*H*), 6.81 (2H, d, J 9, Ar-*H*), 6.47 (1H, d, J 4, CONHNH), 6.30 (1H, d, J 9, CONH), 4.61 (1H, t, J 9, CONHCH(CHCH₂CH₃)), 1.99 – 1.53 (19H, m, Ad-*H*), 1.24 – 1.10 (2H, m, CONHCH(CHCH₂CH₃)), 0.98 (3H, d, J 7, CONHCH(CHCH₂CH₃)), 0.91 (3H, t, J 8, CONHCH(CHCH₂CH₃)); d_C (75 MHz, CDCl₃) 178.7 (CONHNH), 172.1 (CONH), 150.7 (*ipso* Ar-C), 126.4 (*ipso*-Ar-C), 112.8 (Ar-C), 55.5 (CONHCH(CHCH₂CH₃)), 40.8 (*ipso*-Ar-C), 39.1 (Ar-C), 36.9 (*ipso*-Ar-C), 36.3 (Ar-C), 27.9 (Ar-C) 24.9 (CONHCH(CHCH₂CH₃)) 15.6 (CONHCH(CHCH₂CH₃)), 10.9 (CONHCH(CHCH₂CH₃)); m/z (ES⁺) 452 (MH⁺); HRMS (ES⁺) Found MH⁺, 452.2175 (C₂₄H₃₃F₃N₃O₂ requires 452.2480).

Chapter 6: Experimental section

5.2 General Experimental Information of Biological Assessment

5.2.1 Cell Lines

The mycobacterial strains and cell lines used in this study can be found in (Table 13)

Strain	Genotype	Comments	Reference
<i>Mtb</i> mc ² 7000	Δ RD1(esx1):GFP Δ panCD	Deletion of esx1 or RD1 responsible for virulence factor secretion, ESAT-6 and CFP-10 replaced with GFP. Pantothenate auxotroph.	W. Jacobs, Albert Einstein College of Medicine.
<i>Mtb</i> mc ² 7902	Δ leuCD Δ panCD Δ argB	mc ² 6206 derived, arginine auxotroph	Vilcheze et al. 10.1128/mbio.00938-18
<i>Mtb</i> mc ² 8245	Δ panCD Δ leuCD Δ argB Δ 2116169–2162530	mc ² 7902 derived, Δ 2116169–2162530; INH-Resistant	Vilcheze et al. 10.1128/mbio.00938-18
<i>Mtb</i> mc ² 8250	Δ panCD Δ leuCD Δ argB <i>rpoB</i> (H445Y) Δ 2122397–2170320	mc ² 8247 derived, Δ 2122397–2170320; INH-Resistant , <i>rpoB</i> His445 --> Lys; RIF resistant	Vilcheze et al. 10.1128/mbio.00938-18
<i>Mtb</i> mc ² 8257	Δ panCD Δ leuCD Δ argB <i>rpoB</i> (H445Y) <i>katG</i> (V1A)	mc ² 8247 derived, <i>rpoB</i> His445 --> Lys; RIF resistant , <i>katG</i> Val1 --> Ala; INH-Resistant	Vilcheze et al. 10.1128/mbio.00938-18
<i>Mtb</i> AKB7002	Δ RD1(esx1):GFP Δ panCD; Kan ^R <i>rpoB</i> (H445Y)	As <i>Mtb</i> mc ² 7000 pMV261, generated spontaneous mutant, rifampicin-resistant , <i>rpoB</i> His445→Lys.	Brown, A.K. et al. <i>Molecules</i> , 25 (10), p.2387
<i>Mtb</i> AKB7021	Δ RD1(esx1):GFP Δ panCD; Kan ^R <i>katG</i> (S315N)	As <i>Mtb</i> mc ² 7000 pMV261, generated spontaneous mutant, isoniazid-resistant , <i>katG</i> Ser315→Asp.	Brown, A.K. et al. <i>Molecules</i> , 25 (10), p.2387

Table 8: The mycobacterial strains and cell lines used.

Chapter 5. Experimental section.

5.2.2 Bacterial Growth Conditions

Mycobacterial species were developed in Middlebrook 7H9 broth or Middlebrook 7H10 agar media, which were supplemented with albumin–dextrose–catalase (ADC) or oleic acid–albumin–dextrose–catalase (OADC) enrichments. Additionally, the media contained 0.2% glycerol, 0.2% casamino acids, 24 µg/mL pantothenate, 1 µg/mL penicillin G, and 10 µg/mL cyclohexamide purchased from BD Biosciences. The reagents were obtained from Sigma-Aldrich, Gillingham, UK, unless otherwise specified.

5.2.3 *In vitro* bacterial inhibitory assay

Minimum inhibitory concentrations (MICs) of the final compounds on different mycobacterial strains were determined using broth micro-dilution assay in 96-well plates. Bacterial colonies from LJ slants were scraped and re-suspended in Middlebrook 7H9GC medium. Homogeneous mycobacterial suspension was prepared in sterile water, vortexed with glass beads (1-5 mm) for five minutes. After aerosol settlement, the colony-forming unit (CFU) of the suspension was determined by the measurement of optical density (OD) using the SmartSpec™ Plus spectrophotometer (BIO-RAD, CA, USA) at an excitation of 530 nm with an emission of 590 nm. The concentration of stock for each test compound is 10 mg/mL and then a 2-fold serial dilution was prepared (250 to 0.24 µg/mL) in Middlebrook 7H9 medium supplemented with OADC and glycerol as aforementioned. The correct mycobacterial strain suspension was added to an equal volume (100 µL) of test compounds solutions in each well to obtain the final concentration of 1×10^7 CFU/mL for *Mtb* strains. The untreated bacterial suspension and sterile medium were used as positive and negative growth controls. The plates were then incubated at 37°C for 7 days in an oven incubator. A volume of 20 µL of 0.02% (w/v) resazurin dye was added to each well at the end of the incubation period. The color change was evaluated after ~48 h for *Mtb* strains. Resazurin assay is a colorimetric assay in which the viable cells reduce blue resazurin into fluorescent pink resorufin. MIC of each compound on the susceptible, mono-resistant and double-resistant *Mtb* strains was determined visually and defined as the lowest concentration remained in.

Chapter 5. Experimental section.

5.2.4 Cytotoxicity assay method.

Up to 2000 mammalian cells were added to each well of a 96-well plate and left overnight to adhere to the bottom of the wells. Drugs at the relevant concentration, were added to the wells and incubated for 24h. The media was changed and cells incubated for a further 3-4 days before adding MTS solution {Promega MTS kit}. Absorbance was measured at 490 nm via an ELISA plate reader and this was directly proportional to the number of viable cells. Percentage cell viability was determined by comparing the absorbance of treated wells to that of control wells (untreated cells).

5.2.5 Calculation of the percentage yield of the compound

The actual yield of a chemical process is the amount of product that is produced. The theoretical yield is the amount that is determined using the limiting reagent and the balanced chemical equation. The actual amount of product obtained divided by the theoretical amount, stated as a percentage, is known as the percent yield.

Percent Yield = Actual Yield / Theoretical Yield × 100 %.

Example Calculation

Assume conduct a reaction and obtained 6 grams of the product (actual yield), but the theoretical yield was calculated to be 20 grams, therefore the percentage yield would be

$$\text{Percentage Yield} = (20 \text{ g} / 6 \text{ g}) \times 100 = 40\%$$

This means that, the reaction had an efficiency of 40% in generating the intended product.

Theoretical yield calculation:

The theoretical yield of a chemical reaction is the quantity of product obtained considering the reactants fully react.

To calculate theoretical yield:

1. Formulate the balanced chemical equation for the reaction.
2. Determine the limiting reactant.

Chapter 5. Experimental section.

3. Convert grammes of the limiting reactant to moles.
4. Apply the mole ratio between the limiting reactant and the product to get the theoretical number of moles of the product.
5. Convert the moles of product to grammes.

6. References

6. References

- (1) Floyd, K.; Glaziou, P.; Zumla, A.; Raviglione, M. The global tuberculosis epidemic and progress in care, prevention, and research: an overview in year 3 of the End TB era. *The Lancet Respiratory Medicine* **2018**, *6* (4), 299-314.
- (2) Skrahina, A.; Hurevich, H.; Zalutskaya, A.; Sahalchyk, E.; Astrauko, A.; Hoffner, S.; Rusovich, V.; Dadu, A.; Colombani, P. d.; Dara, M. Multidrug-resistant tuberculosis in Belarus: the size of the problem and associated risk factors. *Bulletin of the World Health Organization* **2013**, *91*, 36-45.
- (3) Krieger, E.; Nabuurs, S. B.; Vriend, G. Homology modeling. *Structural bioinformatics* **2003**, *44*, 509-523.
- (4) Organization, W. H. *GLOBAL TUBERCULOSIS REPORT*; 2022.
- (5) Bahuguna, A.; Rawat, D. S. An overview of new antitubercular drugs, drug candidates, and their targets. *Medicinal Research Reviews* **2020**, *40* (1), 263-292.
- (6) Cruz, A. T.; Starke, J. R. Clinical manifestations of tuberculosis in children. *Paediatric respiratory reviews* **2007**, *8* (2), 107-117.
- (7) Kiazky, S.; Ball, T. Tuberculosis (TB): Latent tuberculosis infection: An overview. *Canada Communicable Disease Report* **2017**, *43* (3-4), 62.
- (8) Daniel, B. D.; Grace, G. A.; Natrajan, M. Tuberculous meningitis in children: Clinical management & outcome. *The Indian Journal Of Medical Research* **2019**, *150* (2), 117.
- (9) Leonard, J. M. Central nervous system tuberculosis. *Tuberculosis and Nontuberculous Mycobacterial Infections* **2017**, 331-341.
- (10) Olness, K. Effects on brain development leading to cognitive impairment: a worldwide epidemic. *Journal of Developmental & Behavioral Pediatrics* **2003**, *24* (2), 120-130.
- (11) Lyon, S. M.; Rossman, M. D. Pulmonary tuberculosis. *Microbiology Spectrum* **2017**, *5* (1), 10.1128/microbiolspec.tnmi1127-0032-2016.
- (12) Wells, W. F. *Airborne contagion and air hygiene: an ecological study of droplet infections*; Commonwealth Fund, **1955**.
- (13) Gupta, A.; Singh, A.; Srivastava, S.; Sharma, M. TUBERCULOSIS: AN OVERVIEW. *Webology* **2021**, *18* (1), 1746-1750.
- (14) Jankute, M.; Cox, J. A.; Harrison, J.; Besra, G. S. Assembly of the mycobacterial cell wall. *Annual Review Of Microbiology* **2015**, *69*, 405-423.
- (15) Rohde, M. The Gram-positive bacterial cell wall. *Microbiology Spectrum* **2019**, *7* (3), 10.1128/microbiolspec.gpp1123-0044-2018.
- (16) Silhavy, T. J.; Kahne, D.; Walker, S. The bacterial cell envelope. *Cold Spring Harbor perspectives in biology* **2010**, *2* (5), a000414.
- (17) Mir, M. A. *Human Pathogenic Microbes: Diseases and Concerns*; Academic Press, **2022**.
- (18) Maitra, A.; Munshi, T.; Healy, J.; Martin, L. T.; Vollmer, W.; Keep, N. H.; Bhakta, S. Cell wall peptidoglycan in Mycobacterium tuberculosis: An Achilles' Feel for the TB-causing pathogen. *FEMS Microbiology Reviews* **2019**, *43* (5), 548-575.
- (19) Vilchèze, C. Mycobacterial cell wall: a source of successful targets for old and new drugs. *Applied Sciences* **2020**, *10* (7), 2278.
- (20) Abrahams, K. A.; Besra, G. S. Mycobacterial cell wall biosynthesis: a multifaceted antibiotic target. *Parasitology* **2018**, *145* (2), 116-133.
- (21) Grover, S. Molecular and biochemical characterisation of mycobacterial cell wall drug targets-Lipoarabinomannan. University of Birmingham, **2014**.
- (22) Pieters, J. Mycobacterium tuberculosis and the macrophage: maintaining a balance. *Cell Host & Microbe* **2008**, *3* (6), 399-407.
- (23) Aderem, A.; Underhill, D. M. Mechanisms of phagocytosis in macrophages. *Annual Review Of Immunology* **1999**, *17* (1), 593-623.
- (24) Schmid, S. L. Clathrin-coated vesicle formation and protein sorting: an integrated process. *Annual Review Of Biochemistry* **1997**, *66* (1), 511-548.

6. References

- (25) Knutson, K. L.; Hmama, Z.; Herrera-Velitz, P.; Rochford, R.; Reiner, N. E. Lipoarabinomannan of *Mycobacterium tuberculosis* Promotes Protein Tyrosine Dephosphorylation and Inhibition of Mitogen-activated Protein Kinase in Human Mononuclear Phagocytes: ROLE OF THE Src HOMOMOLOGY 2 CONTAINING TYROSINE PHOSPHATASE 1. *Journal of Biological Chemistry* **1998**, *273* (1), 645-652.
- (26) Chan, J.; Fan, X.; Hunter, S. W.; Brennan, P. J.; Bloom, B. R. Lipoarabinomannan, a possible virulence factor involved in persistence of *Mycobacterium tuberculosis* within macrophages. *Infection and Immunity* **1991**, *59* (5), 1755-1761.
- (27) Zhai, W.; Wu, F.; Zhang, Y.; Fu, Y.; Liu, Z. The immune escape mechanisms of *Mycobacterium tuberculosis*. *International Journal Of Molecular Sciences* **2019**, *20* (2), 340.
- (28) Chen, S.; Saeed, A. F.; Liu, Q.; Jiang, Q.; Xu, H.; Xiao, G. G.; Rao, L.; Duo, Y. Macrophages in immunoregulation and therapeutics. *Signal Transduction and Targeted Therapy* **2023**, *8* (1), 207.
- (29) Pagán, A. J.; Ramakrishnan, L. Immunity and immunopathology in the tuberculous granuloma. *Cold Spring Harbor Perspectives In Medicine* **2015**, *5* (9).
- (30) Heemskerck, D.; Caws, M.; Marais, B.; Farrar, J. Tuberculosis in adults and children. **2015**.
- (31) Rao, M.; Ippolito, G.; Mfinanga, S.; Ntoumi, F.; Yeboah-Manu, D.; Vilaplana, C.; Zumla, A.; Maeurer, M. Latent TB infection (LTBI)–*Mycobacterium tuberculosis* pathogenesis and the dynamics of the granuloma battleground. *International Journal of Infectious Diseases* **2019**, *80*, S58-S61.
- (32) Aaron, L.; Saadoun, D.; Calatroni, I.; Launay, O.; Memain, N.; Vincent, V.; Marchal, G.; Dupont, B.; Bouchaud, O.; Valeyre, D. Tuberculosis in HIV-infected patients: a comprehensive review. *Clinical Microbiology And Infection* **2004**, *10* (5), 388-398.
- (33) Gengenbacher, M.; Kaufmann, S. H. *Mycobacterium tuberculosis*: success through dormancy. *FEMS Microbiology Reviews* **2012**, *36* (3), 514-532.
- (34) Delogu, G.; Sali, M.; Fadda, G. The biology of mycobacterium tuberculosis infection. *Mediterranean Journal Of Hematology And Infectious Diseases* **2013**, *5* (1).
- (35) Colditz, G. A.; Brewer, T. F.; Berkey, C. S.; Wilson, M. E.; Burdick, E.; Fineberg, H. V.; Mosteller, F. Efficacy of BCG vaccine in the prevention of tuberculosis: meta-analysis of the published literature. *Jama* **1994**, *271* (9), 698-702.
- (36) Abubakar, I.; Pimpin, L.; Ariti, C.; Beynon, R.; Mangtani, P.; Sterne, J.; Fine, P.; Smith, P.; Lipman, M.; Elliman, D. Systematic review and meta-analysis of the current evidence on the duration of protection by bacillus Calmette-Guérin vaccination against tuberculosis. *Health Technology Assessment (Winchester, England)* **2013**, *17* (37), 1.
- (37) Brewer, T. F. Preventing tuberculosis with bacillus Calmette-Guerin vaccine: a meta-analysis of the literature. *Clinical Infectious Diseases* **2000**, *31* (Supplement_3), S64-S67.
- (38) Maurya, S. K.; Aqdas, M.; Das, D. K.; Singh, S.; Nadeem, S.; Kaur, G.; Agrewala, J. N. A multiple T cell epitope comprising DNA vaccine boosts the protective efficacy of Bacillus Calmette–Guérin (BCG) against *Mycobacterium tuberculosis*. *BMC Infectious Diseases* **2020**, *20*, 1-14.
- (39) Marinova, D.; Gonzalo-Asensio, J.; Aguilo, N.; Martin, C. MTBVAC from discovery to clinical trials in tuberculosis-endemic countries. *Expert Review Of Vaccines* **2017**, *16* (6), 565-576.
- (40) Dockrell, H. M.; Smith, S. G. What have we learnt about BCG vaccination in the last 20 years? *Frontiers In Immunology* **2017**, *8*, 1134.
- (41) Schatz, A.; Robinson, K. The true story of the discovery of streptomycin. *Actinomycetes* **1993**, *4* (2), 27-39.
- (42) Council, M. R. Streptomycin treatment of pulmonary tuberculosis. *Bmj* **1948**, *2* (4582), 769-782.
- (43) Fox, W.; Sutherland, I. A FIVE-YEAR ASSESSMENT OF PATIENTS IN A CONTROLLED TRIAL OF STREPTOMYCIN, PARA-AMINOSALICYLIC ACID, AND STREPTOMYCIN PLUS PARA-AMINOSALICYLIC ACID, IN PULMONARY TUBERCULOSIS1: Report to the Tuberculosis Chemotherapy Trials Committee of the Medical Research Council. *QJM: An International Journal of Medicine* **1956**, *25* (2), 221-244.

6. References

- (44) Fox, W.; Sutherland, I.; Daniels, M. A Five-Year Assessment of Patients in a Controlled Trial of Streptomycin in Pulmonary Tuberculosis. *Quarterly Journal of Medicine* **1954**, *23* (91), 347-366.
- (45) Keshavjee, S.; Farmer, P. E. Tuberculosis, drug resistance, and the history of modern medicine. *New England Journal of Medicine* **2012**, *367* (10), 931-936.
- (46) Sotgiu, G.; Sulis, G.; Matteelli, A. Tuberculosis—A world health organization perspective. *Tuberculosis and Nontuberculous Mycobacterial Infections* **2017**, 211-228.
- (47) Kai Johnsson, D. S. K., * and Peter G. Schultz* .*. Studies on the Mechanism of Action of Isoniazid and Ethionamide in the Chemotherapy of Tuberculosis
- (48) Marriner, G. A.; Nayyar, A.; Uh, E.; Wong, S. Y.; Mukherjee, T.; Via, L. E.; Carroll, M.; Edwards, R. L.; Gruber, T. D.; Choi, I.; et al. The Medicinal Chemistry of Tuberculosis Chemotherapy. In *Third World Diseases, Topics in Medicinal Chemistry*, **2011**; pp 47-124.
- (49) Mitchison, D.; Davies, G. The chemotherapy of tuberculosis: past, present and future [State of the art]. *The International Journal of Tuberculosis and Lung Disease* **2012**, *16* (6), 724-732.
- (50) Grayson, M. L.; Crowe, S. M.; McCarthy, J. S.; Mills, J.; Mouton, J. W.; Norrby, S. R.; Paterson, D. L.; Pfaller, M. A. *Kucers' The Use of Antibiotics Sixth Edition: A Clinical Review of Antibacterial, Antifungal and Antiviral Drugs*; CRC press, **2010**.
- (51) Dutt, A. K.; Moers, D.; Stead, W. W. Undesirable side effects of isoniazid and rifampin in largely twice-weekly short-course chemotherapy for tuberculosis. *American Review of Respiratory Disease* **1983**, *128* (3), 419-424.
- (52) Kim, J.-H.; Moon, J.-I.; Kim, J. E.; Choi, G.-S.; Park, H.-S.; Ye, Y.-M.; Yim, H. Cutaneous leukocytoclastic vasculitis due to anti-tuberculosis medications, rifampin and pyrazinamide. *Allergy, Asthma & Immunology Research* **2010**, *2* (1), 55-58.
- (53) Gopal, P.; Sarathy, J. P.; Yee, M.; Rangunathan, P.; Shin, J.; Bhushan, S.; Zhu, J.; Akopian, T.; Kandror, O.; Lim, T. K. Pyrazinamide triggers degradation of its target aspartate decarboxylase. *Nature Communications* **2020**, *11* (1), 1661.
- (54) Zhang, Y.; Shi, W.; Zhang, W.; Mitchison, D. Mechanisms of pyrazinamide action and resistance. *Microbiology Spectrum* **2014**, *2* (4), 10.1128/microbiolspec.mgm1122-0023-2013.
- (55) Hussain, Z.; Zhu, J.; Ma, X. Metabolism and hepatotoxicity of pyrazinamide, an antituberculosis drug. *Drug Metabolism and Disposition* **2021**, *49* (8), 679-682.
- (56) Shih, T.-Y.; Pai, C.-Y.; Yang, P.; Chang, W.-L.; Wang, N.-C.; Hu, O. Y.-P. A novel mechanism underlies the hepatotoxicity of pyrazinamide. *Antimicrobial Agents and Chemotherapy* **2013**, *57* (4), 1685-1690.
- (57) Ma, Z.; Ginsberg, A.; Spigelman, M. Comprehensive medicinal chemistry II. *Triggle D* **2007**.
- (58) Foye, W. O. *Foye's principles of medicinal chemistry*; Lippincott Williams & Wilkins, 2008.
- (59) Shahab, F.; Kobarfard, F.; Shafaghi, B.; Dadashzadeh, S. Preclinical pharmacokinetics of KBF611, a new antituberculosis agent in mice and rabbits, and comparison with thiacetazone. *Xenobiotica* **2010**, *40* (3), 225-234.
- (60) Organization, W. H. *Global tuberculosis report 2013*; World Health Organization, 2013.
- (61) Brammachary, U.; Ramachandra, V.; Palavesam, S.; Kapalamurthy, V. R. C.; Muralidhar, A.; Muthaiah, M. Mechanisms and Action of Drug Resistance on Mycobacterium tuberculosis. *Antibiotic Resistance-New Insights* **2022**.
- (62) Shibeshi, W.; Sheth, A. N.; Admasu, A.; Berha, A. B.; Negash, Z.; Yimer, G. Nephrotoxicity and ototoxic symptoms of injectable second-line anti-tubercular drugs among patients treated for MDR-TB in Ethiopia: a retrospective cohort study. *BMC Pharmacology and Toxicology* **2019**, *20*, 1-10.
- (63) Tiberi, S.; Scardigli, A.; Centis, R.; D'Ambrosio, L.; Munoz-Torrico, M.; Salazar-Lezama, M. A.; Spanevello, A.; Visca, D.; Zumla, A.; Migliori, G. B. Classifying new anti-tuberculosis drugs: rationale and future perspectives. *International Journal of Infectious Diseases* **2017**, *56*, 181-184.

6. References

- (64) Seaworth, B. J.; Griffith, D. E. Therapy of multidrug-resistant and extensively drug-resistant tuberculosis. *Tuberculosis and Nontuberculous Mycobacterial Infections* **2017**, 129-158.
- (65) Pallo-Zimmerman, L. M.; Byron, J. K.; Graves, T. K. Fluoroquinolones: then and now. *Compend Contin Educ Vet* **2010**, 32 (7), E1-9.
- (66) Moadebi, S.; Harder, C. K.; Fitzgerald, M. J.; Elwood, K. R.; Marra, F. Fluoroquinolones for the treatment of pulmonary tuberculosis. *Drugs* **2007**, 67, 2077-2099.
- (67) Berning, S. E. The role of fluoroquinolones in tuberculosis today. *Drugs* **2001**, 61, 9-18.
- (68) OTTEN, H. IX. Thioamides: Ethionamide (ETH), Prothionamide (PTH). *Antituberculosis Drugs* **2013**, 84, 167.
- (69) Schaaf, H.; Victor, T.; Venter, A.; Brittle, W.; Jordaan, A.; Hesselning, A.; Marais, B.; Van Helden, P.; Donald, P. Ethionamide cross-and co-resistance in children with isoniazid-resistant tuberculosis. *The International Journal of Tuberculosis and Lung Disease* **2009**, 13 (11), 1355-1359.
- (70) Tala, E.; Tevola, K. Side effects and toxicity of ethionamide and prothionamide. *Ann. Clin. Res.* **1969**, 1 (1), 32-35.
- (71) Huang, W.-C.; Huang, C.-W.; Hsu, K.-M.; Chien, S.-H.; Yu, M.-C. High Incidence of Treatment-Related Hypothyroidism in Multidrug-Resistant Tuberculosis Patients. *胸腔醫學* **2014**, 29 (4), 209-217.
- (72) Tiberi, S.; Munoz-Torrico, M.; Duarte, R.; Dalcolmo, M.; D'Ambrosio, L.; Migliori, G. B. New drugs and perspectives for new anti-tuberculosis regimens. *Pulmonology* **2018**, 24 (2), 86-98. DOI: 10.1016/j.rppnen.2017.10.009.
- (73) Halouska, S.; Fenton, R. J.; Zinniel, D. K.; Marshall, D. D.; Barletta, R. I. G.; Powers, R. Metabolomics analysis identifies d-Alanine-d-Alanine ligase as the primary lethal target of d-Cycloserine in mycobacteria. *Journal of Proteome Research* **2014**, 13 (2), 1065-1076.
- (74) Kendig, I. V.; Charen, S.; Lepine, L. T. Psychological side effects induced by cycloserine in the treatment of pulmonary tuberculosis. *American Review of Tuberculosis and Pulmonary Diseases* **1956**, 73 (3), 438-441.
- (75) Roelens, M.; Battista Migliori, G.; Rozanova, L.; Estill, J.; Campbell, J. R.; Cegielski, J. P.; Tiberi, S.; Palmero, D.; Fox, G. J.; Guglielmetti, L. Evidence-based definition for extensively drug-resistant tuberculosis. *American Journal of Respiratory and Critical Care Medicine* **2021**, 204 (6), 713-722.
- (76) Khoshnood, S.; Goudarzi, M.; Taki, E.; Darbandi, A.; Kouhsari, E.; Heidary, M.; Motahar, M.; Moradi, M.; Bazayr, H. Bedaquiline: Current status and future perspectives. *Journal of Global Antimicrobial Resistance* **2021**, 25, 48-59.
- (77) Felipe dos Santos Fernandes, G.; Hartmann Jornada, P.; de Souza, C.; Man Chin, C.; Rogerio Pavan, F.; Leandro dos Santos, J. Current advances in antitubercular drug discovery: Potent prototypes and new targets. *Current Medicinal Chemistry* **2015**, 22 (27), 3133-3161.
- (78) Sutherland, H. S.; Lu, G.-L.; Tong, A. S.; Conole, D.; Franzblau, S. G.; Upton, A. M.; Lotlikar, M. U.; Cooper, C. B.; Palmer, B. D.; Choi, P. J. Synthesis and structure-activity relationships for a new class of tetrahydronaphthalene amide inhibitors of Mycobacterium tuberculosis. *European Journal of Medicinal Chemistry* **2022**, 229, 114059.
- (79) Nizamuddin, S.; Khan, F. A.; Khan, A. R.; Kamaal, C. M. Assessment of hearing loss in multidrug resistant tuberculosis (MDR-TB) patients undergoing aminoglycoside treatment. *Int J Res Med Sci* **2015**, 3 (7), 1734-1740.
- (80) Andries, K.; Villellas, C.; Coeck, N.; Thys, K.; Gevers, T.; Vranckx, L.; Lounis, N.; de Jong, B. C.; Koul, A. Acquired resistance of Mycobacterium tuberculosis to bedaquiline. *PLOS One* **2014**, 9 (7), e102135.
- (81) Brooks, J. V.; Furney, S. K.; Orme, I. M. Metronidazole therapy in mice infected with tuberculosis. *Antimicrobial Agents and Chemotherapy* **1999**, 43 (5), 1285-1288.
- (82) Mudde, S. E.; Upton, A. M.; Lenaerts, A.; Bax, H. I.; De Steenwinkel, J. E. Delamanid or pretomanid? A Solomonic judgement! *Journal of Antimicrobial Chemotherapy* **2022**, 77 (4), 880-902.

6. References

- (83) Zhang, J.; Ba, Y.; Wang, S.; Yang, H.; Hou, X.; Xu, Z. Nitroimidazole-containing compounds and their antibacterial and antitubercular activities. *European Journal of Medicinal Chemistry* **2019**, *179*, 376-388.
- (84) Tasneen, R.; Williams, K.; Amoabeng, O.; Minkowski, A.; Mdluli, K. E.; Upton, A. M.; Nueremberger, E. L. Contribution of the nitroimidazoles PA-824 and TBA-354 to the activity of novel regimens in murine models of tuberculosis. *Antimicrobial Agents and Chemotherapy* **2015**, *59* (1), 129-135.
- (85) Hedaya, M. A.; Thomas, V.; Abdel-Hamid, M. E.; Kehinde, E. O.; Phillips, O. A. Comparative pharmacokinetic study for linezolid and two novel antibacterial oxazolidinone derivatives in rabbits: Can differences in the pharmacokinetic properties explain the discrepancies between their in vivo and in vitro antibacterial activities? *Pharmaceutics* **2017**, *9* (3), 34.
- (86) Wen, S.; Gao, X.; Zhao, W.; Huo, F.; Jiang, G.; Dong, L.; Zhao, L.; Wang, F.; Yu, X.; Huang, H. In Vitro efficacy comparison of linezolid, tedizolid, sutezolid and delpazolid against rapid growing Mycobacteria isolated in Beijing, China. *BioRxiv* **2020**, 2020.2006. 2025.172742.
- (87) Wallis, R. S.; Dawson, R.; Friedrich, S. O.; Venter, A.; Paige, D.; Zhu, T.; Silvia, A.; Gobey, J.; Ellery, C.; Zhang, Y. Mycobactericidal activity of sutezolid (PNU-100480) in sputum (EBA) and blood (WBA) of patients with pulmonary tuberculosis. *PLoS One* **2014**, *9* (4), e94462.
- (88) Reddy, V. M.; Dubuisson, T.; Einck, L.; Wallis, R. S.; Jakubiec, W.; Ladukto, L.; Campbell, S.; Nacy, C. A. SQ109 and PNU-100480 interact to kill Mycobacterium tuberculosis in vitro. *Journal of Antimicrobial Chemotherapy* **2012**, *67* (5), 1163-1166.
- (89) Appetecchia, F.; Consalvi, S.; Scarpecci, C.; Biava, M.; Poce, G. SAR analysis of small molecules interfering with energy-metabolism in Mycobacterium tuberculosis. *Pharmaceutics* **2020**, *13* (9), 227.
- (90) Pethe, K.; Bifani, P.; Jang, J.; Kang, S.; Park, S.; Ahn, S.; Jiricek, J.; Jung, J.; Jeon, H. K.; Cechetto, J. Discovery of Q203, a potent clinical candidate for the treatment of tuberculosis. *Nature Medicine* **2013**, *19* (9), 1157-1160.
- (91) Yathursan, S.; Wiles, S.; Read, H.; Sarojini, V. A review on anti-tuberculosis peptides: Impact of peptide structure on anti-tuberculosis activity. *Journal of Peptide Science* **2019**, *25* (11), e3213.
- (92) Di, L.; Kerns, E. H.; Hong, Y.; Chen, H. Development and application of high throughput plasma stability assay for drug discovery. *International Journal of Pharmaceutics* **2005**, *297* (1-2), 110-119.
- (93) Rodriguez, L. M. D. L.; Kaur, H.; Brimble, M. A. Synthesis and bioactivity of antitubercular peptides and peptidomimetics: an update. *Organic & Biomolecular Chemistry* **2016**, *14* (4), 1177-1187.
- (94) Sharma, S.; Verma, I.; Khuller, G. Biochemical interaction of human neutrophil peptide-1 with Mycobacterium tuberculosis H37Ra. *Archives of Microbiology* **1999**, *171*, 338-342.
- (95) Davies, S. J.; Ayscough, A. P.; Beckett, R. P.; Bragg, R. A.; Clements, J. M.; Doel, S.; Grew, C.; Launchbury, S. B.; Perkins, G. M.; Pratt, L. M. Structure-activity relationships of the peptide deformylase inhibitor BB-3497: modification of the methylene spacer and the P1' side chain. *Bioorganic & Medicinal Chemistry Letters* **2003**, *13* (16), 2709-2713.
- (96) Barqi, M. M.; Ashar, A.; Bhutta, Z. A.; Javed, M.; Abdellah, I. M.; Eletmany, M. R. Comprehensive Investigation of the Potential of Hydrazine and its Derivatives for the Synthesis of Various Molecules with Biological Activity. *Chemistry and Industry* **2023**, *4*, 6.
- (97) Angelova, V. T.; Valcheva, V.; Vassilev, N. G.; Buyukliev, R.; Momekov, G.; Dimitrov, I.; Saso, L.; Djukic, M.; Shivachev, B. Antimycobacterial activity of novel hydrazide-hydrazone derivatives with 2H-chromene and coumarin scaffold. *Bioorganic & Medicinal Chemistry Letters* **2017**, *27* (2), 223-227.
- (98) Murray, C. J.; Ikuta, K. S.; Sharara, F.; Swetschinski, L.; Aguilar, G. R.; Gray, A.; Han, C.; Bisignano, C.; Rao, P.; Wool, E. Global burden of bacterial antimicrobial resistance in 2019: a systematic analysis. *The Lancet* **2022**, *399* (10325), 629-655.

6. References

- (99) Batoool, R.; Khan, S. W.; Imran, M.; Barry, Z.; Ali, S. Z. Culture conversion and six months interim outcomes in retreatment cases of pulmonary MDRTB—a six month interim analysis. *JPMA. The Journal of the Pakistan Medical Association* **2021**, *71* (12), 2710-2716.
- (100) Uplekar, M. Involving private health care providers in delivery of TB care: global strategy. *Tuberculosis* **2003**, *83* (1-3), 156-164.
- (101) Calligaro, G. L.; Moodley, L.; Symons, G.; Dheda, K. The medical and surgical treatment of drug-resistant tuberculosis. *Journal of Thoracic Disease* **2014**, *6* (3), 186.
- (102) Gandhi, N. R.; Shah, N. S.; Andrews, J. R.; Vella, V.; Moll, A. P.; Scott, M.; Weissman, D.; Marra, C.; Laloo, U. G.; Friedland, G. H. HIV coinfection in multidrug-and extensively drug-resistant tuberculosis results in high early mortality. *American Journal of Respiratory and Critical Care Medicine* **2010**, *181* (1), 80-86.
- (103) Bai, J.; Li, W.; Huang, Y.-M.; Guo, Y. Bibliometric study of research and development for neglected diseases in the BRICS. *Infectious Diseases of Poverty* **2016**, *5* (1), 1-10.
- (104) Almeida Da Silva, P. E.; Palomino, J. C. Molecular basis and mechanisms of drug resistance in Mycobacterium tuberculosis: classical and new drugs. *Journal of Antimicrobial Chemotherapy* **2011**, *66* (7), 1417-1430.
- (105) Coll, F.; McNerney, R.; Preston, M. D.; Guerra-Assunção, J. A.; Warry, A.; Hill-Cawthorne, G.; Mallard, K.; Nair, M.; Miranda, A.; Alves, A. Rapid determination of anti-tuberculosis drug resistance from whole-genome sequences. *Genome Medicine* **2015**, *7* (1), 1-10.
- (106) Feldgarden, M.; Brover, V.; Haft, D. H.; Prasad, A. B.; Slotta, D. J.; Tolstoy, I.; Tyson, G. H.; Zhao, S.; Hsu, C.-H.; McDermott, P. F. Validating the AMRFinder tool and resistance gene database by using antimicrobial resistance genotype-phenotype correlations in a collection of isolates. *Antimicrobial Agents and Chemotherapy* **2019**, *63* (11), 10.1128/aac.00483-00419.
- (107) Prasad, M. S.; Bhole, R. P.; Khedekar, P. B.; Chikhale, R. V. Mycobacterium enoyl acyl carrier protein reductase (InhA): A key target for antitubercular drug discovery. *Bioorganic Chemistry* **2021**, *115*, 105242.
- (108) Goldstein, B. P. Resistance to rifampicin: a review. *The Journal of Antibiotics* **2014**, *67* (9), 625-630.
- (109) Njire, M.; Tan, Y.; Mugweru, J.; Wang, C.; Guo, J.; Yew, W.; Tan, S.; Zhang, T. Pyrazinamide resistance in Mycobacterium tuberculosis: Review and update. *Advances In Medical Sciences* **2016**, *61* (1), 63-71.
- (110) Zhang, S.; Chen, J.; Shi, W.; Liu, W.; Zhang, W.; Zhang, Y. Mutations in panD encoding aspartate decarboxylase are associated with pyrazinamide resistance in Mycobacterium tuberculosis. *Emerging Microbes & Infections* **2013**, *2* (1), 1-5.
- (111) Zhang, Z.; Wang, Y.; Pang, Y.; Kam, K. M. Ethambutol resistance as determined by broth dilution method correlates better than sequencing results with embB mutations in multidrug-resistant Mycobacterium tuberculosis isolates. *Journal of Clinical Microbiology* **2014**, *52* (2), 638-641.
- (112) Khawbung, J. L.; Nath, D.; Chakraborty, S. Drug resistant Tuberculosis: A review. *Comparative immunology, microbiology and infectious diseases* **2021**, *74*, 101574.
- (113) Kabir, S.; Tahir, Z.; Mukhtar, N.; Sohail, M.; Saqalein, M.; Rehman, A. Fluoroquinolone resistance and mutational profile of gyrA in pulmonary MDR tuberculosis patients. *BMC Pulmonary Medicine* **2020**, *20*, 1-6.
- (114) Nath, H.; Ryoo, S. First- and Second-Line Drugs and Drug Resistance. In *Tuberculosis - Current Issues in Diagnosis and Management*, **2013**.
- (115) Laborde, J.; Deraeve, C.; Duhayon, C.; Pratviel, G.; Bernardes-Génisson, V. Ethionamide biomimetic activation and an unprecedented mechanism for its conversion into active and non-active metabolites. *Organic & Biomolecular Chemistry* **2016**, *14* (37), 8848-8858.
- (116) Vilchèze, C.; Jacobs Jr, W. R. Resistance to isoniazid and ethionamide in Mycobacterium tuberculosis: genes, mutations, and causalities. *Molecular Genetics of Mycobacteria* **2014**, 431-453.

6. References

- (117) Kerantzas, C. A.; Jacobs Jr, W. R. Origins of combination therapy for tuberculosis: lessons for future antimicrobial development and application. *MBio* **2017**, *8* (2), 10.1128/mbio. 01586-01516.
- (118) Zheng, J.; Rubin, E. J.; Bifani, P.; Mathys, V.; Lim, V.; Au, M.; Jang, J.; Nam, J.; Dick, T.; Walker, J. R. para-Aminosalicylic Acid Is a Prodrug Targeting Dihydrofolate Reductase in Mycobacterium tuberculosis♦. *Journal of Biological Chemistry* **2013**, *288* (32), 23447-23456.
- (119) Brown, A. K.; Aljohani, A. K.; Gill, J. H.; Steel, P. G.; Sellars, J. D. Identification of novel benzoxa-[2, 1, 3]-diazole substituted amino acid hydrazides as potential anti-tubercular agents. *Molecules* **2019**, *24* (4), 811.
- (120) Hutt, A.; Tan, S. Drug chirality and its clinical significance. *Drugs* **1996**, *52*, 1-12.
- (121) Robey, J. M.; Maity, S.; Aleshire, S. L.; Ghosh, A.; Yadaw, A. K.; Roy, S.; Mear, S. J.; Jamison, T. F.; Sirasani, G.; Senanayake, C. H. Application of Chiral Transfer Reagents to Improve Stereoselectivity and Yields in the Synthesis of the Antituberculosis Drug Bedaquiline. *Organic Process Research & Development* **2023**, *27* (11), 2146-2159.
- (122) Nguyen, L. A.; He, H.; Pham-Huy, C. Chiral drugs: an overview. *International Journal of Biomedical Science: IJBS* **2006**, *2* (2), 85.
- (123) Aljohani, A. K. Design, synthesis and SAR Evaluation of novel benzoxa-[2, 1, 3]-diazole amino acid hydrazides against mycobacterium tuberculosis. Newcastle University, **2022**.
- (124) Sun, H.; Tawa, G.; Wallqvist, A. Classification of scaffold-hopping approaches. *Drug Discovery Today* **2012**, *17* (7-8), 310-324.
- (125) Hessler, G.; Baringhaus, K.-H. The scaffold hopping potential of pharmacophores. *Drug Discovery Today: Technologies* **2010**, *7* (4), e263-e269.
- (126) Harvey, A. L. Natural products in drug discovery. *Drug Discovery Today* **2008**, *13* (19-20), 894-901.
- (127) Brown, A. K.; Aljohani, A. K.; Alsalem, F. M.; Broadhead, J. L.; Gill, J. H.; Lu, Y.; Sellars, J. D. Identification of substituted amino acid hydrazides as novel anti-tubercular agents, using a scaffold hopping approach. *Molecules* **2020**, *25* (10), 2387.
- (128) de Jager, V. R.; Dawson, R.; van Niekerk, C.; Hutchings, J.; Kim, J.; Vanker, N.; van der Merwe, L.; Choi, J.; Nam, K.; Diacon, A. H. Telacebec (Q203), a new antituberculosis agent. *New England Journal of Medicine* **2020**, *382* (13), 1280-1281.
- (129) Brown, A. K.; Aljohani, A. K. B.; Alsalem, F. M. A.; Broadhead, J. L.; Gill, J. H.; Lu, Y.; Sellars, J. D. Identification of Substituted Amino Acid Hydrazides as Novel Anti-Tubercular Agents, Using a Scaffold Hopping Approach. *Molecules* **2020**, *25* (10). DOI: 10.3390/molecules25102387.
- (130) Staneva, D.; Yordanova, S.; Vasileva-Tonkova, E.; Stoyanov, S.; Grabchev, I. Synthesis of a new fluorescent poly (propylene imine) dendrimer modified with 4-nitrobenzofurazan. Sensor and antimicrobial activity. *Journal of Photochemistry and Photobiology A: Chemistry* **2020**, *395*, 112506.
- (131) Cook, M. A.; Wright, G. D. The past, present, and future of antibiotics. *Science Translational Medicine* **2022**, *14* (657), eabo7793.
- (132) Samanta, S.; Kumar, S.; Aratikatla, E. K.; Ghorpade, S. R.; Singh, V. Recent developments of imidazo [1, 2-a] pyridine analogues as antituberculosis agents. *RSC Medicinal Chemistry* **2023**.
- (133) Bagdi, A. K.; Santra, S.; Monir, K.; Hajra, A. Synthesis of imidazo [1, 2-a] pyridines: a decade update. *Chemical Communications* **2015**, *51* (9), 1555-1575.
- (134) Mohana Roopan, S.; Patil, S. M.; Palaniraja, J. Recent synthetic scenario on imidazo [1, 2-a] pyridines chemical intermediate. *Research on Chemical Intermediates* **2016**, *42*, 2749-2790.
- (135) Kang, S.; Kim, Y. M.; Kim, R. Y.; Seo, M. J.; No, Z.; Nam, K.; Kim, S.; Kim, J. Synthesis and structure-activity studies of side chain analogues of the anti-tubercular agent, Q203. *European Journal of Medicinal Chemistry* **2017**, *125*, 807-815.
- (136) Benedetto Tiz, D.; Bagnoli, L.; Rosati, O.; Marini, F.; Sancineto, L.; Santi, C. New halogen-containing drugs approved by FDA in 2021: An overview on their syntheses and pharmaceutical use. *Molecules* **2022**, *27* (5), 1643.

6. References

- (137) Feder, H. M. J.; Osier, C.; Maderazo, E. G. Chloramphenicol: a review of its use in clinical practice. *Reviews of Infectious Diseases* **1981**, *3* (3), 479-491.
- (138) Costa, B.; Vale, N. Efavirenz: History, Development and Future. *Biomolecules* **2022**, *13* (1), 88.
- (139) Han, S.-Y.; Kim, Y.-A. Recent development of peptide coupling reagents in organic synthesis. *Tetrahedron* **2004**, *60* (11), 2447-2467.
- (140) Al Musaimi, O.; Jad, Y. E.; Kumar, A.; Collins, J. M.; Basso, A.; de la Torre, B. G.; Albericio, F. Investigating green ethers for the precipitation of peptides after global deprotection in solid-phase peptide synthesis. *Current Opinion in Green and Sustainable Chemistry* **2018**, *11*, 99-103.
- (141) Katawera, V.; Siedner, M.; Boum li, Y. Evaluation of the modified colorimetric resazurin microtiter plate-based antibacterial assay for rapid and reliable tuberculosis drug susceptibility testing. *BMC Microbiology* **2014**, *14*, 1-4.
- (142) Palomino, J.-C.; Martin, A.; Camacho, M.; Guerra, H.; Swings, J.; Portaels, F. Resazurin microtiter assay plate: simple and inexpensive method for detection of drug resistance in *Mycobacterium tuberculosis*. *Antimicrobial Agents and Chemotherapy* **2002**, *46* (8), 2720-2722.
- (143) Moraski, G. C.; Miller, P. A.; Bailey, M. A.; Ollinger, J.; Parish, T.; Boshoff, H. I.; Cho, S.; Anderson, J. R.; Mulugeta, S.; Franzblau, S. G. Putting tuberculosis (TB) to rest: transformation of the sleep aid, Ambien, and "anagrams" generated potent antituberculosis agents. *ACS Infectious Diseases* **2015**, *1* (2), 85-90.
- (144) Valverde, T. L.; Sampiron, E. G.; Montaholi, D. C.; Baldin, V. P.; Insaurralde, D. D.; Alves-Olher, V. G.; Siqueira, V. L.; Caleffi-Ferracioli, K. R.; Cardoso, R. F.; Vandresen, F. 3, 5-dinitrobenzoylhydrazone derivatives as a scaffold for antituberculosis drug development. *Future Microbiology* **2022**, *17* (4), 267-280.
- (145) Scarim, C. B.; Pavan, F. R. Recent advancement in drug development of nitro (NO₂)-heterocyclic compounds as lead scaffolds for the treatment of *Mycobacterium tuberculosis*. *Drug Development Research* **2022**, *83* (4), 842-858.
- (146) Noriega, S.; Cardoso-Ortiz, J.; López-Luna, A.; Cuevas-Flores, M. D. R.; Flores De La Torre, J. A. The Diverse Biological Activity of Recently Synthesized Nitro Compounds. *Pharmaceuticals* **2022**, *15* (6), 717.
- (147) Eke, I. E.; Williams, J. T.; Haiderer, E. R.; Albrecht, V. J.; Murdoch, H. M.; Abdalla, B. J.; Abramovitch, R. B. Discovery and characterization of antimycobacterial nitro-containing compounds with distinct mechanisms of action and in vivo efficacy. *Antimicrobial Agents and Chemotherapy* **2023**, *67* (9), e00474-00423.
- (148) Cheng, Y.; Xie, J.; Lee, K.-H.; Gaur, R. L.; Song, A.; Dai, T.; Ren, H.; Wu, J.; Sun, Z.; Banaei, N. Rapid and specific labeling of single live *Mycobacterium tuberculosis* with a dual-targeting fluorogenic probe. *Science translational medicine* **2018**, *10* (454), eaar4470.
- (149) Chikhale, R. V.; Barmade, M. A.; Murumkar, P. R.; Yadav, M. R. Overview of the development of DprE1 inhibitors for combating the menace of tuberculosis. *Journal of Medicinal Chemistry* **2018**, *61* (19), 8563-8593.
- (150) Christophe, T.; Jackson, M.; Jeon, H. K.; Fenistein, D.; Contreras-Dominguez, M.; Kim, J.; Genovesio, A.; Carralot, J.-P.; Ewann, F.; Kim, E. H. High content screening identifies decaprenyl-phosphoribose 2' epimerase as a target for intracellular antimycobacterial inhibitors. *PLoS Pathogens* **2009**, *5* (10), e1000645.
- (151) Li, L.; Lv, K.; Yang, Y.; Sun, J.; Tao, Z.; Wang, A.; Wang, B.; Wang, H.; Geng, Y.; Liu, M. Identification of N-benzyl 3, 5-dinitrobenzamides derived from PBTZ169 as antitubercular agents. *ACS Medicinal Chemistry Letters* **2018**, *9* (7), 741-745.
- (152) Karabanovich, G.; Němeček, J.; Valášková, L.; Carazo, A.; Konečná, K.; Stolaříková, J.; Hrabálek, A.; Pavliš, O.; Pávek, P.; Vávrová, K. S-substituted 3, 5-dinitrophenyl 1, 3, 4-oxadiazole-2-thiols and tetrazole-5-thiols as highly efficient antitubercular agents. *European Journal of Medicinal Chemistry* **2017**, *126*, 369-383.

6. References

- (153) Karabanovich, G.; Zemanová, J.; Smutný, T. s.; Székely, R.; Šarkan, M.; Centárová, I.; Vocat, A.; Pávková, I.; Čonka, P.; Němeček, J. Development of 3, 5-dinitrobenzylsulfanyl-1, 3, 4-oxadiazoles and thiadiazoles as selective antitubercular agents active against replicating and nonreplicating *Mycobacterium tuberculosis*. *Journal of Medicinal Chemistry* **2016**, *59* (6), 2362-2380.
- (154) Shea, J.; Halse, T. A.; Kohlerschmidt, D.; Lapierre, P.; Modestil, H. A.; Kearns, C. H.; Dworkin, F. F.; Rakeman, J. L.; Escuyer, V.; Musser, K. A. Low-level rifampin resistance and *rpoB* mutations in *Mycobacterium tuberculosis*: an analysis of whole-genome sequencing and drug susceptibility test data in New York. *Journal of Clinical Microbiology* **2021**, *59* (4), 10.1128/jcm.01885-01820.
- (155) Probes, C. F. RICHARD P. HAUGLAND. *Excited States of Biopolymers* **1983**, 29.
- (156) Occhineri, S.; Matucci, T.; Rindi, L.; Tiseo, G.; Falcone, M.; Riccardi, N.; Besozzi, G. Pretomanid for tuberculosis treatment: an update for clinical purposes. *Current Research In Pharmacology and Drug Discovery* **2022**, *3*, 100128.
- (157) Kim, P.; Zhang, L.; Manjunatha, U. H.; Singh, R.; Patel, S.; Jiricek, J.; Keller, T. H.; Boshoff, H. I.; Barry III, C. E.; Dowd, C. S. Structure– activity relationships of antitubercular nitroimidazoles. 1. Structural features associated with aerobic and anaerobic activities of 4-and 5-nitroimidazoles. *Journal of Medicinal Chemistry* **2009**, *52* (5), 1317-1328.
- (158) Baker, W. R. B., (WA), Shaopei, Cai (Seattle, WA), Keeler, Eric L. (Seattle, WA). Nitroimidazole antibacterial compounds and methods of use thereof. United States 1997.
- (159) Marcotullio, M. C.; Campagna, V.; Sternativo, S.; Costantino, F.; Curini, M. A new, simple synthesis of N-tosyl pyrrolidines and piperidines. *Synthesis* **2006**, 2760-2766.
- (160) Swamy, K. K.; Kumar, N. B.; Balaraman, E.; Kumar, K. P. Mitsunobu and related reactions: advances and applications. *Chemical Reviews* **2009**, *109* (6), 2551-2651.
- (161) Clayden, J.; Greeves, N.; Warren, S. *Organic chemistry*; Oxford University Press, USA, 2012.
- (162) Volante, R. A new, highly efficient method for the conversion of alcohols to thioesters and thiols. *Tetrahedron Letters* **1981**, *22* (33), 3119-3122.
- (163) Tipson, R. S. On esters of p-toluenesulfonic acid. *The Journal of Organic Chemistry* **1944**, *9* (3), 235-241.
- (164) Eglinton, G.; Whiting, M. 721. Researches on acetylenic compounds. Part XXVII. The preparation and properties of the toluene-p-sulphonates of acetylenic alcohols. *Journal of the Chemical Society (Resumed)* **1950**, 3650-3656.
- (165) Agarwal, D.; Soni, J.; Sethiya, A.; Sahiba, N.; Teli, P.; Agarwal, S. Recent advancements on imidazole containing heterocycles as antitubercular agents. *Imidazole-Based Drug Discovery* **2021**, 133-166.
- (166) Aly, H.; El-Shafie, A. S.; El-Azazy, M. Utilization of 7-chloro-4-nitrobenzo-2-oxa-1, 3-diazole (NBD-Cl) for spectrochemical determination of L-ornithine: A multivariate optimization-assisted approach. *RSC Advances* **2019**, *9* (38), 22106-22115.
- (167) Pesnot, T.; Gershater, M. C.; Ward, J. M.; Hailes, H. C. Phosphate mediated biomimetic synthesis of tetrahydroisoquinoline alkaloids. *Chemical Communications* **2011**, *47* (11), 3242-3244.
- (168) Kim, Y.; Cramer, C. J.; Truhlar, D. G. Steric effects and solvent effects on SN2 reactions. *The Journal of Physical Chemistry A* **2009**, *113* (32), 9109-9114.
- (169) Jung, M. E.; Dong, T. A.; Cai, X. Improved synthesis of 4-amino-7-nitrobenzo-2, 1, 3-oxadiazoles using NBD fluoride (NBD-F). *Tetrahedron letters* **2011**, *52* (20), 2533-2535.
- (170) Štimac, A.; Šekutor, M.; Mlinarić-Majerski, K.; Frkanec, L.; Frkanec, R. Adamantane in drug delivery systems and surface recognition. *Molecules* **2017**, *22* (2), 297.
- (171) Zelmer, A.; Carroll, P.; Andreu, N.; Hagens, K.; Mahlo, J.; Redinger, N.; Robertson, B. D.; Wiles, S.; Ward, T. H.; Parish, T. A new in vivo model to test anti-tuberculosis drugs using fluorescence imaging. *Journal of Antimicrobial Chemotherapy* **2012**, *67* (8), 1948-1960.
- (172) Mohi-Ud-Din, R.; Chawla, A.; Sharma, P.; Mir, P. A.; Potoo, F. H.; Reiner, Ž.; Reiner, I.; Ateşşahin, D. A.; Sharifi-Rad, J.; Mir, R. H. Repurposing approved non-oncology drugs for cancer

6. References

therapy: A comprehensive review of mechanisms, efficacy, and clinical prospects. *European Journal of Medical Research* **2023**, *28* (1), 345.

(173) Lv, S.; Zhang, Y.; Song, J.; Chen, J.; Huang, B.; Luo, Y.; Zhao, Y. Cerulenin suppresses ErbB2-overexpressing breast cancer by targeting ErbB2/PKM2 pathway. *Medical Oncology* **2022**, *40* (1), 5.

7. Appendix

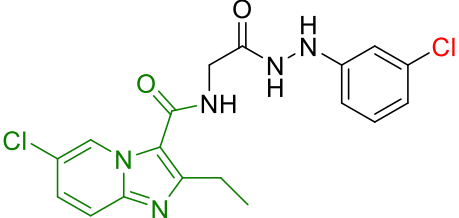
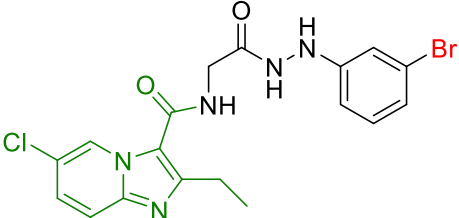
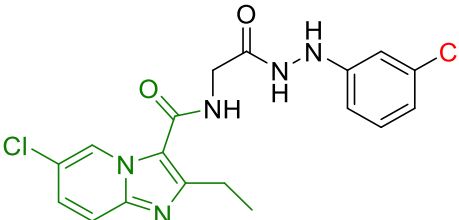
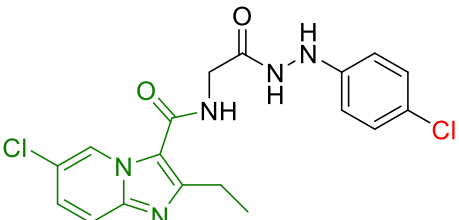
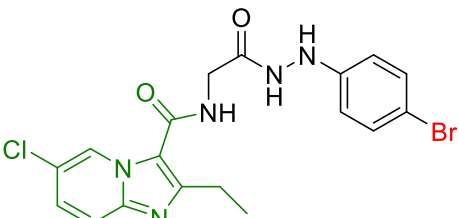
7. Appendix

7.1 The biological data for *in vitro* evaluating antitubercular activity

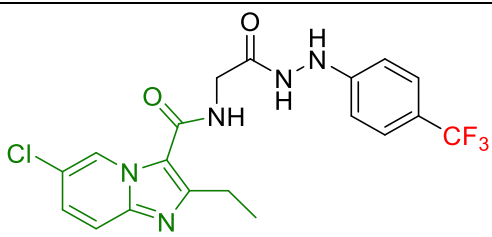
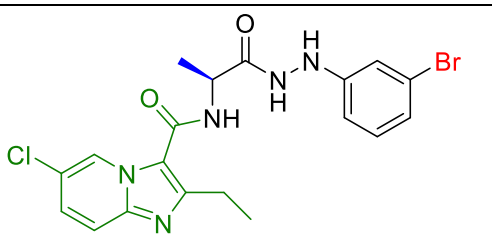
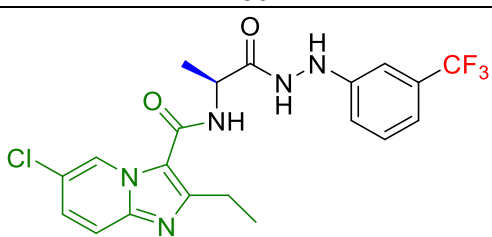
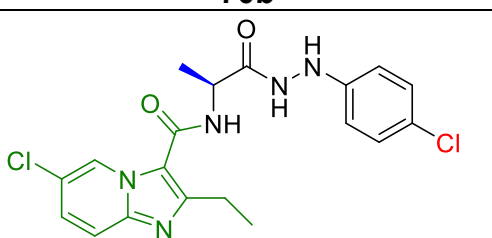
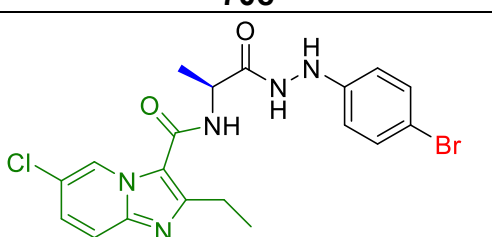
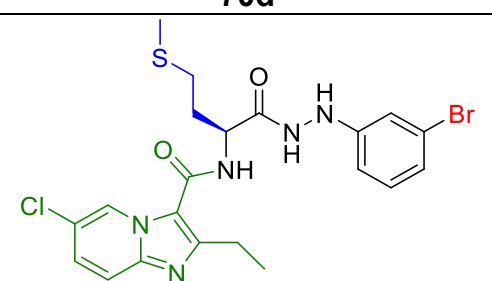
As observed for *in vitro* antitubercular screening, the MIC results of the imidazo [1, 2a] pyridine substituted amino acid hydrazide compounds **69a** - **75f** against wild-type *Mtb*, isoniazid-resistant *Mtb* strain and rifampicin-resistant *Mtb* were obtained.

7.1.1 Q203 analogues MIC values.

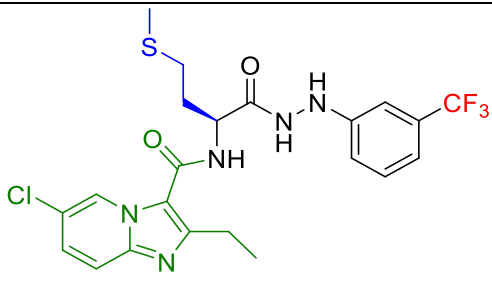
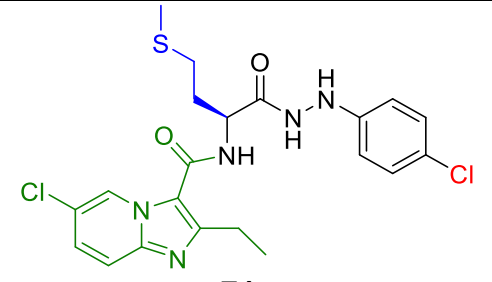
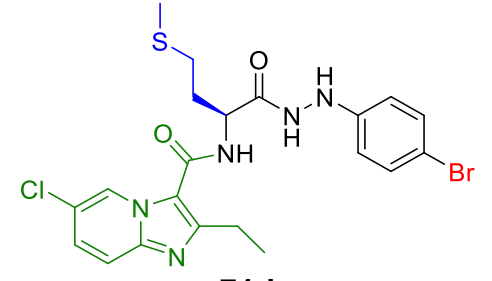
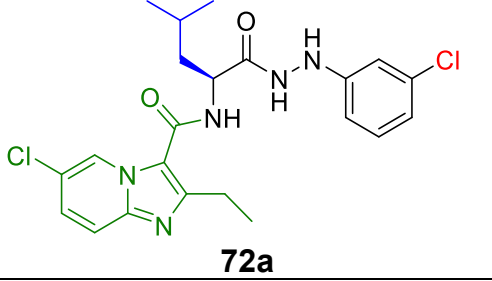
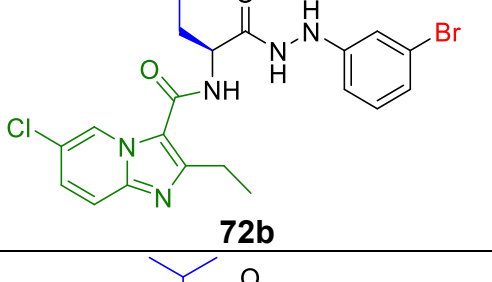
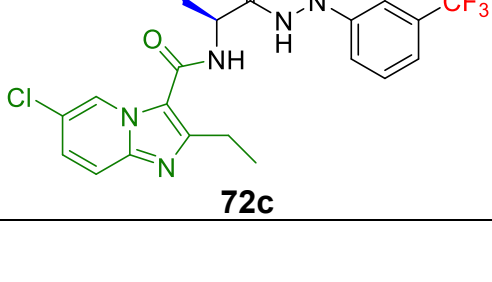
7. Appendix

Compound Structure	7902 WT (μM)	8245 INH ^R (μM)	8250 RIF/INH ^R (μM)	8258 RIF/INH ^R (μM)
 <p>69a</p>	39	39	39	39
 <p>69b</p>	71	71	71	71
 <p>69c</p>	–	–	–	–
 <p>69d</p>	79	79	79	79
 <p>69e</p>	71	35	35	35

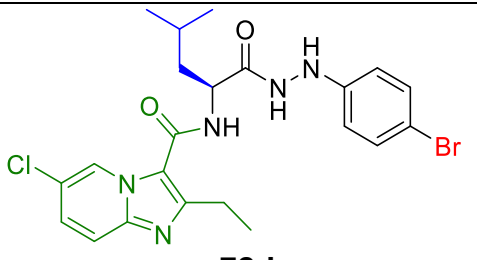
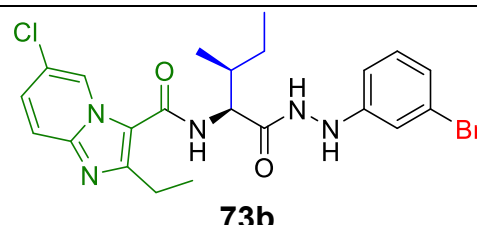
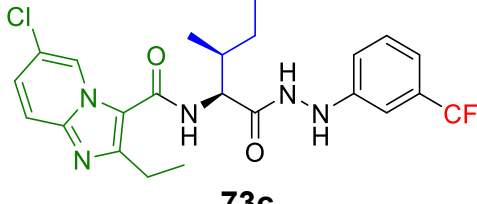
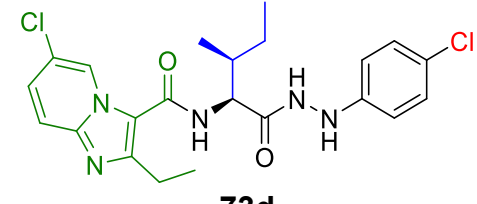
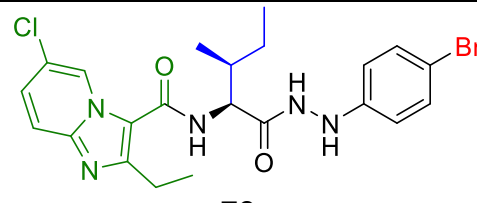
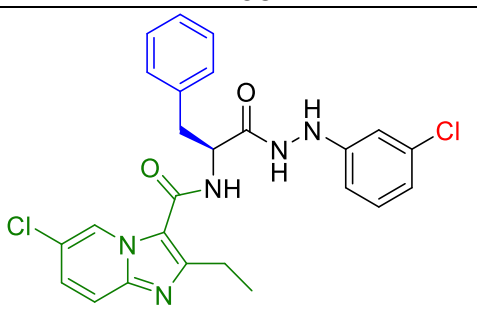
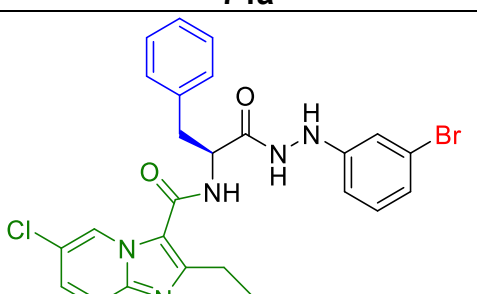
7. Appendix

 <p>69f</p>	36	36	36	36
 <p>70a</p>	69	138	—	69
 <p>70b</p>	—	—	—	—
 <p>70c</p>	—	—	—	—
 <p>70d</p>	152	152	152	152
 <p>71a</p>	—	—	—	—

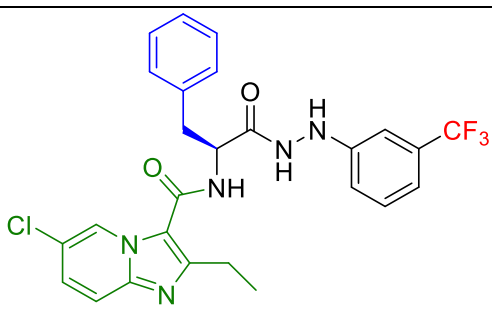
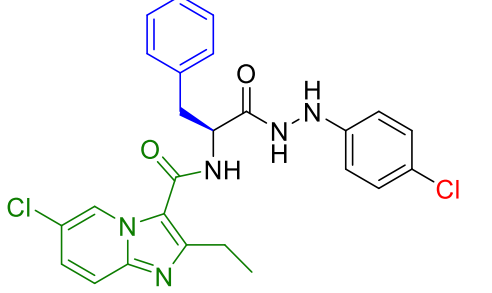
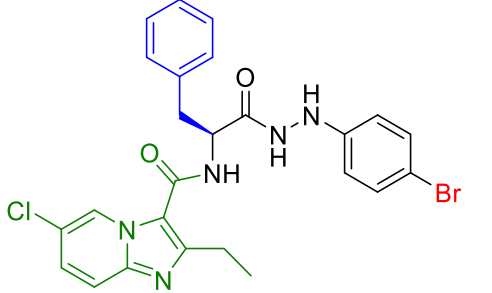
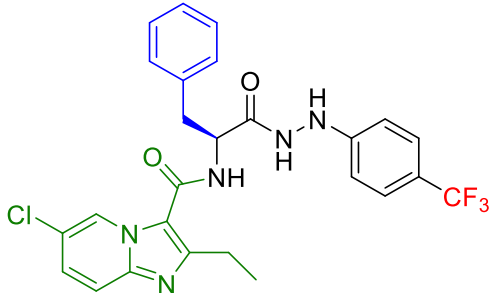
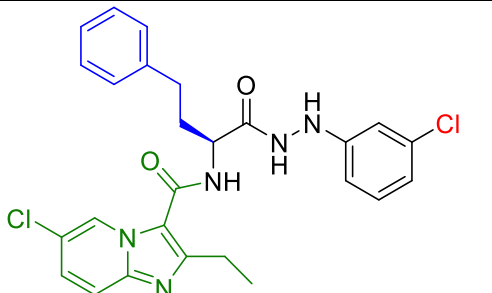
7. Appendix

 <p>71b</p>	125	125	125	125
 <p>71c</p>	-	-	-	-
 <p>71d</p>	-	-	-	-
 <p>72a</p>	-	-	-	-
 <p>72b</p>	126	126	126	126
 <p>72c</p>	-	-	-	-

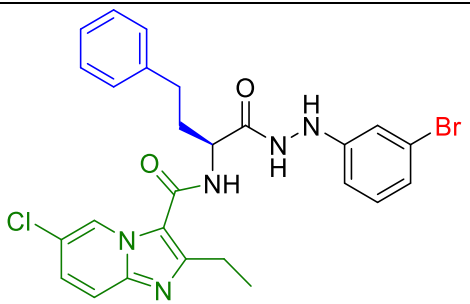
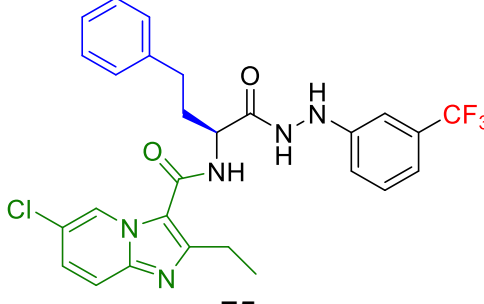
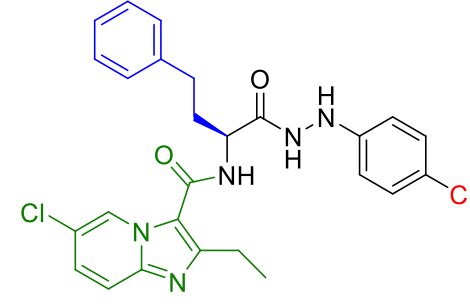
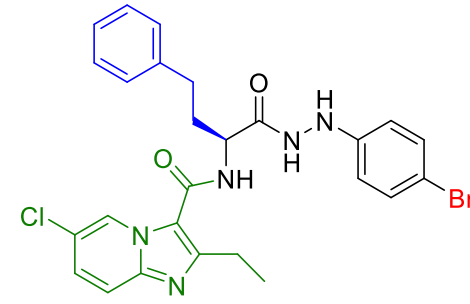
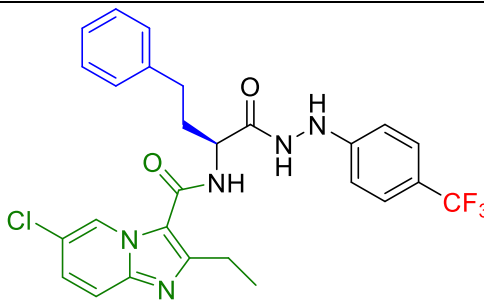
7. Appendix

 <p>72d</p>	-	-	-	-
 <p>73b</p>	-	-	-	-
 <p>73c</p>	-	-	-	-
 <p>73d</p>	-	-	-	-
 <p>73e</p>	-	-	-	-
 <p>74a</p>	-	-	-	-
	-	-	-	-

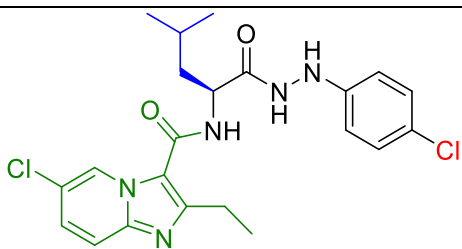
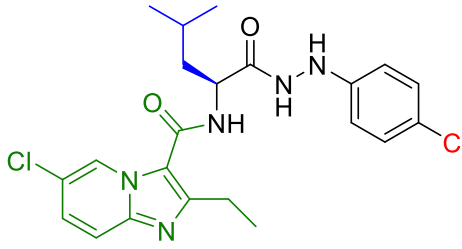
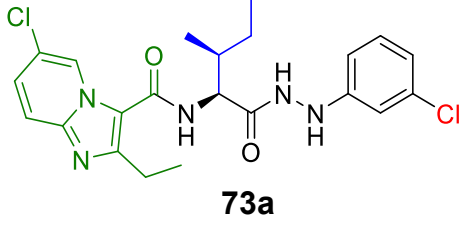
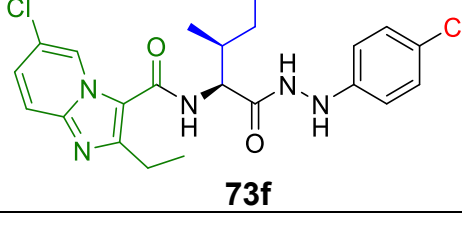
7. Appendix

<p style="text-align: center;">74b</p>  <p style="text-align: center;">74c</p>	-	-	-	-
 <p style="text-align: center;">74d</p>	-	-	-	-
 <p style="text-align: center;">74e</p>	-	-	-	-
 <p style="text-align: center;">74f</p>	60	60	60	60
 <p style="text-align: center;">75a</p>	-	-	-	-

7. Appendix

 <p>75b</p>	-	-	-	-
 <p>75c</p>	-	-	-	-
 <p>75d</p>	-	-	-	-
 <p>75e</p>	-	-	-	-
 <p>75f</p>	118	118	118	118

7. Appendix

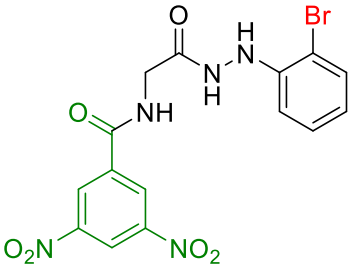
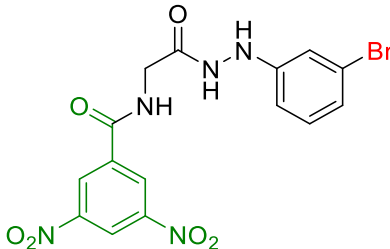
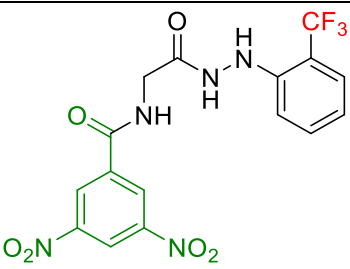
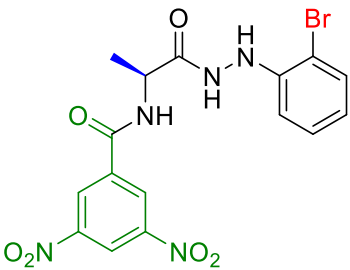
Compound structure	7000 WT (μM)	7002 RIF ^R (μM)	7021 INH ^R (μM)
 <p>71d</p>	-	-	-
 <p>71f</p>	-	-	-
 <p>73a</p>	65	-	65
 <p>73f</p>	-	-	-

7. Appendix

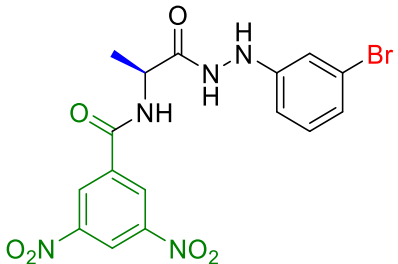
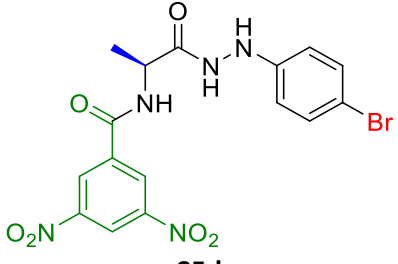
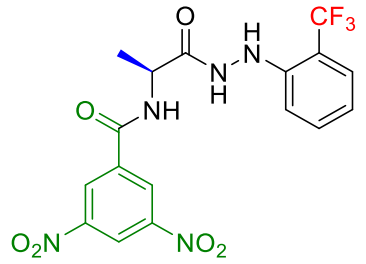
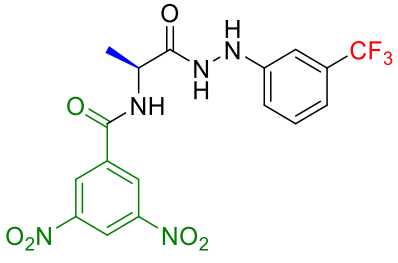
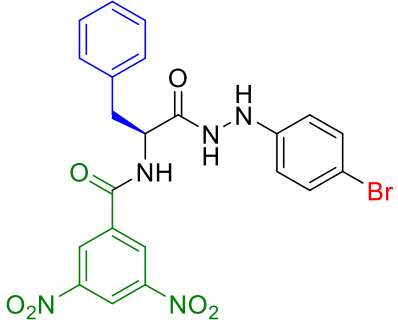
7.1.2 3,5-dinitrobenzene amino acid hydrazide compounds MIC values.

The *in vitro* antitubercular screening, the MIC results of the 3,5-dinitrobenzene substituted amino acid hydrazide compounds **84a** - **89h** against wild-type *Mtb*, isoniazid-resistant *Mtb* strain and rifampicin-resistant *Mtb* were obtained.

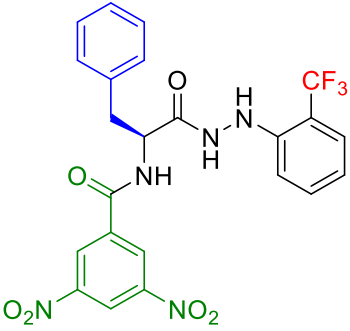
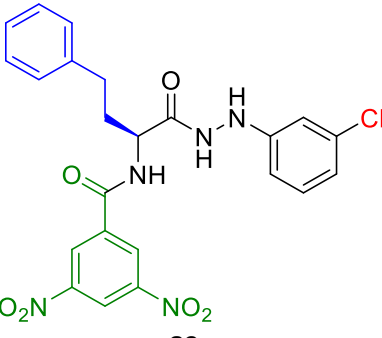
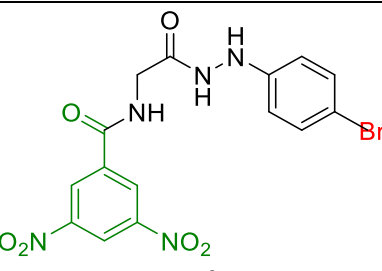
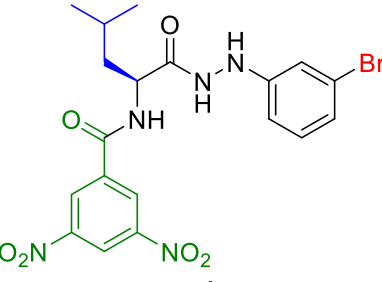
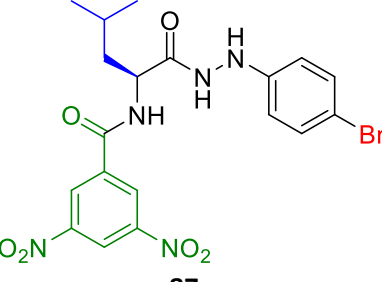
7. Appendix

Compound Structure	7902 WT (μM)	8245 INH ^R (μM)	8247 RIF ^R	8250 RIF/INH ^R (μM)	8258 RIF/INH ^R (μM)
 <p>84c</p>	18	18		18	18
 <p>84d</p>	-	-		-	-
 <p>Log P: 1.99 84f</p>	37	37		37	37
 <p>85b</p>	35	35		35	35

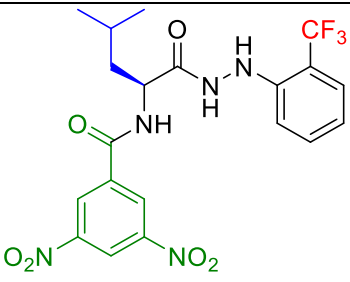
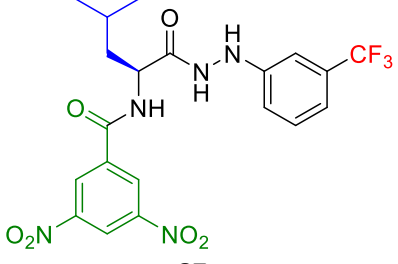
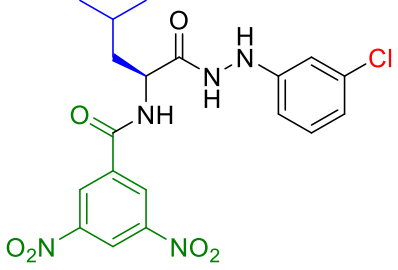
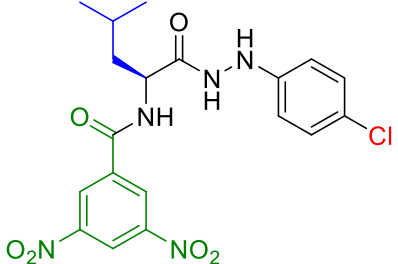
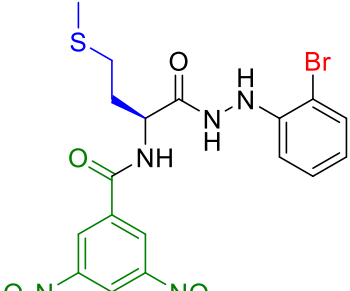
7. Appendix

 <p>85c</p>	18	18		18	18
 <p>85d</p>	35	35		35	35
 <p>Log P: 2.31 85e</p>	18	18		18	18
 <p>85f</p>	36	36		36	36
 <p>86e</p>	-	-		-	-

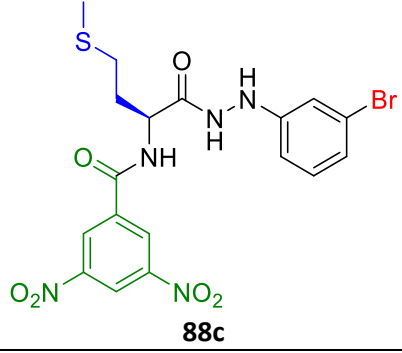
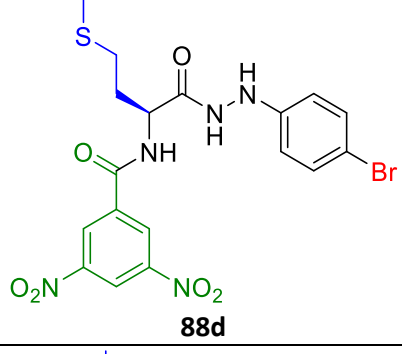
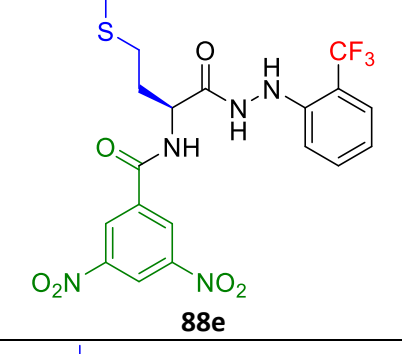
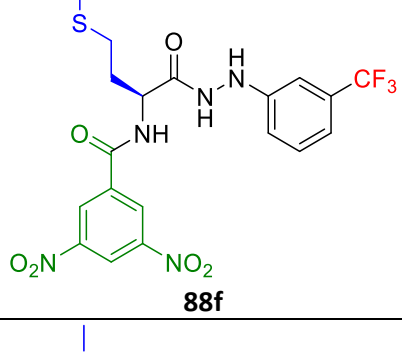
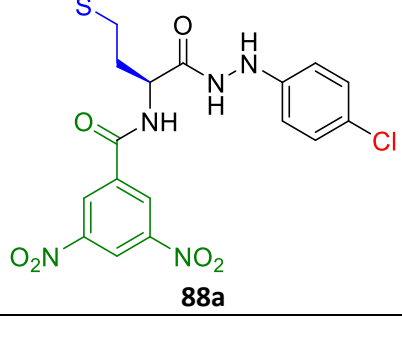
7. Appendix

 <p>Log P: 3.79 86f</p>	4	4		4	4
 <p>89a</p>	8	8		8	8
Compound structure	7902 WT	7902 pMV	8245 INH^R	8247 RIF^R	8050 INH^R/RIF^R
 <p>84d</p>	9	9	9	9	9
 <p>87d</p>	129	64	64	129	129
 <p>87e</p>	16	16	8	16	16

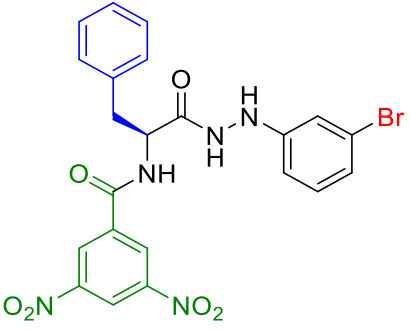
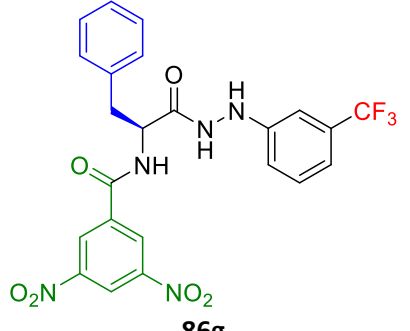
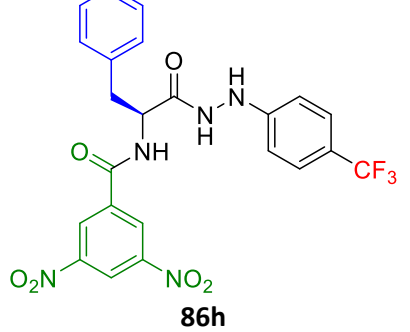
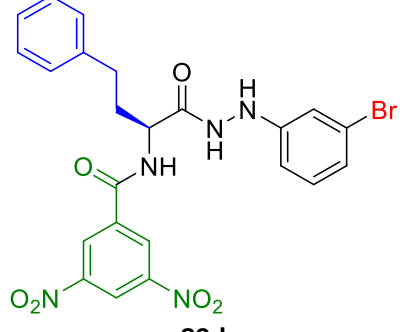
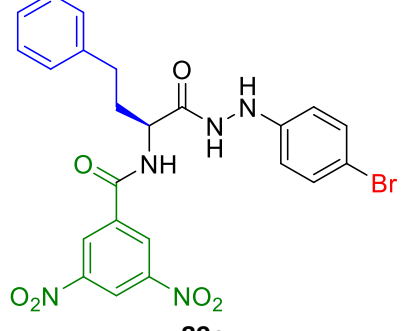
7. Appendix

 <p>87f</p>	8	8	8	8	8
 <p>87g</p>	17	8	8	17	17
 <p>87a</p>	18	9	9	9	9
 <p>87b</p>	18	18	9	18	18
 <p>88b</p>	16	16	16	16	16

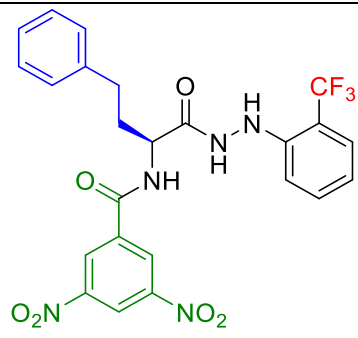
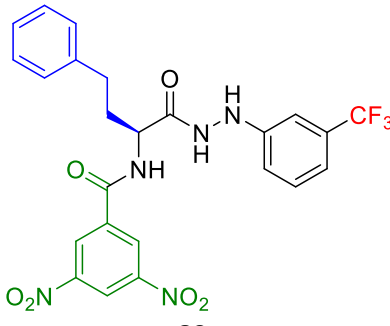
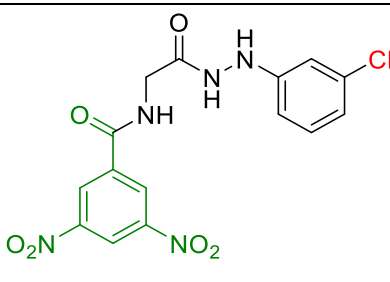
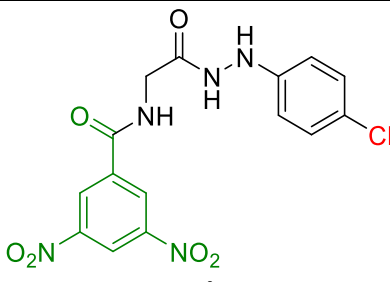
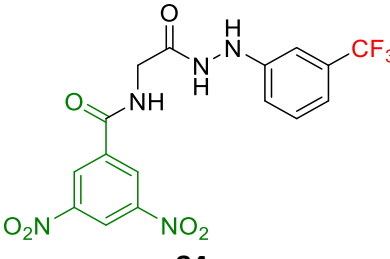
7. Appendix

 <p>88c</p>	63	63	63	63	31
 <p>88d</p>	125	125	63	125	125
 <p>88e</p>	16	16	16	16	16
 <p>88f</p>	32	16	16	64	32
 <p>88a</p>	34	34	17	34	34

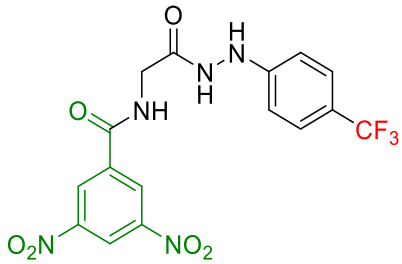
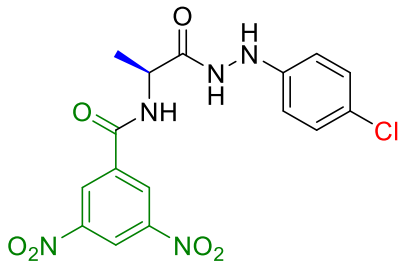
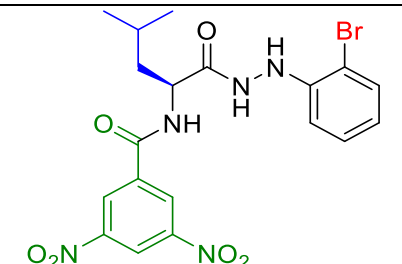
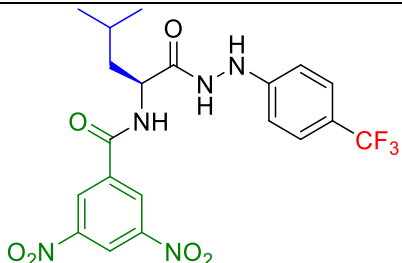
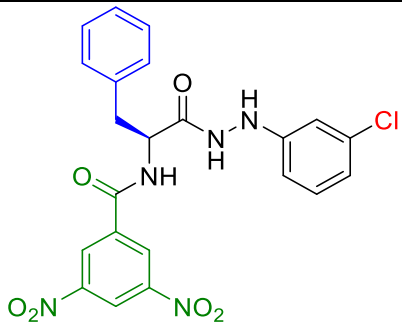
7. Appendix

 <p>86d</p>	15	15	15	30	30
 <p>86g</p>	124	124	124	124	124
 <p>86h</p>	16	16	16	16	16
 <p>89d</p>	7	4	4	7	7
 <p>89e</p>	15	15	7	30	30

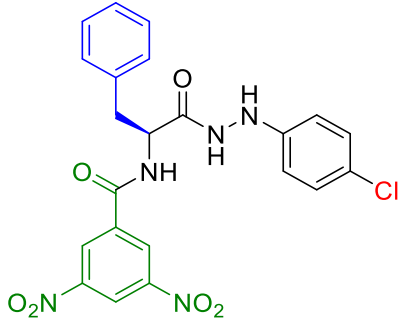
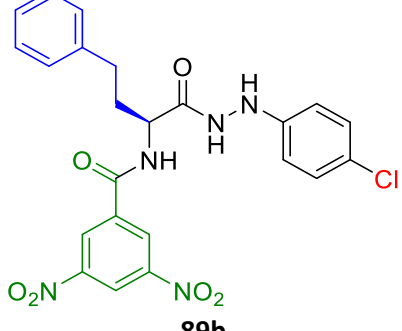
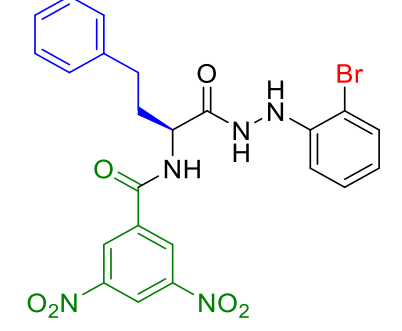
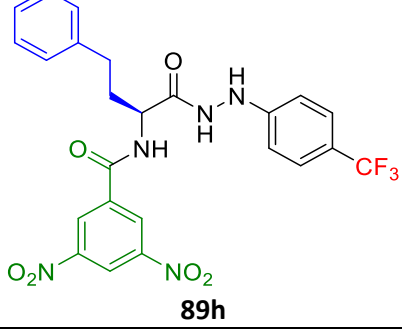
7. Appendix

 <p>89f</p>	30	30	15	30	30
 <p>89g</p>	60	60	30	60	60
<p>Compound structure</p>					
 <p>84a</p>	41	20	163	41	81
 <p>84b</p>	41	10	41	20	20
 <p>84g</p>	19	9	37	9	19

7. Appendix

 <p>84h</p>	19	9	37	9	19
 <p>85a</p>	20	10	39	20	20
 <p>87c</p>	16	16	32	8	16
 <p>87h</p>	8	4	8	8	8
 <p>86a</p>	8	4	8	4	8

7. Appendix

 <p>86b</p>	17	17	33	8	17
 <p>89b</p>	16	16	32	16	16
 <p>Log P: 4.15 89c</p>	2	2	2	2	2
 <p>89h</p>	15	8	30	8	15

7. Appendix

7.2 Crystal structure determination of: jds220006 (C₁₄H₂₀ClN₃O₃)

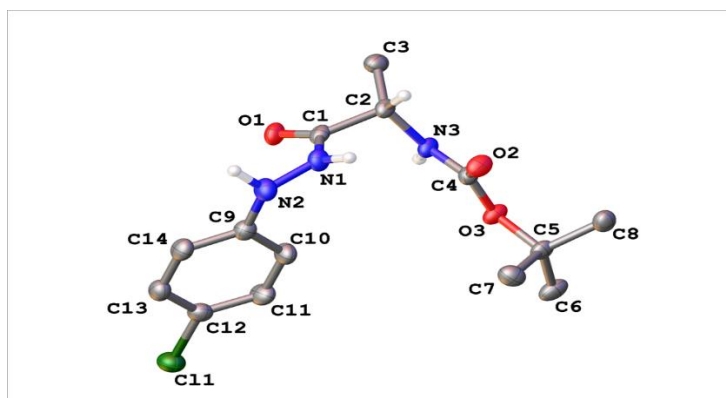


Table 1 : Crystal data and structure refinement for jds220006.

Identification code	jds220006
Empirical formula	C ₁₄ H ₂₀ ClN ₃ O ₃
Formula weight	313.78
Temperature/K	150.0(2)
Crystal system	orthorhombic
Space group	P2 ₁ 2 ₁ 2 ₁
a/Å	5.03010(10)
b/Å	10.8437(3)
c/Å	28.3729(7)
α/°	90
β/°	90
γ/°	90
Volume/Å ³	1547.60(7)
Z	4
ρ _{calc} /cm ³	1.347

7. Appendix

μ/mm^{-1}	2.311
F(000)	664.0
Crystal size/ mm^3	$0.26 \times 0.1 \times 0.07$
Radiation	Cu K α ($\lambda = 1.54184$)
2 Θ range for data collection/ $^\circ$	6.23 to 147.228
Index ranges	$-6 \leq h \leq 4, -13 \leq k \leq 13, -28 \leq l \leq 35$
Reflections collected	14518
Independent reflections	3066 [$R_{\text{int}} = 0.0247, R_{\text{sigma}} = 0.0173$]
Data/restraints/parameters	3066/0/204
Goodness-of-fit on F^2	1.027
Final R indexes [$I \geq 2\sigma(I)$]	$R_1 = 0.0232, wR_2 = 0.0595$
Final R indexes [all data]	$R_1 = 0.0240, wR_2 = 0.0600$
Largest diff. peak/hole / $e \text{ \AA}^{-3}$	0.16/-0.16
Flack parameter	-0.004(5)